

**IMMUNOPHILINS FKBP52 AND FKBP51 MODULATE GLUCOCORTICOID  
RECEPTOR DISTRIBUTION IN NEURONS AND ARE ALTERED IN HIV AND  
MAJOR DEPRESSIVE DISORDER**

by

**Erick Thomas Tatro**

Bachelor of Science, The Ohio State University, 2004

Submitted to the Graduate Faculty of  
School of Medicine in partial fulfillment  
of the requirements for the degree of  
Doctor of Philosophy  
in Cellular and Molecular Pathology

University of Pittsburgh

2008

UNIVERSITY OF PITTSBURGH

School of Medicine

This Dissertation was presented

by

Erick Thomas Tatro

It was defended on

July 28, 2008

and approved by

Committee Chair: Robert P. Bowser, PhD, Department of Pathology

Cristian L. Achim, MD, PhD, Department of Pathology

Stephen C. Strom, PhD, Department of Pathology

Ruth G. Perez, PhD, Department of Neurology

Teresa G. Hastings, PhD, Department of Neurology

Dissertation Advisor: Cristian L. Achim, MD, PhD, Department of Pathology

Copyright © by Erick T. Tatro

2008

**IMMUNOPHILINS FKBP52 AND FKBP51 MODULATE GLUCOCORTICOID RECEPTOR DISTRIBUTION IN NEURONS AND ARE ALTERED IN HIV AND MAJOR DEPRESSIVE DISORDER**

Erick T. Tatro, PhD

University of Pittsburgh, 2008

The class of proteins known as immunophilins, that are cis-trans prolyl isomerases perform diverse chaperone roles. The immunophilins FKBP52 and FKBP51 (FK506 Binding Proteins) are adapter proteins involved in the trafficking of the glucocorticoid receptor (GR), in which FKBP52 facilitates binding of retrograde molecular motor protein dynein and the GR, while FKBP51 binds only the GR. This body of work presents: 1. An analysis of the FKBP family of proteins and their potential for involvement of neuropathogenesis and identifies FKBP52 and FKBP51 as an evolutionarily divergent duo in mammals, 2. The changes in gene and protein levels of these immunophilins in the frontal cortex of patients with HIV and Major Depressive Disorder (MDD), and 3. A role for FKBP52 in the ligand-activated redistribution of GR in neurons.

Using primary human mixed neuron-glia cultures, we tested the hypothesis that immunophilin ligands, like FK506, may alter the kinetics of FKBP52 or FKBP51-mediated trafficking of the GR in neurons. We treated the neuron-glia cultures with hydrocortisone with or without FK506 pretreatment, and found that FK506 altered the distribution of GR. By knocking down expression of FKBP52 using siRNA in a differentiated neuroblastoma cell line, hydrocortisone-mediated nuclear translocation of GR was slowed.

Treatment of neuroblastoma cells media supplemented with 10% conditioned media of HIV-infected microglia lead to increased expression of both immunophilins. In a parallel study, we assessed the transcriptional and postranscriptional levels of the GR adapter proteins FKBP52 and FKBP51 in autopsy tissues from the frontal cortex of patients with MDD with and without HIV. We found increased expression of both proteins in HIV infected patients. FKBP51 was increased in MDD while expression of FKBP52 was the highest in the HIV population with MDD.

These data support the hypothesis that the immunophilins described here modulate the cellular function of the GR in the brain and expression levels may be related to mood disorders. In general, viral infection and inflammation increase expression, of both immunophilins, which may alter the cortisol-induced trafficking of GR.

## TABLE OF CONTENTS

<b>PREFACE.....</b>	<b>XXX</b>
<b>1.0 INTRODUCTION.....</b>	<b>1</b>
<b>1.1 OVERVIEW.....</b>	<b>1</b>
<b>1.2 OVERVIEW OF STUDY ONE - A REVIEW OF THE INVOLVEMENT OF THE IMMUNOPHILIN FAMILY OF PROTEINS IN THE MOLECULAR BASIS FOR NEUROLOGIC DISEASE .....</b>	<b>4</b>
<b>1.3 OVERVIEW OF STUDY TWO - IMMUNOPHILIN FKBP52 AND FKBP51 EXPRESSION IN THE FRONTAL CORTEX IN HIV AND MAJOR DEPRESSIVE DISORDER.....</b>	<b>5</b>
<b>1.4 OVERVIEW OF STUDY THREE - MODULATION OF DISTRIBUTION OF GLUCOCORTICOID RECEPTOR IN NEURONS .....</b>	<b>10</b>
<b>2.0 INVOLVEMENT OF THE IMMUNOPHILIN FAMILY OF PROTEINS IN THE MOLECULAR BASIS FOR NEUROLOGIC DISEASES, A REVIEW .....</b>	<b>12</b>
<b>2.1 ABSTRACT.....</b>	<b>12</b>
<b>2.2 INTRODUCTION .....</b>	<b>13</b>
<b>2.3 MOLECULAR PROPERTIES OF FK506 BINDING PROTEINS .....</b>	<b>14</b>
<b>2.3.1 FK506 Binding-Protein Gene Family.....</b>	<b>14</b>
<b>2.3.1.1 Amino Acid Sequence Analysis of Three Immunophilin Proteins.</b>	<b>18</b>

2.3.2	FK506 Binding Protein Biochemical Properties .....	20
2.3.3	Immunophilin Ligands .....	22
2.4	FK506 BINDING PROTEINS IN PROTEIN FOLDING AND TRAFFICKING.....	26
2.4.1	FKBP12 As Accessory to Transmembrane Proteins .....	27
2.4.2	FKBP12 and Soluble Protein Targets .....	30
2.4.3	FKBP52/59 and Hormone Receptor Activation.....	32
2.5	EMERGING ROLES FOR FKBP38 IN NEURAL CELL FUNCTION AND DEVELOPMENT.....	36
2.5.1	FKBP38 and Apoptosis.....	36
2.5.2	FKBP38 and the Proteasome .....	39
2.5.3	FKBP38 and Neurodevelopment.....	40
2.6	CONCLUSION .....	41
3.0	EXPRESSION OF IMMUNOPHILINS FKBP52 AND FKBP51 IS INCREASED IN FRONTAL CORTEX OF HIV <sup>+</sup> PATIENTS AND DIFFERENTIALLY EXPRESSED IN DEPRESSION.....	42
3.1	INTRODUCTION .....	43
3.2	MATERIALS AND METHODS.....	44
3.2.1	Demographic Information and Analysis.....	44
3.2.2	FKBP52 and FKBP51 Protein Determination .....	50
3.2.3	<i>FKBP4</i> and <i>FKBP5</i> Gene Expression Determination .....	51
3.2.4	HIV-Induced In Vitro Changes in <i>FKBP4</i> and <i>FKBP5</i> Transcript.....	52
3.2.5	<i>FKBP5</i> Genotyping of Patient Cohort .....	53

3.2.6	Immunohistochemistry.....	54
3.3	<b>RESULTS</b> .....	55
3.3.1	Protein Analysis .....	55
3.3.2	Immunophilin Gene Expression .....	59
3.3.2.1	Correlation of Gene and Protein Expression .....	63
3.3.3	Single Nucleotide Polymorphism Analysis .....	67
3.3.4	Immunophilin Response in Cultured Neuronal Cells Exposed to HIV .	70
3.3.5	Immunohistochemistry of FKBP52 and FKBP51 in Frontal Cortex.....	73
3.4	<b>DISCUSSION</b> .....	79
3.4.1	Immunophilin FKBP51 and FKBP52 Expression in HIV and MDD ....	79
3.4.2	Balance of FKBP4 and FKBP5 Genes .....	81
3.4.3	Polymorphism Analysis of <i>FKBP5</i> in MDD .....	82
3.4.4	Immunohistochemistry of FKBP51 and FKBP52.....	88
3.4.5	Limitations and Further Questions.....	90
3.4.6	Conclusion .....	95
4.0	<b>IMMUNOPHILIN FKBP52 MODULATES THE DISTRIBUTION OF ACTIVATED GLUCOCORTICOID RECEPTOR IN NEURONS</b> .....	96
4.1	<b>INTRODUCTION</b> .....	97
4.2	<b>MATERIALS AND METHODS</b> .....	101
4.2.1	Cells .....	101
4.2.2	Immunoprecipitation.....	103
4.2.3	Western Blotting .....	105
4.2.4	PCR and siRNA Synthesis .....	105

4.2.5	Cortisol and FK506 Exposure.....	106
4.2.6	Quantitative PCR.....	107
4.2.7	Imaging .....	108
4.2.8	Quantitative Imaging of Glucocorticoid Receptor Nuclear Translocation in SH-SY5Y Cells .....	108
4.3	<b>RESULTS</b> .....	112
4.3.1	FKBP52-Dynein-Glucocorticoid Complex in SH-SY5Y Cells.....	112
4.3.2	FK506 Inhibits Cortisol-Induced Redistribution of GR and FKBP51 in Neurons	114
4.3.3	siRNA Knockdown of <i>FKBP4</i> Slows GR Translocation .....	124
4.3.3.1	Immunofluorescence Imaging and Quantification of Nuclear and Cytoplasmic GR.....	127
4.3.3.2	Analysis of Nuclear Fluorescence Intensity.....	129
4.3.3.3	Analysis of Cytoplasmic Fluorescence Intensity .....	131
4.3.3.4	Analysis of Percentage of GR in Nucleus .....	132
4.4	<b>DISCUSSION</b> .....	134
4.4.1	FKBP52 and FKBP51 Co-Immunoprecipitations .....	134
4.4.1.1	Limitations and Further Questions.....	135
4.4.2	Immunofluorescence of GR and FKBP51 in Neuronal Cultures .....	137
4.4.2.1	Limitations and Further Questions.....	138
4.4.3	Knockdown of FKBP52 by siRNA Slows Cortisol-Induced GR Nuclear Localization.....	140
4.4.4	Conclusion .....	142

<b>5.0</b>	<b>CONCLUSION AND FUTURE DIRECTIONS .....</b>	<b>143</b>
<b>5.1</b>	<b>IMMUNOPHILINS AND GLUCOCORTICOID RECEPTOR.....</b>	<b>144</b>
<b>5.2</b>	<b>IMMUNOPHILINS IN HIV AND DEPRESSION.....</b>	<b>145</b>
	<b>APPENDIX A .....</b>	<b>149</b>
	<b>APPENDIX B .....</b>	<b>161</b>
	<b>BIBLIOGRAPHY .....</b>	<b>164</b>

## LIST OF TABLES

Table 2-1. Summary Information for the Human Immunophilin - FK506 Binding Proteins. The thirteen immunophilin genes are shown with summaries of function, cell compartment. For reference, PubMed Gene identification is given with key citations on structure and function. Modular structures are listed to illustrate genetic expansion of FKBP genes and divergence of function. FK506 Binding domain (FKB), TM (transmembrane), TPR (tetratricopeptide repeat), CaM-BD (calmodulin binding domain), Efh (E-F hand).....	17
Table 3-1. Demographic Description of Patients in Study .....	46
Table 3-2. Sex composition of study groups by HIV status. Chi-square analysis indicates there are significantly more males in the HIV groups (p=0.006) than non-HIV groups. ....	49
Table 3-3. Sex composition of nonHIV groups by diagnosis. The sex composition is balanced in the non-HIV groups by mental diagnosis (p=0.709). ....	49
Table 3-4. Genotype Frequencies for SNP rs 3800373 of <i>FKBP5</i> Gene. Genotypes of each case in Table 3-1 was determined from genomic DNA by allelic discrimination assay described in Section 3.2.5. Based on the published allelic frequencies $f(A) = 0.688$ , $f(C) = 0.312$ , <i>Expected</i> genotype frequencies are calculated based on Hardy-Weinberg equilibrium and compared to <i>Observed</i> genotypes for the study groups. $\chi^2$ analysis comparing <i>Expected</i> with <i>Observed</i>	

values determines significant deviation in the patient groups from the population, significance is considered at  $p < 0.05$ . ..... 68

Table 3-5. Allelic Frequencies for SNP rs3800373 of *FKBP5* Gene. Genotypes of each case in Table 3-1 was determined from genomic DNA by allelic discrimination assay described in Section 3.2.5. Based on the published allelic frequencies  $f(A) = 0.688$ ,  $f(C) = 0.312$ , *Expected* allele frequencies are calculated based on group size and compared to *Observed* genotypes for the study groups.  $\chi^2$  analysis comparing *Expected* with *Observed* values determines significant deviation in the patient groups from the population, significance is considered at  $p < 0.05$ . ..... 69

Table 3-6. Genotype Frequencies for SNP rs1360780 of *FKBP5* Gene. Genotypes of each case in Table 3-1 was determined from genomic DNA by allelic discrimination assay described in Section 3.2.5. Based on the published allelic frequencies  $f(C) = 0.758$ ,  $f(T) = 0.242$ , *Expected* genotype frequencies are calculated based on Hardy-Weinberg equilibrium and compared to *Observed* genotypes for the study groups.  $\chi^2$  analysis comparing *Expected* with *Observed* values determines significant deviation in the patient groups from the population, significance is considered at  $p < 0.05$ . ..... 69

Table 3-7. Allelic Frequencies for SNP rs1360780 of *FKBP5* Gene. Genotypes of each case in Table 3-1 was determined from genomic DNA by allelic discrimination assay described in Section 3.2.5. Based on the published allelic frequencies  $f(A) = 0.688$ ,  $f(C) = 0.312$ , *Expected* allele frequencies are calculated based on group size and compared to *Observed* genotypes for the study groups.  $\chi^2$  analysis comparing *Expected* with *Observed* values determines significant deviation in the patient groups from the population, significance is considered at  $p < 0.05$ . ..... 69

Table 3-8. Summary of Previous Studies Involving *FKBP5* SNP's rs1360780 and rs3800373.. 88

Table 4-1. Bonferroni post test comparing nuclear  $\hat{I}_{\text{siControl}}$  vs  $\hat{I}_{\text{siFKBP4}}$  at each time point after treatment with 100 nM cortisol showing effect of si-RNA. .... 130

Table 4-2. Bonferroni post test comparing nuclear  $\hat{I}_0$  vs  $\hat{I}_{\text{Time points}}$  at each siRNA group, showing effect of Time with 100 nM cortisol. .... 131

Table 4-3. Bonferroni post test comparing cytoplasmic  $I_{\text{siControl}}$  vs  $I_{\text{siFKBP4}}$  at each time point, showing effect of siRNA group on cytoplasmic intensity. .... 132

Table 4-4. Bonferroni post test comparing cytoplasmic  $I_0$  vs  $I_{\text{time point}}$  in each siRNA group, showing effect of Time with 100 nM cortisol on cytoplasmic intensity. .... 132

Table 4-5. Bonferroni post test comparing %GR in Nucleus<sub>siControl</sub> vs %GR in Nucleus<sub>siFKBP4</sub> at each time point, showing effect of siRNA group on percent of GR in nucleus. .... 133

Table 4-6. Bonferroni post test comparing %GR in Nucleus<sub>Time0</sub> vs %GR in Nucleus<sub>Time point</sub> in each siRNA group, showing effect of Time with 100 nM cortisol on %GR in Nucleus for each group. .... 134

## LIST OF FIGURES

Figure 1-1. FKBP52 and FKBP51 Expression is Enriched in the Hippocampus, Dentate Gyrus, the Cerebral Cortex and the Cerebellum of the Mouse. Data were mined from the Allen Brain Map [48, 49] and images of fluorescence in situ hybridization for mRNA encoding the androgen receptor (AR), glucocorticoid receptor (GR), FKBP52, and FKBP51 in sagittal sections of the adult male mouse brain. For orientation, the Nissl stain is labeled for relevant brain regions are outlined: cortex (CTX), hippocampus (HIP), dentate gyrus (DG), thalamus (TH), and hypothalamus (HY)..... 8

Figure 2-1. Crystal structure of the Human FKBP52 Protein Depicting FKBP-Binding Domains, TPR Domains, and CaM-Binding Domain. Sample large molecular immunophilin FKBP52 showing modular domains of two FK506-Binding Protein (FKBP) Domains, tetratricopeptide repeat (TPR) domains, and C-terminal calmodulin (CaM) binding domains..... 17

**Figure 2-2. Cross-Phyla Cladogram of *FKBP4*, *FKBP5*, and *FKBP1A* Analogues. In order to identify homologous proteins in various species for the immunophilins FKBP51, FKBP52, and FKBP12, the *Homologene* database available online through the National Center for Biological Informatics and the National Library of Medicine was used. The cladogram was constructed using the JalView Java Alignment Editor, the amino acid sequences of identified homologous proteins were sorted using the ClustalW Multiple**

**Sequence Alignment algorithm and the tree was constructed using the Neighbor Joining Using Percent Identity algorithm [99]. The NCBI Accession numbers are as follows (from top to bottom of the tree): NP\_508026.1, NP\_002005, XP\_534923.1, NP\_34349.1, NP\_004108.1, XP\_001172411.1, XP\_538880.2, NP\_0334350.1, NP\_001012174.1, NP\_524895.2, XP\_508927.2, XP\_342764.3, NP\_189160.3, NP\_001021722.1, NP\_000792.1, NP\_032045.1, XP\_001053006.1, XP\_001167897.1, NP\_523792.2, NP\_014264.1, AB028739.**

..... 19

Figure 2-3. Ribbon Diagram and 3-D Structure of FKBP12 With FK506 Bound. The prolyl isomerase active site is highlighted in yellow of the ribbon structure, and color coded for hydrophobicity in the three-dimensional structure [102]. Active-site residues are non-continuous and come together inside the hydrophobic pocket [100]...... 21

Figure 2-4. FKBP12 Modulates Function of the Ryanodine Receptor (A) with FKBP12 bound, the RyR open conformation duration is shorter, allowing less Ca<sup>2+</sup> to pass from the mitochondria to the cytoplasm, large arrow pushing equilibrium toward left in (A). (B) Glutathione blocks binding of FKBP12 and its modulation, allow for redox-control of Ca<sup>2+</sup> gating mediated through FKBP12, larger arrow pushing equilibrium toward right in (B). ..... 24

Figure 2-5. The Mechanism of Signal Transduction Modulation Mediated By Immunophilins and the roles for cofactors and drugs. Binding of the immunophilin to the transducing protein (top), which could be an enzyme or ion channel, modulates its function (middle). Further attenuation is achieved by the presence of cofactors or exogenous immunophilin ligands (bottom). Stars indicate downstream signaling..... 24

Figure 2-6. Model that FKBP12 Accelerates Fibril Formation of  $\alpha$ -Synuclein in an Enzymatic Fashion. FKBP12 causes insoluble fibril formation of  $\alpha$ -synuclein in an enzymatic fashion. It is

thought formation of insoluble fibrils is protective to protein processing machinery from insoluble  $\alpha$ -synuclein protofibrils..... 31

Figure 2-7. FKBP52 and FKBP51 Modulate Activation of Glucocorticoid Receptor (GR). The GR is in complex with HSP90 (90) and FKBP51 (-51). Upon cortisol (C) binding, an immunophilin switch from -51 to FKBP52 (-52). Through -52, the GR complex is linked to the molecular motor protein dynein, shuttling it toward the nucleus. This interaction may be important in large cells with extensive microtubule polymers, extensive endoplasmic reticulum networks where diffusion may be limited. These immunophilins -51 and -52 are expressed in the brain, as shown in Figure 1-1 and in large pyramidal neurons shown in Section 3.3.5. .... 34

Figure 2-8. FKBP38 Regulates Apoptosis Through Its Protein-Trafficking Function of Bcl2. FKBP38 (-38) has a weak mitochondrial signal sequence as transmembrane region, with the functional domain on the cytoplasmic side. FKBP38 can be present on the outer mitochondrial membrane or the Golgi apparatus, its subcellular localization may be altered by posttranslational modification like phosphorylation or association with CaM. The protein Bcl2 is anti-apoptotic by inactivating Bax. Bcl2's association with -38 stabilizes Bcl2; and when -38 is either returned to the Golgi or degraded, Bcl2 becomes inactive or is degraded; and Bax activates apoptosis. .. 37

Figure 3-1. Age Does Not Correlate With Gene Expression of *FKBP4* (A) or *FKBP5* (B). Gene expression from cortical grey matter all the patients listed in Table 3-1 is determined by qPCR using the  $\Delta\Delta$ CT method and normalizing the gene of interest to *GAPDH* expression as explained in Section 3.2.3. Fold-Control is plotted versus age. Linear regression shows no correlation for either gene with Age. .... 47

Figure 3-2. Brain pH Does Not Correlate With Gene Expression of *FKBP4* (A) or *FKBP5* (B). Gene expression from cortical grey matter of patients listed in Table 3-1 for whom brain pH data

were available is determined by qPCR using the  $\Delta\Delta\text{CT}$  method and normalizing the gene of interest to *GAPDH* expression as explained in Section 3.2.3. Fold-Control is plotted versus Brain pH. Linear regression shows no correlation for either gene with Brain pH. .... 48

Figure 3-3. Postmortem Interval (PMI) Does Not Correlate With Gene Expression of *FKBP4* (A) or *FKBP5* (B). Gene expression from cortical grey matter of patients listed in Table 3-1 is determined by qPCR using the  $\Delta\Delta\text{CT}$  method and normalizing the gene of interest to *GAPDH* expression as explained in Section 3.2.3. Fold-Control is plotted versus PMI. Linear regression shows no correlation for either gene with PMI..... 48

Figure 3-4. Expression of *FKBP4* (A) and *FKBP5* (B) is the same in male and female. Gene expression from cortical grey matter of patients listed in Table 3-1 is determined by qPCR using the  $\Delta\Delta\text{CT}$  method and normalizing the gene of interest to *GAPDH* expression as explained in Section 3.2.3. Non-HIV patients are divided into male and female groups and Fold-Control plotted, illustrated is a box-and-whisker plot showing the standard deviation about the mean in the box and the interquartile range in the whiskers. Student's t test comparing male versus female expression showed no significant difference based on sex for expression of *FKBP4*  $p = 0.179$  (A) or *FKBP5* (B)  $p = 0.716$ . .... 50

Figure 3-5. Western Analysis of FKBP52 in MDD and HIV/MDD Patients. Tissue was dissected (100  $\mu\text{g}$ ) from frozen tissue of cortical grey matter of the cases listed in Table 3-1. Tissue was homogenized and 50  $\mu\text{g}$  total soluble protein was run separated by PAGE. Cases representing each study group were included in every gel. After transfer and immobilization on PVDF membrane, proteins were probed by Western blot for FKBP52. Membranes were stripped of antibodies and reprobbed for Actin. Densitometry determined Area Under the Curve for

FKBP52 and Actin signal, and  $\text{Fold-Actin} = \text{Area}_{\text{FKBP52}} / \text{Area}_{\text{Actin}}$ , and plotted to the right are corresponding Fold-Actin values as detailed in Section 3.2.2 and Appendix A. .... 56

Figure 3-6. FKBP52 Protein Level is Increased in HIV Group. Normalized Fold-Actin values are calculated from the Fold-Actin values determined in Figure 3-5. Values are normalized to controls on their respective gels,  $\text{Normalized Fold-Actin} = \text{Fold-Actin}_{\text{Patient}} / \text{Fold-Actin}_{\text{ControlMean}}$  as detailed in Appendix B. The area within the bar delineates the standard deviation about the mean ( $\mu \pm \sigma$ ). Two-way ANOVA and Dunn's Multiple Comparison test were used to test for significance (\*  $p < 0.05$ ). .... 57

Figure 3-7. Western Analysis of FKBP51 in MDD and HIV/MDD Patients. Tissue was dissected (100  $\mu\text{g}$ ) from frozen tissue of cortical grey matter of the cases listed in Table 3-1. Tissue was homogenized and 50  $\mu\text{g}$  total soluble protein was run separated by PAGE. Cases representing each study group were included in every gel. After transfer and immobilization on PVDF membrane, proteins were probed by Western blot for FKBP51. Membranes were stripped of antibodies and reprobed for Actin. Densitometry determined Area Under the Curve for FKBP51 and Actin signal, and  $\text{Fold-Actin} = \text{Area}_{\text{FKBP51}} / \text{Area}_{\text{Actin}}$ , and plotted to the right are corresponding Fold-Actin values as detailed in Section 3.2.2 and Appendix A. .... 58

Figure 3-8. FKBP51 Protein is Altered in MDD Groups Compared to Control and Trended Toward Elevated in HIV. Normalized Fold-Actin values are calculated from the Fold-Actin values determined in Figure 3-5. Values are normalized to controls on their respective gels,  $\text{Normalized Fold-Actin} = \text{Fold-Actin}_{\text{Patient}} / \text{Fold-Actin}_{\text{ControlMean}}$  as detailed in Appendix B. The area within the bar delineates the standard deviation about the mean ( $\mu \pm \sigma$ ). Two-way ANOVA and Dunn's Multiple Comparison test were used to test for significance at  $p < 0.05$ . .... 59

Figure 3-9. *FKBP4* (A) and *FKBP5* (B) Expression is Increased in HIV and HIV with MDD. Gene expression from cortical grey matter of patients listed in Table 3-1 is determined by qPCR using the  $\Delta\Delta CT$  method and normalizing the gene of interest to *GAPDH* expression as explained in Section 3.2.3. Fold-Control is plotted for each of the study groups, ● represent individual patients and bars represent median within the group. One-way ANOVA with Dunn's Multiple Comparison Test tested for significant difference among the groups (\*  $p < 0.05$ ). ..... 60

Figure 3-10. Correlation of *FKBP4* and *FKBP5* Expression in Frontal Cortex Separated by Group. Gene expression from cortical grey matter of patients listed in Table 3-1 is determined by qPCR using the  $\Delta\Delta CT$  method and normalizing the gene of interest to *GAPDH* expression as explained in Section 3.2.3. Fold-Control is plotted for each of the study group, plotting the *FKBP4* expression on the y-axis, and *FKBP5* expression on the x-axis. Pearson's test for correlation showed a correlation between *FKBP4* and *FKBP5* ( $R^2 = 0.55$ ,  $p = 0.0085$ , goodness of fit, and probability that the non-zero slope is due to chance) expression in the Control (●) Group. In the MDD (■) and MDD/Psych (□) groups, the curve was flat, ( $p = 0.52$  and  $0.49$ , respectively) and no correlation ( $R^2 = 0.15$  and  $0.08$ , respectively). For both HIV (▲) and HIV/MDD (△) there was no correlation and the curves were flat ( $R^2 = 0.04$  and  $0.04$ ,  $p = 0.74$  and  $0.66$ , respectively). The curves represent linear regression of the *FKBP4* versus *FKBP5* (solid bold = Control, black = MDD, black dashed = MDD/Psych, grey solid = HIV, grey dashed = HIV/MDD). ..... 62

Figure 3-11. Expression of *FKBP4* (A) and *FKBP5* (B) in the CNTN Groups Separated by Most Recent Episode. Gene expression from cortical grey matter of patients for whom MDD clinical data were available is determined by qPCR using the  $\Delta\Delta CT$  method and normalizing the gene of interest to *GAPDH* expression as explained in Section 3.2.3. Patients are divided based on

MDD Episode Within 1 Month or Within 6 Months and Fold-Control plotted, ● represent individuals and bars represent median. Student's *t* test comparing the two groups' expression showed a nonsignificant trend based on most recent MDD episode for expression of *FKBP4*,  $p = 0.11$  (A); or *FKBP5*,  $p = 0.15$  (B)..... 63

Figure 3-12. Gene Expression of *FKBP4* and Protein Levels of FKBP52 do not correlate. Control group (A), MDD (B), MDD/Psyc (C), HIV (D), HIV/MDD (E), all groups combined (F) are plotted separately. Gene expression from cortical grey matter of patients listed in Table 3-1 is determined by qPCR using the  $\Delta\Delta CT$  method and normalizing the gene of interest to *GAPDH* expression as explained in Section 3.2.3, and Fold Control for *FKBP4* is plotted on the y axes. Normalized Fold-Actin values representing FKBP52 Expression are calculated from the Fold-Actin values determined in Figure 3-5. Values are normalized to controls on their respective gels,  $FKBP52 \text{ Protein Expression} = \text{Fold-Actin}_{\text{patient}} / \text{Fold-Actin}_{\text{ControlMean}}$  as detailed in Appendix B and is plotted on the x axes, ■ represent individual cases. Lines illustrate linear regression and Pearson's Test for Correlation  $R^2$  values for correlation and  $p$  values for probability that a non-zero slope is due to chance are reported..... 65

Figure 3-13. Gene Expression of *FKBP5* versus Protein Levels of FKBP51. Gene Expression of *FKBP5* and Protein Levels of FKBP51 correlate positively in the MDD group (B) and negatively in the HIV/MDD group (E). Control group (A), MDD (B), MDD/Psyc (C), HIV (D), HIV/MDD (E), all groups combined (F) are plotted separately. Gene expression from cortical grey matter of patients listed in Table 3-1 is determined by qPCR using the  $\Delta\Delta CT$  method and normalizing the gene of interest to *GAPDH* expression as explained in Section 3.2.3, and Fold Control for *FKBP5* is plotted on the y axes. Normalized Fold-Actin values representing FKBP51 Expression are calculated from the Fold-Actin values determined in Figure 3-5. Values

are normalized to controls on their respective gels, FKBP51 Protein Expression =  $\text{Fold-Actin}_{\text{Patient}} / \text{Fold-Actin}_{\text{ControlMean}}$  as detailed in Appendix B and is plotted on the x axes, ■ represent individual cases. Lines illustrate linear regression and Pearson's Test for Correlation  $R^2$  values for correlation and p values for probability that a non-zero slope is due to chance are reported. .... 66

Figure 3-14. Transcription Factor Binding Sites and SNP Locations on *FKBP5* Gene. The genomic organization of the *FKBP5* gene is illustrated, exons are numbered with black bars, distance between bars represent relative lengths of the introns. The locations of the two polymorphisms, rs1360780 and rs3800373 are indicated by ▲ and location of hormone responsive elements are indicated with ◆ ..... 68

Figure 3-15. Expression of *FKBP4* in SH-SY5Y Cells Exposed to HIV-Conditioned Media. Differentiated SH-SY5Y cells were exposed for 6 Hours (A) or 24 Hours (B) to conditioned 10% Conditioned Media from HIV-infected microglia. Microglia had been infected with HIV for 15 days, with media removed every third day. On day 15, supernatant (Sup) was removed and used to supplement the SH-SY5Y media to 10% Conditioned Media. Control Media were supplemented with Microglia media, D15 M Sup is supplemented from non-infected microglia grown in parallel to the HIV infection, D0 HIV Sup is supplemented from supernatant of the microglia cultures immediately prior to HIV – infection, D15 HIV Sup is supernatant from the actual infection. RNA was isolated and qRT-PCR for *FKBP4* gene using the  $\Delta\Delta\text{CT}$  method comparing *FKBP4* expression with *GAPDH* and calibrating Control Media. Fold-changes are plotted and two-way ANOVA compares among the groups (\* p <0.01). .... 71

Figure 3-16. Expression of *FKBP5* in SH-SY5Y Cells Exposed to HIV-Conditioned Media. Differentiated SH-SY5Y cells were exposed for 6 Hours (A) or 24 Hours (B) to conditioned 10%

Conditioned Media from HIV-infected microglia. Microglia had been infected with HIV for 15 days, with media removed every third day. On day 15, supernatant (Sup) was removed and used to supplement the SH-SY5Y media to 10% Conditioned Media. Control Media were supplemented with Microglia media, D15 M Sup is supplemented from non-infected microglia grown in parallel to the HIV infection, D0 HIV Sup is supplemented from supernatant of the microglia cultures immediately prior to HIV – infection, D15 HIV Sup is supernatant from the actual infection. RNA was isolated and qRT-PCR for *FKBP5* gene using the  $\Delta\Delta$ CT method comparing *FKBP4* expression with *GAPDH* and calibrating Control Media. Fold-changes are plotted and two-way ANOVA compares among the groups (\* p <0.01). ..... 72

Figure 3-17. Cellular layers of human cortex showing (left) Golgi stain cytoplasm, (middle) Nissl stain cell bodies, (right) myelin sheaths, from Brodmann (1912) [183]. ..... 74

Figure 3-18. No Primary Antibody Control - Frontal Cortex. Paraffin embedded section from the frontal cortex was subjected to immunohistochemistry protocol in Section 3.2.6, lacking primary antibody. Sections were cut at 8  $\mu$ m thick, mounted on glass slides, deparaffinized, rehydrated, permeablized in 1% Triton-X100. Endogenous peroxidases were blocked in 0.3% H<sub>2</sub>O<sub>2</sub> in methanol. Sections were incubated in a pressure cooker at 125°C 10 min. Sections incubated in secondary antibody (HRP conjugated Donkey anti Mouse and Donkey anti Rabbit, 1:1000) 2 hr RT, and after washing, incubated with Nova Red. Sections were counterlabeled with hematoxylin (5 min). Sections were imaged in a 40X objective. Non-specific or endogenous peroxidase reaction in dark red was not observed. .... 75

Figure 3-19. Immunohistochemical staining for FKBP52 in Frontal Cortex from paraffin embedded tissue. Paraffin embedded section from the frontal cortex was subjected to immunohistochemistry protocol in Section 3.2.6. Sections were cut at 8  $\mu$ m thick, mounted on

glass slides, deparaffinized, rehydrated, and permeablized in 1% Triton-X100. Endogenous peroxidases were blocked in 0.3% H<sub>2</sub>O<sub>2</sub> in methanol. Sections were incubated in a pressure cooker at 125°C, 10 min for antigen unmasking and blocked in 10% normal donkey serum. Sections were then incubated with primary antibody (Mouse anti FKBP52, 1:200) overnight at 4°C, then after washing, incubated with secondary antibody (HRP conjugated Donkey anti Mouse, 1:1000) for 2 hr at RT, finally after washing, immunoperoxidase reaction was developed with Nova Red. Specific staining is dark red. Sections were counterlabeled with hematoxylin (5 min) and imaged in a 40X objective. 10X images created the composite image (left). Cytoplasmic neuronal staining is indicated by ▲, perinuclear staining is indicated at △. Specific neuronal staining for FKBP52 was observed in Cortical Layers II, III, IV, and V. .... 76

Figure 3-20. Immunohistochemical staining for FKBP51 in Frontal Cortex from paraffin embedded tissue. Paraffin embedded section from the frontal cortex was subjected to immunohistochemistry protocol in Section 3.2.6. Sections were cut at 8 µm thick, mounted on glass slides, deparaffinized, rehydrated, and permeablized in 1% Triton-X100. Endogenous peroxidases were blocked in 0.3% H<sub>2</sub>O<sub>2</sub> in methanol. Sections were incubated in a pressure cooker at 125°C, 10 min for antigen unmasking and blocked in 10% normal donkey serum. Sections were incubated with primary antibody (Rabbit anti FKBP51, 1:100) overnight at 4°C, then after washing, incubated with secondary antibody (biotin conjugated Donkey anti Rabbit, 1:1000) for 2 hr at RT, then in ABC complex for 30 min at RT, finally after washing, immunoperoxidase reaction was developed with Nova Red. Specific staining is dark red. Sections were counterlabeled with hematoxylin and imaged in a 40X objective. 10X images created the composite image (left). Cytoplasmic neuronal staining is indicated by ▲, axonal tract

staining is indicated at  $\triangleright\triangleright$ . Specific staining for FKBP51 was observed in Cortical Layers III, IV, V, and VI. .... 77

Figure 4-1. LDH Measurements From Exposure of Primary Human Neuron-Glia Cultures to 100 nM Cortisol and 10  $\mu$ M FK506. Primary human neuron-glia cultures grown for 4 weeks on glass coverslips and exposed to 10  $\mu$ M FK506, 100 nM cortisol, both FK506+cortisol, or media alone. Supernatant (10  $\mu$ L) was removed at 0, 30, 60, and 360 min and LDH activity measured by ELISA in CytoTox assay. Positive control is a cell-lysis suspension from cultures grown in parallel. The treatments were not toxic..... 103

Figure 4-2. Quantification methods for nuclear and cytoplasmic fluorescent labeling of GR. Tagged image format (TIF) files were analyzed in Image J software. A representative image is shown in (A). The green and blue color channels were separated and converted the greyscale bitmap (B). A threshold was set for the blue image to delineate the nuclei (C). Image math, subtracting the thresholded image from the green image yielded the nuclear staining (D left). Subtracting the inverted thresholded image from the green image yielded cytoplasmic staining (D right). The text file of the intensity histograms were exported to Excel for analysis and summed across all ten images, (E) shows histogram from one image. .... 110

Figure 4-3. SHSY5Y Cells Express *FKBP4*, *FKBP5*, and *NR3C1* (GR) Genes. RNA was isolated from differentiated SH-SY5Y cells, and reverse transcriptase – PCR reaction performed using primers specific for human *FKBP4*, *FKBP5*, and *NR3C1* (GR) genes. The expected molecular weights were *FKBP4* 600bp, *FKBP5* 650bp, and *NR3C1* 350 bp. The PCR product was separated in 1% agarose gel and imaged in ultraviolet light with ethidium bromide staining. .... 112

Figure 4-4. Co-immunoprecipitation of (A) Dynein and (B) GR with FKBP52 and FKBP51. FKBP51 and FKBP52 were immunoprecipitated from whole cell lysates according to Section 3.2.2. Cells were preincubated in and immunoprecipitation buffers supplemented with 100 nM cortisol or 10  $\mu$ M FK506. Immunoprecipitation products were eluted in tris-tricine running buffer and separated by SDS-PAGE and probed for dynein (74 kD) (A) or GR (97 kD) (B). Dynein was detected with FKBP51. GR was detected with FKBP52 only in the presence of cortisol..... 113

Figure 4-5. Characterization of primary human neuron-glia cultures. Primary human neuronal cultures were cultivated according to Appendix B and cultured according to Section 4.2.1. Cultures on glass coverslips were permeablized in 1% TritonX-100, blocked with normal serum, and incubated with primary antibody overnight at 4°C. Coverslips were incubated in Alexafluor 488 and Alexafluor 547 conjugated secondary antibodies at RT for 2 hr. Nuclei were counterlabeled with Hoechst, 10 min RT (blue). (A) Astrocytes labeled with anti-GFAP (green) and GR (red) indicate astrocytic expression of GR at 40X (left) and 100X (right). (B) Neuronal cells were immunofluorescently labeled with neurofilament and MAP2 (green) and GR (red). (C) Together neurons labeled for neurofilament and MAP2 (green) and astrocytes labeled for GFAP (red) in culture indicate maturation of neurons and approximately 1:1 mixture glia:neurons..... 115

Figure 4-6. Cortisol-induced nuclear translocation of GR slowed in primary human neuronal cultures with preincubation with 10  $\mu$ M FK506. Primary human neuron-glia cultures were pre-treated with vehicle (1:500 ethanol) or 10  $\mu$ M FK506 for 2 hr and subsequently treated with 100 nM Cortisol for 30, 60, 180 min. Cells were labeled for neurons with MAP2 and neurofilament (green), immunostained for GR (red), and nuclei counterstained with Hoechst (blue). More focal

subnuclear staining of GR was apparent in a time-dependent manner with cortisol. More cytoplasmic GR is delineated with  $\Delta$  at 60 min at 180 min if pretreated with FK506..... 118

Figure 4-7. Localization of FKBP51 in primary human neuronal cultures is altered in the presence of 10  $\mu$ M FK506. Primary human neuron-glia cultures were pre-treated with vehicle (1:500 ethanol) or 10  $\mu$ M FK506 for 2 hr and subsequently treated with 100 nM Cortisol for 60 and 180 min. Cells were labeled for neurons with MAP2 and neurofilament (green), immunostained for FKBP51 (red), and nuclei counterstained with Hoechst (blue). 3-D reconstruction showed diffused nuclear staining of FKBP51 with and without cortisol present as indicated in top panels with  $\blacktriangle$ . Pretreatment with FK506 caused exclusion of FKBP51 from the nucleus. .... 120

Figure 4-8. SH-SY5Y Cells Express DAT, TH, Synapsin, D2DR, and  $\beta$ -3-Tubulin. Total cell lysate from differentiated SH-SY5Y cells treated with or without 10  $\mu$ M FK506 for 24 hr was separated by SDS PAGE and transferred to PVDF membrane. Lysates were probed for dopamine transporter (DAT), tyrosine hydroxylase (TH), synapsin, and D2-dopamine receptor. Differentiated SH-SY5Y cells were grown on glass coverslips, fixed in 4% paraformaldehyde, permeabilized in 1% triton-X100, and immunolabeled for Synapsin (red) and  $\beta$ -III-tubulin. Differentiated SH-SY5Y cells, with and without FK506, are of the dopaminergic neuronal phenotype..... 121

Figure 4-9. Differentiated SH-SY5Y Cells Show Neuritic Networks and Arborization. SH-SY5Y cells were grown in glass coverslips coated with poly-ornithine and laminin, after differentiated in retinoic acid for 6 days, cells extend neuritic networks and arborization. Cells were imaged in culture in phase contrast using 20X objective..... 122

Figure 4-10. FK506 Inhibits Cortisol - Induced Gene Expression of (A) *FKBP5* and (B) *Bcl2-l1* in Differentiated SH-SY5Y cells. Differentiated SH-SY5Y cells were exposed 100 nM cortisol for up to 48 hr with (▲) or without (■) pretreatment with 10  $\mu$ M FK506. Saline controls are indicated by  $\nabla$ , plotted are mean and standard deviation of 3 measurements. RNA was isolated and qRT-PCR was performed as described in Section 4.2.6, percent of control comparing to Time 0 for each treatment and time point for the (a) *FKBP5* and (b) *Bcl2-l1* transcripts are plotted. One way ANOVA and Dunn's multiple comparison tests compared the treatments ( $p < 0.05$  for significance). \* Indicate significant difference at a particular timepoint of 100 nM Cortisol compared to Vehicle Control, and # indicate significant difference between 100 nM Cortisol compared to the FK506 pre-treated group. There is low induction of *FKBP5* (A) with cortisol treatment (■) that is slowed but not abrogated by FK506 (▲). Induction of *Bcl2-l1* is abrogated by FK506. The vehicle control ( $\nabla$ ) elevated *Bcl2-l1* (B) expression after 24 hr compared to Time point 0, which was not observed in the Cortisol +FK506 group (▲). ..... 123

Figure 4-11. Confirmation of siRNA knockdown of *FKBP4* in SH SY5Y cells. The half-life of FKBP52 was determined by incubating differentiated SHSY5Y cells with 100  $\mu$ g/mL cycloheximide for various time points, and cell lysates were subjected to western and densitometry analysis, triplicate measurements and nonlinear regression to exponential decay ( $R^2 = 0.852$ ) determined that FKBP52 has a half-life of 13.6 (2.2) hr (mean and 95%CI) (A). Differentiated SHSY5Y cells on glass coverslips in 24 well plates were exposed to 250 ng siRNA generated against the *FKBP4* gene or against a control gene, encoding GFP provided by the manufacturer, for 24 hr; protein was isolated for Western and densitometry analysis and RNA isolated for qRT-PCR (B). Two independent siRNA experiments are illustrated (B) and achieved a 70% reduction in protein and 15% reduction in mRNA. To ensure that a difference in

GR immunofluorescence was not due to altered GR protein content, GR was measured by Western analysis, triplicate measurements (mean and SD) of fold-control versus median control value are illustrated (B). To test the appearance of non-specific bands in the western blots, membranes were developed with primary antibody (C-left), without primary antibody (C-middle) and without both secondary and antibody (C-right center), and determined that the non-specific band is from the avidin-biotin amplification system (C). Immunoprecipitation of FKBP52 from cell lysates and probing for FKBP52 by Western blot further confirmed that the non-specific band is a component in total protein, which could be removed through pre-clearing the lysate (C-right) with streptavidin magnetic beads (C)..... 126

Figure 4-12. Quantification of nuclear and cytoplasmic immunofluorescent staining of GR after treatment with 100 nM cortisol and siRNA to *FKBP4*. Differentiated SHSY5Y cells were grown on glass coverslips and exposed to 250 nmol control (top) and *FKBP4* (bottom) siRNA for 24 hr and then 100 nM cortisol for 0, 15, 30, 60 min. Following fixation, cells were fluorescently labeled for GR (green) and nuclei (blue). Using Image J and Slidebook, nuclear and non-nuclear GR staining was partitioned according to the Methods and Supplementary Information and quantified in 10 images for each treatment. Fluorescence histograms were plotted and fitted by non-linear regression to a Boltzman distribution for nuclear staining and exponential decay distribution for cytoplasmic staining and normalized, which are shown below representative images. Geometric mean ( $\hat{I}$ , for nuclear) and half-maximal ( $I_{1/2}$ , for cytoplasmic) intensities with 95% confidence intervals are shown below the images. The total percentage of nuclear fluorescence intensities among the conditions are plotted below the images. Two-way ANOVA compared the effects of siRNA or time-with cortisol on  $\hat{I}$  (bottom center),  $I_{1/2}$ (bottom left), and %Nuclear GR (bottom right). Significance is represented by \* ( $p < 0.01$ ) between the siRNA

groups at a particular timepoint and # represent significant difference due to time with cortisol. Si-*FKBP4* contributed to lower nuclear staining intensity, slower nuclear translocation, and higher cytoplasmic staining intensity..... 128

Figure 5-1. Model of control of GR signaling in neurons by immunophilins; dysregulation in chronic inflammation or mood disorder. The working model is that FKBP52 and FKBP51 balance to act as gatekeepers to GR signaling in mature neurons. FKBP51 may act to promote stability of of GR in the nucleus and cytoplasm, while FKBP52 links GR to the retrograde molecular motor dynein. Factors such as chronic stress, genetic components, or paracrine signaling from nearby activated microglia may cause an imbalance in immunophilin expression, leading to abberant GR signaling in the brain, and thus contributing to HPA axis dysfunction. 143

## PREFACE

### Acknowledgements

I would like to thank my advisor, Dr Cristian Achim, for the intellectual and academic support for the past four years. Cris is a true practitioner of the academic mission and his enthusiasm for science, interesting problems, and life is infectious. His emphasis on independent thought fostered realization of full potential in all of his trainees. I thank my thesis committee for their thoughtful suggestions to experiments and analyses that greatly improved my work and inspired me around the final bend to finish with a sprint and enjoy the adrenaline rush of the long, long run.

Thanks to my family. Scott Tatro, for teaching me the rewards of hard work, and laying the foundation of ethics, fairness, and motivation. Tanya Gureck, for being supportive in times of need, moral, and physical. Especially, Tom and Mom, for the best Christmas present ever: a monthly supply of coffee delivered timely to my door. Uncle Dan for encouraging and supporting my decision to go to college in the first place and grad school in the second.

Thanks to the University of Pittsburgh, the School of Medicine, the faculty of Department of Pathology, and the McGowan Institute for Bioengineering for scholastic training, support, and funding.

Knowing what I know now about brain development, cognition, and the formation of habits and vocabulary, I must thank my fifth grade teacher. Ms. Dolores Zebelian inspired me to

enjoy reading, to pick up a book, and changed the trajectory of my life. Other instructors in college, Drs. Lowary in chemistry and Curtis in biology, gave me a chance to hone my skills as an amateur scientist, taught me not only scientific knowledge but skills and methods; and they were inspirations to go to grad school.

Thanks to gang at UCSD and the Burnham Institute, Britta Hult, Gursh Chana, Ginger Lucero for providing technical, emotional, and mental support in the lab, at the desk, in the pub, on the beach, and on the trail. Thanks to Dr. Kaul for showing me how to navigate the microscope; Ricky Muang and Katie Medders were great purveyors of enlightenment. Nina Korzeniewski and the Biweekly-Triweekly Dinner Club of the Interdisciplinary Biomedical Science Program matriculating class of 2004 should be acknowledged for the good food, the good times, the random movie nights, and the late-night scientific and philosophical discussions over poker. Lenny Boss was an awesome tennis partner and is great friend. Thanks Andrew Levin, for challenging my brain, being a good music buddy, and teaching me to do proper squats; healthy body has a healthy mind and a healthy mind can survive grad school. Thanks Chris Stewart and Charles Serafy for emotional support in all the random places grad school took me. The Grad Studies office in the School of Medicine was super helpful and patient and Cindy Duffy's contribution to each grad student is hugely understated and she deserves a medal for dealing with my manias alone.

My sanity would not have remained in tact without Endnote, Mac OSX, iTunes, podcasts, lots of coffee, John Williams, New Balance shoes, Schenley Park, Buffy the Vampire Slayer, and the Pacific Ocean.

#### List of abbreviations

3-D	three dimensional
3'UTR	three prime untranslated region

5'UTR	five prime untranslated region
A/C	adenosine to cytosine
A260/A280	Absorbance at 260nm : Absorbance at 280nm ratio
AA	adenosine homozygous
ABC	adenosine triphosphate binding cassette
AC	adenosine cytosine heterozygous
ACTH	adrenocorticotropic hormone
AD	Alzheimer's disease
AIDS	acquired immune deficiency syndrome
ALCOH POIS	alcohol poisoning
ALS	amyotrophic lateral sclerosis
APP	amyloid precursor protein
AR	androgen receptor
Asn	asparagine
ATP	adenosine triphosphate
Bcl2	B-cell lymphoma 2 protein
bp	basepairs
C/T	cytosine to thymine
Ca	calcium
Ca <sup>2+</sup>	calcium II ion
CaM-BD	calmodulin binding domain
CaN	calcineurin
CARDIAC	cardiac arrest
CC	cytosine homozygous
CCAAT	cytosine-cytosine-adenine-adenine-thymine promoter sequence
cDNA	complementary DNA strand
CNS	central nervous system
CNTN	California NeuroAIDS Tissue Network
CORT	cortisol
CRH	corticotropin release hormone
CT	cytosine thymine heterozygous
D	day
Δ CT	change in cycle threshold
DA	dopamine
DAT	dopamine transporter
Dk	donkey
DMEM	Dulbelco's modified Eagle's medium
DNA	deoxyribunucleic acid
EDTA	ethylenediaminetetraacetic acid
Efh	E-f-hand - calcium binding
ELISA	enzyme linked immunosorbant assay
ER	endoplasmic reticulum
F	female
FKB	FK506 binding domain
FKBP	FK506 binding protein
FKBP12	FK506 binding protein of 12 kilodaltons

FKBP12.6	FK506 binding protein of 12.6 kilodaltons
<i>FKBP1A</i>	Gene FK506 binding protein-1A
<i>FKBP1B</i>	Gene FK506 binding protein-1B
<i>FKBP2</i>	Gene FK506 binding protein-2
<i>FKBP3</i>	Gene FK506 binding protein-3
FKBP38	FK506 binding protein of 38 kilodaltons
<i>FKBP4</i>	Gene FK506 binding protein-4
<i>FKBP5</i>	Gene FK506 binding protein-5
FKBP51	FK506 binding protein of 51 kilodaltons
FKBP52	FK506 binding protein of 52 kilodaltons
<i>FKBP8</i>	Gene FK506 binding protein-8
FoxA2	forkhead box A-2
GABA	$\gamma$ -aminobutyric acid
<i>GAPDH</i>	glyceraldehyde 3-phosphate dehydrogenase gene
GFAP	glial fibrillary acid protein
GFP	green fluorescent protein
GR	glucocorticoid receptor
GSW	gunshot wound
Gt	goat
GTP	guanosine triphosphate
HEK293	human emryonic kidney-293 cell line
HEPES	4-(2-hydroxyethyl)-1-piperazineethanesulfonic acid
HIV	human immunodeficiency virus
HPA	hypothalamus-pituitary-adrenal
HRE	hormone responsive element
HRP	horseradish peroxidase
HSP56	heat shock protein of 56 kilodaltons
HSP90	heat shock protein of 90 kilodaltons
IgG	immunoglobulin G isoform
Ile	isoleucine
IP	immunoprecipitate
kD	kilodaltons
LDH	lactate dehydrogenase
M	male
$\mu\pm\sigma$	mean plus or minus standard deviation
MAP2	microtubule associated protein 2
MDD	major depressive disorder
MDD/Psych	major depressive disorder with psychotic features
MDR	multidrug resistance genes
$\mu\text{g}$	microgram
mg	miligram
min	minutes
mL	mililiter
$\mu\text{L}$	microliter
mM	milimolar
$\mu\text{M}$	micromolar

Mo	mouse
mRNA	messenger ribonucleic acid
MVA	motor vehicle accident
n	sample size
NCBI	National Center for Bioinformatics
ng	nanograms
NIH	National Institutes of Health
nm	nanometers
nM	nanomolar
NO	nitric oxide
<i>NR3C1</i>	Nuclear Receptor Subfamily 3, Group C, Member 1 (Glucocorticoid Receptor gene)
OD	overdose
p24	protein 24 antigen
PBS	phosphate buffered saline
PCR	polymerase chain reaction
PD	Parkinson's disease
PFC	prefrontal cortex
pg	picograms
PGP	p-glycoprotein
Phe	phenylalanine
PULM EMBOL	pulmonary embolism
qPCR	quantitative polymerase chain reaction
Rb	rabbit
RCA1	Riccinnus communis agglutinin I
rpt2	regulatory particle triple-A protein
RyR	ryadonine receptor
SDS-PAGE	sodium dodecyl sulfate polyacrylamide gel electrophoresis
SH-SY5Y	third generation neuroblastoma from SK-NSH
siRNA	small-interfering ribonucleic acids
SNP	single nucleotide polymorphism
SUIC	suicide
Sup	supernatant
TGF- $\beta$	transforming growth factor beta
TH	tyrosine hydroxylase
TM	transmembrane
TPR	tetratricopeptide repeat
Tris-HCl	2-amino-2(hydroxymethyl)1,3-propanediol hydrochloride
Trp	tryptophan
TT	thymine homozygous
Tyr	tyrosine
<i>uca</i>	ultracurvata
Val	valine
VMAT2	vesicular monamine transporter 2
WB	Western blot
WNT1	wingless-related mmtv integration site 1

## 1.0 INTRODUCTION

### 1.1 OVERVIEW

FK506-Binding proteins (FKBP's) are a class of proteins expressed in all prokaryotic organisms. In multicellular organisms, they are expressed in many tissues and in vertebrates, particularly highly expressed in the brain [1, 2]. The higher molecular weight immunophilins arose through classic gene duplication and increased in size by fusion of the classic immunophilin domain that forms the FKBP12 protein to other protein modules, such as tetratricopeptide repeat (TPR) domains, signal sequences, calcineurin (CaN) binding domain, and transmembrane domains [3, 4]. The function of immunophilins varies depending on its modules and localization, but the function of the immunophilin-domain as a rotamase is to serve as a molecular chaperone, promoting stability, maintenance of a particular conformation, and proper folding [5, 6]. The high molecular weight immunophilins, FKBP52 and FKBP51 are only expressed in multicellular organisms, FKBP51 expressed exclusively in vertebrates, and the evolution of the high molecular weight immunophilins has diverged greatly to serve different functions in more complex organisms compared to other prolyl isomerases [7].

FKBP12 is expressed in the brain is more highly expressed in neuroinflammation and neurodegeneration [8]. Neurodegenerative diseases such as Parkinson's disease (PD), Alzheimer's disease (AD), and amyotrophic lateral sclerosis (ALS) are often characterized by

selective loss of a particular neuronal phenotype and by abnormal accumulation of proteins in the later stages of disease [9]. Proteins often found in these accumulations are:  $\alpha$ -synuclein, hyperphosphorylated tau, ubiquitin,  $\beta$ -amyloid, and neurofilament. These proteins are ubiquitously expressed in neurons and in other cells types, so why are dopaminergic neurons susceptible to degeneration and accumulation of protein aggregates in PD? Why spinal cord neurons in ALS? Why hippocampal neurons in AD? In the frontal cortex, synaptic density and dendritic arborization is reduced in Major Depressive Disorder (MDD), thought to be due to excessive glucocorticoid signaling [10-12] [13]. There must be a distinctive biochemical milieu to specific neuronal phenotypes rendering them susceptible to degeneration. Indeed, there seems to be divergent mechanisms of toxicity among the various neuronal phenotypes leading to convergent outcomes: synaptic loss, neuronal degeneration, and aggregation of ubiquitously expressed proteins. In Chapter 2, the functions and properties of immunophilins are broadly reviewed in the context of evolution and neural cell biology. We review some of the observed biochemical and genetic properties of immunophilins and apply these properties to possible mechanisms of neuronal function, specifically synaptic plasticity and stability.

The sequence analysis performed in Chapter 2 recognized that the amino acid sequence of immunophilin FKBP51 falls within the FKBP52 clade, and both of these genes diverge greatly in humans compared to other organisms. These two proteins are thought to be involved in modulation of hormone signaling and differentially regulate the function of the GR [14]. Aberrant glucocorticoid signaling and hypercortisolemia are thought to be contributors to the physiologic basis for MDD [13, 15-17]. With that in mind, in Chapter 3, we aimed to study whether these proteins and genes are differentially expressed in patients suffering from Major Depressive Disorder (MDD) compared to the normal population. Since hypercortisolemia [18,

19]and MDD [20]are comorbid to HIV and the fact that cytokines produced by HIV-infected cells [21, 22]impairs GR signaling [23-26], we included in our study patients with HIV infection who suffered from MDD as well . We found changes in expression of the immunophilins most strongly correlated to HIV infection.

In Chapter 4, we determine whether these immunophilins modulate the trafficking of the GR in neurons. There is abundant literature on the effects of glucocorticoid excess and brain function [27, 28]. The widely accepted model is that chronic glucocorticoid signaling in neurons renders them vulnerable to degeneration leading to decreased volume of brain structures such as the hippocampus [17]. The decreased volume is not necessarily due to neuronal loss per se, but rather reduction in the size of neurons and their synaptic and dendritic fields [29]. While this model may be accurate, we still know little about the molecular events that occur in a neuron making it “vulnerable” to GR activity. Furthermore, although some neural populations are identified as particularly susceptible to cortisol-induced vulnerability (for example the CA1 and CA3 fields of the hippocampus), no molecular mechanism explains how this occurs [30]. Identifying and studying mechanisms like the steroid co-activation or repression of GR-mediated signaling may offer an explanation for the molecular basis of depression and offer routes for novel interventions.

## **1.2 OVERVIEW OF STUDY ONE - A REVIEW OF THE INVOLVEMENT OF THE IMMUNOPHILIN FAMILY OF PROTEINS IN THE MOLECULAR BASIS FOR NEUROLOGIC DISEASE**

Neurodegenerative diseases such as PD, AD, and ALS are often characterized by selective loss of a particular neuronal phenotype and by abnormal accumulation of proteins in the later stages of disease. Theoretically, to identify etiology of these diseases, one approach would be to identify the specific properties that characterize the susceptible neuronal phenotype. For example: How is a dopamine (DA) neuron different from other neurons? Answering this question assists in answering the corollary question: Why is it susceptible to degeneration in PD? The presence of DA, its intermediates and oxidative byproducts, the presence of the dopamine transporter (DAT), tyrosine hydroxylase (TH), vesicular monoamine transporter 2 (VMAT2), and D2-DA receptors provide a singular biochemical environment to the dopaminergic neuron. The human brain is equipped with more extensive basal ganglia than other mammals, possessing as much as 590,000 DA neurons compared to 165,000 in *Macaca*, while the overall brain size is increased only 2-3 times, approximately in correlation to body weight [31]. Humans and not monkeys suffer from PD, therefore not only identifying the unique properties of susceptible neuronal populations, but identifying unique properties of the human physiologic milieu and aging could lead to uncovering the etiology of neurodegenerative disease.

It has been long reported that immunophilins are expressed in levels 50-times higher in the brain compared to other tissues and that immunophilins are specifically expressed higher in the basal ganglia, substantia nigra, and hippocampus compared to the other brain regions [1]. We have shown recently by immunohistochemistry that immunophilin FK506-binding protein of 12 kD (FKBP12, gene ID *FKBP1A*) is expressed at higher levels in cells expressing TH and

DAT than other neuronal types [32]. The observation that immunophilin ligands have neurotrophic effects coupled with the reported higher expression of immunophilins in dopaminergic neurons is noteworthy and warrants further study [33, 34]. The review provided in Chapter 2 serves to link the various studies of genetics, biochemistry, and bioinformatics of immunophilin proteins to the molecular mechanisms of brain disease.

### **1.3 OVERVIEW OF STUDY TWO - IMMUNOPHILIN FKBP52 AND FKBP51 EXPRESSION IN THE FRONTAL CORTEX IN HIV AND MAJOR DEPRESSIVE DISORDER**

In Chapter 3, we investigate through autopsy studies whether the expression levels of FKBP52 and FKBP51 are different in the brains of depressed patients compared to controls. The rationale for studying the levels of immunophilins in the frontal cortex of depression patients lies in the basic premise that depression has a physiological basis in the brain. The volume and metabolic activity of the prefrontal cortex (PFC) is reduced in severe depression [35]. The PFC facilitates complex cognitive operations and responds to external cues that could control the function of the amygdala, hypothalamus, and brain stem. Cortisol, in humans, alters processes associated with PFC functions, including inhibitory control, attention regulation, and planning [36]. In rats, cortisol causes a reorganization of PFC dendritic fibers [29]. Cortisol-induced impairment of the PFC leads to disinhibition of the hypothalamus-pituitary-adrenal (HPA) axis, which leads to enhanced cortisol secretion: this highlights the feed-forward mechanism of the glucocorticoid cascade hypothesis of depression that is discussed below [17].

Particularly relevant to depression, the amygdala is involved in regulation of emotion and behavior. In depression, the amygdala shows increased activity, which inhibits the function of the PFC and activates the HPA [37]. Cells of the amygdala express the GR and corticosteroids enhance amygdala activity, facilitating the embedding of emotion-related memory [38]. Hyperactivity of the amygdala enhances cortisol release, which in turn increases amygdala activity. Thus the amygdala is involved in a self-perpetuating cycle of hyperactivity that leads to deleterious effects on the PFC, hippocampus, and brain-stem; and ultimately is clinically manifested as depression [39].

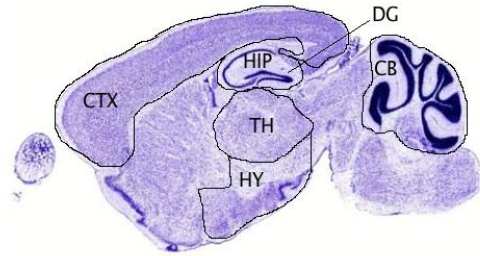
The volume and the function of the hippocampus are reduced in patients suffering from major depression [40]. The volume and functional loss are due to reduced synaptic and dendritic densities and neuronal size rather than loss of neurons [41]. Activation of the GR in hippocampal neurons promotes long-term depression, alters hippocampal morphology, and alters cognitive ability [42-44]. Furthermore, damage to the hippocampus impairs its ability to contribute to feedback inhibition of the HPA axis, so excess cortisol signalling contributes to changes that further promote its secretion [39]. The expression of the GR co-activator FKBP52 and the inhibitor FKBP51 is high in the hippocampus compared to other brain regions Figure 1-1, and may be involved in GR-mediated effects of cortisol on the hippocampus.

The glucocorticoid-cascade hypothesis postulates a feed-forward mechanism of decreased feedback inhibition with increased sensitivity of the brain to cortisol. With aging and stress over time, long-term exposure to cortisol decreases the ability of the hypothalamus to downregulate secretion of corticotrophin releasing hormone (CRH) after a stressor. While the levels of circulating cortisol may not increase with age, older animals show a longer recovery time from stress-induced cortisol surges than younger ones. The longer duration of elevated

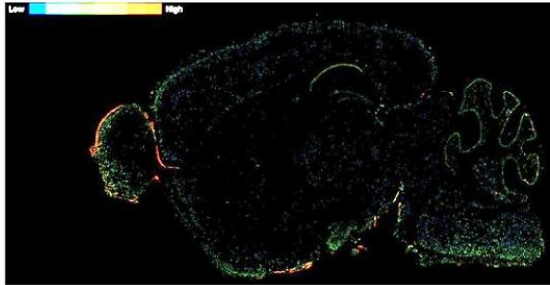
cortisol also causes a decreased sensitivity to the feed-back inhibition loop, further exacerbating the problem [17].

FKBP52 (gene ID *FKBP4*) consists of two classic immunophilin domains at the N-terminus, followed by tetratricopeptide repeat (TPR) domains, and a calmodulin-binding domain [45]. Yeast and lower life-forms do not express FKBP52. The promoter region of the gene contains a binding site for Sp1, an important transcription factor for constitutively active genes [46]. It also contains a consensus binding sequence for heat-shock factor therefore it is important to note that increased expression may be inducible. FKBP52 is expressed in all tissues.

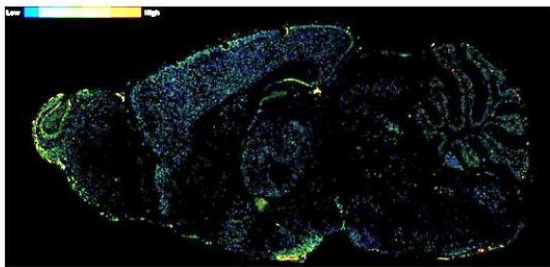
Figure 1-1, compiled from the Allen Brain Map, shows through in situ hybridization that the FKBP4 gene is expressed in the cortex, and particularly enriched in CA1 and CA3 region of the hippocampus, as well as the thalamus and cerebellum of the mouse [47]. GR expression is also enriched in these regions but it has not yet been determined whether expression of *FKBP4* is altered in these regions during disease-state.



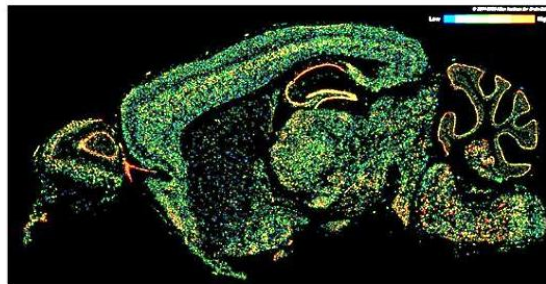
Nissl



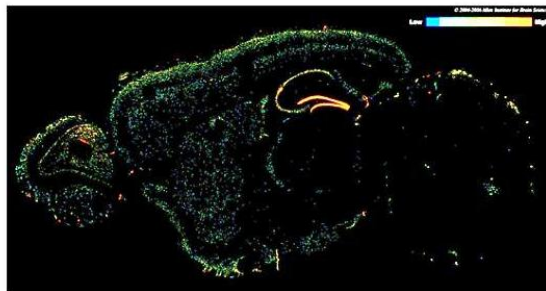
AR



GR



FKBP52



FKBP51

**Figure 1-1. FKBP52 and FKBP51 Expression is Enriched in the Hippocampus, Dentate Gyrus, the Cerebral Cortex and the Cerebellum of the Mouse. Data were mined from the Allen Brain Map [48, 49] and images of fluorescence in situ hybridization for mRNA encoding the androgen receptor (AR), glucocorticoid**

**receptor (GR), FKBP52, and FKBP51 in sagittal sections of the adult male mouse brain. For orientation, the Nissl stain is labeled for relevant brain regions are outlined: cortex (CTX), hippocampus (HIP), dentate gyrus (DG), thalamus (TH), and hypothalamus (HY).**

In an autopsy study of patients with major depression, there were more neurons in the paraventricular region of the hypothalamus expressing CRH than in control brains [50]. Through these neurons, norepinephrin secretion is promoted by cortisol [51]. However, cortisol acts in a negative manner on the hypothalamic CRH neurons that signal to the pituitary. In depressed patients, this negative feedback loop is deficient at reducing elevated cortisol levels [36]. The precise means by which cortisol secretion may be inhibited (through feedback) is not yet established but it is reasonable to propose that it may be mediated by GR [17], and thus may be affected by the co-activator and inhibitor, FKBP52 and FKBP51, of GR that are the focus of the current body of work. Mice lacking GR have increased corticosterone levels and reduced anxiety suggesting that GR function plays a role in emotion and behavior [52]. Based on these observations it is feasible that decreased FKBP52 (the coactivator) and increased FKBP51 (the inhibitor) would have similar (and possibly reversible or controllable) effects as decreasing GR. Conversely, increased FKBP52 and decreased FKBP51 would promote aberrantly increased GR signaling. In Chapter 3, we tested these hypotheses.

## **1.4 OVERVIEW OF STUDY THREE - MODULATION OF DISTRIBUTION OF GLUCOCORTICOID RECEPTOR IN NEURONS**

In Chapter 4, we determine whether the immunophilin ligand, FK506 alters association of the GR with adapter proteins. Furthermore, we use microscopy to determine whether the cellular localization, particularly to the nucleus, and formation of GR-complexes in the nucleus was altered by FK506 or by knocking down expression of FKBP52.

The rationale for studying glucocorticoid signaling in neurons is that chronically elevated cortisol due to stress causes pathology in the brain. Glucocorticoids, particularly cortisol in humans, are secreted by the adrenal glands in response to signals from the hypothalamus/pituitary. While the hypothalamus and pituitary are largely involved in regulating autonomic functions, and cortisol secretion is part of circadian rhythm (i.e. elevated after awakening and decreasing throughout the day), the HPA axis is also involved in the stress response and is integrated into other “higher” functional areas of the brain as well.

In response to stress, both emotional and physical, CRH is secreted by the hypothalamus, signaling to the pituitary to release adrenocorticotrophic hormone (ACTH), which enters the blood stream and eventually stimulates cells of the adrenal cortex to increase the production of corticosteroids, mainly glucocorticoids. Glucocorticoids have a vast array of systemic effects on almost all organs of the body, known overall as the “flight or fight” response.

Like other tissues, the brain contains GR, and activation of GR affects neuronal function. The brain responded to glucocorticoids leads to feedback inhibition of the HPA axis to reduce CRH secretion and returns the body to normal metabolic state. “Higher” functions, such as emotion can induce this response to signals that arise from the prefrontal cortex, amygdala, and hippocampus, which in turn will prompt the hypothalamus to initiate a stress response.

The effects of glucocorticoid excess and brain function have been abundantly reported [28, 53]. A model that is widely accepted is that chronic glucocorticoid signaling in neurons renders them vulnerable to degeneration, leading to decreased volume of brain structures such as the hippocampus [17]. The decreased volume is not necessarily due to neuronal loss, but rather reduction in the size of neurons and their synaptic and dendritic fields [29].

While this model may be accurate, the molecular events leading to vulnerability are poorly understood. Furthermore, although some neural populations are identified as particularly susceptible to cortisol-induced vulnerability (for example the CA1 and CA3 fields of the hippocampus), no molecular mechanism explains how this occurs [30].

Identifying and studying mechanisms like the steroid co-activation or repression of GR-mediated signaling may offer an explanation for the molecular basis of depression and offer routes for therapeutic interventions.

## 2.0 INVOLVEMENT OF THE IMMUNOPHILIN FAMILY OF PROTEINS IN THE MOLECULAR BASIS FOR NEUROLOGIC DISEASES, A REVIEW

### 2.1 ABSTRACT

FK506-Binding Proteins (FKBP's), called immunophilins, are involved in a wide variety of biochemical and cellular functions. Some FKBP's expressed in the brain, genes *FKBP1A*, *FKBP1B*, *FKBP4*, *FKBP5*, (protein names FKBP12, FKBP12.6, FKBP52, and FKBP51, respectively) are more highly expressed in neuroinflammation and neurodegeneration. *FKBP8* (protein FKBP38) is important for neurodevelopment. We outline here diverse biochemical and cellular functions of immunophilins that are of interest to the molecular basis for a wide variety of neuropathologic conditions, including stress-related neuropathies,  $\alpha$ -synucleinopathies,  $\beta$ -amyloidopathies, and diseases involving mitochondrial function. FKBP's are involved in hormone signaling, protein folding, and signal transduction modulation. Many are abundantly expressed in neurons of the hippocampus, in all layers of the frontal cortex, and in the basal ganglia. Many of the biochemical mechanisms underlying these functions are very recently discovered and could some day prove pertinent to the pathogenesis of various diseases of the central nervous system. The review serves to link the various new studies of genetics, biochemistry, bioinformatics of immunophilin proteins to the molecular mechanisms of brain disease.

## 2.2 INTRODUCTION

FK506-binding proteins (FKBP's) are a family of prolyl isomerases that catalyze the cis/trans orientation about proline residues; a rate-limiting step in the folding of many proteins [7]. New data suggest that some of these FKBP's may have recently evolved to perform specific functions apart from generalized protein folding, particularly in the brain. The biochemical and cellular functions of these FKBP's indicate that they may play a role in the pathogenesis of some neurodegenerative and cognitive disorders. In some neurodegenerative and cognitive diseases FKBP's are upregulated, downregulated, or mutated [8]. The purpose of this review is to discuss the recent discoveries of the molecular and cellular functions of the FKBP's with regard to brain specific functions; specifically their roles in protein folding and trafficking, apoptosis, and signal transduction modulation. Elucidating how these three processes are regulated by immunophilins, of high abundance in the brain, may prove important to understanding some features of the molecular pathogenesis of neurodegeneration or even mechanisms of neuroprotection [1].

## 2.3 MOLECULAR PROPERTIES OF FK506 BINDING PROTEINS

### 2.3.1 FK506 Binding-Protein Gene Family

There are 13 human genes in the protein family of FKBP's, they comprise part of the Immunophilin class of isomerases, their activity is to flip the peptide bond about a proline from *cis* to *trans* position, also called *rotamase*. They are called “immunophilins” because they were originally identified as “receptors” for immunosuppressive drugs such as FK506 (tacrolimus) and cyclophilin [54-56]. While protein binding partners are identified, no endogenous small molecule ligand, in other words cofactor, has been identified for immunophilins in humans, however the possibility exists and will be discussed below. FK506 was shown to have neurotrophic effects in vitro and in vivo, there is debate as to the “importance” of which FKBP mediates this effect and how, however discussion of the neurotrophic effects of immunophilin ligands is beyond the scope of this dissertation, for a review on that topic see Gold (2003) [34, 57]. Instead, we will highlight how the molecular functions may be involved in the pathogenesis of various neurodegenerative or cognitive diseases. In order to do so, we must first discuss the basic molecular properties of FKBP's.

The FKBP's are one of three distinct families in the rotamase (*cis/trans* isomerase enzymes) class of proteins, the other two are the cyclophilins and parvulins. Pemberton and Kay (2005) compared the prolyl isomerase repertoires of human, fruit fly, nematode, and yeast [58, 59]. They performed analyses of the amino acid sequences and constructed dendograms depicting the evolutionary history of prolyl isomerase repertoires in these species, revealing that FKBP's are expanded in human more than would be expected compared to the other isomerases. The repertoires of the organisms have both isomerases with common function and those that

appear distinct for any given organism. The proportion of cyclophilins and parvulins with cross-species orthologues is high, whereas the proportion seen with the FKBP's is low by comparison. They concluded that cyclophilins and parvulins have evolved to perform conserved functions, while the FKBP's have evolved to fill divergent or ever-changing niches within constantly evolving organisms [60]. This theme is revisited when we consider the role of *FKBP4* and *FKBP5* in humans and monkeys, and how slight alterations in expression led to physiological differences between *Homo sapiens* and monkeys. There are large inserts in the monkey FKBP51 protein that does not exist in the human analogue. Biochemical analysis showed that the monkey FKBP51 protein does not bind GR as efficiently as the human [61], which helps to stabilize it in the HSP90 complex [14, 62]. X-ray crystallography attributes this inefficiency due to conformational differences leading to GR to not have efficient access to its binding location in the monkey FKBP51 protein [63]. The general glucocorticoid resistance in New World monkeys is attributed to both higher expression of its lack of ability to chaperone and stabilize the GR [63].

To illustrate the role of divergent evolution in the higher molecular weight immunophilins, a cladogram of the FKBP52, FKBP51, and FKBP12 protein sequences across various phyla was constructed and is described below in Section 2.2.1.1. Clearly, the FKBP12 amino acid sequence was highly conserved and the FKBP52 and FKBP51 sequences diverged.

The FKBP family of proteins arose through classic gene-duplication of the archetypal immunophilin FKBP12 (gene name *FKBP1A*). All other FKBP's arise from duplication of this gene and transposing throughout genomes to other functional modules, such as the tetratricopeptide repeat domains (TPR), calcium-binding domains, or signal sequences [64]. Figure 2-1 shows the crystal structure of the FKBP52 protein and its protein modules. The N-

terminal [65] and C-terminal[66] crystal structures were solved separately. Table 1-1 lists all of the FKBP's in humans, their sizes, their domain architecture, and their cellular location. Given that FKBP's may perform the rate-limiting step in protein folding pathways, and the expansion of the FKBP family described by Pemberton and Kay (2005), it could be that they are evolving to serve this increased requirement for chaperoning in higher organisms and in specific cell-types, driven independently within each organism or tissue, thus leading to their observed lack of cross-phyla orthology. A recent bioinformatics report on the evolution of the FKBP12 gene supports the notion the cyclophilins are evolving to perform specific conserved functions within the different organisms, while the FKBP's are evolving, in most cases, to meet the more individual needs for protein chaperoning [59, 60].

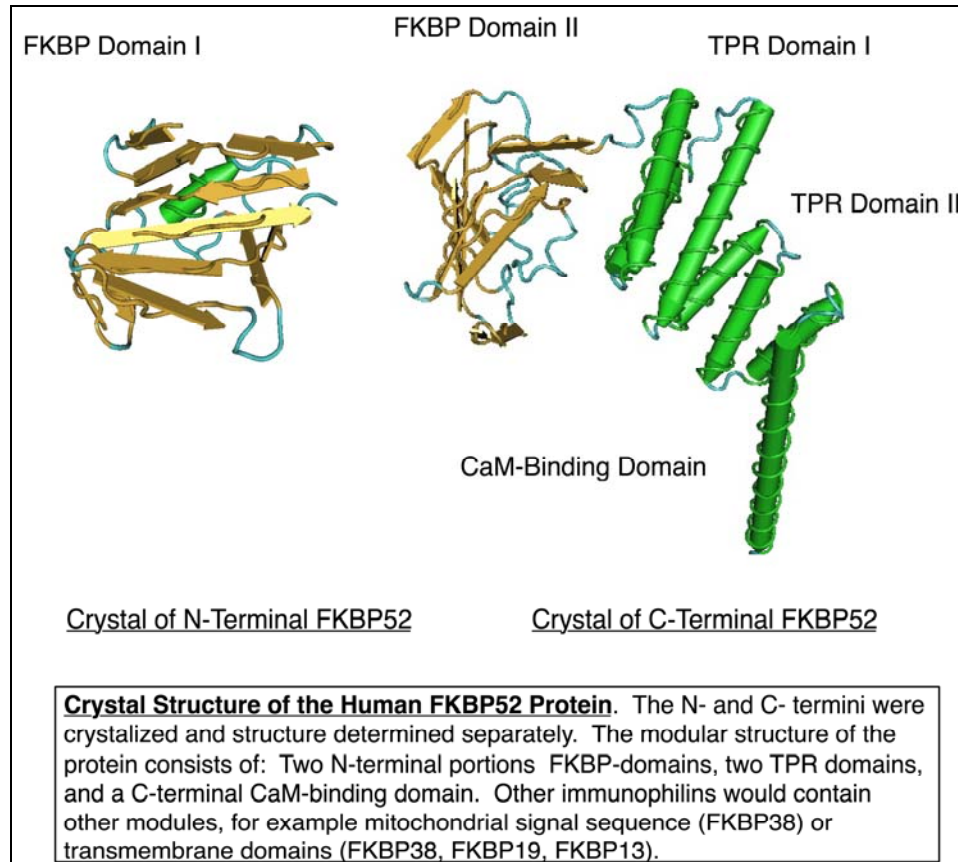


**Figure 2-1. Crystal structure of the Human FKBP52 Protein Depicting FKBP-Binding Domains, TPR Domains, and CaM-Binding Domain. Sample large molecular immunophilin FKBP52 showing modular domains of two FK506-Binding Protein (FKBP) Domains, tetratricopeptide repeat (TPR) domains, and C-terminal calmodulin (CaM) binding domains.**

**Table 2-1. Summary Information for the Human Immunophilin - FK506 Binding Proteins.** The thirteen immunophilin genes are shown with summaries of function, cell compartment. For reference, PubMed Gene identification is given with key citations on structure and function. Modular structures are listed to illustrate genetic expansion of FKBP genes and divergence of function. FK506 Binding domain (FKB), TM (transmembrane), TPR (tetratricopeptide repeat), CaM-BD (calmodulin binding domain), Efh (E-F hand).

Table 2-1. Summary Information for Human Immunophilin – FK506 Binding Proteins.

FKBP	PubMed GeneID	Molec Weight (kD)	Brain Level	Cell Compartment	Modular Structure	Function	Citation
<i>FKBP1A</i>	2280	12	high	Cytoplasm	1X FKB	Protein Folding and Trafficking, Ca mobilization Intracellular signalling modulation	[67-71]
<i>FKBP1B</i>	2281	12.6	low	Cytoplasm	1X FKB	Protein Folding and Trafficking, Ca Mobilization	[72, 73]
<i>FKBP2</i>	2286	13	moderate	ER membrane	1X FKB 1XTM	ER Chaperone	[74, 75]
<i>FKBP3</i>	2287	25	low	Nuclear	2X FKB	Transcription Cofactor, Protein trafficking	[76-78]
<i>FKBP4</i>	2288	52 or 59	high	Cytoplasm	3X FKB 3X TPR	Hormone Receptor Trafficking	[45, 79-82]
<i>FKBP5</i>	2289	51	high	Cytoplasm	3X FKB 1X TPR 1X CaM-BD	Hormone Receptor Modulation and Trafficking	[63, 79, 81]
<i>FKBP6</i>	8468	36	none	Nuclear	1X FKB 1X TPR	Mitosis, Chromosome Segregation	[83, 84]
<i>FKBP7</i>	14231	23	low	ER	1X FKB 2X Efh	ER Chaperone	[85]
<i>FKBP8</i>	23770	38	moderate	ER - Mt memb	1X FKB 2XTPR 1X TM	Protein Trafficking, Apoptosis, Ca Signaling, Proteasome	[86-91]
<i>FKBP9</i>	11328	63	moderate	ER	4XFKBP 2XEFh	ER Chaperone	
<i>FKBP10</i>	60681	65	none	ER	4XFKB 2XEFh	ER Chaperone	[92, 93]
<i>FKBP11</i>	51303	19	none	ER membrane	1X FKBP 1XTM	Protein Folding	[94, 95]
<i>FKBP14</i>	55033	22	none	ER	1X FKB 2XEFh	ER Chaperone	[96, 97]

### 2.3.1.1 Amino Acid Sequence Analysis of Three Immunophilin Proteins

Comparison of amino acid sequences of proteins over evolutionary history tell much about biochemical niches. For example, the amino acid sequences of histones remained quite constant from early eukaryotes to complex mammals [98]. While the biochemical milieu of cells expands with gene-duplications and modular formation of new proteins, the diversity of proteins expands

as mutations are selected for or against. Since other authors showed that immunophilin genes comprise a class of genes undergoing fast evolution [59], we sought to compare homologous proteins to the immunophilins FKBP52 and FKBP51. The analysis provided insight into the comparison between humans and recent ancestors.

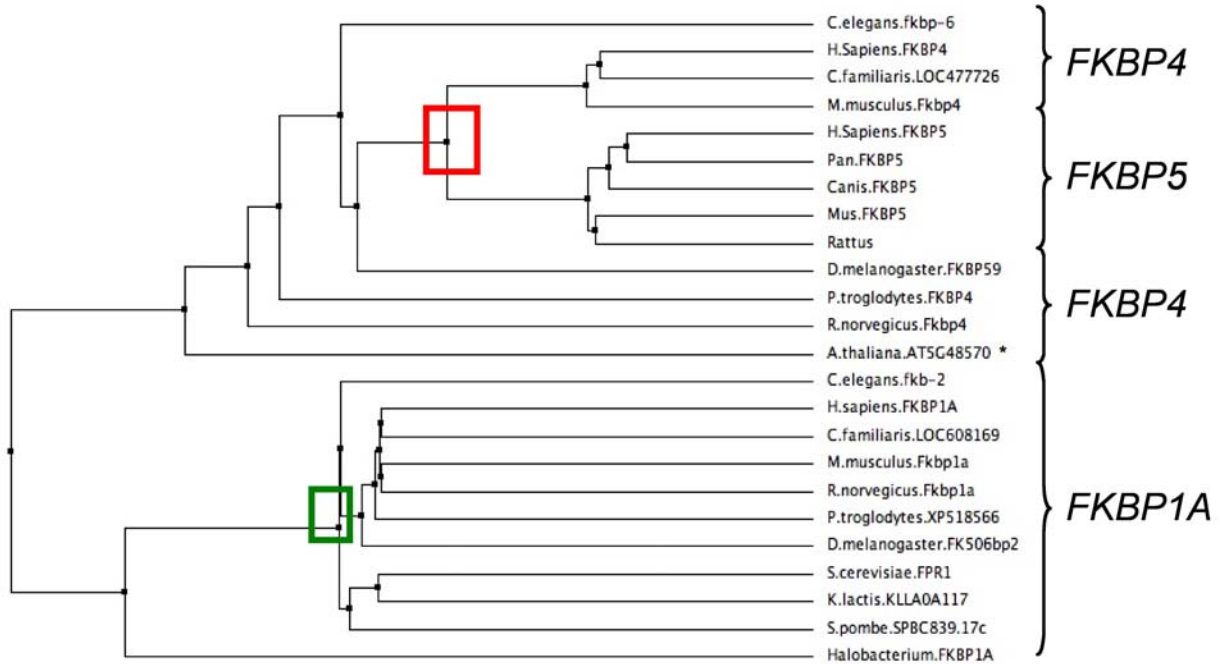


**Figure 2-2. Cross-Phyla Cladogram of *FKBP4*, *FKBP5*, and *FKBP1A* Analogues. In order to identify homologous proteins in various species for the immunophilins FKBP51, FKBP52, and FKBP12, the *Homologene* database available online through the National Center for Biological Informatics and the National Library of Medicine was used. The cladogram was constructed using the JalView Java Alignment Editor, the amino acid sequences of identified homologous proteins were sorted using the ClustalW Multiple Sequence Alignment algorithm and the tree was constructed using the Neighbor Joining Using Percent Identity algorithm [99]. The NCBI Accession numbers are as follows (from top to bottom of the tree): NP\_508026.1, NP\_002005, XP\_534923.1, NP\_34349.1,**

NP\_004108.1, XP\_001172411.1, XP\_538880.2, NP\_0334350.1, NP\_001012174.1, NP\_524895.2, XP\_508927.2, XP\_342764.3, NP\_189160.3, NP\_001021722.1, NP\_000792.1, NP\_032045.1, XP\_001053006.1, XP\_001167897.1, NP\_523792.2, NP\_014264.1, AB028739.

In Figure 2-2, the horizontal distance between nodes corresponds to sequence similarity of homologues. The large distances between those of the higher molecular weight immunophilins, *FKBP4* and *FKBP5*, indicate fast genetic divergence throughout evolution, particularly among vertebrates, compared to the amino acid sequence for the FKBP12 protein (green box). There exists a plant homologue for FKBP52 in *Arabidopsis thaliana* (\*), and the distance between it and the node for animals is shorter than that between *Pan troglodytes* and *Homo sapiens*, indicating that among mammals, this gene has changed to occupy different biochemical niches, perhaps to be cell-, tissue-, or organism-specific. Interestingly, the FKBP51 clade falls *within* the FKBP52 clade (red box), indicating its recent emergence and high similarity with FKBP52. Since FKBP51 is a modulator for the hormone-receptor chaperone function of FKBP52, this phenomenon suggests a recent emergence of the capacity to modulate hormone function and introduce a higher level of complexity for increasingly complex organisms. With regard to function in the nervous system, this represents at least one pinpoint of difference between humans and recent ancestors.

### **2.3.2 FK506 Binding Protein Biochemical Properties**

The FKBP domain consists of a single  $\alpha$ -helix with five  $\beta$ -pleated sheets, the last sheet being interrupted by a turn, and the whole structure resembling a miniature “beta barrel” [100]. A loose

consensus sequence for the target proteins is the hydrophobic side chains of the leucine-leucine-proline sequence [101]. The active site of the FKBP domain, which performs the isomerase function, is a hydrophobic pocket deep in the middle of the barrel and the conserved residues necessary for activity are not continuous but located on different  $\beta$ -sheets and facing inside the pocket [102]. The crystal structure of FKBP12 with FK506 bound is illustrated in Figure 2-3, the prolyl isomerase active site is highlighted in yellow of the ribbon structure, and color coded for hydrophobicity in the three-dimensional structure [102]. Active-site residues are non-continuous and come together inside the hydrophobic pocket [100]. This is important because the mechanism of

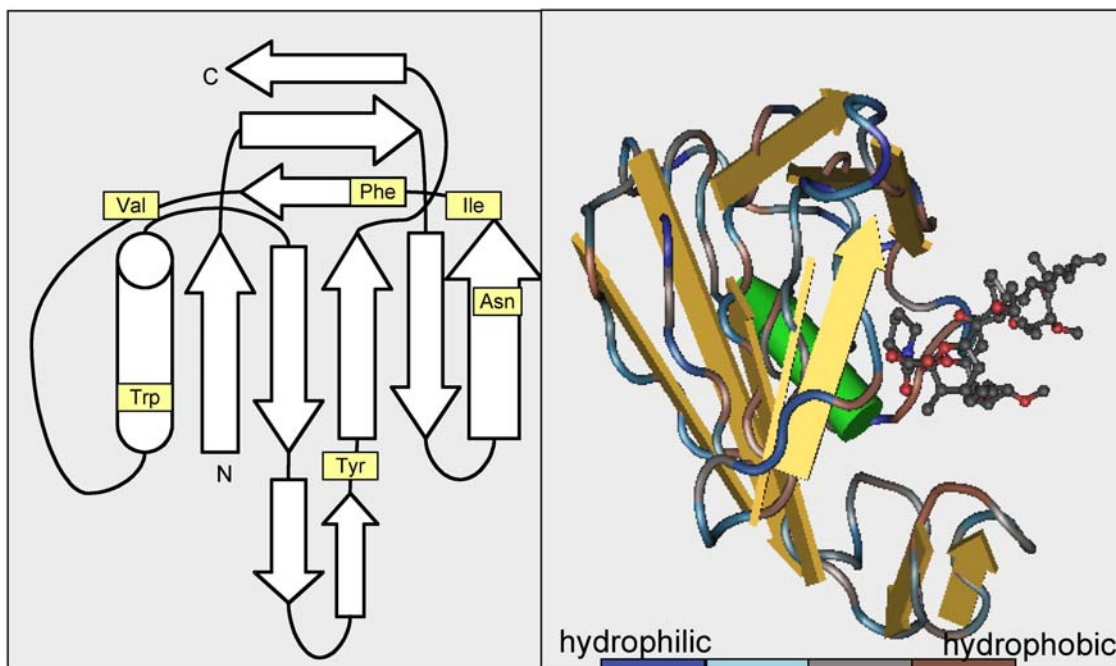


**Figure 2-3. Ribbon Diagram and 3-D Structure of FKBP12 With FK506 Bound. The prolyl isomerase active site is highlighted in yellow of the ribbon structure, and color coded for hydrophobicity in the three-dimensional structure [102]. Active-site residues are non-continuous and come together inside the hydrophobic pocket [100].**

the isomerase enzymatic activity is to lower the polarity of the microenvironment surrounding the substrate proline allowing for twisting of the proline residue about the backbone of the target protein [103] [6]. Any substitution that would increase the polarity of the active site would cause loss of isomerase function, but not necessarily loss of binding (due to the high hydrophobicity of the pocket), which would imply that natural competitive inhibitors could easily evolve by substitution mutation, or that chaperone function may be “allowed” to be independent of isomerase activity. Indeed, this is the case with the *FKBP4/FKBP5* interaction discussed below, and may explain why pharmacologic ligands that bind the active pocket do not necessarily inhibit interaction of the target proteins. This is an important point to consider for the mechanism of drug interactions. Binding of small organic molecule ligands (like FK506) to the active site of the FKBP domain may simply lower the polarity of the microenvironment, and increase the energy of dissociation of the hydrophobic pocket of the FKBP domain from the substrate proline on the target proteins. For example CaN (CaN) is a target of FKBP12 normally, and the presence of FK506 causes FKBP12 to bind irreversibly and permanently inhibit the phosphatase activity of CaN [54, 104, 105]. A molecule that inhibits the FKBP-to-target interaction would have to bind the hydrophobic pocket of the FKBP domain, but have polar moieties further away, sufficient to “repel” the non-polar substrate region of the target protein.

### **2.3.3 Immunophilin Ligands**

Endogenous small molecule ligands as cofactors have not yet been identified for FKBP's, though it is possible that they exist. In a few diverse systems, small molecules like amino acid threonine, nitric oxide, glutathione, ATP, and GTP have been identified to regulate some signal transduction modulation pathways by cytoplasmic FKBP's that are of high abundance in the

brain [106]; a general mechanism by which these are thought to function is shown in Figure 2-5. In yeast, FKBP12 is shown to control methionine and aspartate metabolic flux [107]. The synthesis of methionine/serine/threonine in yeast follows a pathway beginning with the phosphorylation of aspartate by aspartokinase. The phosphorylation of aspartate by aspartokinase is feedback-inhibited by the end-product, threonine, which binds in the active site but is not phosphorylated. The feedback inhibition is facilitated by FKBP12, and in fact, without FKBP12, toxic amounts of metabolic intermediates accumulate if downstream enzymes are also mutated [108]. The precise molecular mechanism of the modulation is unknown, though it could be that FKBP12 stabilizes the inactive form of aspartokinase, potentially holding the inhibitory threonine in place [108]. The immunophilin FKBP52 binds ATP and GTP in the FKB-Domain II, which is isomerase-inactive owing to a phenylalanine to tryptophan (increasing polarity) amino acid substitution [45, 106]. The physiologic function of FKBP52 with regard to hormone receptor signaling is discussed below. Whether ATP/GTP binding has a biologic consequence on these functions is unknown, though it is tempting to speculate that ATP/GTP binding could be another level of hormone signaling modulation.

Aracena et al (2005) showed that S-nitrosylation of the ryanodine receptor (RyR) causes decreased affinity of FKBP12, increasing the activity of the calcium channel, leading to a model whereby NO selectively increases ryanodine receptor sensitivity to  $\text{Ca}^{2+}$  activation due to s-nitrosylation-induced decrease in the interaction of the channel with FKBP12 [109]. Figure 2-4 illustrates how FKBP12 modulates function of the RyR, in which the closed conformation is favored with FKBP12 bound, therefore upon ryanodine binding and opening of the channel, if FKBP12 is bound, the time spent open is shorter, allowing less  $\text{Ca}^{2+}$  through. This is an example of the general mechanism for FKBP-mediated signal transduction modulation

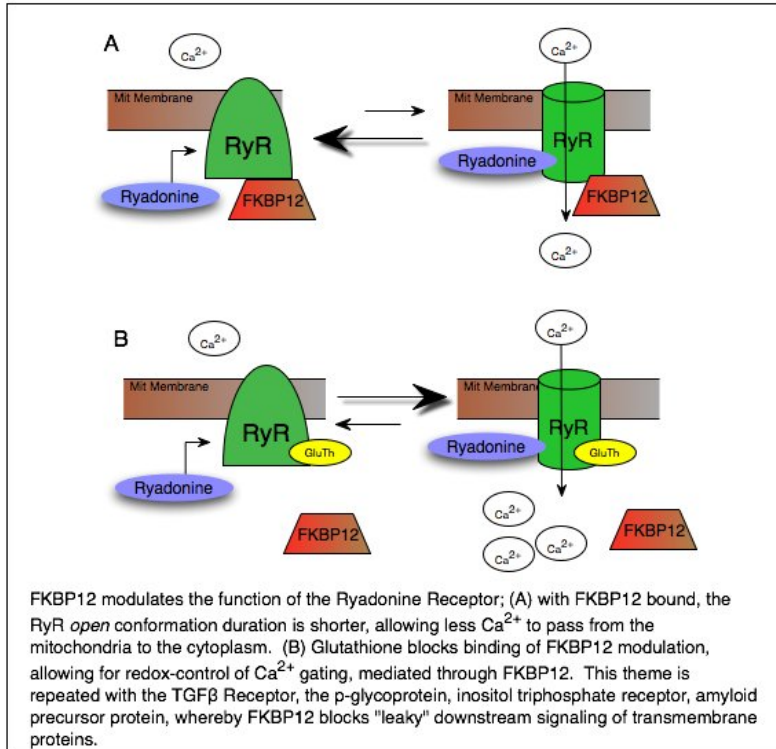


**Figure 2-4. FKBP12 Modulates Function of the Ryadonine Receptor (A) with FKBP12 bound, the RyR open conformation duration is shorter, allowing less  $\text{Ca}^{2+}$  to pass from the mitochondria to the cytoplasm, large arrow pushing equilibrium toward left in (A). (B) Glutathione blocks binding of FKBP12 and its modulation, allow for redox-control of  $\text{Ca}^{2+}$  gating mediated through FKBP12, larger arrow pushing equilibrium toward right in (B).**

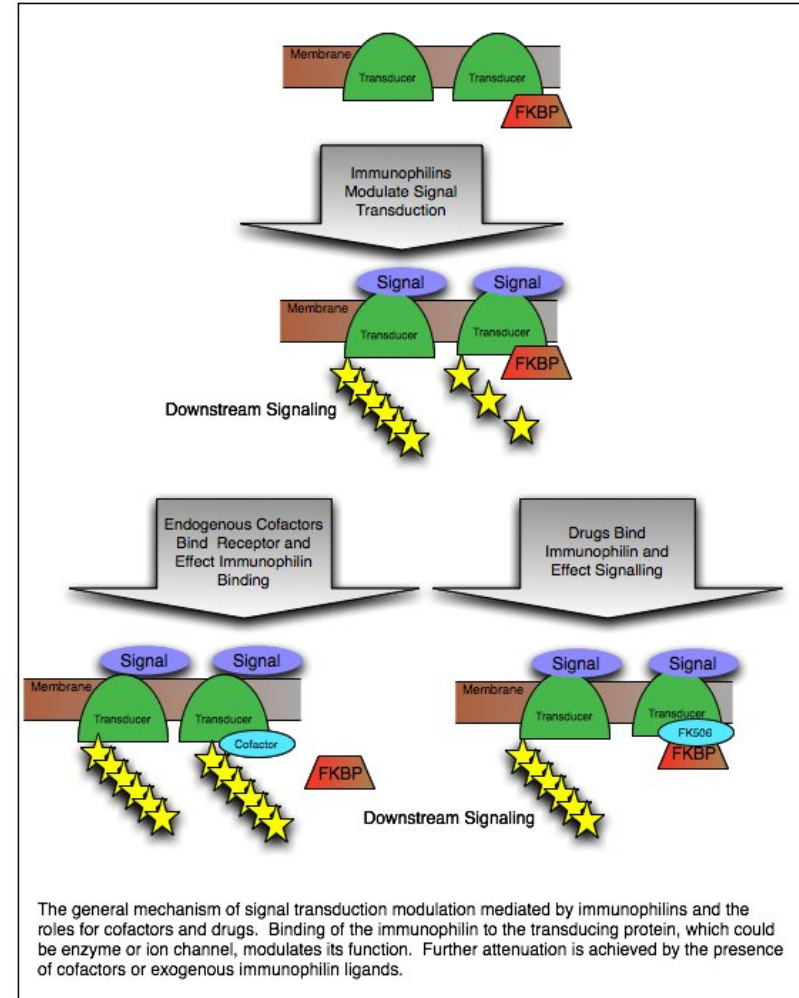


**Figure 2-5. The Mechanism of Signal Transduction Modulation Mediated By Immunophilins and the roles for cofactors and drugs. Binding of the immunophilin to the transducing protein**

**(top), which could be an enzyme or ion channel, modulates its function (middle). Further attenuation is achieved by the presence of cofactors or exogenous immunophilin ligands (bottom). Stars indicate downstream signaling.**

whereby the immunophilin acts as an accessory to transmembrane proteins, which is shown in Figure 2-5.

Finally, binding of glutathione to the ryanodine receptor causes increased affinity of FKBP12 and homologous protein FKBP12.6 to the channel, decreasing its “open” state, indicating redox regulation of the ryanodine receptor facilitated by FKBP12/12.6 [73, 109]. Furthermore, there is evidence that glutathione binds the RyR at the FKBP12-binding site [73, 109]. This interaction is reminiscent of the FKBP12-FK506-CaN interaction. In the pharmacologic (FK506) interaction, the molecule binds the immunophilin, but in natural instances, it is the protein target that is modified by small molecules which changes immunophilin-binding affinity. In the context of neurons, this may be of importance because the redox conditions are unusual, there are neurotransmitters, cofactors, and ion gradients present in neurons that are different from other systems that have been characterized (for example cardiac muscle cells or lymphocytes). Figure 2-5 highlights the general proposed mechanisms that were outlined here by which immunophilins modulate signal transduction, as well as the role for drugs like FK506, rapamycin, or GPI1046 and endogenous cofactors like NO or glutathione. Further study of mechanisms of immunophilin function in the biochemical milieu of neurons and neuronal sub-types (eg. dopaminergic, glutamergic, GABA-ergic) may uncover interesting interactions of importance to neural function and survival.

#### **2.4 FK506 BINDING PROTEINS IN PROTEIN FOLDING AND TRAFFICKING**

Because proline isomerization can be a rate-limiting step in the synthesis and proper folding of proteins, it was originally hypothesized that the main function of FKBP's would be as molecular

chaperones, assisting in general protein folding. This was found to not entirely be the case. The immunophilin domain is promiscuous with regard to its binding and isomerase activity. In large molecular weight FKBP's, specificity is conferred by the other functional modules and subcellular localization. For example, FKBP52 and -51 interact with androgen and GR complexes in all tissues (including the brain) through the TPR domains [110]. FKBP38 interacts with Bcl through its immunophilin domain and shuttles it from the Golgi to mitochondria via FKBP38's C-terminal signal sequence. The low molecular weight immunophilins (FKBP12, -12.6, -13) interact with a wide range of proteins and bind with varying degrees of affinity. The FKBP's localized in the lumen of the ER bind  $Ca^{2+}$  and have general chaperone function to facilitate folding of many proteins, but the ER-localized FKBP's are not substantially expressed in the brain and we will exclude them from our discussion [74, 75, 111]. Cytosolic immunophilins are involved in the trafficking of hormone complexes, folding of soluble proteins, trafficking and stabilization of transmembrane proteins; the involvement of these interactions in the context of brain function is poorly understood, but once could apply the modulation-function of immunophilins to specific cellular processes and extrapolate the cellular processes to neuronal and brain functions.

#### **2.4.1 FKBP12 As Accessory to Transmembrane Proteins**

The archetypal immunophilin, FKBP12, is involved in the stabilization of a number of membrane-bound proteins including TGF $\beta$ -Receptor, ryadonine receptor, inositol triphosphate receptor [69, 112-116]. An intriguing interaction that has received little attention in neuroscience is the FKBP12 to p-glycoprotein interaction. P-glycoproteins (PGP), components of multi-drug resistance genes (MDR), also called ABC (ATP binding cassette); are key functional components of the MDR3 system in the blood-brain barrier [117]. The PGPs and relatives form

an important transmembrane transport system that pumps xenobiotics and other molecules that had passed into brain capillary endothelial cells back into the blood; preventing the passage of undesirable molecules from blood into the brain and also ridding the brain of endogenously produced toxins [118]. There is currently an immense amount of study on the blood-brain barrier and its role in neurodegeneration, CNS infection, acute brain injury, and pharmacokinetics. Studies of PGP and FKBP's have been published in non-mammalian cellular systems such as *Saccharomyces* and *Arabidopsis* [119]. The major theme is that function of the PGP is dependent upon an FKBP. In *Arabidopsis*, it is the immunophilin AtFKBP42, and yeast, it is the *FKBP1A* orthologue called *fpr1* (yeast do not express the high molecular weight immunophilins).

In drug sensitive yeast, FKBP12 was shown to be necessary for function of p-glycoprotein and proper function of MDR3 at the plasma membrane [119]. In an FKBP12-null strain, PGP-mediated drug resistance is severely compromised, but transfection with both wild-type and mutant FKBP12 lacking isomerase activity restores PGP function. An MDR3-FKBP12 complex has not been detected by coprecipitation or affinity chromatography, so the interaction may be indirect or transient or the detection-methods may have been insufficient or the interaction does not occur in mammalian cells [119]. The p-glycoprotein is a 12-pass transmembrane protein synthesized at the rough ER membrane and trafficked through the trans-Golgi to be expressed at the cell surface. The authors speculated that hydrophobic residues of FKBP12 may allow proper folding of the cytosolic portions of the p-glycoprotein as it folds to be a functionally mature protein expressed at the plasma membrane [119]. Hemenway and Heitman (1996) specifically addressed and excluded roles for CaN and cyclophilin A in p-glycoprotein function [119]. Some studies on the effects of FK506 and its binding proteins operated under the assumption that all FKBP12 effects are mediated through the inhibition of CaN, but this is shown not to be the case here and elsewhere.

In *Arabidopsis*, the immunophilin involved in MDR function is a large molecular weight and transmembrane FKBP, AtFKBP42 [120]. This protein has homology with both human FKBP52 (*FKBP4*) and FKBP38 (*FKBP8*) [121]. It resembles FKBP52 in general domain architecture of having N-terminal FKBP, three TPR domains, and a calmodulin-binding domain (CaM-BD). Like FKBP38, AtFKBP42 contains a transmembrane C-terminus, but is located at the plasma membrane (while FKBP38 is located at cytosolic leaflet of the outer mitochondrial membrane) [121] [120]. The AtFKBP42 protein was originally discovered in the dwarf mutant *uca* (ultracurvata) [122]. This mutant displayed dwarfed stems and a developmental defect caused by hyperactive signaling of a plant steroid, auxin, due to dysfunctional MDR complex [122]. The AtFKBP42-to-MDR interaction has been mapped to the segment of the MDR protein (called AtPGP1) harboring the second ATP-binding cassette. Weiergraber et al (2006) speculate that binding of AtFKBP42 might regulate access of ATP to the MDR or facilitate its ATPase activity [121]. This interaction, if applicable to the MDR genes that function in the mammalian blood brain barrier, would be pertinent to brain pathologies associated with function of the blood brain barrier as well as pharmacokinetics of drugs intended to act in the CNS. It remains to be elucidated however, whether any of the cytosolic immunophilins play a real-life in vivo role in the blood brain barrier, though the molecular evidence points to [119, 121, 123] facilitative role to the function of the p-glycoproteins [124].

Both cyclosporine A and FK506 are known to inhibit the p-glycoprotein and confer drug sensitivity to cancer cells expressing the p-glycoprotein. One study determined that pharmacologic suppression of peptide-prolyl isomerase and CaN activities were not responsible for the inhibition of p-glycoprotein function [123]. They conclude that the FK506 and cyclosporine A – inhibition of p-glycoprotein must be independent of isomerase activity and CaN function. These results are in-line with the yeast genetic results whereby mutant FKBP12 was isomerase-inactive and yet still restored MDR function [119]. However, the mammalian

FKBP-repertoire is larger than the yeast's and chaperone activity on the MDR may be mediated by cytosolic immunophilins other than FKBP12. It would be interesting to see whether, which, and how immunophilins regulate the function of the MDR at the blood brain barrier.

The simplest protein of the immunophilin family, FKBP12 may have the largest variety of protein targets. It binds to and influences the function of intracellular calcium channels, TGF $\beta$  receptor, and CaN [54, 104, 105, 112, 114]. A recent report of preliminary data showed that FKBP12 interacts with the intracellular domain of the amyloid precursor protein (APP) and that the interaction is inhibited competitively by the neurotrophic ligand FK506 [125]. Further studies are underway to determine the specific effect of FKBP12-binding to the intracellular domain of APP. The general theme of FKBP12 function is to prevent aberrant signaling or to stabilize transmembrane proteins. Determining whether FKBP12 influences cleavage of APP by the proteolytic enzymes  $\beta$ - and  $\gamma$ - secretases would show a direct role for FKBP12 in the pathogenesis of Alzheimer's Disease. The observed upregulation of FKBP12 in Alzheimer's Disease may be an attempt by neurons to modulate APP cleavage in an as yet-undetermined fashion [8, 126].

#### **2.4.2 FKBP12 and Soluble Protein Targets**

FKBP12 was shown to accelerate the aggregation of  $\alpha$ -synuclein in vitro [71]. The role of  $\alpha$ -synuclein in neuroprotection and neurodegeneration is reviewed extensively in Sidhu et al (2004) [127].  $\alpha$ -Synuclein has emerged as a central player in the pathophysiology of dopaminergic degeneration among other forms of neurodegeneration, the term "synucleinopathy" was invented and propagated from this role [128-130]. Though the wild-type normal function of  $\alpha$ -synuclein may be to regulate dopamine content and synaptic tone in dopaminergic neurons, the inherent hydrophobicity of the  $\alpha$ -synuclein lends its susceptibility to form oligomers in solution. The

soluble oligomers of  $\alpha$ -synuclein may be toxic to neurons by disrupting the synaptic vesicle packaging and trafficking machinery as well as the protein trafficking and recycling systems of neurons; particularly at the synapse, locations at significant distances from the cell bodies. Removal of oligomeric  $\alpha$ -synuclein from solution by forming insoluble aggregates may be cytoprotective to the neurons because in aggregated form, it cannot interact with the cellular vesicle and protein trafficking and recycling machinery [127]. Although  $\alpha$ -synuclein does not have the Leu-Leu-Pro sequence that is loosely the consensus binding sequence for FKBP12, it does contain a number of prolines and hydrophobic stretches. Gerard et al showed that fibril formation of  $\alpha$ -synuclein is accelerated by FKBP12 in an enzymatic fashion that is blocked by isomerase inhibition [71]. Figure 2-6 illustrates a possible pathway showing  $\alpha$ -synuclein associated with vesicles, perhaps regulating synaptic tone, and FKBP12 promoting aggregate formation. The physiologic significance of this action remains to be seen, but it is a very interesting observation that would link the protein folding / chaperone function of FKBP12 directly to a phenomenon observed frequently in  $\alpha$ -synucleinopathies.

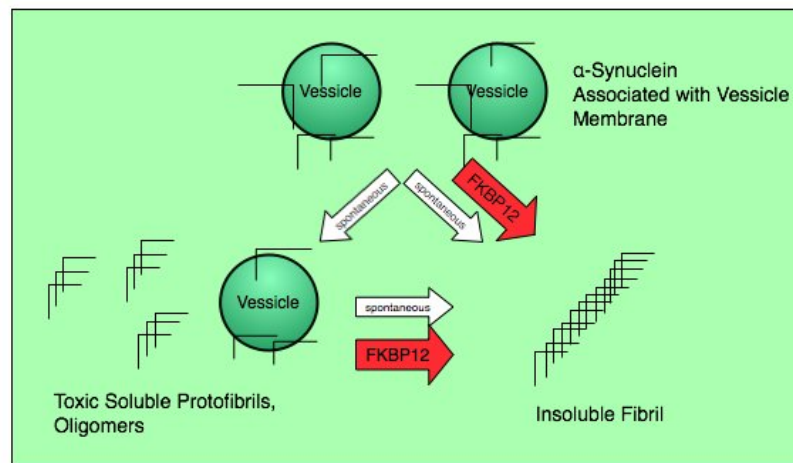


**Figure 2-6. Model that FKBP12 Accelerates Fibril Formation of  $\alpha$ -Synuclein in an Enzymatic Fashion. FKBP12 causes insoluble fibril formation of  $\alpha$ -synuclein in an enzymatic fashion. It is thought**

**formation of insoluble fibrils is protective to protein processing machinery from insoluble  $\alpha$ -synuclein protofibrils.**

### **2.4.3 FKBP52/59 and Hormone Receptor Activation**

The gene product of FKBP4 is an immunophilin of 52 kD and 59 kD, and there is no known functional difference between the two forms. Both were shown to bind to the molecular motor dynein through the FKBP domain I. Dynein is a retrograde molecular motor that shuttles protein or vesicle cargo retrograde along microtubules. FKBP52 colocalizes with microtubules, binds specifically to dynein by its N-terminal prolyl isomerase domain, and its enzymatic activity is required for this interaction [131-134]. FKBP52 was determined to be the same protein as “HSP56” that co-immunoprecipitates with the glucocorticoid receptor (GR) / HSP90 complex. Hormone activation and nuclear translocation of the GR is dependent on the FKBP52 binding through its TPR domain and by N-terminal isomerase activity on dynein [110] and we illustrate this function in Figure 2-7. The relevance of GR signaling in neurons has been demonstrated and it is hypothesized that expedited nuclear translocation is important in specialized mammalian cells like neurons, where the traveling distance may be long [14]. The FKBP52 knockout mouse displays decreased prostate development, malformed seminal vesicles, and reproductive abnormalities that correlate to decreased androgen levels or inadequate androgen receptor (AR) response [135-137]. Loss of FKBP51 appears to be neutral with respect to developmental control by AR, although the double-knockout *FKBP5-/FKBP4-* is perinatal lethal [135]. Hormone-induced reporter activity of AR is increased with FKBP52 overexpression and decreased with FKBP52 knock-down by siRNA [137]. Since the AR also binds other chaperone molecules that promote ubiquitination and degradation, it is hypothesized that the presence of FKBP52 or the activities of other co-chaperones will influence whether the AR is degraded or functional.

Certain species of New World primates have general resistance to glucocorticoids. Since they do in fact express the GR, which binds to cortisol, the mechanism of the resistance was puzzling. It was found that a soluble cytosolic factor, FKBP51, from the cytosol of monkey lymphocytes inhibits binding of cortisol to GR [61]. Furthermore, FKBP51 expression is 13-fold higher in these primates, and that FKBP52 expression less than one-half compared to humans; effectively rendering them resistant to the GR-mediated effects of cortisol [138] [139]. Firstly, differences in the amino acid sequences in the protein regions linking the immunophilin domains to the TPR domains is highly variable comparing human to monkey [61]. Secondly, the promoter regions may be different, the monkey gene may have more constitutive promoters elements and the human may have more inducible promoter elements, a thorough genetic analysis could determine this. FKBP51 does not have a functional isomerase domain and acts as a competitive inhibitor of FKBP52 in the context of GR signaling [63, 82]. Figure 2-7 illustrates the molecular mechanism of GR-modulation by immunophilins, the cell may control its “competency” to respond to cortisol by its expression levels of FKBP51 and FKBP52. An analysis of the amino acid sequences of the FKBP52 and FKBP51 genes in Figure 2-1 showed relatively recent emergence of the FKBP51 protein, and in fact, the FKBP51 clade falls within the FKBP52 clade. This finding suggests that FKBP51 and FKBP52 are closely related, and that FKBP52 must have environmental pressure for divergence. With these proteins, the environment is the cell, and the differing pressures may be differing chaperoning needs.

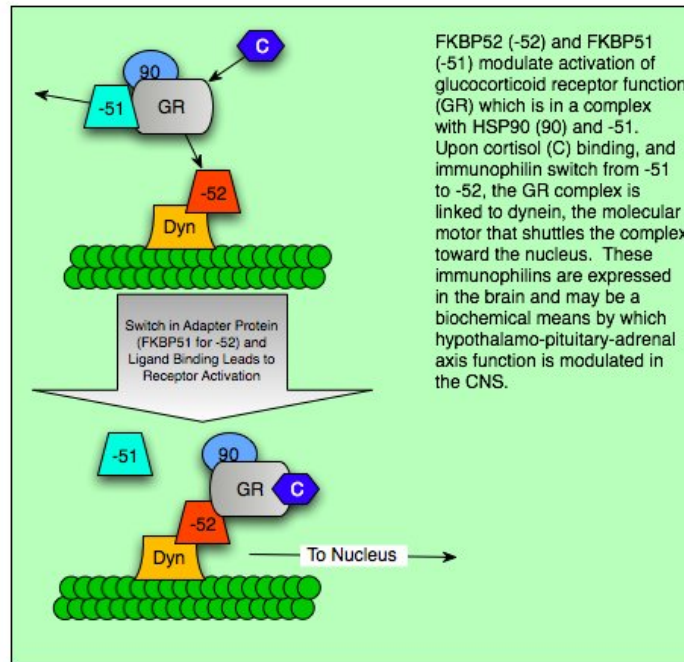


**Figure 2-7. FKBP52 and FKBP51 Modulate Activation of Glucocorticoid Receptor (GR).** The GR is in complex with HSP90 (90) and FKBP51 (-51). Upon cortisol (C) binding, an immunophilin switch from -51 to FKBP52 (-52). Through -52, the GR complex is linked to the molecular motor protein dynein, shuttling it toward the nucleus. This interaction may be important in large cells with extensive microtubule polymers, extensive endoplasmic reticulum networks where diffusion may be limited. These immunophilins -51 and -52 are expressed in the brain, as shown in Figure 1-1 and in large pyramidal neurons shown in Section 3.3.5.

Recent studies of the molecular properties of FKBP51 and FKBP52 found that they differentially regulate dynein interaction with GR in mammalian cells [79]. FKBP52 facilitates the interaction of GR with dynein, and thus the shuttling of the activated receptor to the nucleus, where GR-steroid action can take place [131]. FKBP51 inhibits this interaction and GR-steroid complexes cannot carry out its effects on gene transcription [14]. This activator/inhibitor interplay would be particularly important in cells where the distance between the receptor and the nucleus is long, such as neurons. Since the steroid receptor and its coactivator and inhibitor are highly expressed in regions of the brain that are affected by excessive cortisol in depression, these immunophilins may play a role in the molecular basis and pathogenesis of stress-related

mental illnesses such as late-life depression, major depressive disorder, and post-traumatic stress disorder.

A genome-wide scan determined that single nucleotide polymorphisms (SNP's) are linked to unipolar depression in the gene encoding FKBP51 (gene ID *FKBP5*) [140, 141]. The specific molecular consequences of these SNP's are not known [142]. This study linked polymorphisms in *FKBP5* gene to increased recurrence of depressive episodes and rapid response to drugs. The authors identified two polymorphisms that affect FKBP51 protein levels in the blood, but not the mRNA levels. The group also identified functional polymorphisms in the GR gene that associate with different responsiveness to the dexamethasone-suppression-test after treatment for depression [143].

As previously mentioned, the involvement of immunophilins FKBP52 and FKBP51 in brain pathologies is tightly related to HPA axis function and the role that glucocorticoids would play in brain function or dysfunction. A widely accepted model of the role of HPA axis dysregulation leading to MDD is that chronic glucocorticoid signaling in neurons renders them vulnerable to degeneration leading to decreased volume of brain structures such as the hippocampus [144]. The decreased volume is not necessarily due to neuronal loss per se, but rather reduction in the size of neurons and their synaptic and dendritic fields [11, 145].

While this model may be accurate, we still know little about the molecular events that occur in neurons making them “vulnerable” to GR activity. Furthermore, although some neural populations are identified as particularly susceptible to cortisol-induced vulnerability (for example the CA1 and CA3 fields of the hippocampus), no molecular mechanism explains how this occurs (for review of aging, stress, and the hippocampus, see Miller, 2005) [43, 144, 146, 147]. The glucocorticoid-cascade hypothesis first put forward by Sapolsky postulates a feed-forward mechanism of decreased feedback inhibition with increased sensitivity of the brain to

cortisol [13, 17]. With aging and stress over time, long-term exposure to cortisol restrains the ability of the hypothalamus to downregulate secretion of corticotropin-release hormone after a stressor [148]. While the levels of circulating cortisol may not increase with age, older animals show a longer recovery time from stress-induced cortisol surges than younger ones [149]. The longer duration of elevated cortisol also causes a unresponsiveness to the feed-back inhibition loop, further exacerbating the problem. The regulation of protein trafficking by the interplay of FKBP52 and FKBP51 with the GR and dynein complex may be critically important to changes in the brain caused by chronic stress.

*FKBP4* and *FKBP5* genes are expressed in the cortex and particularly enriched in CA1 and CA3 regions of the hippocampus, as well as the thalamus and cerebellum of the mouse. GR expression is also enriched in these regions; it would be interesting to determine whether expression of *FKBP4* or *FKBP5* is altered in these regions during disease-state.

## **2.5 EMERGING ROLES FOR FKBP38 IN NEURAL CELL FUNCTION AND DEVELOPMENT**

### **2.5.1 FKBP38 and Apoptosis**

The gene product of *FKBP8* is FKBP38 and it consists of an N-terminal immunophilin domain, three TPR domains, followed by a C-terminal CaM-BD. The immunophilin domain lacks specific aromatic residues that are essential for FK506 binding and its rotamase activity must be activated. Additionally, FKBP38 contains a mitochondrial signal sequence. Like *FKBP4*, the *FKBP8* gene has a CCAAT box and two Sp-1 binding sites in the promoter region. Also similar to *FKBP4*, the protein product has regulatory function through its capacity to facilitate protein trafficking. It is expressed in the forebrain and at particularly high levels in the hippocampus

[150]. An *FKBP8*-promoter region in a  $\beta$ -galactosidase reporter showed that the *FKBP8* gene contains a specific forebrain promoter, the protein is involved in neurodevelopment, apoptosis (see Figure 2-8), and proteasomal function [151].

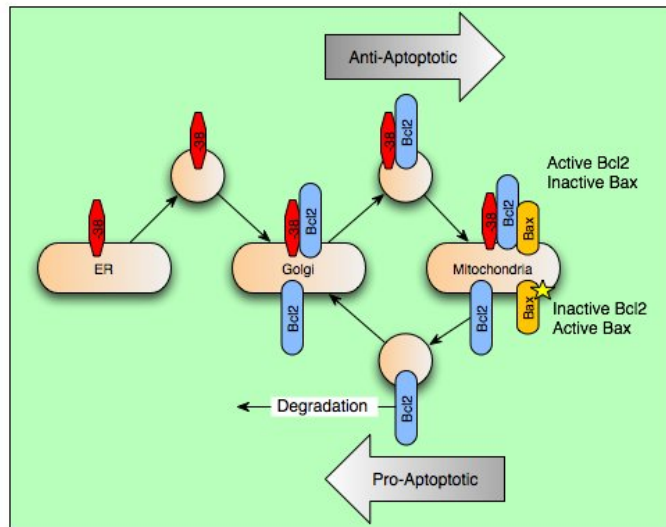


**Figure 2-8. FKBP38 Regulates Apoptosis Through Its Protein-Trafficking Function of Bcl2.**

**FKBP38 (-38) has a weak mitochondrial signal sequence as transmembrane region, with the functional domain on the cytoplasmic side. FKBP38 can be present on the outer mitochondrial membrane or the Golgi apparatus, its subcellular localization may be altered by posttranslational modification like phosphorylation or association with CaM. The protein Bcl2 is anti-apoptotic by inactivating Bax. Bcl2's association with -38 stabilizes Bcl2; and when -38 is either returned to the Golgi or degraded, Bcl2 becomes inactive or is degraded; and Bax activates apoptosis.**

FKBP38 is thought to play a major role in the neurotrophic and neuroprotective properties of immunophilin ligands FK506 and GPI-1046. The mechanism underlying FKBP38-mediated neuroprotection is a current topic of study and debate and may be related to its interactions with Bcl2. In Figure 2-8, the antiapoptotic role for FKBP38 by means of protein trafficking is illustrated. An antiapoptotic protein, Bcl2 localizes to the ER, Golgi, and mitochondria. Its presence in the mitochondria suppresses apoptosis in a variety of ways: preventing release of

proteases and caspases, regulating  $\text{Ca}^{2+}$  homeostasis, and neutralizing death effector properties of Bax.

It was initially believed that FKBP38 was an inherent inhibitor of CaN; it was hypothesized that the binding site of the FKBP12/FK506 complex was structurally similar to the FKBP38 binding site and that FKBP38 itself was an endogenous inhibitor of CaN [90]. This was found to be partly true. FKBP38 does not have inherent isomerase activity, but is activated only in the presence of  $\text{Ca}^{2+}$  at concentrations found intracellularly after  $\text{Ca}^{2+}$  bursts and in complex with calmodulin (CaM) [89]. FKBP38 is only enzymatically active and only binds to CaN when complexed with  $\text{Ca}^{2+}$ /CaM. The phosphatase CaN was shown to bind to Bcl2 in a maltose-binding-protein and amylose column system and FKBP38/Ca/CaM interrupted the interaction. This effect is abolished in the presence of the neuroprotective immunophilin ligand GPI 1046. One mechanism of neuroprotection may be that the immunophilin ligand prevents the FKBP38/Ca/CaM complex from interrupting the Bcl2/CaN interaction and there is less cytosolic CaN and potentially more dephosphorylated Bcl2. Bcl2 is shown to be dephosphorylated by PP2A and interacts with CaN in neuronal tissue [152, 153]. Interestingly, when activated by  $\text{Ca}^{2+}$ /CaM, FKBP38 increases the solubility of Bcl2 [154].

The physiologic function of the Bcl2/FKBP38 interaction may be cell-specific. In yeast L40 and human embryonic kidney (HEK)-293 cells, FKBP38 was observed to associate with Bcl2 directly and target Bcl2 to mitochondria. In SH-SY5Y cells, FKBP38 was found to only interact with Bcl2 in the presence of the  $\text{Ca}^{2+}$ /CaM complex [87, 155]. It was observed that: 1. phosphorylated Bcl2 localizes primarily to the ER, 2. phosphorylated Bcl2 has lower affinity for FKBP38, 3. cells depleted in FKBP38 have a switch from mitochondrial to ER localization of Bcl2 [156]. It is believed that FKBP38 may somehow mediate post-translational modifications of Bcl2 in its large unstructured loop by direct binding to this loop [154, 157]. Ubiquitination and phosphorylation regulate the stability, activity, or localization of Bcl2 and diverse stimuli cause

these modifications [158, 159]. It would be interesting to determine whether FKBP38-modulates ubiquitination of Bcl2, which then changes in response to excitation, neurotoxin, neuronal stressors, or neuronal growth factors. Presenilins –1 and –2 were shown to bind to FKBP38 and inhibit its interaction with Bcl-2 [88]. Familial Alzheimer’s disease – linked mutations in Presenilins 1 and 2 cause enhanced inhibition of FKBP38 activity; this may be important for the anti-apoptotic role of Bcl-2 as well as the function of the proteasome as described below.

## **2.5.2 FKBP38 and the Proteasome**

Of particular interest to the study of molecular pathology of Parkinson’s and Alzheimer’s Diseases, FKBP38 was recently shown to bind to components of the 26S proteasome and localize it to the cytosolic leaflet of the mitochondrial membrane similar to its role in shuttling Bcl-2 to the mitochondrial membrane. The 26S proteasome is present in the cytoplasm and nucleus. In the cytoplasm, the proteasome is associated with different organelles to fulfill compartment-specific functions. Nakayama (2007) presents evidence that FKBP38 tethers the proteasome to the mitochondrial membrane, increasing the amount and activity of the proteasome [91]. Since a yeast orthologue to the S4 subunit, called Rpt2, is responsible for gating of the 20S proteasome, it may be that FKBP38 modulates gating in addition to serving as an adapter protein for trafficking [160].

The ubiquitin-oxproteasome system is important to neurodegenerative diseases like Alzheimer’s and Parkinson’s diseases as well as synaptic homeostasis (see Ross, 2004 and Hegde, 2002 for reviews [161-163]). Since mitochondria are present in high numbers near the synapse and important for maintaining a healthy synapse as an energy supply, FKBP38 may play a role in maintaining synaptic integrity by serving as a link between mitochondria and the ubiquitin-proteasome system [164]. The degradation and clearance of poly-ubiquitinated

proteins is vital to function of the synapse at which there are high amounts of membrane and membrane-bound proteins, 20% of the surface area of the average synaptic vesicle is actually occupied by membrane-bound proteins [165]. The effects of depletion or inhibition of FKBP38 on the synapse is unknown, but the data suggest that FKBP38 would be important for maintaining synaptic homeostasis by facilitating the function of the proteasome and allowing for healthy clearance of poly-ubiquitinated proteins and preventing toxic accumulation of proteins targeted for proteolytic degradation.

### **2.5.3 FKBP38 and Neurodevelopment**

With respect to neurodevelopment, FKBP38 is also shown to be an important factor for dorsoventral patterning of the central nervous system. A mouse knockout of FKBP38 resulted in ventralization of the developing neural tube. In other words, in development of the neural tube, the markers for the ventral components were expanded (e.g. *Foxa2*), there was defective dorsoventral patterning, and the most-dorsal neural tube markers (e.g. *WNT1*) were absent. The authors showed that loss of the *FKBP8* gene caused ligand-independent activation of sonic hedgehog pathway and conclude that FKBP38 is required to suppress sonic hedgehog signaling in neural tissue [166]. The molecular mechanism is as yet unknown but the phenomenon seems to be specific to neural tissues. Exaggerated sonic hedgehog signaling in humans leads to a variety of diseases including holoprosencephaly and cancers of the skin and brain and is reviewed by Nieuwenhuis and Hui (2005); it remains to be seen if perhaps loss FKBP38 function could be a factor in these conditions [167].

## 2.6 CONCLUSION

The immunophilins represent a family of proteins with diverse functions and mechanisms throughout many different species and even many different tissues in a given organism. Many biochemical, bioinformatics, and genetic studies have discovered a wide array of functions ranging from stabilization of calcium release channels, modulation of p-glycoprotein, influencing apoptosis, hormone receptor signaling, and many more. These molecular functions have specific roles in pathogenesis in the central nervous system. Although the specific and direct links between Immunophilin → Target Protein → Molecular Basis of Disease have not yet been uncovered, the wide range of studies from various systems covering many biochemical pathways seem to be converging toward that goal. Since small molecule ligands are already developed that bind to immunophilins, modulate their functions, cross the blood brain barrier, and are approved for clinical use in another context the immunophilins FKBP12, FKBP12.1, FKBP38, FKBP51, and FKBP52 may be prime pharmacologic targets for a host of neurodegenerative conditions. Furthermore, since the cellular and brain-regional distribution of immunophilins is altered in neurodegeneration, the immunophilins and their ligands may serve as good diagnostic or imaging tools in the future. The field is very close to linking the diverse molecular functions outlined here to the biochemical milieu of neurons and the brain. The human brain is exceedingly complex and uniquely susceptible to loss of homeostasis leading to neurodegeneration, discoveries about the functions of immunophilins, that may be specifically adapted with increased brain complexity, may lead to insights regarding the pathogenesis of neurodegeneration.

### **3.0 EXPRESSION OF IMMUNOPHILINS FKBP52 AND FKBP51 IS INCREASED IN FRONTAL CORTEX OF HIV<sup>+</sup> PATIENTS AND DIFFERENTIALLY EXPRESSED IN DEPRESSION**

Patients infected with HIV have a higher risk of developing MDD than the population at large. This may be due a biological effect related to chronic viral infection in the brain. Immunophilins FKBP52 and FKBP51 are expressed in cortical neurons and differentially regulate the function of the GR. Previous reports have shown genetic variants in the gene encoding FKBP51 called *FKBP5* are linked to unipolar depression, to traumatic dissociation, and to response to drugs; however these findings are controversial and the genetic link was not found in a subsequent study. We sought to determine whether immunophilins are upregulated in the frontal cortex during HIV infection by comparison of protein and gene expression in an HIV cohort. Furthermore, in order to determine whether the interplay between FKBP52 and FKBP51 plays a role in depression, we compared protein and gene expression in the frontal cortex of patients with and without MDD who were or were not infected with HIV. We found an upregulation of both immunophilins in HIV infected brain. In MDD, *FKBP5* is upregulated. In the HIV<sup>+</sup> population with MDD, *FKBP5* is highly variable, and *FKBP4* is significantly upregulated compared to controls.

### 3.1 INTRODUCTION

Immunophilins are a class of chaperone and adapter proteins that are widely expressed in most tissues, but particularly highly expressed in the brain, predominantly in neurons [1, 168]. FKBP52 and FKBP51 are the products of the *FKBP4* and *FKBP5* genes, respectively. FKBP52 functions as an adapter protein in the GR -HSP90 complex that links the hormone-bound receptor complex to the molecular motor dynein, allowing for shuttling of the activated receptor complex to the nucleus [79]. In contrast to FKBP52, the FK506-binding domain of FKBP51 lacks isomerase function, but is shown to bind the GR through the tetratricopeptide repeat domains and therefore functions as a competitive inhibitor to formation of the GR-FKBP52-dynein complex [61, 138]. Sapolsky's glucocorticoid-cascade hypothesis proposes a feed-forward mechanism of decreased feedback inhibition with increased sensitivity of the brain to cortisol. The action of the GR in the brain may be central to the molecular mechanism whereby the HPA axis feedback loop is dysregulated in the hypercortisolemia observed in depression [13, 149]. Therefore, the modulation of GR signaling in the cortex may be a site of regulation that could affect the susceptibility of neurons to lose synaptic and dendritic density, which is found in hypercortisolemia and depression [11, 169].

A genome-wide scan identified single nucleotide polymorphisms (SNP's) linked to unipolar depression in the *FKBP5* gene [140]. The specific molecular consequences of these SNP's are not known. Polymorphisms were linked to increased recurrence of depressive episodes and rapid response to drugs. The authors identified two polymorphisms that link to decreased FKBP51 protein levels in the blood. The same polymorphisms in *FKBP5* were linked with peritraumatic dissociation in traumatically injured children, who had been victims of a

motor vehicle accident or assault [141]. A subsequent study failed to definitively assign the designated SNP's association with monopolar depression or affective disorder [142]. However, *FKBP5* may play a role only in some depression cases, with other genes involved in the glucocorticoid system responsible for disturbances of the HPA-axis during depressive episodes.

Since the frequency of MDD is significantly elevated in people with HIV infection [19, 20, 170, 171], we sought to determine whether there was a relationship between HIV infection, MDD, and the expression of immunophilins in the frontal cortex. Neuropathologically, in MDD there is reduced cortical glial density as well as dendritic and synaptic simplification. Our lab previously showed an increase, in deep grey matter, of the related protein FKBP12, which we hypothesize to be a protective response for the basal ganglia [19, 20, 170, 171]. Our study here shows an increase in FKBP51 and FKBP52 in HIV, however expression of *FKBP5* is not significantly higher in HIV<sup>+</sup> individuals with MDD.

## **3.2 MATERIALS AND METHODS**

### **3.2.1 Demographic Information and Analysis**

Fresh frozen tissue was kindly donated by the Stanley Foundation and the California NeuroAIDS Tissue Network. Standard universal precaution following University of San Diego California Environmental Health and Safety procedures was observed in handling fresh frozen tissue, including personal protective wear consisting of goggles, lab coats, double latex gloves. Also engineering designs using covered bucket centrifuges, biosafety cabinet, and sealed and covered biohazard waste and sharps containers. Personnel attended laboratory safety training in blood born pathogens and chemical hygiene. Twelve cases from each group were studied with an age range of 24-63. The cases were divided into five study groups: control, MDD, MDD with psychosis

(MDDP<sub>sync</sub>), HIV<sup>+</sup>, and HIV<sup>+</sup> with MDD (see Table 1). The cause of death in the control group was mainly cardiac arrest, while the depressed groups cause of death was predominantly suicide. The cause of death for the two HIV groups was not recorded by the CNTN, nor was brain pH, general scizophrenia is the only disease where pH is routinely ascertained. The postmortem interval (PMI) was generally within 24 hours (the average in the CNTN cohort approximately 12 hours and approximately 35 hours from the Stanley Foundation cohort). For RNA and protein analysis, slices were cut from the frontal cortex, included all cortical layers, and care was taken to avoid meninges.

**Table 3-1. Demographic Description of Patients in Study**

Patient ID	Age	Sex	PMI	pH	Cause of Death
Control					
1	48	M	12	6.51	CARDIAC
2	24	M	17	6.6	MVA
3	50	F	35	6.31	CARDIAC
4	44	M	27	6.82	AC ALCOH POIS
5	35	M	31	6.59	MVA
6	63	M	40	6.91	CARDIAC
7	50	M	11	6.5	CARDIAC
8	63	M	37	6.5	CARDIAC
9	34	M	9	6.56	MVA
10	56	F	29	6.78	CARDIAC
11	56	F	31	6.66	OBESITY
12	39	F	24	6.88	CARDIAC
Means	46.8	8M, 4F	25.3	6.64	
MDD					
13	32	F	19	6.8	SUIC
14	47	F	25	6.88	SUIC
15	56	M	38	6.59	SUIC
16	33	M	25	6.86	SUIC
17	45	F	29	6.9	CARDIAC
18	24	M	21	6.61	SUIC
19	56	F	15	6.59	BURNS
20	44	M	24	6.52	CARDIAC
21	34	M	24	6.79	SUIC
22	53	M	21	6.64	CARDIAC
23	45	M	29	6.75	SUIC
24	45	F	13	6.58	SUIC
Means	42.8	7M, 5F	23.6	6.71	
MDD Psychosis					
25	48	F	24	6.36	SUIC
26	40	M	52	6.48	OD
27	28	M	26	6.7	SUIC
28	28	F	40	6.68	SUIC
29	62	M	65	6.57	SUIC
30	28	F	40	6.68	SUIC
31	32	F	19	6.7	SUIC
32	63	M	31	6.6	SUIC
33	51	F	36	6.3	UNKNOWN
34	40	F	49	6.72	SUIC
35	35	M	36	6.6	SUIC
36	36	F	32	6.74	PULM EMBOL
Means	41.5	5M, 7F	35.8	6.59	

Patient ID	Age	Sex	PMI	pH	Cause of Death
HIV+					
38	45	M	12		
39	57	M	12		
40	35	M	5		
41	55	M	5		
42	57	M	12		
43	54	M	12		
44	49	M	10		
45	37	F	1		
46	40	M	10		
47	47	F	12		
48	46	M	12		
Mean	46.6	9M, 2F	8.8		
HIV+ MDD					
49	43	M	12		
50	43	M	31		
51	34	M	10		
52	55	M	120		
53	59	M	12		
54	54	M	11		
55	35	M	10		
56	38	M	7		
57	38	M	10		
58	39	M	12		
59	34	M	4		
Mean	44.7	12M, 0F	15.2		

Possible confounding variables to a human postmortem study that would affect the results are taken into consideration. They are: age, brain pH, postmortem interval (PMI, or time elapsed between death and autopsy). Gene expression of the genes of interest, *FKBP4* and *FKBP5*, could correlate to these variables and tests for linear correlation were performed and are illustrated in Figures 3-1, 3-2, and 3-3. Since gene expression is calculated as  $\text{Fold-Change} = 2^{-\Delta\Delta\text{CT}}$ , a value of 0.5 corresponds to a two-fold decrease, therefore, a  $\text{Log}_2$  scale for the y-axis is used so that 0.5 and 2 are equidistant from baseline; regression analyses for correlation account for this. Expression was plotted versus age, PMI, and brain pH and Pearson's Test for Correlation was performed and nonlinear ( $\text{Log}_2 y = m x + b$  where  $m$  is the slope and  $b$  is the y intercept) regressions are plotted in Figures 3-1, 3-2, and 3-3. For all three characteristics, there were no correlations with gene expression,  $R^2 < 0.50$ .

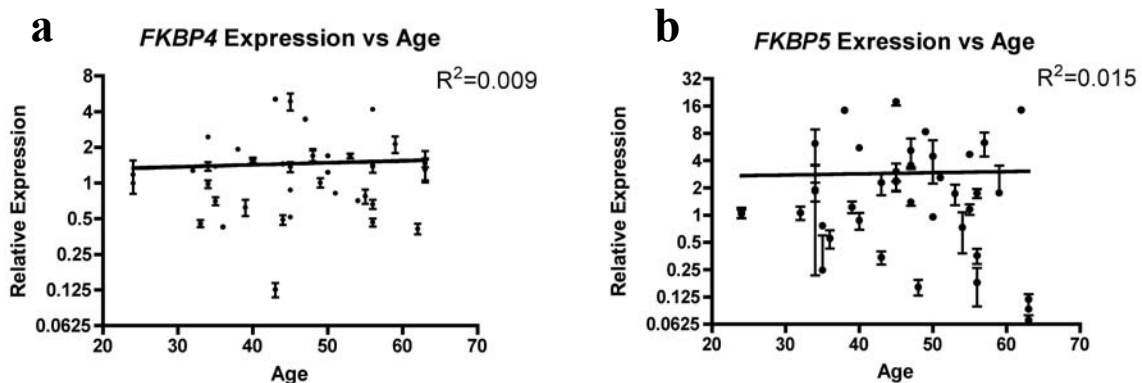


**Figure 3-1. Age Does Not Correlate With Gene Expression of *FKBP4* (A) or *FKBP5* (B).** Gene expression from cortical grey matter all the patients listed in Table 3-1 is determined by qPCR using the  $\Delta\Delta\text{CT}$  method and normalizing the gene of interest to *GAPDH* expression as explained in Section 3.2.3. Fold-Control is plotted versus age. Linear regression shows no correlation for either gene with Age.

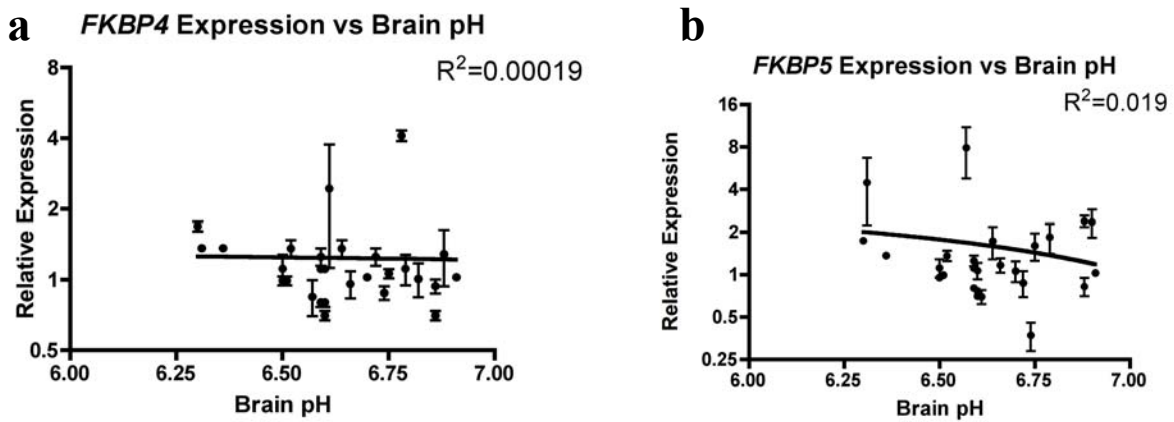


Figure 3-2. Brain pH Does Not Correlate With Gene Expression of *FKBP4* (A) or *FKBP5* (B). Gene expression from cortical grey matter of patients listed in Table 3-1 for whom brain pH data were available is determined by qPCR using the  $\Delta\Delta$ CT method and normalizing the gene of interest to *GAPDH* expression as explained in Section 3.2.3. Fold-Control is plotted versus Brain pH. Linear regression shows no correlation for either gene with Brain pH.

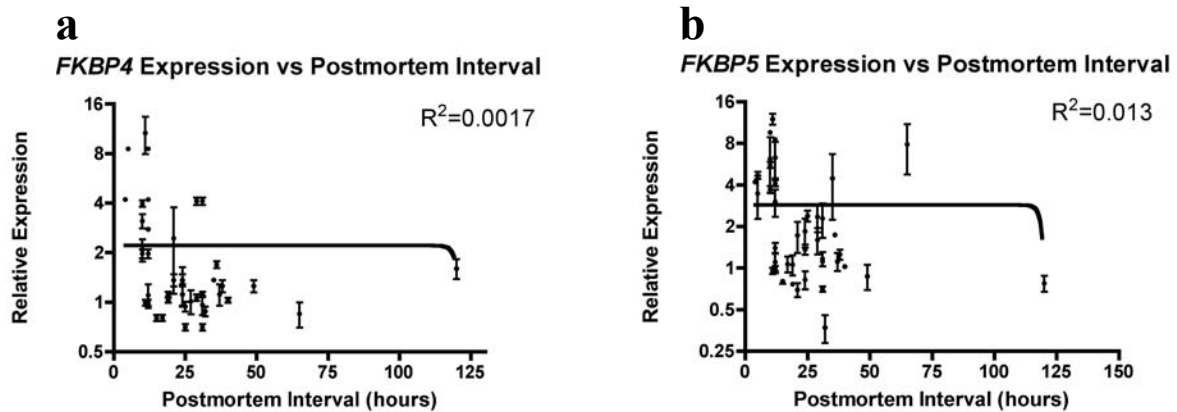


Figure 3-3. Postmortem Interval (PMI) Does Not Correlate With Gene Expression of *FKBP4* (A) or *FKBP5* (B). Gene expression from cortical grey matter of patients listed in Table 3-1 is determined by qPCR using the  $\Delta\Delta$ CT method and normalizing the gene of interest to *GAPDH* expression as explained in Section 3.2.3. Fold-Control is plotted versus PMI. Linear regression shows no correlation for either gene with PMI.

In examining Table 3-1, one can see that the HIV<sup>+</sup> specimens obtained from the CNTN had more males, and this is shown by Chi-square analysis in Table 3-2. The HIV-negative groups obtained from the Stanley Foundation had stastically indistinguishable male:female compositions, Table 3-3. T-tests comparing expression in non-HIV males to expression in non-HIV females of the two immunophilin genes found no difference between the sexes with respect to immunophilin expression, which are plotted in Figure 3-4, showing 95% confidence intervals interquartile ranges. Since there was no difference between male and female expression of *FKBP4* ( $p = 0.179$ ) and *FKBP5* ( $p=0.716$ ), sex is unlikely to be a confounder to the analysis. No other study known to the authors has assessed gene expression in the brain of *FKBP4* or *FKBP5* or that age, PMI, sex, brain pH correlate to gene expression. One study showed expression of *FKBP5* in peripheral blood mononuclear cells correlating to blood plasma cortisol levels in a specific subpopulation of patients who are homozygous for the T allele at locus rs1360780, which is a polymorphism analyzed in this work (Materials Section 3.2.5 and Results Section 3.3.3) [140].

**Table 3-2. Sex composition of study groups by HIV status. Chi-square analysis indicates there are significantly more males in the HIV groups ( $p=0.006$ ) than non-HIV groups.**

	NonHIV	HIV	$\chi^2$ $p$
Male	21	21	<b>0.006</b>
Female	15	2	

**Table 3-3. Sex composition of nonHIV groups by diagnosis. The sex composition is balanced in the non-HIV groups by mental diagnosis ( $p=0.709$ ).**

	Control	MDD	MDD/Psyc	$\chi^2$ $p$
Male	8	7	6	0.709
Female	4	5	6	

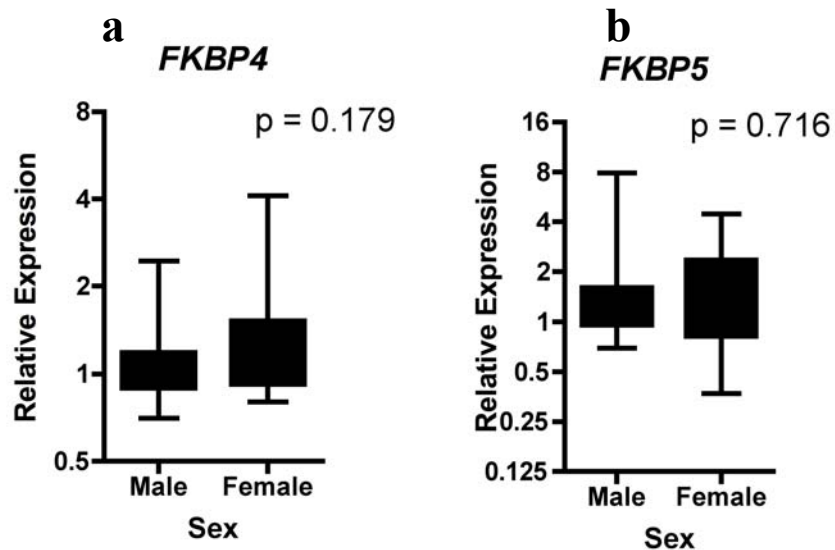


Figure 3-4. Expression of *FKBP4* (A) and *FKBP5* (B) is the same in male and female. Gene expression from cortical grey matter of patients listed in Table 3-1 is determined by qPCR using the  $\Delta\Delta\text{CT}$  method and normalizing the gene of interest to *GAPDH* expression as explained in Section 3.2.3. Non-HIV patients are divided into male and female groups and Fold-Control plotted, illustrated is a box-and-whisker plot showing the standard deviation about the mean in the box and the interquartile range in the whiskers. Student's t test comparing male versus female expression showed no significant difference based on sex for expression of *FKBP4*  $p = 0.179$  (A) or *FKBP5* (B)  $p = 0.716$ .

### 3.2.2 FKBP52 and FKBP51 Protein Determination

One hundred mg tissue was cut and homogenized in 0.9 mL ice-cold lysis buffer consisting of 50 mM Tris-HCl, 1% sodium dodecyl sulfate, 150 mM NaCl, 1 mM EDTA, 1 mM phenylmethylsulfonyl fluoride, 1  $\mu\text{g}/\text{mL}$  aprotinin, 1 mM  $\text{Na}_3\text{VO}_4$ , pH 7.4. 50  $\mu\text{g}$  of total protein from each case was electrophoresed in 10% polyacrylamide gels and transferred to polyvinylidene fluoride (PVDF) membranes. Western blotting analysis for immunophilins

FKBP52 and FKBP51 was performed using Mouse anti FKBP52 (Stressgen SRA1400) at 1:5000, and rabbit (Rb) anti FKBP51 (Abcam ab2901) at 1:1000 and primary antibody was incubated overnight, shaking, 4°C. Secondary antibodies were horseradish peroxidase conjugated donkey (Dk) anti Mouse and Dk anti Rb, respectively, at 1:5000, purchased from Jackson Immunoresearch. The chemiluminescence signal was developed according to manufacturer's protocols (Perkin Elmer NEL103001) and quantitated using densitometric analysis with Image J software, the detailed steps are expounded on in Appendix A, changes are expressed as Fold-Actin, and Normalized Fold-Actin.

### **3.2.3 *FKBP4* and *FKBP5* Gene Expression Determination**

For RNA isolation, 100 mg of tissue was cut and homogenized in ice cold TRIzol reagent (Invitrogen) and by following manufacturer's instructions. RNA quality was assessed by spectrophotometry, whereby A260/A280, absorbances at 260 nm and 2680 nm were measured, an A260/A280 ration greater than or equal to 1.8, downstream analysis is only performed when this criterion was met. cDNA synthesis was performed using 1ug of RNA using the SuperScript III kit from Invitrogen. For quantitative PCR, 40ng cDNA per reaction was used and 20X prevalidated fluorescently-labeled (using carboxyfluorescence, 5-FAM) probes were purchased from Applied Biosystems. For *FKBP5*, assay Hs00188025\_m1; for *FKBP4*, assay Hs00427038\_g1; and for *GAPDH*, assay Hs02758991\_g was used. TaqMan master mix (2X) purchased from Applied Biosystems was used in 20µL reactions on 96 well-plates and assays were performed at the University of San Diego Center for AIDS Research Genomics Core. Gene expression is reported as fold-control versus the median of the control-group using the  $\Delta\Delta$ -CT method comparing to housekeeping gene *GAPDH* whereby  $\Delta\text{CT} = \text{CT}_{\text{GAPDH}} - \text{CT}_{\text{Gene}}$ ,  $\Delta\Delta\text{CT} = \Delta\text{CT}_{\text{Control}} - \Delta\text{CT}_{\text{Disease}}$ , and  $\text{Fold-Control} = 2^{-\Delta\Delta\text{CT}}$ . A test for normality showed that not all

groups are distributed in a Gaussian curve, therefore non-parametric statistical analyses were performed, which included Kruskal Wallace Rank Sums test and Dunn's Multiple Comparison to compare the groups.

### **3.2.4 HIV-Induced In Vitro Changes in *FKBP4* and *FKBP5* Transcript**

To test the hypothesis that neuronal exposure to HIV leads to increased immunophilin expression, we utilized the neuroblastoma cell line, SH-SY5Y, after differentiation, exposed to supernatant from primary human microglia infected with HIV-BaL. HIV-BaL is a macrophage-tropic (m-tropic) HIV-1 strain (Catalogue Number 11446 of the NIH AIDS Research and Reference Reagent Program, Bethesda, MD), obtained through the Center for AIDS Research at the University of California San Diego (La Jolla, CA). SH-SY5Y cells were plated at  $5 \times 10^5$  cells/well in six-well plates coated with laminin by incubating with 2  $\mu\text{g/mL}$  laminin in  $\text{H}_2\text{O}$  (Sigma L2020) overnight at 37°C. SH-SY5Y cells were grown in media composed of 1:1 mixture of Ham's F-12 Media (Gibco 31765-035) and DMEM (Gibco 11960-044) supplemented with glutamate, sodium bicarbonate (Gibco 25080-094), pyruvate (Gibco P333-1000), and 10% fetal bovine serum (Gibco 16140-071). After three days in culture, 80% confluency, the media were supplemented with 1  $\mu\text{g/mL}$  retinoic acid for differentiation; media were changed daily until cells showed neuritic networks, typically 3-5 days. Microglia were obtained from primary human fetal CNS tissue and grown in DMEM, 10% fetal bovine serum, 25 mM HEPES buffer (Gibco 15630-130), 1 mM L-glutamine (Gibco 21051-024) at 37°C 5%  $\text{CO}_2$  for two weeks and exposed to HIV. HIV was propagated in microglial for seven weeks, with media changes every three days. Supernatant was stored at -20°C and viral production was assessed by quantitation of the viral capsid protein, p24, by using ELISA (Perkin Elmer NEK050B001KT), a reliable method for monitoring viral production clinically [172]. Appendix B shows the p24

concentrations during the viral propagation. After differentiation of SH-SY5Y cells, media were changed, and cultures were supplemented with 10% HIV-infected microglia supernatant. Four conditions were assessed: Media alone, Day 15 HIV<sup>-</sup>Microglia supernatant, Day 15 HIV<sup>+</sup>Microglia supernatant, and Day 0 HIV<sup>+</sup>Microglia supernatant. The “Days” correspond to the days-of-infection of the microglia. Media exposed to virus and pipette tips exposed to said media were treated in a 10% aqueous bleach solution prior to disposal. Quantitative real-time polymerase chain reaction (qPCR) for *FKBP4* and *FKBP5* was performed as described in Section 3.2.3.

### **3.2.5 *FKBP5* Genotyping of Patient Cohort**

Genotyping of previously published alleles of the *FKBP5* gene, implicated in mood disorders, was performed. Genomic DNA from the patients was isolated from the tissue following manufacturer’s instructions using the DNeasy kit (Qiagen #69504). Genotyping was performed using 20ng DNA following manufacturer’s protocols of the SNP Genotyping Assay from Applied Biosystems: an A/C substitution in the 3’ untranslated region of *FKBP5* gene, SNP rs3800373, (Applied Biosystems Assay ID C\_27489960\_10) and a C/T substitution in Intron 1 of the *FKBP5* gene, SNP rs1360780 (Applied Biosystems Assay ID C\_8852038\_10). A five by three table was constructed of the possible genotypes with the five test-groups and Chi Square analysis compared the expected genotype frequencies with the actual frequencies observed. Expected frequencies are determined by genotype frequency in North American Caucasian population deposited in NCBI SNP database; for rs3800373 record ID ss2334697 and for rs1360780 record ID ss4777328 were used [173]. Because the published genotype frequencies were used in for a Caucasian population, non-caucasians were removed from our patient panel

for genotyping analysis. Two by five tables were constructed. Allelic frequencies and Chi-square analysis compared the expected versus observed frequencies.

### **3.2.6 Immunohistochemistry**

Paraffin embedded tissue from the frontal cortex of the patients described above were provided by the CNTN. In order to ascertain which cortical layers and cells in the brain expressed the immunophilins, 14 µm sections were immunolabeled for FKBP52 and FKBP51. Sections were incubated overnight at 50°C and deparaffinized in Citrisolve (2X 5 min), and rehydrated by serial incubation in 100%, 90%, 70% ethanol in water, and then washed in PBS with 0.2% Tween-20 followed by antigen unmasking by incubation in 10 mM sodium citrate pH 6.4 on high setting, 125°C and 15 pounds per square inch, in a pressure cooker for 10 min. Endogenous peroxidases were blocked in 0.3% H<sub>2</sub>O<sub>2</sub> in methanol. Following blocking in 10% normal donkey serum (NDS), primary antibody was incubated overnight at 4°C in PBS-T with 5% NDS. Antibodies: Mo anti FKBP52 (Stressgen #SRA-1400, 1:200), Rb anti FKBP51 (Novus NB300-519, 1:100). After washing 3X5 min in PBST, secondary antibody was incubated 2hr at room temperature (Dk anti Rb and Dk anti Mouse – HRP conjugated). Staining was visualized following manufacturer's instructions with Nova Red (Vector Laboratories) and sections were counterlabeled by immersion in Meyer's Haematoxylin for 5 min.

### 3.3 RESULTS

#### 3.3.1 Protein Analysis

The Western blots illustrated in Figure 3-5 and Figure 3-7 showed a wide variation in expression of both immunophilin proteins in the Control group, Patients 1-12 in blue, indicating that expression varies in the population at large, and likely is dependent on many physiologic factors. Plots showing Fold-Actin calculated by densitometric analysis, whose detailed analyses are described in Appendix A, are illustrated to the right of the immunoblots. Since exposure levels were different among the blots, in order to compare across all patients and all groups from the five immunoblots on one graph, the Fold-Actin values were normalized to the average Control-value on a particular immunoblot, and is illustrated in Figure 3-6, the blue bar indicates the standard deviation about the mean of the Control Group ( $1.056 \pm 0.3641$ ). FKBP52 was elevated in HIV group (Pink, Patients 38-39) compared to Control (Blue, Patients 1-12),  $p = 0.0084$ . In comparing HIV with HIV/MDD (Red, Patients 49-60), the HIV/MDD group, although more variable than Control did not elevate to the same as HIV without MDD. Indeed patient 54 seemed to lack FKBP52 in the sampled section altogether. Among the MDD and MDD/Psychosis Groups, expression of FKBP52 is more variable than control, with the MDD mean above the standard deviation of the mean Control, however not stastically different.

#### FKBP51

The immunoblots and Fold-Actin graphs for FKBP51 across the five study groups are illustrated in Figure 3-7. In order to compare all patients across the five immunoblots, the same normalization procedure was performed with the FKBP51 densitometry values and plotted in Figure 3-8, the blue bar indicates the standard deviation about the mean for the Control Group ( $1.06 \pm 0.43$ ).

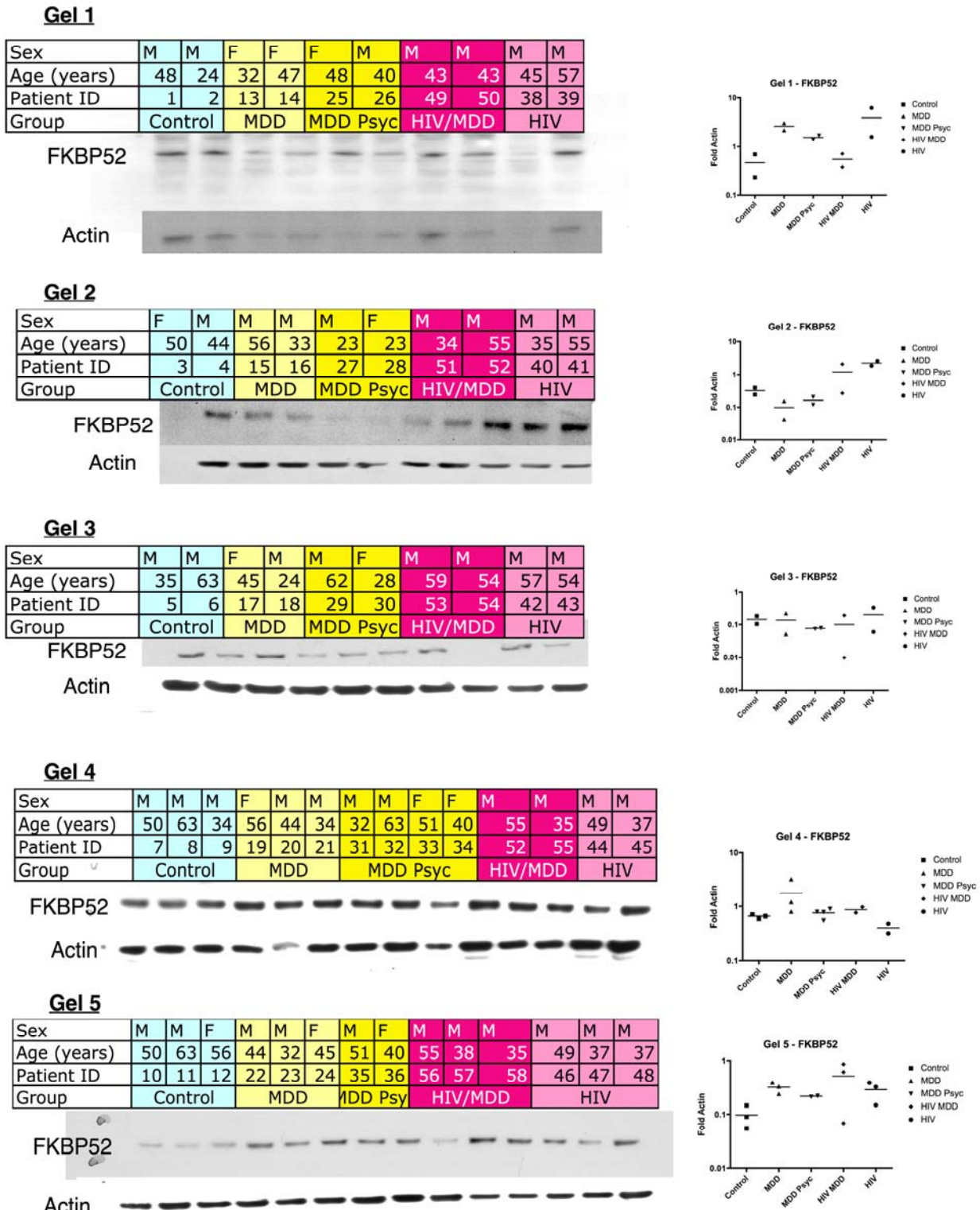


Figure 3-5. Western Analysis of FKBP52 in MDD and HIV/MDD Patients. Tissue was dissected (100  $\mu$ g) from frozen tissue of cortical grey matter of the cases listed in Table 3-1. Tissue was homogenized and 50  $\mu$ g total soluble protein was run separated by PAGE. Cases representing each study group were included in every gel. After transfer and immobilization on PVDF membrane, proteins were probed by

Western blot for FKBP52. Membranes were stripped of antibodies and reprobed for Actin. Densitometry determined Area Under the Curve for FKBP52 and Actin signal, and  $\text{Fold-Actin} = \text{Area}_{\text{FKBP52}} / \text{Area}_{\text{Actin}}$ , and plotted to the right are corresponding Fold-Actin values as detailed in Section 3.2.2 and Appendix A.

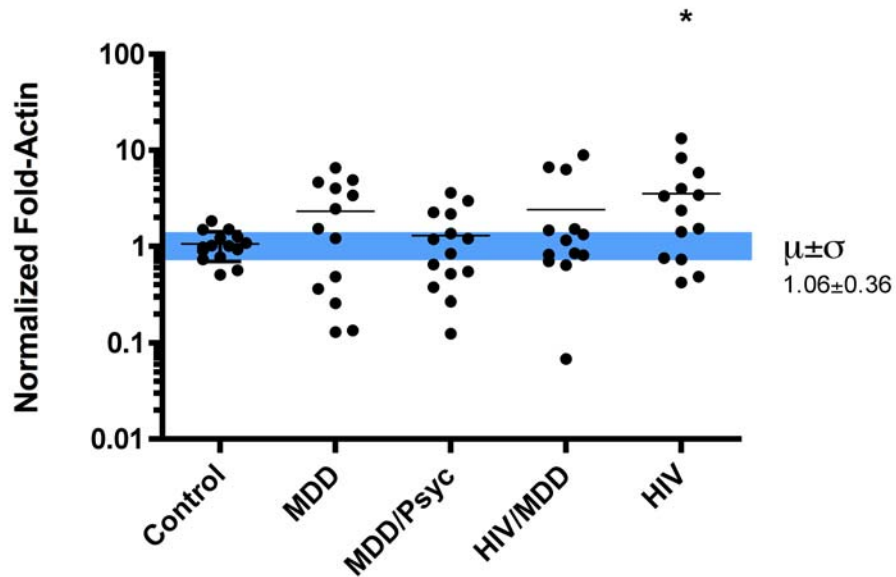
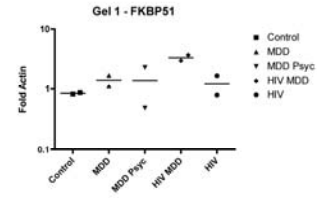


Figure 3-6. FKBP52 Protein Level is Increased in HIV Group. Normalized Fold-Actin values are calculated from the Fold-Actin values determined in Figure 3-5. Values are normalized to controls on their respective gels,  $\text{Normalized Fold-Actin} = \text{Fold-Actin}_{\text{Patient}} / \text{Fold-Actin}_{\text{ControlMean}}$  as detailed in Appendix B. The area within the bar delineates the standard deviation about the mean ( $\mu \pm \sigma$ ). Two-way ANOVA and Dunn's Multiple Comparison test were used to test for significance (\*  $p < 0.05$ ).

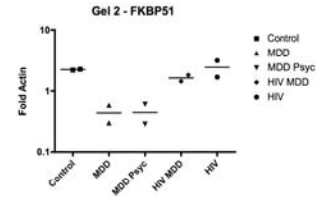
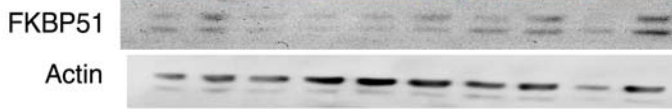
**Gel 1**

Sex	M	M	F	F	F	M	M	M	M	M
Age (years)	48	24	32	47	48	40	43	43	45	57
Patient ID	1	2	13	14	25	26	49	50	38	39
Group	Control		MDD		MDD Psyc		HIV/MDD		HIV	



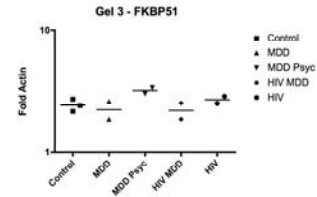
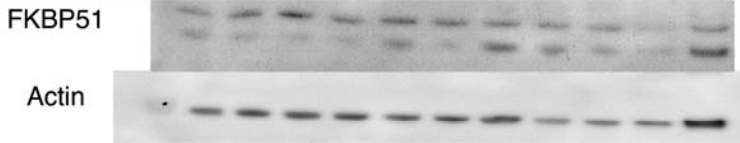
**Gel 2**

Sex	F	M	M	M	M	F	M	M	M	M
Age (years)	50	44	56	33	23	23	34	55	35	55
Patient ID	3	4	15	16	27	28	51	52	40	41
Group	Control		MDD		MDD Psyc		HIV/MDD		HIV	



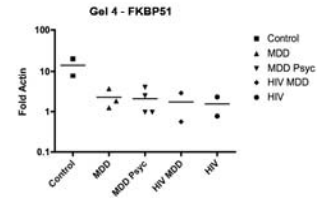
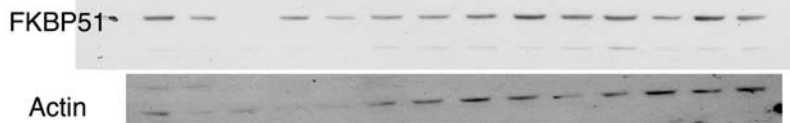
**Gel 3**

Sex	M	M	F	M	M	F	M	M	M	M
Age (years)	35	63	45	24	62	28	59	54	57	54
Patient ID	5	6	17	18	29	30	53	54	42	43
Group	Control		MDD		MDD Psyc		HIV/MDD		HIV	



**Gel 4**

Sex	M	M	M	F	M	M	M	M	F	F	M	M	M	M
Age (years)	50	63	34	56	44	34	32	63	51	40	55	35	49	37
Patient ID	7	8	9	19	20	21	31	32	33	34	52	55	44	45
Group	Control			MDD			MDD Psyc			HIV/MDD			HIV	



**Gel 5**

Sex	M	M	F	M	M	F	M	F	M	M	M	M	M	M	
Age (years)	50	63	56	44	32	45	51	40	55	38	35	49	37	37	
Patient ID	10	11	12	22	23	24	35	36	56	57	58	46	47	48	
Group	Control			MDD			MDD Psyc			HIV/MDD			HIV		

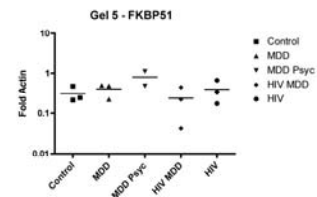
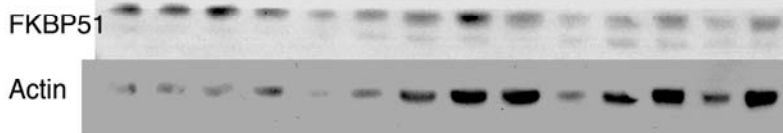


Figure 3-7. Western Analysis of FKBP51 in MDD and HIV/MDD Patients. Tissue was dissected (100 µg) from frozen tissue of cortical grey matter of the cases listed in Table 3-1. Tissue was homogenized and 50 µg total soluble protein was run separated by PAGE. Cases representing each study group were included in

every gel. After transfer and immobilization on PVDF membrane, proteins were probed by Western blot for FKBP51. Membranes were stripped of antibodies and reprobed for Actin. Densitometry determined Area Under the Curve for FKBP51 and Actin signal, and  $\text{Fold-Actin} = \text{Area}_{\text{FKBP51}} / \text{Area}_{\text{Actin}}$ , and plotted to the right are corresponding Fold-Actin values as detailed in Section 3.2.2 and Appendix A.

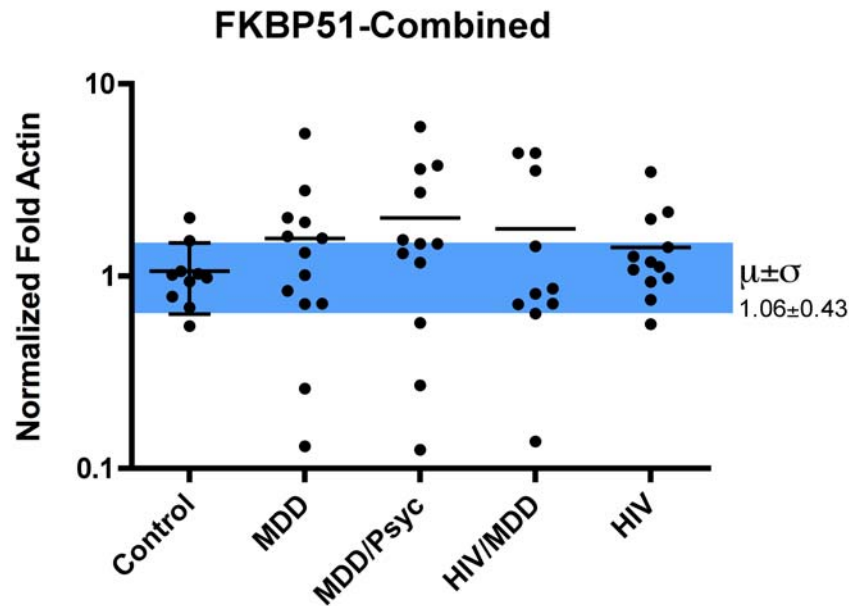


Figure 3-8. FKBP51 Protein is Altered in MDD Groups Compared to Control and Trended Toward Elevated in HIV. Normalized Fold-Actin values are calculated from the Fold-Actin values determined in Figure 3-5. Values are normalized to controls on their respective gels,  $\text{Normalized Fold-Actin} = \text{Fold-Actin}_{\text{Patient}} / \text{Fold-Actin}_{\text{ControlMean}}$  as detailed in Appendix B. The area within the bar delineates the standard deviation about the mean ( $\mu \pm \sigma$ ). Two-way ANOVA and Dunn's Multiple Comparison test were used to test for significance at  $p < 0.05$ .

### 3.3.2 Immunophilin Gene Expression

Figure 3-9 shows the fold-control of the (a) *FKBP4* and (b) *FKBP5* gene expression across the five study groups. In order to represent the natural variation in the population at large, fold-

control was calculated against the median  $\Delta\text{CT}$  value from the Control Group. Therefore half of the Controls appear above and half below 1. As shown in Figure 3-9, the majority of patients in the two HIV<sup>+</sup> populations showed higher expression of *FKBP4* and *FKBP5* above the Control median. For the *FKBP4* gene, HIV<sup>+</sup> patients exhibited a fold-increase of  $3.2 \pm 2.6$  (mean  $\pm$  standard deviation) and HIV<sup>+</sup>MDD patients exhibited a fold-increase of  $3.1 \pm 3.3$ . For the *FKBP5* gene, HIV<sup>+</sup> patients showed  $13.5 \pm 15.8$  fold increase over Control and HIV<sup>+</sup>MDD patients showed  $9.6 \pm 12.7$  fold increase over Control. In the HIV<sup>+</sup>MDD population, *FKBP5* was more variable in the patient populations, ranging from 0.7-44.3 -fold change in HIV+MDD and in HIV<sup>+</sup> from 1.4-50 -fold increase.

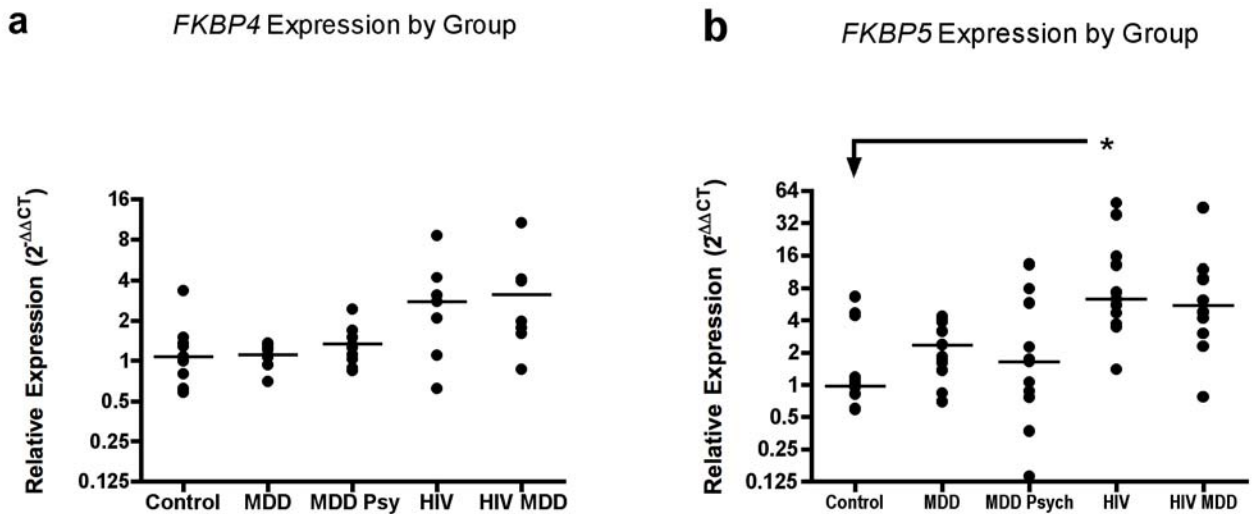


Figure 3-9. *FKBP4* (A) and *FKBP5* (B) Expression is Increased in HIV and HIV with MDD. Gene expression from cortical grey matter of patients listed in Table 3-1 is determined by qPCR using the  $\Delta\Delta\text{CT}$  method and normalizing the gene of interest to *GAPDH* expression as explained in Section 3.2.3. Fold-Control is plotted for each of the study groups, ● represent individual patients and bars represent median within the group. One-way ANOVA with Dunn's Multiple Comparison Test tested for significant difference among the groups (\*  $p < 0.05$ ).

In the HIV negative MDD group, there is a trend toward increased expression of *FKBP5* with median expression 2.4 fold higher than control (Figure 3-9b), however, no change is apparent for *FKBP4* this group. The HIV<sup>+</sup> groups with and without MDD show expression levels of both *FKBP4* and *FKBP5* trending toward being elevated than the three HIV<sup>-</sup> groups. This suggests that the viral infection contributes more than depression to the increased immunophilin expression. The HIV infection is the contributing variable here, the factors causing differences in *FKBP4* and *FKBP5*, the proteins for these genes were found in neurons in Section 3.3.5, and neurons do not get infected by the virus. Therefore, it is likely that factors of long-term, chronic, subtle CNS inflammation, increased cytokine and interleukin production, due to HIV infection and the interaction between infected monocytes and glia with the neuronal cells cause the upregulation.

We hypothesized that there would be a balance between *FKBP4* and *FKBP5* expression and the balance would be disrupted in MDD, MDD/Psychosis, or HIV/MDD. In plotting the *FKBP4* expression on the y-axis, and *FKBP5* expression on the x-axis, we analyzed possible correlation of expression between the two genes. Pearson's test for correlation showed a moderate correlation between *FKBP4* and *FKBP5* ( $R^2 = 0.55$ ,  $p = 0.0085$ , goodness of fit, and probability that the non-zero slope is due to chance) expression in the Control (●) group which is absent in all other groups (Figure 3-10). In the MDD (■) and MDD/Psych (□) groups, the curve was flat, ( $p = 0.52$  and  $0.49$ , respectively) and no correlation ( $R^2 = 0.15$  and  $0.08$ , respectively). For both HIV (▲) and HIV/MDD (△), the curves were shifted upwards, but flat with no correlation ( $R^2 = 0.04$  and  $0.04$ ,  $p = 0.74$  and  $0.66$ , respectively).

In the tissue acquired from the CNTN, we had available patient history of the MDD and MDD/Psych patients regarding their most recent MDD episode and it was either within the last 1 month or 6 months of death. The *FKBP4* and *FKBP5* expression was higher in the MDD

patients who had MDD episodes within 1 month, but did not reach statistical significance,  $p = 0.11$  and  $p = 0.15$  respectively (Figure 3-11).

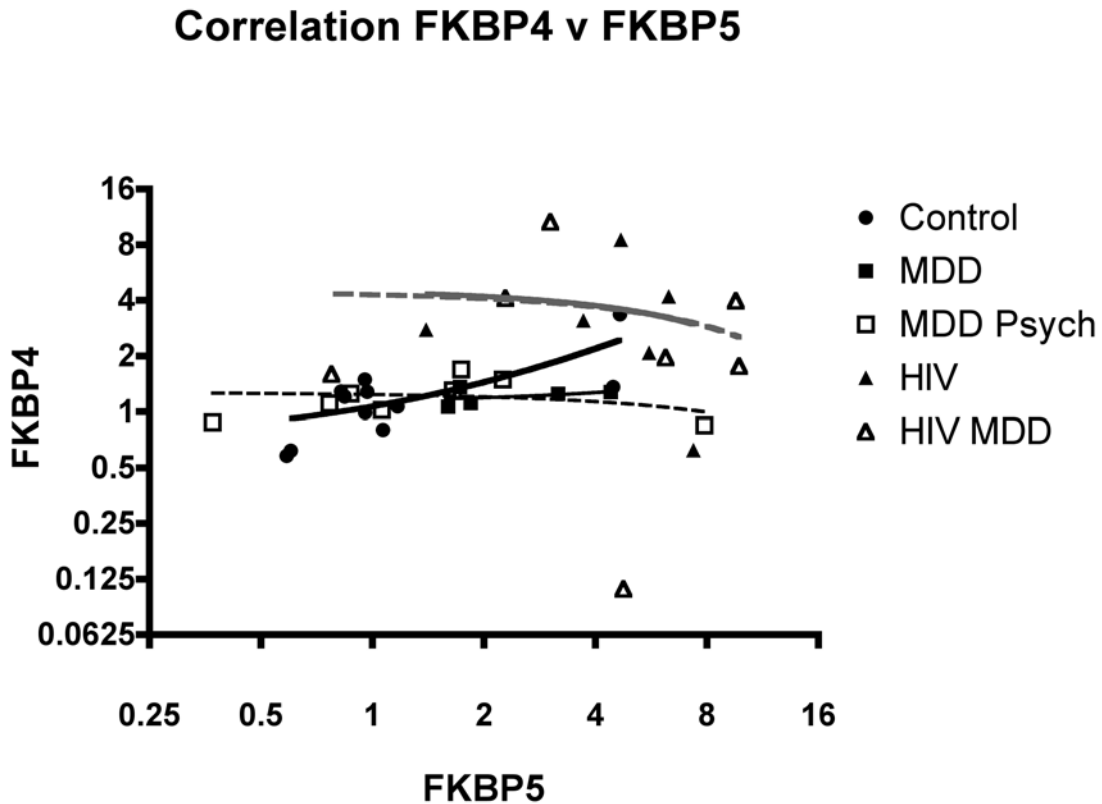


Figure 3-10. Correlation of *FKBP4* and *FKBP5* Expression in Frontal Cortex Separated by Group. Gene expression from cortical grey matter of patients listed in Table 3-1 is determined by qPCR using the  $\Delta\Delta$ CT method and normalizing the gene of interest to *GAPDH* expression as explained in Section 3.2.3. Fold-Control is plotted for each of the study group, plotting the *FKBP4* expression on the y-axis, and *FKBP5* expression on the x-axis. Pearson's test for correlation showed a correlation between *FKBP4* and *FKBP5* ( $R^2 = 0.55$ ,  $p = 0.0085$ , goodness of fit, and probability that the non-zero slope is due to chance) expression in the Control (●) Group. In the MDD (■) and MDD/Psych (□) groups, the curve was flat, ( $p = 0.52$  and  $0.49$ , respectively) and no correlation ( $R^2 = 0.15$  and  $0.08$ , respectively). For both HIV (▲) and HIV/MDD (△) there was no correlation and the curves were flat ( $R^2 = 0.04$  and  $0.04$ ,  $p = 0.74$  and  $0.66$ , respectively). The curves represent linear regression of the *FKBP4* versus *FKBP5* (solid bold = Control, black = MDD, black dashed = MDD/Psych, grey solid = HIV, grey dashed = HIV/MDD).

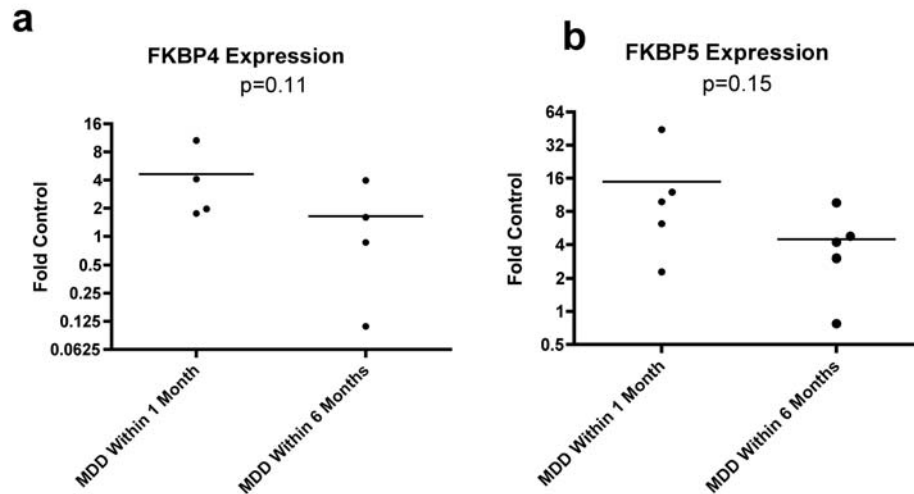


Figure 3-11. Expression of *FKBP4* (A) and *FKBP5* (B) in the CNTN Groups Separated by Most Recent Episode. Gene expression from cortical grey matter of patients for whom MDD clinical data were available is determined by qPCR using the  $\Delta\Delta$ CT method and normalizing the gene of interest to *GAPDH* expression as explained in Section 3.2.3. Patients are divided based on MDD Episode Within 1 Month or Within 6 Months and Fold-Control plotted, ● represent individuals and bars represent median. Student's *t* test comparing the two groups' expression showed a nonsignificant trend based on most recent MDD episode for expression of *FKBP4* ,  $p = 0.11$  (A); or *FKBP5*,  $p = 0.15$  (B).

### 3.3.2.1 Correlation of Gene and Protein Expression

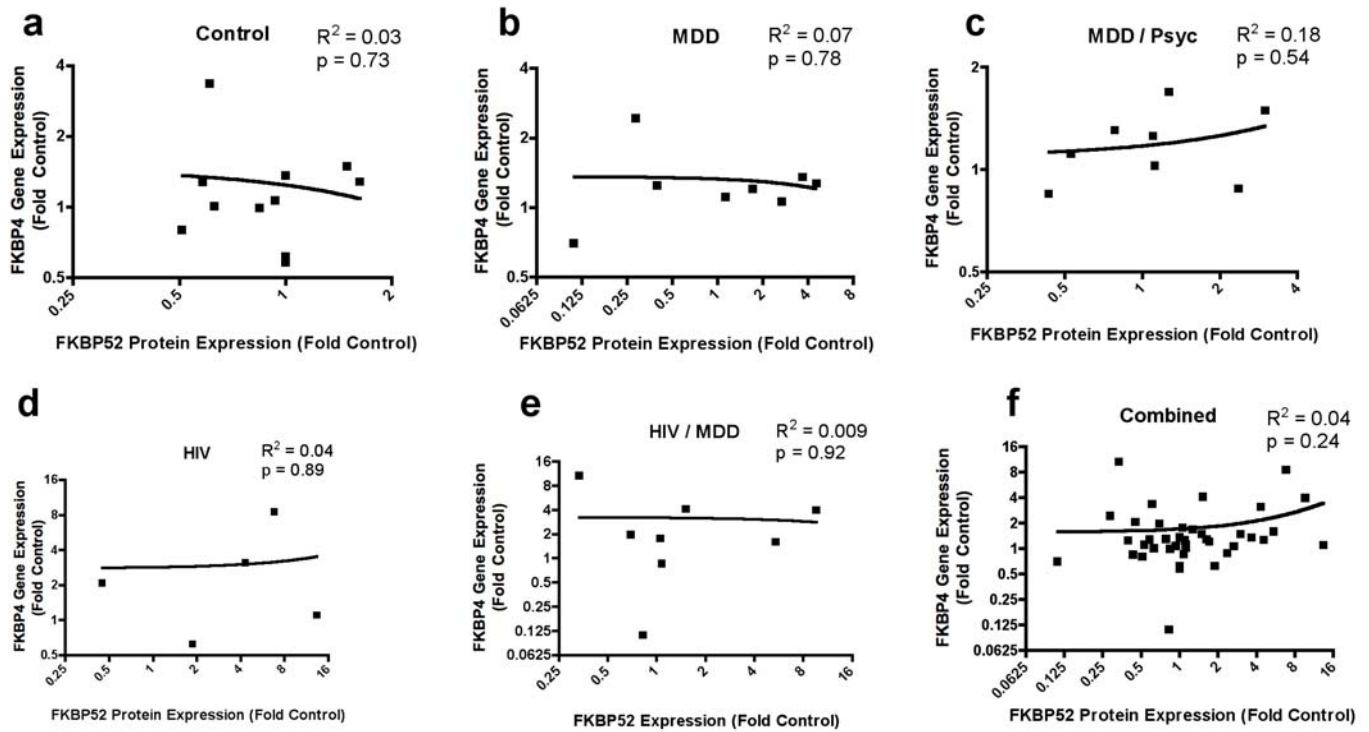
Gene expression and corresponding level of proteins they encode do not always correlate. In eukaryotes, gene expression of mRNA and protein translation occur in different compartments, the nucleus and the cytoplasm, respectively; allowing for modulation on many levels. The amount of mRNA of a particular transcript is affected by direct active transcription from the genome. Polyadenylation of the pre-mRNA affects its stability and transport from the nucleus. There are hundreds of RNA-binding proteins that modify, edit, stabilize, or degrade mRNA. Trans-acting RNA's also modify the stability of RNA, for example micro-RNA or short-interfering RNA's [174]. Any of these factors acting alone or in concert could affect

mRNA levels irrespective of the amount of gene-product. Conversely, these factors could change the rate of protein translation without changing mRNA levels. The corresponding protein is altered by gene translation and protein turnover. Processes such as the ubiquitin, small ubiquitin-like modification (SUMO), and proteasome systems can modify specific protein levels without a corresponding change in mRNA levels [175, 176].

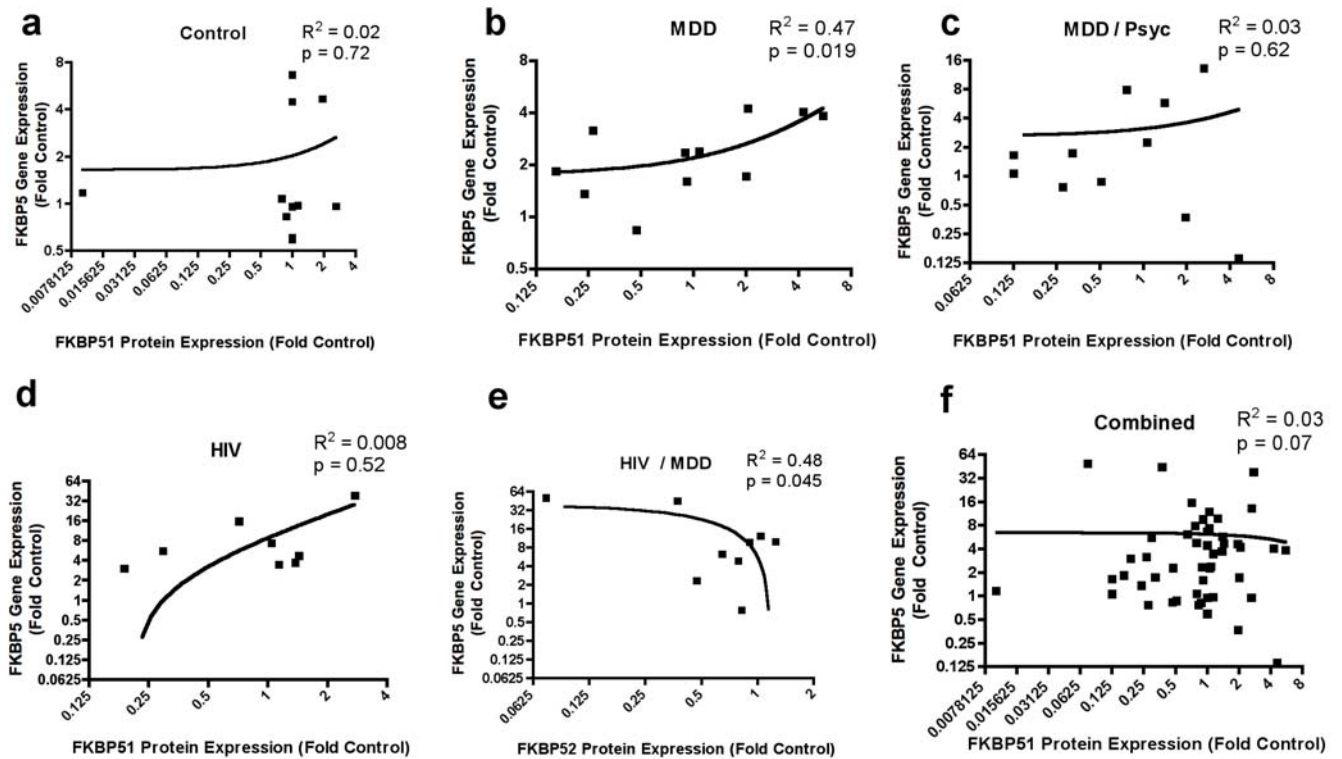
The *FKBP4* and *FKBP5* gene expressions trended toward increase in HIV and HIV/MDD, most significantly for *FKBP4* in the HIV group (Figure 3-9). The mean values for the FKBP52 protein were higher in HIV and HIV/MDD, and protein levels were much more variable in all groups than gene expression. The mean values of FKBP51 protein trended toward higher in MDD, HIV, and HIV/MDD. This indicates that perhaps gene transcription is induced by some unidentified factor in HIV-infection, for example, chronically activated microglia secreting TGF- $\beta$ , IL-1 $\alpha$ , or IL-1 $\beta$  [21-24, 177, 178]. Perhaps protein levels are altered by mechanisms independent of mRNA levels in the MDD/Phyc or MDD groups. It would be desirable to know whether mRNA levels correspond to protein levels. In order to determine whether the gene transcript levels and the protein levels that we observed correlate, we plotted gene expression versus protein levels determined above for the individual cases. We performed Spearman's test for correlation setting. P-values are reported, derived from the  $R^2$  value of the Spearman's rank-test, which indicate the probability that a non-zero slope of linear regression is due to chance,  $p < 0.05$  is considered significant.

Figure 3-12 shows the correlation plots of *FKBP4* expression versus FKBP52 protein amounts for (a) Control, (b) MDD, (c) MDD/Phyc, (d) HIV, (e) HIV/MDD, and all groups (f) Combined. The gene expression and corresponding protein levels did not correlate. Figure 3-13 shows the correlation plots of *FKBP5* expression versus FKBP51 protein amounts for each study group and groups combined. In the MDD and HIV groups, gene transcript-levels did correlate positively with protein levels (Figure 3-13b and 3-13d, respectively). In the HIV/MDD group,

*FKBP5* gene and FKBP51 protein correlated negatively (Figure 3-13e). When all groups are combined (Figure 3-13f), *FKBP5* and FKBP51 protein do not correlate. This suggests complex regulation of the immunophilin genes and proteins.



**Figure 3-12. Gene Expression of *FKBP4* and Protein Levels of FKBP52 do not correlate.** Control group (A), MDD (B), MDD/Psyc (C), HIV (D), HIV/MDD (E), all groups combined (F) are plotted separately. Gene expression from cortical grey matter of patients listed in Table 3-1 is determined by qPCR using the  $\Delta\Delta\text{CT}$  method and normalizing the gene of interest to *GAPDH* expression as explained in Section 3.2.3, and Fold Control for *FKBP4* is plotted on the y axes. Normalized Fold-Actin values representing FKBP52 Expression are calculated from the Fold-Actin values determined in Figure 3-5. Values are normalized to controls on their respective gels,  $\text{FKBP52 Protein Expression} = \text{Fold-Actin}_{\text{Patient}} / \text{Fold-Actin}_{\text{ControlMean}}$  as detailed in Appendix B and is plotted on the x axes, ■ represent individual cases. Lines illustrate linear regression and Pearson's Test for Correlation  $R^2$  values for correlation and p values for probability that a non-zero slope is due to chance are reported.



**Figure 3-13. Gene Expression of *FKBP5* versus Protein Levels of FKBP51.** Gene Expression of *FKBP5* and Protein Levels of FKBP51 correlate positively in the MDD group (B) and negatively in the HIV/MDD group (E). Control group (A), MDD (B), MDD/Psyc (C), HIV (D), HIV/MDD (E), all groups combined (F) are plotted separately. Gene expression from cortical grey matter of patients listed in Table 3-1 is determined by qPCR using the  $\Delta\Delta\text{CT}$  method and normalizing the gene of interest to *GAPDH* expression as explained in Section 3.2.3, and Fold Control for *FKBP5* is plotted on the y axes. Normalized Fold-Actin values representing FKBP51 Expression are calculated from the Fold-Actin values determined in Figure 3-5. Values are normalized to controls on their respective gels,  $\text{FKBP51 Protein Expression} = \text{Fold-Actin}_{\text{Patient}} / \text{Fold-Actin}_{\text{ControlMean}}$  as detailed in Appendix B and is plotted on the x axes, ■ represent individual cases. Lines illustrate linear regression and Pearson's Test for Correlation  $R^2$  values for correlation and p values for probability that a non-zero slope is due to chance are reported.

### 3.3.3 Single Nucleotide Polymorphism Analysis

Using the allelic discrimination assay, we tested two polymorphisms: rs38000373, an A to C transversion substitution in the 3' untranslated region (3'UTR) of the *FKBP5* gene and rs1360780, which is a C to T transition substitution in the second intron of the *FKBP5* gene. SNP rs1360780 is located in a region where transcription factors may bind, where hormone response elements (HRE) are located as shown in Figure 3-14, this may alter transcription and has been implicated in mood disorders [179, 180]. SNP rs3800373 is located in a region which may alter stability and half-life of the mRNA molecule.

The SNP rs3800373 had associations with MDD and MDD/Psych groups. The heterozygous genotype, AC, and the minor allele homozygous CC, were significantly more frequent than expected based on Hardy-Weinberg assumptions of the North American Caucasian population and previously published allelic and genotype frequencies (Table 3-4) [173]. The HIV/MDD groups did not have the same deviation from expected as noted in the HIV negative MDD group. The MDD with Psychosis group had increased frequency of the C allele compared with the North American Caucasian population and the Control group in this study (Table 3-5).

In the genotype frequencies of the Intron II polymorphism were were significantly different in the MDD/Psych group from North American Caucasian population. The AC and CC genotypes were increased in the MDD Psychosis as well as significant increase in the minor, C, allele; Tables 3-5 and 3-6. A possible confound may be associated with our observation that the Control and the HIV populations differed from the Expected values.

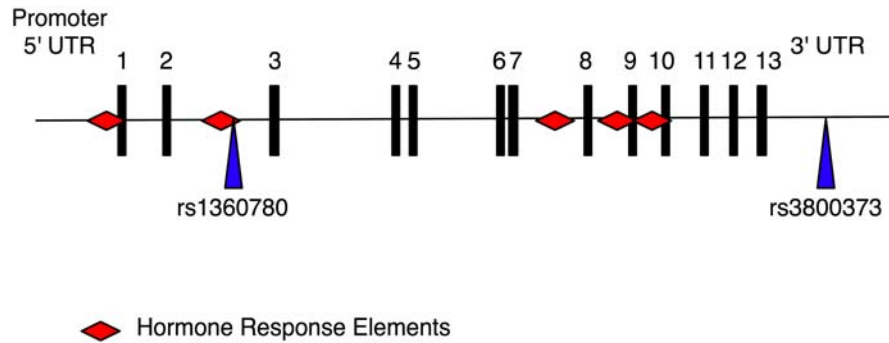


Figure 3-14. Transcription Factor Binding Sites and SNP Locations on *FKBP5* Gene. The genomic organization of the *FKBP5* gene is illustrated, exons are numbered with black bars, distance between bars represent relative lengths of the introns. The locations of the two polymorphisms, rs1360780 and rs3800373 are indicated by ▲ and location of hormone responsive elements are indicated with ◆.

Table 3-4. Genotype Frequencies for SNP rs 3800373 of *FKBP5* Gene. Genotypes of each case in Table 3-1 was determined from genomic DNA by allelic discrimination assay described in Section 3.2.5. Based on the published allelic frequencies  $f(A) = 0.688$ ,  $f(C) = 0.312$ , *Expected* genotype frequencies are calculated based on Hardy-Weinberg equilibrium and compared to *Observed* genotypes for the study groups.  $\chi^2$  analysis comparing *Expected* with *Observed* values determines significant deviation in the patient groups from the population, significance is considered at  $p < 0.05$ .

	<i>Expected</i>			<i>Observed</i>			$\chi^2$ <i>p-Value</i>
	AA	AC	CC	AA	AC	CC	
Control (n=13)	5.4	7.0	0.5	8	4	1	0.232
MDD (n=11)	5.0	6.5	0.5	7	2	2	<b>0.015</b>
MDD Psych (n=10)	4.6	6.0	0.5	2	6	2	<b>0.037</b>
HIV (n=9)	3.8	4.9	0.4	2	6	1	0.350
HIV MDD (n=8)	3.3	4.3	0.3	3	5	0	0.790

**Table 3-5. Allelic Frequencies for SNP rs3800373 of FKBP5 Gene.** Genotypes of each case in Table 3-1 was determined from genomic DNA by allelic discrimination assay described in Section 3.2.5. Based on the published allelic frequencies  $f(A) = 0.688$ ,  $f(C) = 0.312$ , *Expected* allele frequencies are calculated based on group size and compared to *Observed* genotypes for the study groups.  $\chi^2$  analysis comparing *Expected* with *Observed* values determines significant deviation in the patient groups from the population, significance is considered at  $p < 0.05$ .

	Expected		Observed		$\chi^2$ p-value
	A	C	A	C	
Control (n=26)	18	8	20	6	0.371
MDD (n=22)	15	7	16	6	0.691
MDD Psych (n=20)	14	6	10	10	0.070
HIV (n=18)	12	6	10	8	0.225
HIV MDD (n=16)	11	5	11	5	0.997

**Table 3-6. Genotype Frequencies for SNP rs1360780 of FKBP5 Gene.** Genotypes of each case in Table 3-1 was determined from genomic DNA by allelic discrimination assay described in Section 3.2.5. Based on the published allelic frequencies  $f(C) = 0.758$ ,  $f(T) = 0.242$ , *Expected* genotype frequencies are calculated based on Hardy-Weinberg equilibrium and compared to *Observed* genotypes for the study groups.  $\chi^2$  analysis comparing *Expected* with *Observed* values determines significant deviation in the patient groups from the population, significance is considered at  $p < 0.05$ .

	Expected			Observed			$\chi^2$ p-Value
	CC	CT	TT	CC	CT	TT	
Control (n=13)	7.5	4.8	0.8	7	3	3	<b>0.026</b>
MDD (n=12)	6.9	4.4	0.7	4	7	1	0.238
MDD Psych (n=11)	6.4	4.0	0.6	3	6	2	0.062
HIV (n=9)	6.3	4.0	0.6	1	7	1	<b>0.033</b>
HIV MDD (n=8)	4.6	2.9	0.5	3	5	0	0.290

**Table 3-7. Allelic Frequencies for SNP rs1360780 of FKBP5 Gene.** Genotypes of each case in Table 3-1 was determined from genomic DNA by allelic discrimination assay described in Section 3.2.5. Based on the published allelic frequencies  $f(A) = 0.688$ ,  $f(C) = 0.312$ , *Expected* allele frequencies are calculated based on group size and compared to *Observed* genotypes for the study groups.  $\chi^2$  analysis comparing *Expected* with

*Observed* values determines significant deviation in the patient groups from the population, significance is considered at  $p < 0.05$ .

	Expected		Observed		$\chi^2$ p-value
	C	T	C	T	
Control (n=28)	20	6	17	9	0.215
MDD (n=24)	18	6	15	9	0.128
MDD Psych (n=24)	17	5	12	10	<b>0.020</b>
HIV (n=22)	14	4	9	9	<b>0.011</b>
HIV MDD (n=22)	12	4	11	5	0.510

### 3.3.4 Immunophilin Response in Cultured Neuronal Cells Exposed to HIV

In order to test the hypothesis that HIV infection leads to increased expression of immunophilins in neuronal cells, differentiated SH-SY5Y cells were exposed to media supplemented with 10% HIV-infected microglia-conditioned medium. In order to determine whether factors secreted by microglia in the absence of infection would alter expression, cells were given conditioned media from HIV negative microglia grown in parallel with, were cultivated from the same source and grown in identical conditions, except that the HIV<sup>+</sup> group were exposed in vitro to HIV. In order to allow for soluble factors from the conditioned media to have an effect on translation of induced genes, RNA was harvested at 6 hours from the exposed SH-SY5Y cells, and in order to determine whether any induction would be sustained, RNA was harvest at 24 hours. Figure 3-15 shows increased *FKBP4* expression after 6 hours of exposure to HIV-infected microglia, which returns to baseline by 24 hours, while exposure to HIV-negative supernatant did not lead to an appreciable change in *FKBP4* expression.

**A**

**B**

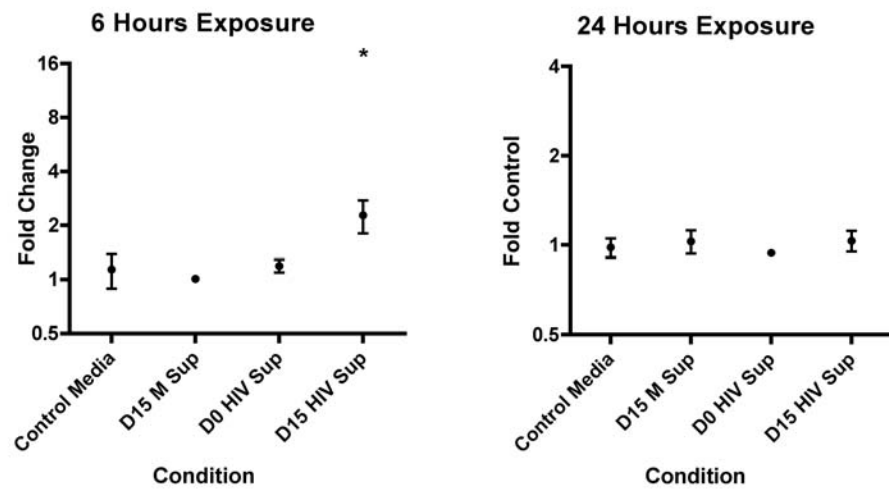


**Figure 3-15. Expression of *FKBP4* in SH-SY5Y Cells Exposed to HIV-Conditioned Media.** Differentiated SH-SY5Y cells were exposed for 6 Hours (A) or 24 Hours (B) to conditioned 10% Conditioned Media from HIV-infected microglia. Microglia had been infected with HIV for 15 days, with media removed every third day. On day 15, supernatant (Sup) was removed and used to supplement the SH-SY5Y media to 10% Conditioned Media. Control Media were supplemented with Microglia media, D15 M Sup is supplemented from non-infected microglia grown in parallel to the HIV infection, D0 HIV Sup is supplemented from supernatant of the microglia cultures immediately prior to HIV – infection, D15 HIV Sup is supernatant from the actual infection. RNA was isolated and qRT-PCR for *FKBP4* gene using the  $\Delta\Delta\text{CT}$  method comparing *FKBP4* expression with *GAPDH* and calibrating Control Media. Fold-changes are plotted and two-way ANOVA compares among the groups (\*  $p < 0.01$ ).

**A**

**B**

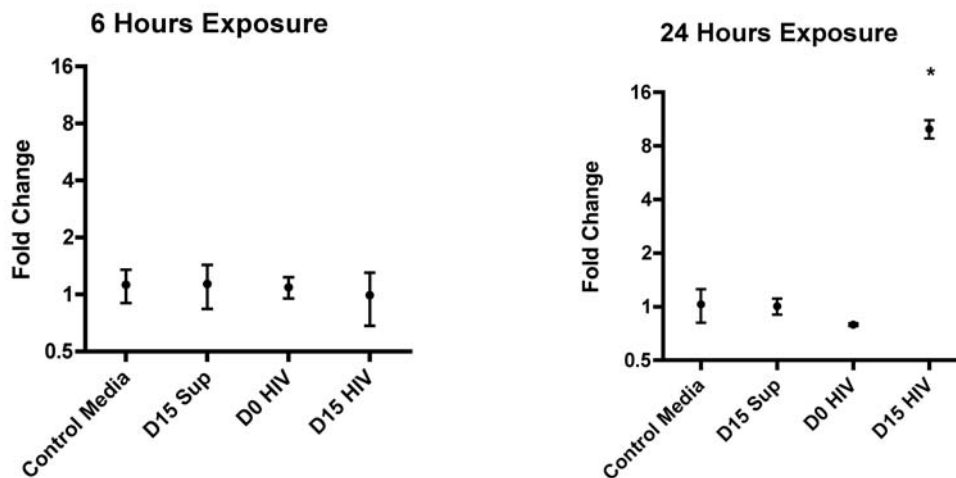


**Figure 3-16. Expression of *FKBP5* in SH-SY5Y Cells Exposed to HIV-Conditioned Media.** Differentiated SH-SY5Y cells were exposed for 6 Hours (A) or 24 Hours (B) to conditioned 10% Conditioned Media from HIV-infected microglia. Microglia had been infected with HIV for 15 days, with media removed every third day. On day 15, supernatant (Sup) was removed and used to supplement the SH-SY5Y media to 10% Conditioned Media. Control Media were supplemented with Microglia media, D15 M Sup is supplemented from non-infected microglia grown in parallel to the HIV infection, D0 HIV Sup is supplemented from supernatant of the microglia cultures immediately prior to HIV – infection, D15 HIV Sup is supernatant from the actual infection. RNA was isolated and qRT-PCR for *FKBP5* gene using the  $\Delta\Delta\text{CT}$  method comparing *FKBP4* expression with *GAPDH* and calibrating Control Media. Fold-changes are plotted and two-way ANOVA compares among the groups (\*  $p < 0.01$ ).

In contrast to the gene encoding the GR-adaptor protein, *FKBP4*, the inhibitory *FKBP5* gene did not change after six hours, but *did* increase after 24 hours, Figure 3-16. Indicating a temporal difference between how the two genes respond to stressors. Microglial supernatant alone was not enough to induce a change in expression in either gene. Exposure to supernatant of HIV– infected microglial lead to an increase in the immunophilin genes; *FKBP5* expression increased later than *FKBP4*. Microglia infected with HIV secrete cytokines and chemokines such as tumor necrosis factor- $\alpha$  (TNF- $\alpha$ ), interleukin 1  $\alpha$  and  $\beta$  (IL-1 $\alpha$  and IL-1 $\beta$ ) [181]. The

increase in *FKBP4* may have been a transient increase in response to such factors, while the increase in *FKBP5* could have been a secondary, later effect.

### **3.3.5 Immunohistochemistry of FKBP52 and FKBP51 in Frontal Cortex**

The tissue distribution of the immunophilins in the brain has not yet been studied. Although it has been shown that *FKBP4* is expressed in the brain [182], and in situ hybridization shown in Chapter 1 from the rat brain showed expression in the cellular cortical layers of the rat brain, it is unknown which cells in the brain express these immunophilins. To that end, we utilized paraffin embedded frontal cortex tissue obtained from the CNTN and immunolabeled FKBP52 and FKBP51. For comparison, the classic cortical layer diagram from Brodmann [181] is illustrated in Figure 3-17, with Golgi stain on the left showing cytoplasm, Nissl stain in the middle showing cell bodies, and myelin stain on the right showing axons [183].

FKBP52 immunohistochemistry is illustrated in Figure 3-19 and FKBP51 immunohistochemistry is illustrated in Figure 3-20. Negative Controls (Figure 3-18) shows no background Nova Red staining, and purple nuclei stain of the Hematoxylin counterstain. We found that FKBP52 was expressed in the large pyramidal cells of layer III and V. It stained cytoplasm in the cell bodies. It was also expressed in a subset of, what may be, interneurons of Layer IV. FKBP51 was seen more in processes. Immunoreactivity was also seen in a subset of cells in Layer III and in Layer V, though this qualitative assessment seems to show FKBP51 in fewer pyramidal cells than FKBP52. FKBP51 stained, like FKBP52, in a subset of smaller cell bodies in Layer IV. In addition, FKBP51 was present in axonal tracts of the cortical white matter.

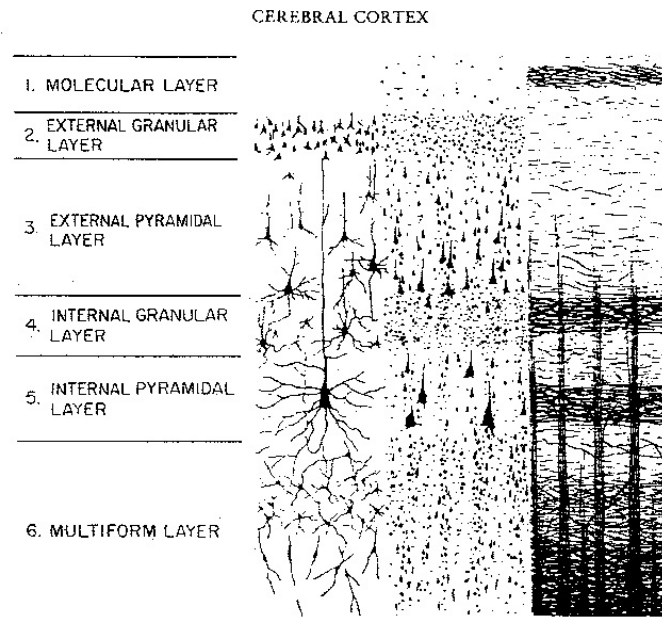


**Figure 3-17. Cellular layers of human cortex showing (left) Golgi stain cytoplasm, (middle) Nissl stain cell bodies, (right) myelin sheaths, from Brodmann (1912) [183].**

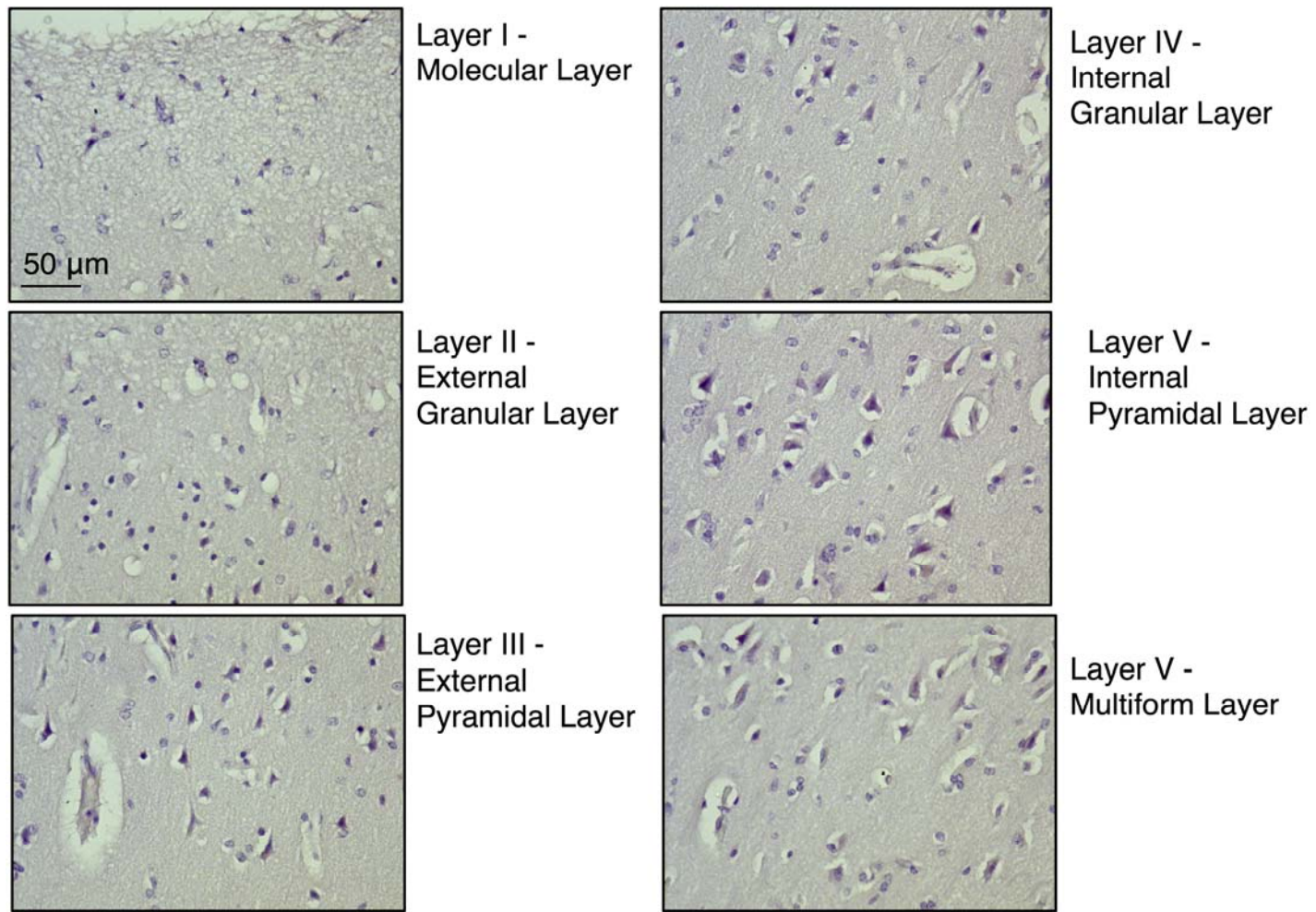


**Figure 3-18. No Primary Antibody Control - Frontal Cortex.** Paraffin embedded section from the frontal cortex was subjected to immunohistochemistry protocol in Section 3.2.6, lacking primary antibody. Sections were cut at 8 µm thick, mounted on glass slides, deparaffinized, rehydrated, permeablized in 1% Triton-X100. Endogenous peroxidases were blocked in 0.3% H<sub>2</sub>O<sub>2</sub> in methanol. Sections were incubated in a pressure cooker at 125°C 10 min. Sections incubated in secondary antibody (HRP conjugated Donkey anti Mouse and Donkey anti Rabbit, 1:1000) 2 hr RT, and after washing, incubated with Nova Red. Sections were counterlabeled with hematoxylin (5 min). Sections were imaged in a 40X objective. Non-specific or endogenous peroxidase reaction in dark red was not observed.

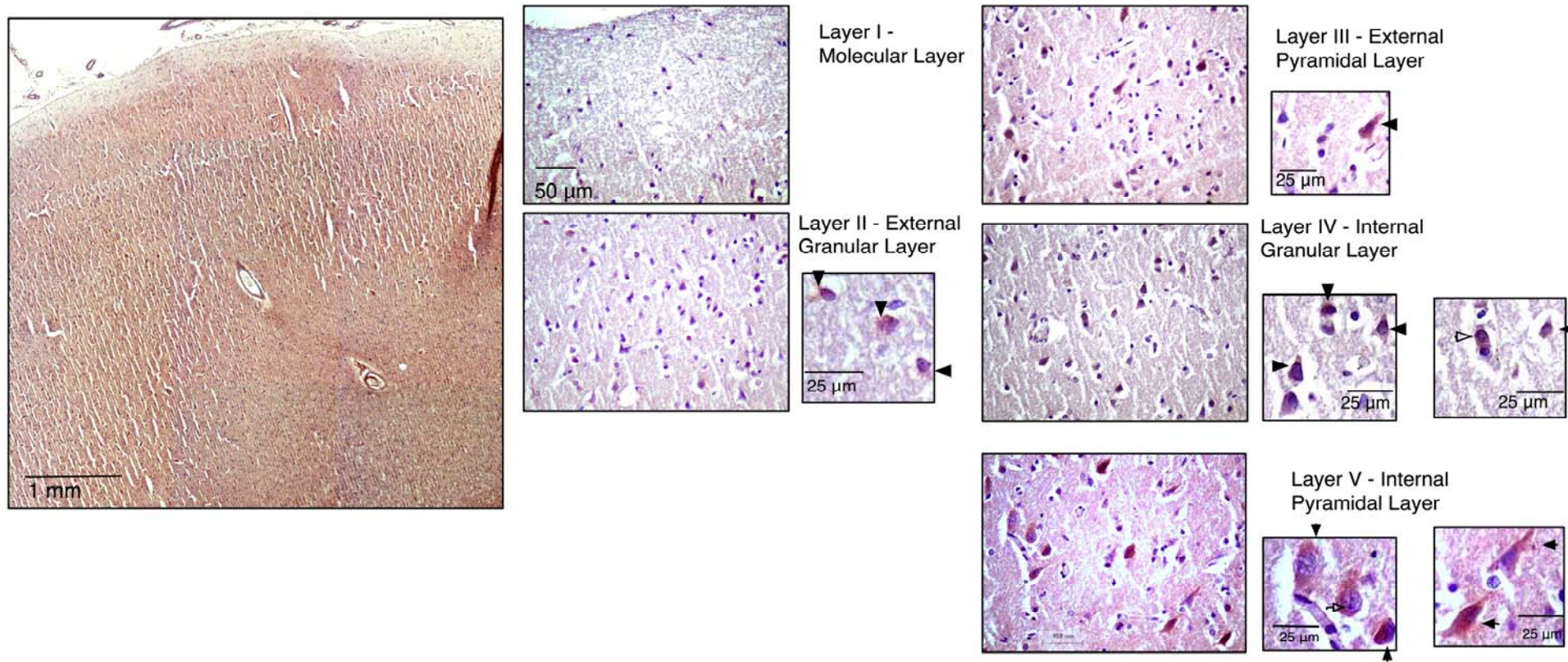


**Figure 3-19. Immunohistochemical staining for FKBP52 in Frontal Cortex from paraffin embedded tissue.** Paraffin embedded section from the frontal cortex was subjected to immunohistochemistry protocol in Section 3.2.6. Sections were cut at 8 µm thick, mounted on glass slides, deparaffinized, rehydrated, and permeablized in 1% Triton-X100. Endogenous peroxidases were blocked in 0.3% H<sub>2</sub>O<sub>2</sub> in methanol. Sections were incubated in a pressure cooker at 125°C, 10 min for antigen unmasking and blocked in 10% normal donkey serum. Sections were then incubated with primary antibody (Mouse anti FKBP52, 1:200) overnight at 4°C, then after washing, incubated with secondary antibody (HRP conjugated Donkey anti Mouse, 1:1000) for 2 hr at RT, finally after washing, immunoperoxidase reaction was developed with Nova Red. Specific staining is dark red. Sections were counterlabeled with hematoxylin (5 min) and imaged in a 40X objective. 10X images created the composite image (left). Cytoplasmic neuronal

staining is indicated by ▲, perinuclear staining is indicated at △. Specific neuronal staining for FKBP52 was observed in Cortical Layers II, III, IV, and V.

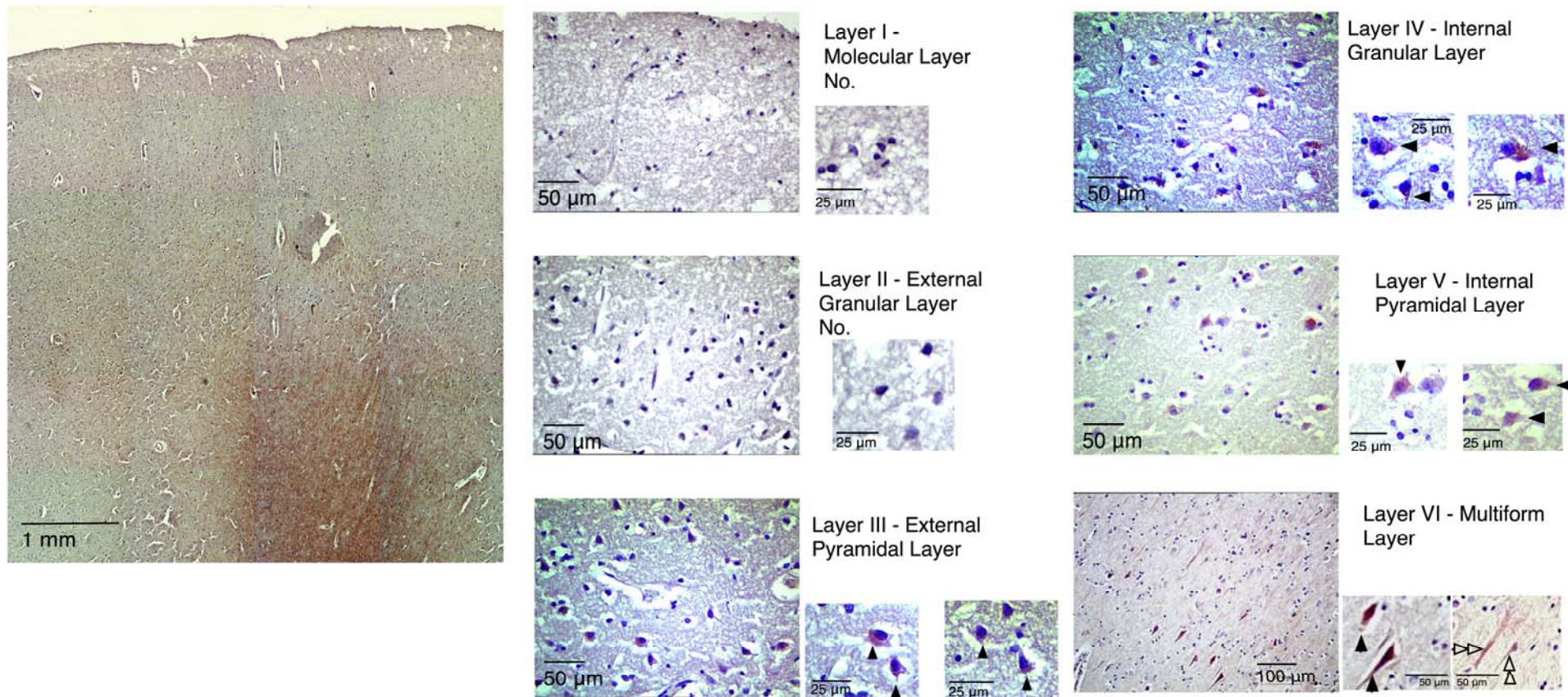


**Figure 3-20. Immunohistochemical staining for FKBP51 in Frontal Cortex from paraffin embedded tissue.** Paraffin embedded section from the frontal cortex was subjected to immunohistochemistry protocol in Section 3.2.6. Sections were cut at 8 μm thick, mounted on glass slides, deparaffinized, rehydrated, and permeablized in 1% Triton-X100. Endogenous peroxidases were blocked in 0.3% H<sub>2</sub>O<sub>2</sub> in methanol. Sections were incubated in a pressure cooker at 125°C, 10 min for antigen unmasking and blocked in 10% normal donkey serum. Sections were incubated with primary antibody (Rabbit anti FKBP51, 1:100) overnight at 4°C, then after washing, incubated with secondary antibody (biotin conjugated Donkey anti Rabbit, 1:1000) for 2 hr at RT, then in ABC complex for 30 min at RT, finally after washing, immunoperoxidase reaction was developed with Nova Red. Specific

staining is dark red. Sections were counterlabeled with hematoxylin and imaged in a 40X objective. 10X images created the composite image (left). Cytoplasmic neuronal staining is indicated by ▲, axonal tract staining is indicated at ▷▷. Specific staining for FKBP51 was observed in Cortical Layers III, IV, V, and VI.

## 3.4 DISCUSSION

### 3.4.1 Immunophilin FKBP51 and FKBP52 Expression in HIV and MDD

The observation of unequal variance of transcriptional levels of both *FKBP4* and *FKBP5* determined in Section 3.3.2 among the groups is biologically interesting, it indicates variation in the population and that there are other mechanisms at play and that expression was more variable in the MDD, MDD/Psychosis, HIV, and HIV/MDD groups. The interplay between FKBP51 and FKBP52 in modulating the effects of cortisol at the cellular level may be of some consequence.

We observed higher *FKBP5* gene transcription, median fold-change being 2.4-fold higher in the MDD group that did not reach statistical significance (Figure 3-9). The Control group had two outliers at 4-fold and 6-fold higher than the median of the Control groups. They were Patient 3 and Patient 9. There was nothing particularly irregular regarding the demographics of these two patients, falling close to the average brain pH, spanning the age range at 24 years and 50 years. The PMI's for these two patients were lower than the average (25.3 hours) at 17 hours and 9 hours. *FKBP5* is known to be responsive to cortisol [14]. Hypercortisolemia as a manifestation of HPA axis dysregulation is a component in MDD and other mood disorders. If the MDD patients were chronically hypercortisolemic, it would follow that *FKBP5* would be elevated. It would be technically challenging to analyze the cortisol content of the post-mortem tissue, as it has been in storage at -80°C and the levels measured would be indicative of the physiologic factors at the time and cause of death and not reflective of chronic conditions. Binder et al showed that *FKBP5* was elevated in the blood of patients with unipolar depression, but only when the patient had the minor variant of the rs1360780 locus in the 3'UTR of *FKBP5*. This and

other SNP's of *FKBP5* are associated with peritraumatic dissociative disorder, and PTSD, discussed below.

In HIV patients, immunophilin expression is elevated although not statistically significant except in the case of *FKBP4* gene and the FKBP52 protein for the HIV group. The HIV/MDD group has an outlier with low expression of FKBP52 with the mean fold-control falling above the range of standard deviation of the Control (Figure 3-6). Although gene expression of *FKBP5* trended toward higher in the HIV and HIV/MDD groups, the protein expression for 9/12 of the HIV patients fell within the standard deviation of the Control Group, with 3 above. The gene may be induced in HIV, but the protein levels may not be sustained at higher levels. The HIV status seems to contribute more to elevated immunophilin expression than MDD status because in MDD and MDD/Psyc, the expressions were highly variable; while being more variable, showed a trend toward higher expression in both HIV groups.

The observed increase in immunophilin expression may be a result of chronic neuroinflammation and activation of microglia resulting from the HIV infection. The number of infiltrating macrophages and activated microglia are better predictors of HIV encephalitis than viral load per se [184, 185]. The immunohistochemistry in Section 3.3.5 showed expression of the two immunophilins in neuronal populations and it is important to note that neurons are not infected by HIV, as they do not express the viral receptor CD4 or coreceptor CCR5, but rather microglia and monocytes are. HIV-infected monocytes secrete chemokines and cytokines such as TNF- $\alpha$ , IL-1 $\alpha$  and IL-1 $\beta$  [178, 184]. These two cytokines in particular were shown to alter GR signaling without altering cellular GR concentration [23, 25, 26, 177]. Our *in vitro* data in Figure 3-16 showing transient early increase in *FKBP4* and later increase in *FKBP5* could help explain this phenomenon. Gene transcription was elevated following exposure to conditioned media of HIV-infected microglia, shown in Section 3.3.4. These data are also in-line with a previous study whereby Achim and Avramut showed higher expression of the immunophilin

FKBP12 in the HIV infected brain [8]. If the immunophilins share similar promoter regions, containing SP1 binding elements and CCAAT boxes, discussed in Section 2.2.1, it would make sense that immunophilin genes may be inducible by mechanisms of neuroinflammation such as cytokine signaling mentioned above.

The specific mechanisms of immunophilin upregulation in HIV is undetermined, but they are likely to be different pathways because the timing of the upregulation was different. *FKBP4* upregulation preceded *FKBP5* upregulation (Figure 3-16). The temporal difference between *FKBP4* and *FKBP5* induction may be caused by a feedback loop whereby increased FKBP52 protein causes more transcriptionally active GR-signaling, and subsequent increase in *FKBP5*, and the *FKBP4* induction was transient. How this loop plays out in the chronically infected brain remains to be determined. Furthermore, with HPA axis-regulated elevated cortisol levels, it could be possible that GR signaling in the brain is altered in HIV depending on the cellular levels of FKBP52 protein, which we show is increased in a subset HIV patients, Figure 3-6. By conditioning media from a cell-free supernatant of HIV-infected microglia, we observed an increase in immunophilin expression. Our observations may be a cellular mechanistic explanation for the previously published studies showing cytokines, secreted by HIV-infected microglia, alter GR signaling. Treating SH-SY5Y cells with combinations of  $\text{TNF}\alpha$ ,  $\text{IL-1}\alpha$ , and  $\text{IL-1}\beta$ , knocking-down expression of their receptors, or expressing a dominant-negative mutant of the receptors, then subsequently measuring *FKBP4* and *FKBP5* expression would test this new hypothesis.

### **3.4.2 Balance of FKBP4 and FKBP5 Genes**

Figure 3-11 illustrated a positive correlation between *FKBP4* and *FKBP5* expression in the Control group. This correlation disappeared in the MDD and MDD/Psychosis groups. These

data imply that there may be a homeostatic balance of FKBP51 and FKBP52 that is dysregulated in mood disorders. In the HIV and HIV/MDD group, the correlation also disappeared, and the expression levels of both immunophilins is elevated, which is consistent with the elevation other immunophilins in HIV observed by Avramut et al [32].

Clinical data for the HIV patients from the CNTN groups were available. The HIV/MDD patients had all presented at the clinic with an MDD episode within the past 6 months and a subset had presented within 1 month. The gene expression of both *FKBP4* and *FKBP5* trended toward elevated in the group presenting with an MDD episode within 1 month compared to the 6-month. The small sample size did not allow for statistical significance, but it is interesting nonetheless, indicating that these genes could play a role in an MDD episode through the HPA axis dysregulation and GR dysfunction observed in MDD.

### **3.4.3 Polymorphism Analysis of *FKBP5* in MDD**

To test for the potential association of two polymorphisms of the *FKBP5* gene with MDD in our cohort, we performed allelic discrimination assays for two SNP's, rs1360780 and rs3800373, which had been previously shown to associate with various mood disorders. Our sample size is quite low for gene association study, however our autopsy collection is unique in having prospectively acquired clinical data on the presence of MDD. A standardized clinical instrument at the HIV Neurobehavioral Research Center (San Diego, CA) [186] and the Stanley Foundation (Bethesda, MD) [187] verified MDD in the cohort, and it is important to perform the genotyping of our cohort despite the small sample size. In contrast, other autopsy psychiatric studies do not have MDD diagnoses verified by a standardized instrument rather by either retrospective analysis of clinical notes or by interviews with family members. We therefore are confident in our clinical groupings.

In genotyping, we did not seek to identify new biomarkers, but rather confirm and further characterize our study groups. Furthermore the abstract mathematical association of a polymorphism with a mental diagnosis, while interesting, is not indicative of function. The basis of a polymorphism linkage to MDD may be in underlying regulation of GR signaling as a function of the gene product itself leading to dysfunction in disease. The disease, in this case MDD, is a well-defined description of symptoms but the identification of gene polymorphisms associated with a psychiatric diseases is misleading in that a polymorphism is an actual physical entity with potential functional consequences in cellular and physiologic mechanisms.

These two SNP's are associated with unipolar depression, peritraumatic dissociative disorder, PTSD, and MDD: disorders hallmarked by HPA axis dysfunction [140, 141, 143, 188]. Rather than being biomarkers for a specific disease like MDD, identification of SNP's in psychiatric disorders is informative in two aspects. First, identification of a SNP with potential functional consequences in the cell can relate to the function of its specific gene products and relate to the etiology of disease in order to uncover basic biochemical processes. In that case, processes in frontal cortical neurons. Secondly, in reality the SNP's associate more with a physiologic mechanism than a set of diagnostic criteria, for example HPA axis dysregulation than MDD. The SNP may point toward underlying physiologic mechanisms but it is developmental chance or environment that lead to progression of a specific set of symptoms to classify the disorder as a particular disease.

The SNP, rs1360780, located in Intron II, which contains HRE's, potential alternative promoter regions, and distal enhancer elements, had genotype frequencies significantly different from expected in Control, and HIV. Since genotype should be independent of HIV infection, and also Control should be similar to North American Caucasian population, it is unclear whether the increase in TT genotype of the MDD/Psychosis is of consequence. The expected numbers in our Chi Square analysis were derived from published genotype frequency data in the

GeneCard database for the North American Caucasian population, whose sample size was only 24, Gene Card identifier *ss4777328* [189].

Our sample size is quite small for population genetics-studies, but the observation with regard to the 3' UTR is interesting nonetheless. We found that the rs3800373 CC genotype more frequent in the MDD and MDD/Psychosis group, Table 3-4, this SNP is located in the 3'UTR of the mRNA, and could potentially affect protein translation. In Figure 3-8, we show higher protein levels of the *FKBP5* gene product, FKBP51, in portions of the MDD and MDD/Psychosis groups as compared to Control, while in Figure 3-9, we do not find a change in transcription levels, it may be that this 3'UTR polymorphism affects translation efficiency. Our data comparison methods, based on comparing to Controls, precludes determining whether higher protein amounts are found in the minor C allele, but it would be an interesting next-step. Furthermore, new research on micro-RNAs show that mRNA stability, based on micro-RNA binding in 3'UTRs affects the half-life of certain transcripts [190]. This would be another possibility of another level of modulation of cellular FKBP51 levels and thereby modulation of glucocorticoid signaling and HPA axis function.

The SNP's studied here were identified to be associated with MDD by Binder et al. through a genome scan in a region of chromosome 6 that encompassed the *TULP1*, *FLJ25390*, *CLPS*, and *FKBP5* genes. Four SNP's were identified to associate with MDD in *FKBP5* and strong association was made to rs1360780. The minor allele was associated with both an increased recurrence of episodes and response to therapeutic drug treatment. Indicating that the SNP may be functionally related to HPA axis. This study utilized 339 normal controls and 294 MDD patients [140]. A similar study, however, failed to find association of the two SNP's rs1360780 with response to antidepressive medication when the medication was controlled specifically to be 20 mg / day fluoxetine and that age had a large impact on medication-response

[191]. The genetic background of the two studies was different as well, the Binder study-group being German and the Tsai study-group being Chinese.

The SNP's rs3800373, rs1360780, and rs4713902 in *FKBP5* gene associated with bipolar disorder in a large family-based study. The study recruited a total number of 1,188 individuals in 317 families with 554 bipolar offspring. The minor alleles had a dominant effect in increasing risk for bipolar disorder with  $p = 0.03$  for rs3800373 and  $p = 0.13$  for rs1360780 [192].

The two SNP's analyzed in the current study also correlated to PTSD in adults who had suffered child abuse as adults. This study utilized 725 normal controls, 175 patients, who had childhood traumatic experiences such as witness violence or assault; with a subset being abuse-victims. Both rs3800373 and rs1360780 correlated to development of PTSD in patients only in the patient subset of abuse [188].

A study analyzing peritraumatic dissociation in medically injured children found an association with *FKBP5* polymorphism [141]. Forty-six medically injured children. Medical injury is defined simply as injuries requiring professional medical attention, they resulted mainly from motor vehicle accidents, physical assault by a non-relative, or falls. This study was similar to ours in that it was hypothesis-driven and targeted the specific SNP's: rs3800373 and rs1360780. They found that the minor alleles correlated with dissociation during the accident ( $p < 0.05$  for both SNPs) and stronger correlation with dissociation since the accident ( $p < 0.001$  and  $p < 0.03$  for rs3800373 and rs136078, respectively) [141].

One other study failed to identify *FKBP5* as a genetic marker in mood disorders using affective psychosis as a study group [142]. This study grouped manic-depressive and MDD patients together in "affective psychosis," 188 patients with 248 control subjects. It was a case-controlled prospective study that recruited and followed individuals prior to diagnosis. Although no significant association was made with MDD, there was a nominal association of two-locus

haplotype, meaning both alleles transmitted together on the same chromosome, of rs1360780 (C) and rs3800373 (T).

A recent interesting genotyping experiment recruited 64 normal individuals and subjected them to psychosocial stress and measured recovery from stress based on physiologic parameters and subjective self-reporting [193]. This is unique from the other *FKBP5* association analyses in that it is a before-after experiment measuring physiologic responses in the absence of disease. There was a profound genetic effect of *FKBP5* on cortisol response during “anticipation” period of the stress and impaired recovery of the cortisol secretory response following the psychosocial stress administration. Further, Ising et al reported delayed recovery in self-reporting of anxiety. Interestingly, there was no association with the ACTH response [193]. ACTH is secreted by the pituitary to signal to cells of the adrenal medulla for secretion of glucocorticoids, namely cortisol. ACTH secretion is stimulated by CRF from the hypothalamus, which itself is stimulated in response to external stress and stimuli. If the ACTH response is independent of *FKBP5* allele while cortisol and self-reported anxiety do associate with the *FKBP5* polymorphism, it may be that *FKBP5*'s role in mood disorders is more closely tied with the cortisol response in the brain than peripheral stress response.

Table 3-8 summarizes the findings of eight genotyping studies that analyzed the *FKBP5* SNP's that we have studied in our CNTN / Stanley Foundation cohorts of MDD and HIV. In general, either SNP associates with a mood disorder. The disorders studied here all have in common that they are mood disordered characterized, in part, by dysfunction HPA axis. These results, along with ours, support the notion that *FKBP5* and its gene product, the protein FKBP51, could be involved in glucocorticoid signaling in the brain and dysregulation lead to disorder. That the SNP's are located in non-coding regions, implies the mRNA stability or protein translation are key factors in homeostasis.

Future work to uncover the functional consequences of the SNP's could provide interesting insights into the molecular basis neuropathology caused by HPA axis dysregulation. For example, micro-RNA's in the 3'UTR could affect mRNA turnover or protein translation while enhancer or promoter elements in the Intron I could affect gene transcription. In fact, one study did identify alternate intronic promoters for *FKBP5* gene that produces shorter versions of the mRNA . A SNP in a particularly important location could affect expression of these smaller transcripts that have downstream, unforeseen consequences on the balance of FKBP51 protein concentration, and further downstream on GR signaling in pertinent cell types such as neurons in the frontal cortex.

**Table 3-8. Summary of Previous Studies Involving *FKBP5* SNP's rs1360780 and rs3800373**

<u>Citation</u>	<u>Disease</u>	<u>n</u>	<u>Significant SNPs</u>	<u>Notes</u>
[140]	MDD	294 Dis. 339 Cont.	rs1360780	Screened region of Chr 6
[192]	Bipolar	491 Dis. 1118 Total	rs3800373 rs1360780 rs4713902	Family-based study. Effect of minor allele is dominant
[188]	PTSD	175 Dis. 725 Cont.	rs1360780 rs3800373	Correlated to PTSD scale score, p<0.05
[141]	Dissociation Disorder	46 Total	rs1360780 rs3800373	SNP's increased risk for developing disorder after traumatic stress.
[193]	Healthy-Psychosocial Stress	64 Total	rs1360780 rs3800373	Impaired cortisol secretory response, delay reduction of anxiety.
[191]	MDD and Dysthymic Disorder	125 Dis.	rs3800373	No correlation, age significant factor in response to 20 mg/day fluoxetine
[142]	Affective Psychosis	188 Dis. 248 Cont.	rs3800373 rs1360780 rs4713902	No correlation, prospective study, 2-locus haplotype associated weakly
[194]	MDD	1809 Dis. 739 Cont.	rs1360780 rs4713902	-780 associated with MDD, -902 associated with remission. Not significant in American Black pop.

### **3.4.4 Immunohistochemistry of FKBP51 and FKBP52**

The goal of the immunohistochemical analysis was to determine whether neurons express the immunophilins and in which cortical layers. A more detailed stereological analysis would be dependent on availability of tissue of good quality. The majority of the cases analyzed were sections unsuitable for quantitative analysis, but qualitative illustration of neuronal expression is

shown here. For immunohistochemistry of FKBP51 and FKBP52, twenty-four cases were analyzed, two slides each. The optimal antibody concentration was determined and example stainings are illustrated in Figures 3-19 and 3-20. The slides were paraffin embedded tissue from the frontal cortex provided by the CNTN, therefore it should be noted that the slides were from HIV<sup>+</sup> individuals. The Stanley Foundation provided frozen sections mounted on glass slides and we were unable to satisfactorily immunolabel them. Although the materials available were unsuitable for quantitative analysis, the qualitative assessment of FKBP51 and FKBP52 expression in layers of the frontal cortex is informative.

This is the first immunolabeling for FKBP51 and FKBP52 in the frontal cortex known to the author. The immunohistochemistry of FKBP51 and FKBP52 illustrated in Figures 3-19 and 3-20 showed that they are expressed mainly in pyramidal neurons in Layers II and V of the cortex and in a subset of smaller cell bodies of Layer IV. In addition, FKBP51 was also expressed in axonal tracts of the neuropil. The distribution of expression of FKBP51 and FKBP52 in cortical tissue in certain neuronal populations of the cortex may be relevant to mood disorders [10-12, 195]. Chronic corticosteroid exposure in rats caused reorganization of the dendritic fibers in neurons of the external pyramidal layer of the cortex, showing decreased distal Golgi-staining and arborization and increased proximal dendrites to the pyramidal neurons [10]. Chronic glucocorticoid exposure led to a decrease in serotonin and catecholamine receptor sites in the frontal cortex [195]. Since these layers specifically stain in neurons for the immunophilins FKBP52 and FKBP51 which are intracellular modulators of GR signaling, our findings could implicate that if these cells coexpress the GR, they may have an ability to individually regulate GR signaling and this system may be dysregulated in the chronic neuroinflammation characterized by activated microglia and monocytes [196], leading to vulnerability to developing mood disorders like MDD.

### 3.4.5 Limitations and Further Questions

There were some limitations to the study presented here in both the methods and materials worthy of note, and some possible future experiments that would overcome them and confirm findings presented here.

The tissue available for analysis is from the frontal cortex, and is fresh frozen tissue. While staff conducting the autopsy and tissue-archiving may take precautions and perform excellently, the fact remains that the brain is from a deceased individual and that gene expression and protein expression reflect a combination of genetic predisposition, chronic environmental conditions, chronic physiologic factors, and the acute physiologic state of the brain at the time of death. Our five study groups are: Control, MDD, MDD/Psyc, HIV, and HIV/MDD. These disease conditions are what we wish to be our independent variable and in an ideal scientific situation, measurement of protein and gene quantities would be the dependent variable: solely dependent on the disease condition. In reality these measurements also depend on physiologic factors surrounding the conditions at the time of death. Postmortem degradation of protein and RNA are also limitations, which we control for by normalizing to housekeeping genes and proteins, though this procedure itself is imperfect. We control for these factors by taking into account PMI, brain pH (when data available), and match the cohorts for age and sex. Furthermore, well-defined prospective study groups strengthen confidence in psychiatric classification of the cases.

Both the Western and the gene expression analyses were from sections cut from the frontal cortex. The brain is a heterogeneous organ with respect to cell type and cell density. We avoided the meninges, but microvasculature cannot be avoided with our method, laser microdissection may avoid microvasculature. The immunohistochemistry showed no staining in vascular endothelial cells, so differences in vascularity from sample to sample would not affect

the signal of the genes and proteins of interest, but *could* affect the signal of actin and *GAPDH*, the housekeeping protein and gene used to normalize for protein loading and RNA stability. For Western blot, analyzing all the samples from each group would have given a better idea of the spread of expression. Another way for normalization would have been to compare to an unrelated control; for example: signal from the same quantity of RNA or protein isolated from SH-SY5Y cells, comparing all the groups (including the Control group) to the signal from the cultured cells rather than comparing the disease groups to the Control group.

The Western analysis is susceptible to noise from factors unrelated to the actual sample. The transfer of the proteins from the polyacrylamide gel to the PVDF membrane must be even. The chemiluminescent reaction emitting light onto the film can also be variable, the developing time of the film must be consistent, and densitometric analysis is subject to the limitation of how dark the film can be (based on the chemical composition of the film, which may vary from lot to lot and by manufacturer), how many scales of grey the scanner can detect, and the analysis is limited to the range of greyscale (0-255) embedded in an 8-bit tagged image format file (TIFF) image in ImageJ. By running a representation from each sample group on a gel and only comparing within-gel for calculating fold-control, we subjected all the samples from a given gel to the same constraints and biases, so the result is a relative determination; relative to the Control samples run at the same time. Other methods like enzyme-linked immunosorbant assay (ELISA) or quantitative mass-spectrometry could overcome some of these limitations. To date, there are no commercially available ELISA's for the proteins of interest, commercially available antibodies have not been tested for this application, and standards like recombinant purified protein are costly. Matrix-assisted laser desorption ionization – time of flight (MALDI-TOF) mass spectrometry has been used for analysis of proteins in a mixture, however, the technique is best suited to identification rather than quantification; as there may be high background from abundant proteins.

The qPCR determination of *FKBP4* and *FKBP5* were subject to similar constraints as the protein determination. Fold-control was calculated using the  $\Delta\Delta CT$  method, that first compares amplification of the transcript of interest (*FKBP4* and *FKBP5*) to a housekeeping gene that should remain stable (*GAPDH*), and then calibrating to a Control. Our study compared the disease groups to the median of the Control, and also compared all the Controls to that particular median. Therefore the median Control was calibrated to be 1.00, and the other Controls were above and below this value, representing the spread in the normal population. Another method available of analyzing gene expression using qPCR would be calculating copy-number of transcripts. This method would necessitate the construction of standard curves for each sample would have been more costly, requiring a larger volume of reagents and destruction of a greater quantity of precious samples. Northern blotting for the genes of interest would also have been possible, however, all the limitations from Western blotting would apply and Northern analysis would not be superior to qPCR.

In Section 3.3.4, we analyzed the gene expression of *FKBP4* and *FKBP5* after exposure of SH-SY5Y cells to 10% conditioned media of HIV-infected microglia. The SH-SY5Y cells are a well-established neuronal cell line, and in cell culture, provide a homogenous population for quantitative analysis that overcomes the limitations of heterogenous cell populations described above. The responses of SH-SY5Y cells may be more reliably quantified owing to homogeneity, but may not extrapolate perfectly to in vivo human brain conditions. They are a neuroblastoma cell line that can be differentiated to dopaminergic neuronal phenotype. The region of the brain studied here, the frontal cortex, consists primarily of glutamatergic neurons and  $\gamma$ -aminobutyric acid (GABA)-ergic interneurons. We extrapolate our data to make assumptions about chronic conditions of HIV-infection and MDD, while cell culture treatments and analyses are inherently models of acute insult. Nevertheless, we have shown as a first-step that immunophilins are upregulated in neuronal cells in culture in response to HIV-infected

conditioned media. Animal models of HIV infection, for example comparing immunophilin expression in the transgenic mouse model of astrocytic secretion of HIV gp120 [197], a component of the HIV envelope shown to induced neuroinflammation, with control mice would be informative. Even this model has limitations owing to the genetic divergence of the *FKBP4* and *FKBP5* genes in recent evolution described in Section 2.2.1.1. Therefore a human model was desired to show a direct interaction between HIV-infected microglia and neurons that removed the external variables surrounding autopsy studies described above, and so a reproducible neuronal cell line was utilized.

The goal of our genotyping analysis of the two *FKBP5* SNP's was to further characterize our patient populations. The technicalities and interpretations of the assay are straightforward. However, our sample size is inappropriate for extrapolating our findings to identification of a biomarker for MDD or MDD/Psyc. Our study used very specific diagnostic criteria and specifically matched sex and age, analyzing the entire CNTN population disregarding these stricter criteria would provide more power to a genotyping study. Other genotype studies ranged from 1,188 in a family-based bipolar genetic analysis to 64 subjects in an experimental before-after functional analysis of normal individuals.

MDD is a description of symptoms characterized mainly by depressive episodes consisting of: depressed mood, anhedonia, eating disorder, hyper- or in- somnia, lethargy or agitation, self-loathing, impaired concentration, and suicidal thoughts [198]. A polymorphism is an actual physical entity with measurable physical consequences in a cell or tissue, identification of polymorphisms is useful for helping to uncover physiologic mechanisms underlying the symptoms, in case of this study, physiologic mechanisms regarding HPA axis dysregulation in the brain. Physical manifestations of an *FKBP5* SNP may be altered GR signaling in neurons followed by reduced synaptic and dendritic density, which leads in certain environments to MDD. However, assuming that any one SNP of any one gene could be a biomarker for MDD,

would be analogous to assuming that a bacteria culture of the upper respiratory tract would diagnose rhinitis caused by allergy to pollen. Rather, the SNP helps identify underlying cellular mechanisms and identify susceptibility and it is environment or developmental chance that leads to a particular disorder like MDD, bipolar disorder, PTSD, or peritraumatic dissociation.

Immunohistochemistry is subject to limitations as well. Our study used Nova Red as an indicator, and visualization of staining is dependent on peroxidase reaction and endogenous peroxidases must be blocked with a peroxide and methanol mixture as described in the Materials and Methods (Section 3.2.6). Also, concurrent negative controls using no primary antibody will test for such false-positives. The specificity of the antibody should be assured as well. For this reason it is important to use the antibody at the lowest concentration that yields a signal. Competition of the antibody with a blocking peptide that would block binding of the antibody to antigens in the tissue would show specificity. The best assurance would be by immunohistological analysis in knock-out mice that genetically lack the antigen of interest and comparing staining with control. In the case of the FKBP51 and FKBP52 immunophilins, the expected staining patterns based on published mouse situ hybridization images was observed (Compare Figure 1-1 with Figures 3-29 and 3-20), and not all cell types and populations stained positive. It is uncertain whether commercially available antibodies to FKBP51 or FKBP52 would detect the mouse homologues owing to genetic divergence. For example, our lab was unable to stain FKBP52 in a monoclonal mouse antibody generated against human FKBP52 (Stressgen SRA1400) in a paraffin sections of *Rhesus* brain but we achieved successful staining in the corresponding region in human paraffin embedded sections.

There are limitations to the materials and methods used here and there are further controls that could rule out possible false-positives. However, the well-defined clinical characterization and age- and sex- matching in the autopsy patient groups strengthens its findings. The detection and quantification of the proteins and genes is suitable based on available techniques. The cell

cultures are a homogenous neuronal population lending itself to quantification. The immunohistochemistry showed staining above background in specific populations.

### 3.4.6 Conclusion

We hypothesized that FKBP51, as modulator of the nuclear translocation of the GR, would be lower in MDD. The rationale for the hypothesis is that those individuals whose neurons were not able to modulate GR signaling as effectively would be more vulnerable to cortical synaptic and dendritic simplification, neuropathologic conditions noted in depression [11, 169]. Instead, FKBP51 is increased at both the transcript and protein levels in MDD. However, FKBP52, the adapter protein that facilitates active GR trafficking was variable in both directions, elevated *and* decreased in MDD and MDD/Psych. *FKBP4* mRNA and protein is elevated in during HIV infection. In contrast to *FKBP5*, *FKBP4* fold-change was not significantly increased in HIV, but in HIV<sup>+</sup>MDD. Perhaps immunophilins, as a class of chaperone and adapter proteins, are upregulated during chronic inflammation in response to cytokine signaling. If the agonist to GR signaling, in this case *FKBP5* is not significantly upregulated to compensate for increased *FKBP4* expression and thus increased ability of GR to be functionally active. Cortical neurons would be rendered more susceptible to the effects of glucocorticoids and the cascade leading to subtle pathologies of depression.

#### **4.0 IMMUNOPHILIN FKBP52 MODULATES THE DISTRIBUTION OF ACTIVATED GLUCOCORTICOID RECEPTOR IN NEURONS**

Mood disorders associated with dysfunction of HPA axis are common psychiatric conditions. The GR is a steroid-activated nuclear receptor that upon binding to cortisol translocates to the nucleus, targeting genes related to neuronal metabolism and plasticity. In patients suffering from depression, elevated cortisol levels result in a decreased ability of neurons to return to resting conditions.

We investigated the molecular events associated with the FKBP52 and FKBP51 response to cortisol exposure in neuronal cell cultures and subsequent effects on GR translocation. We found that the immunophilin ligand FK506 inhibited nuclear translocation of the GR and expression of GR-responsive genes. Furthermore, si-RNA knockdown of *FKBP4* gene, coding for FKBP52, inhibited cortisol-activated GR nuclear translocation.

We propose that immunophilins are key modulators of the cortisol-HPA axis response to stress and related chronic brain disorders. Altering neuronal gene expression through immunophilin-mediated GR signaling pathways may represent a novel therapeutic avenue in psychiatric diseases.

## 4.1 INTRODUCTION

Mood disorders associated with altered HPA axis function are common psychiatric conditions [199, 200]. In response to physical, emotional, and cognitive stress, CRH is secreted by the hypothalamus, signaling to the pituitary to release ACTH. ACTH then enters the blood stream to stimulate cells of the adrenal cortex to increase the production of corticosteroids, mainly glucocorticoids such as cortisol. Glucocorticoids have an array of physiological effects to prepare the body for fight-or-flight, including effects on neurons and glia of the brain [27, 201].

The type II corticosteroid receptor, GR, has low affinity for cortisol and is expressed in the hypothalamus, hippocampus, and frontal cortex, and acts to mediate feedback inhibition of the HPA axis [202]. GR is a steroid-activated nuclear receptor, and upon cortisol-binding, GR translocates to the nucleus where it binds target DNA sequences as a positive or negative transcription factor to mediate mRNA production of genes related to neuronal plasticity, neuronal activation, and neuronal metabolism [203, 204]. In depressed patients, the negative feedback loop is deficient at reducing elevated cortisol levels, which is the basis of the dexamethasone suppression test for evaluation of HPA function [17]. The dexamethasone suppression test measures HPA axis function by oral administration of the synthetic GR agonist, dexamethasone, and measurement of the patient's circulating cortisol and ACTH. In normal individuals, the feedback inhibition loop of the HPA axis will cause cortisol and ACTH to be lowered and elevate to normal over time [205]. In HPA axis dysregulation, for example

Cushing's Disease and MDD, cortisol and ACTH are not suppressed and patients are called "non-suppressors" [206]. The glucocorticoid cascade hypothesis claims that deficiency of the HPA axis to regulate circulating cortisol results in a feed-forward mechanism of increased cortisol levels during stress and a decreased ability to return to resting conditions, consequently all cells, including neurons, are subject to prolonged GR activation and its downstream effects [17].

This study analyzes the role of two adapter proteins, putative chaperones, to the GR, that are of the immunophilin protein class. Two immunophilins, FK506 Binding Protein of molecular weight 51 (FKBP51) and its related protein FKBP52, are thought to be involved at the cellular level in regulation GR signaling [14]. FKBP51 acts as a competitive inhibitor to its genetic relative FKBP52, whose gene ID is FKBP4 [14]. The protein products of *FKBP4* were originally identified by co-precipitation of the activated GR/HSP90 complex as "HSP56" [207]. Molecular studies have since clarified that it is actually two proteins of 52 and 59 kilodaltons, owing to two poly-adenylation sites of the *FKBP4* gene sequence which would produce two differently-sized mRNA [208]. There is no known functional difference between the long or short form, for our purposes, FKBP52 and FKBP59 are synonymous and we will refer to the protein as FKBP52.

FKBP52 colocalizes with microtubules, binds specifically to dynein by its N-terminal immunophilin (also known as prolyl isomerase) domain, and its enzymatic activity is required for this interaction [209]. The FKBP52 knockout male mouse displays decreased prostate development, malformed seminal vesicles, and reproductive abnormalities that correlated to decreased androgen levels or inadequate androgen receptor response [137]. The female knockout had no uterine receptivity for embryo implantation, a progesterone receptor-

mediated event [136]. The effects of FKBP52 knockout on the developing or adult male and female mouse brain have not yet been studied. FKBP52, through its TPR domains, links GR to the molecular motor protein dynein [210]. Dynein is a retrograde motor protein, this interaction between GR-FKBP52-dynein, may be of particular importance in cells such as neurons where the distance between the receptor and the nucleus may be long.

There are data indicating that GR plays a role in MDD and mood disorders such as PTSD [205]. The administration of reserpine, a drug inducing depressive symptoms, causes altered GR signaling and glucocorticoid resistance [211]. In fact, transgenic mice that under- or overexpress GR have been used as models of depression or post-traumatic stress disorder (PTSD) [15, 212, 213]. Pariante et al showed that antidepressants exert effects on GR function, not expression [23]. It is thought that prolonged high glucocorticoid levels cause GR to be saturated with ligand, signaling to the nucleus, following inactivation, leading to overburdening the recycling capacity of GR, and finally diminishing function of GR [205]. Decreased GR mRNA was found in the frontal cortex of postmortem tissue of depressed, bipolar, and schizophrenic patients [12]. In a rat model of PTSD, which involves subjecting the mice to a single-prolonged stress, long-term potentiation in the CA1 of the hippocampus was impaired, and administration GR antagonist RU40555 prevented this effect [214]. In this model, the rats exhibited enhanced contextual fear conditioning one week following the single-prolonged stress induction, and this effect was also prevented by concomitant administration of the GR antagonist [214]. Interestingly, the abnormal glucocorticoid feedback regulation in HPA axis dysfunction was shown to occur at the level of the brain [215], indicating that GR signaling in the brain would be an interesting target of study for such diseases as MDD.

Species of New World primates have general resistance to glucocorticoids [216]. Since they do express the GR, which when purified, binds to cortisol, the mechanism of resistance was puzzling [217, 218]. It was found that a soluble factor, which turned out to be FKBP51, inhibits binding of cortisol to GR. It turns out that expression of FKBP51 is 13-fold higher in these primates, and FKBP52 expression less than one-half compared to humans; effectively rendering the monkeys resistant to the effects of cortisol mediated by GR [61]. FKBP51 does not have a functional isomerase domain and acts as a competitive inhibitor of FKBP52 in the context of GR signaling [168]. These data, along with indications that GR function is dysregulated in the brain in MDD, indicate that FKBP52 / FKBP51 kinetics may be important in GR-mediated pathologies such as depression.

There may be a genetic component in variants on the gene encoding FKBP51 (gene ID *FKBP5*). Single nucleotide polymorphisms (SNP's) in the gene encoding the immunophilin FKBP51 were recently found to be linked to unipolar depression . The functional significance of these SNP's is unknown [140, 143]. A study by Binder et al linked polymorphisms in the *FKBP5* gene to increased recurrence of depressive episodes and rapid response to drugs. Recently, they linked the *FKBP5* polymorphisms with risk of post traumatic stress disorder (PTSD) symptoms in adults who suffered from abuse during childhood [188]. The same alleles, rs3800373 and rs1360780, were associated with increased occurrence of peritraumatic dissociation in children after physical trauma requiring medical attention, for example motor vehicle accident or assault, [141], which is a risk factor for developing adult PTSD [219]. These findings warrant further investigation into the function of FKBP51 in neurons.

Past studies have shown that FKBP52 and FKBP51 differentially regulate the function of the GR through the interaction of FKBP52 with dynein [14, 79, 132, 133, 209]. Although there

is conflicting evidence whether FK506, which dissociates both immunophilins from the GR, would enhance or inhibit nuclear translocation of the GR [220].

We hypothesized that inhibition or knockdown of FKBP52 would inhibit the effects of cortisol in neuronal cells. We investigated molecular functions of FKBP52 and FKBP51 in the context of cortisol exposure in neuronal cell cultures. Immunophilin ligand FK506, which is commonly used as an immunosuppressant in organ transplant patients, inhibited nuclear translocation of the GR and altered nuclear distribution of the FKBP51 chaperone in neurons. Knockdown by si-RNA of FKBP52 inhibited cortisol-activated GR nuclear translocation.

## **4.2 MATERIALS AND METHODS**

### **4.2.1 Cells**

The neural cell line SH-SY5Y was used for protein extraction and immunoprecipitation. SH-SY5Y cells were also used for transfection with siRNA to knockdown FKBP52 translation and determine whether FKBP52 plays a role in nuclear translocation of GR. Primary human neuroglia cultures were used in qualitative microscopic analyses.

SH-SY5Y cells were plated at  $5 \times 10^5$  cells/well on glass coverslips in 24-well plates which had been coated with poly-L-ornithine and laminin by sequentially incubating overnight at 37°C first with 0.1 mg/mL poly-L-ornithine hydrobromide in H<sub>2</sub>O solution (Sigma P5666) and then 2 µg/mL laminin in H<sub>2</sub>O (Sigma L2020). SH-SY5Y cells were grown in media composed of 1:1 mixture of Ham's F-12 Media (Gibco 31765-035) and Dulbecco's Modified Eagle Media (DMEM) (Gibco 11960-044) supplemented with 2 mM glutamine (Gibco), sodium bicarbonate

(Gibco 25080-094), sodium pyruvate (Gibco P333-1000), and 10% fetal bovine serum (Gibco 16140-071), and 50  $\mu\text{g}/\text{mL}$  penicillin and streptomycin (Invitrogen 15640-055). After three days in culture, the media were supplemented with 1  $\mu\text{g}/\text{mL}$  retinoic acid (Fisher Scientific AC41897) for differentiation, media were changed daily with the retinoic acid supplement until cells showed neuritic networks, typically 3-5 days.

Human forebrain fetal tissue was acquired according to the University of California San Diego Internal Review Board guidelines through Advanced Bioscience Resources (Alameda, CA). Tissue was processed as previously described, and detailed in Appendix B [34, 221]. Cells were seeded at  $10^6$  cells per well on glass coverslips coated with polyornithine and laminin in 24-well plates and maintained in DMEM-F12 media (Gibco 12634-010) supplemented with 2mM glutamine, 5% human serum, and 10  $\mu\text{g}/\text{mL}$  gentamycin sulphate (Gibco 15750) for four weeks with media-change every 3 days. Toxicity of treatments to primary neuroglia cultures is measured by removing 50  $\mu\text{L}$  aliquots of medium and measuring release of lactate dehydrogenase by following manufacturer's protocol of the CytoTox LDH assay (Promega G1780), results are illustrated in Figure 4-1, indicating that none of the treatments were toxic according to measurement of LDH release.

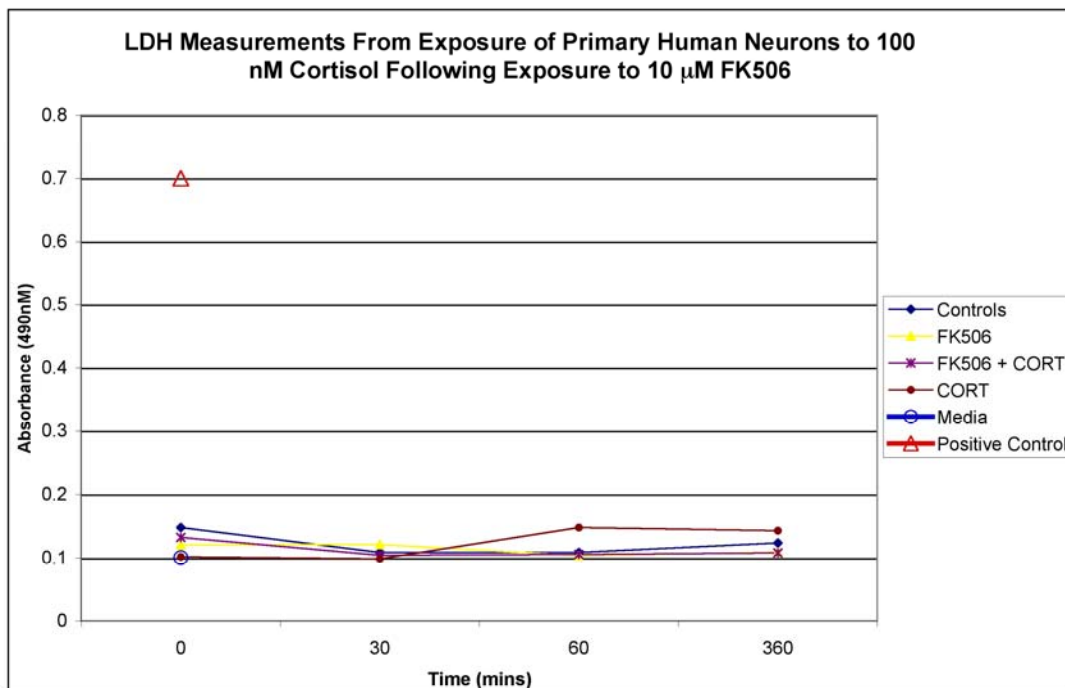


**Figure 4-1. LDH Measurements From Exposure of Primary Human Neuron-Glia Cultures to 100 nM Cortisol and 10  $\mu$ M FK506.** Primary human neuron-glia cultures grown for 4 weeks on glass coverslips and exposed to 10  $\mu$ M FK506, 100 nM cortisol, both FK506+cortisol, or media alone. Supernatant (10  $\mu$ L) was removed at 0, 30, 60, and 360 min and LDH activity measured by ELISA in CytoTox assay. Positive control is a cell-lysis suspension from cultures grown in parallel. The treatments were not toxic.

#### 4.2.2 Immunoprecipitation

SH-SY5Y cells were grown to 80% confluency in T-75 flasks and cells were differentiated using 10  $\mu$ g/mL retinoic acid for three days. Media were changed and supplemented with 10  $\mu$ M FK506 (Fisher Scientific NC9444052) for 2 hr, 100 nM hydrocortisone (Sigma H6909) for 30 min, or nothing prior to lysis. Total protein was obtained by washing media 2 times 10 min in 37°C PBS to remove media, incubating with 0.5 mL ice-cold lysis buffer consisting of 50 mM 2-amino-2(hydroxymethyl)1,3-propanediol hydrochloride (Tris-HCl), pH 7.4, 150 mM NaCl, 0.2

mM Na<sub>3</sub>VO<sub>4</sub>, 1 mM phenylmethanesulfonyl fluoride, 1 mM ethylenediaminetetraacetic acid (EDTA), 5 µg/mL aprotinin, 1% Triton-X 100, and 0.1% sodium dodecyl sulfate (SDS). Lysate was pre-cleared for non-specific binding by incubating with 1:100 streptavidin-coated magnetic beads (New England Biolabs S1420S) for 30 min, 4°C, and separated from solution using a magnetic microfuge tube rack (New England Biolabs S1506S) prior to incubation with primary antibodies. Immunoprecipitation was performed by incubating pre-cleared lysate with primary antibody for 2 hr at room temperature, followed by biotinylated secondary antibody for 2 hr, and complexes were immobilized on streptavidin-coated magnetic beads (New England Biolabs S1420S) for 30 mins, 4°C, and separated from solution using a magnetic rack (New England Biolabs S1506S). After immobilization, magnetic bead with antibody-protein complexes were washed 3X 30 mins 4°C with gentle rotation in wash buffer consisting of 10 mM Tris-HCl, 1 mM EDTA, 1 mM ethyleneglycoltetraacetic acid, 150 mM NaCl, 1% Triton-X 100, 0.2 mM Na<sub>3</sub>VO<sub>4</sub>, 5 µg/mL aprotinin. To maintain complexes caused by presence of ligands, all buffers were supplemented with vehicle (1:1,000 ethanol), 10 µM FK506, or 100 nM cortisol.

Immunoprecipitation products were eluted in 100 µL SDS- PAGE tris-tricine buffer (Biorad 161-0744) and heated to 90°C for 3 min, followed by separation from magnetic beads using the magnetic tube rack, and eluate separated immediately by gel electrophoresis in 10% polyacrilamide gel (Biorad) for western blotting. Antibodies used for immunoprecipitation: mouse anti FKBP52 (1:50, Stressgen #SRA-1400), rabbit anti FKBP51 (1:100 Novus NB300-519), control antibody was mouse IgG (1:100, Jackson # 015-000-03).

### 4.2.3 Western Blotting

Primary antibodies used for Western Blotting: mouse anti dynein (1:200, Affinity Bioreagents MA1-070), rabbit anti GR (1:500, Novus Biologicals # NB300-610). For western blotting of immunoprecipitation product, HRP-conjugated secondary antibodies were purchased from Jackson ImmunoResearch (anti mouse #115-035-166, anti rabbit #111-035-144) and incubated at 1:10,000 at room temp for 2 hr. Chemiluminescence was performed following manufacturer's instructions of luminal reagent (Pierce Biologicals 32106). Because the siRNA experiments were performed in 24-well plates, at low cell numbers, the protein yield and Western signal are low, therefore for western blotting of the siRNA lysates, therefore biotin-conjugated secondary antibodies were used from Jackson ImmunoResearch (anti mouse # 715-065-151, anti rabbit #711-065-152, both 1:1,000, 2 hr room, temperature), and vector ABC kit was used for signal amplification (Vector laboratories PK-4002).

### 4.2.4 PCR and siRNA Synthesis

Prior to treatments, to confirm that SH-SY5Y cells expressed the GR, FKBP52, and FKBP51, reverse transcriptase-PCR was performed using the following primers were utilized from the National Library of Medicine Genbank datase as markers for the human genes: 1. For GR: F- actacacatccctaatgtgtgcc and R-gcatgtaaagctgcagtagcc; expected size 337bp (GenBank Accession G06351), 2. For FKBP52: F- agcgggtaaggctatgctaag and R- acttctcgtgtgtgctgtcca, expected size 650bp; 3. For FKBP51: F-gatccctcgaatgcaactctet and R-gaaaggcagcaaggagaaatga, expected size 650bp. After differentiation of the SH-SY5Y cells, RNA was isolated using Trizol according to the manufacturer's protocols (Invitrogen 15596) and cDNA was synthesized using Superscript

III Reverse Transcriptase (Invitrogen 18064). Forty PCR thermocycles were performed using 2 $\mu$ L cDNA in 50 $\mu$ L PCR reactions of Platinum PCR Supermix (Invitrogen 12532). PCR product was run on 1% agarose gel in Tris-Boric acid-EDTA buffer and visualized with ethidium bromide in UV.

The Dicer siRNA Generation Kit (Gene Therapy Systems # T510001) was used to generate siRNA to FKBP52 following manufacturer's protocols. The mRNA sequence for human *FKBP4* (Accession number NM\_002014) was used to design primers to amplify a 650 base-pair region of the mRNA spanning both Exon 2 and Exon 3, coding for the linker region between the two immunophilin domains, a region of high variation between individuals and very low homology with *FKBP5*. The primers are: FKBP52-T7-F gcg-taatacgactcactatagggag-agcggggaaggctatgctaag, FKBP52-T7-R gcg-taatacgactcactatagggag-acttctcgttgttgcgtcca (leader-T7 RNA polymerase promoter- **target sequence**). Differentiated SH-SY5Y cells were exposed to siRNA (250 ng siRNA, 3.5 $\mu$ L GeneSilencer reagent per well) for 24 hr prior to cortisol exposure. Control siRNA, specific to green fluorescent protein (GFP), was generated using the template plasmid and primers for GFP supplied by the manufacturer.

#### **4.2.5 Cortisol and FK506 Exposure**

Differentiated SH-SY5Y cells or primary human neuroglia cultures were exposed to vehicle or 10nM FK506 for two hours; followed by nothing or 100nM cortisol for various time points. Each treatment (vehicle, FK506, cortisol 30, 60, 180 min, and cortisol pre-treated with FK506) was performed in triplicate and cells were fixed in 4% paraformaldehyde for immunofluorescent labeling of GR and Hoechst 33342 (Molecular Probes H3570). Primary neuronal cultures were labeled for GR (Mouse 1:50 AbCam ab9568), FKBP52 (Mouse 1:100, Stressgen SRA1400), or

FKBP51 (Rabbit 1:40 AbCam ab54992). To determine cell types in culture, counter-labeling was performed. To identify neuronal dendrites and soma: MAP2 (Mouse 1:500 Sigma M9942; or Rabbit 1:1000 Cell Signaling Technologies 4542). To identify neuronal axons: Neurofilament (1:500 Rabbit Covance PRB574C or Mouse 1:1000 Cell Signaling Technologies 2835). To identify astrocytes: GFAP (1:400 Mouse Cell Signaling 3670). To identify microglia: *Ricinus communis* Agglutinin I (biotinylated RCA1, 1:1000 Vector Laboratories B-1085). Cells were permeabilized in 1% Triton X 100 for 30 minutes at room temp, and washed three times briefly with phosphate buffered saline (PBS) with 0.2% TWEEN-20 prior to blocking for 1 hr with 10% normal donkey serum in PBS-Tween. After fixing, washing, and blocking, cells were incubated with primary antibody overnight at 4°C. To reduce non-specific antibody binding to extracellular debris previously observed using rabbit antibodies, the wash buffer was supplemented with 100 mM NaCl for primary antibodies generated in rabbit. Donkey anti-mouse and donkey anti-rabbit Alexafluor 488 and 546 antibodies and Alexafluor 647-conjugated streptavidin were used at 1:2000, and cells were incubated with secondary antibodies at room temp for 2 hr.

#### **4.2.6 Quantitative PCR**

To assess whether GR-responsive genes, *FKBP5* and *BCL21A* are altered due to the presence of FK506, qPCR was performed. RNA was isolated from differentiated cells pretreated with or without 10  $\mu$ M FK506 followed by 100 nM cortisol for various lengths of time. For qPCR, 20 ng cDNA per reaction was used and 6-carboxyfluorocin (FAM) -labeled 20X prevalidated probes were purchased from Applied Biosystems. For *FKBP5*, assay Hs00188025\_m1; for *BCL21A*, assay Hs00236329\_m1; and for endogenous control we used the actin gene, *ACTB*,

assay 4352935E. TaqMan master mix (2X), purchased from Applied Biosystems was used in 20 $\mu$ L reactions on 96 well-plates and assays were performed at the University of San Diego Center for AIDS Research Genomics Core. Gene expression is reported as fold-control versus the median of the control-group using the  $\Delta\Delta$ -CT method comparing to housekeeping gene *ACTB* whereby  $\Delta CT = CT_{ACTB} - CT_{Gene}$ ,  $\Delta\Delta CT = \Delta CT_{Control} - \Delta CT_{Treatment}$ , and Fold-Control =  $2^{-\Delta\Delta CT}$ . Plotted are median fold-changes and error bars represent range as determined in triplicate.

#### **4.2.7 Imaging**

Images were acquired utilizing a 40X objective on a Carl Zeiss Axiovert 40 inverted fluorescent microscope with deconvolution capabilities. For 3D imaging, 10 planes were imaged at 0.5  $\mu$ m steps and deconvolved using the Nearest Neighbor algorithm in the image analysis software Slidebook 4.2 [222]. All the images for a particular experiment were acquired at the same time under identical parameters such as exposure time, intensity, binning, and Normalization settings following the conventions outlined in Slidebook 4.2 [222].

#### **4.2.8 Quantitative Imaging of Glucocorticoid Receptor Nuclear Translocation in SH-SY5Y Cells**

In order to quantify the nuclear and cytoplasmic staining of the GR in the SH-SY5Y cells, a method was adopted from Noursadeghi [223]. Basically, 10 fields from each treatment were acquired in a 40X object on a Carl Zeiss Axiovert 40 inverted microscope. Fields were selected randomly to reduce bias, the user focused only using the blue channel. For each field, 10 images were taken in 0.5  $\mu$ m steps in the z-plane with 2X binning, green channel 1.75 sec, and blue

channel 0.650 sec. After deconvolution, images were exported as tagged image format (TIF) files. A representative image is shown in Figure 4-2a.

Ten fields from a particular treatment were opened in Image J software and converted to a stack to treat all images identically. The green and blue color channels were separated and converted the greyscale bitmap as shown in Figure 4-2b. A threshold was set for the blue image to delineate the nuclei, Figure 4-2c. Image math, subtracting the thresholded image from the green image yielded the nuclear staining, Figure 4-2d, left. Subtracting the inverted thresholded image from the green image yielded cytoplasmic staining, Figure 4-2d, right. The text file of the intensity histograms was exported to Excel for analysis and summed across all ten images, Figure 4-2e shows histogram from one image.

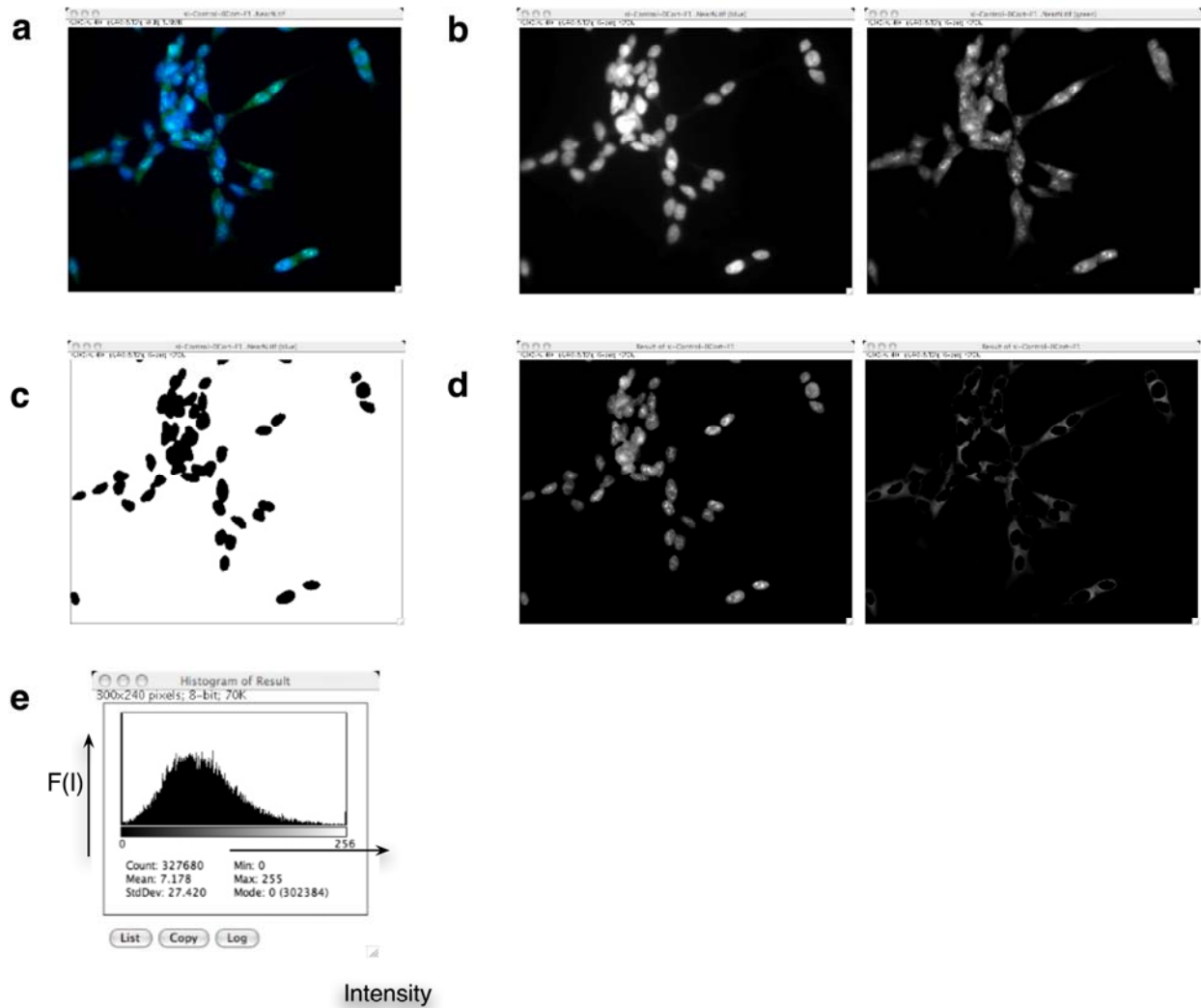


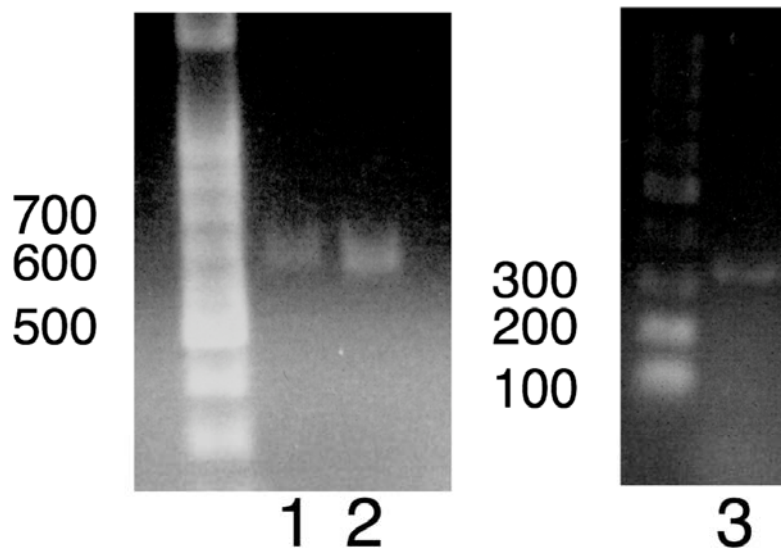
**Figure 4-2.** Quantification methods for nuclear and cytoplasmic fluorescent labeling of GR. Tagged image format (TIF) files were analyzed in Image J software. A representative image is shown in (A). The green and blue color channels were separated and converted the greyscale bitmap (B). A threshold was set for the blue image to delineate the nuclei (C). Image math, subtracting the thresholded image from the green image yielded the nuclear staining (D left). Subtracting the inverted thresholded image from the green image yielded cytoplasmic staining (D right). The text file of the intensity histograms were exported to Excel for analysis and summed across all ten images, (E) shows histogram from one image.

To account for variation in cell count, nuclear size, and cell size, the y-axis of the intensity histogram was converted to Frequency, rather than counts, by dividing each count of pixel intensity by the total number of counts, so the y axis is frequency of the intensity,  $F(I)$ , and the x axis is intensity,  $I$ , Figure 4-12 in Results. For fitting, the nuclear staining histograms were fitted to a Maxwell Boltzman Distribution using four parameters,  $F(I) = A + B I^2 e^{-C(I^2+D)}$ , where A, B, C, and D are fitting parameters. A is the position of the curve relative to the y axis, D the position relative to the x axis, B determines upward the slope of the curve and C the downward tail. The Solver tool of Excel was used to adjust the parameters and to generate a fitting line to maximize  $R^2$  comparing the experimental data to the fit line using a method outlined by Brown [224]. The geometric mean intensity was experimentally determined by integrating the intensity. The fit was confirmed in GraphPad Prism by plotting the fitted curve and the experimental data and using an F-test to compare the values. The 95% CI are determined and plotted, and 95% CI of the geometric mean intensities,  $\hat{I}$ , reported. For the cytoplasmic staining, the same procedure was carried out using an exponential decay equation whereby  $F(I) = A + B e^{-k(I+C)}$ , where A is the position of the graph on the y axis, C the position on the x axis, B relates the slope from the y axis, and k relates tightness of inflection point. Since the distribution of fluorescence intensity modeled a decay function, intensity at half-max value,  $I_{1/2}$ , is calculated in GraphPad Prism and reported with 95% CI.

## 4.3 RESULTS

### 4.3.1 FKBP52-Dynein-Glucocorticoid Complex in SH-SY5Y Cells

It was first necessary to determine that differentiated SH-SY5Y cells would be appropriate to study the GR signaling system with respect to binding of immunophilins. PCR showed that GR, FKBP52, and FKBP51 are expressed in SH-SY5Y cells (Figure 4-3).



1. FKBP52 (600 basepairs, bp)
2. FKBP51 (600 bp)
3. GR (350 bp)

Figure 4-3. SHSY5Y Cells Express *FKBP4*, *FKBP5*, and *NR3C1* (GR) Genes. RNA was isolated from differentiated SH-SY5Y cells, and reverse transcriptase – PCR reaction performed using primers specific for human *FKBP4*, *FKBP5*, and *NR3C1* (GR) genes. The expected molecular weights were *FKBP5* 600bp, *FKBP5* 650bp, and *NR3C1* 350 bp. The PCR product was separated in 1% agarose gel and imaged in ultraviolet light with ethidium bromide staining.

In order to confirm that the proposed model of GR-FKBP complex formation occurs in neuronal cells, we utilized the neuroblastoma cell line SH-SY5Y. We used co-immunoprecipitation to determine whether the proposed model of Dynein-FKBP-GR complex formation was recapitulated in neuronal cells. Dynein co-immunoprecipitated with FKBP52 but not with FKBP51, Figure 4-4a. GR co-immunoprecipitated with FKBP51 and FKBP52, Figure 4-4b. When 100 nM cortisol was added to the cell culture growth media for two hours, and to the lysis-, immunoprecipitation-, and wash- buffers, GR did not co-precipitate with FKBP51 but did with FKBP52. Furthermore, when 10  $\mu$ M FK506, a common immunophilin ligand was added, GR did not co-precipitate with either immunophilin. The complex formation of dynein-to-FKBP52-to-GR was recapitulated in this neuronal system, and 10  $\mu$ M FK506 interrupted the interaction, Figure 4-4.

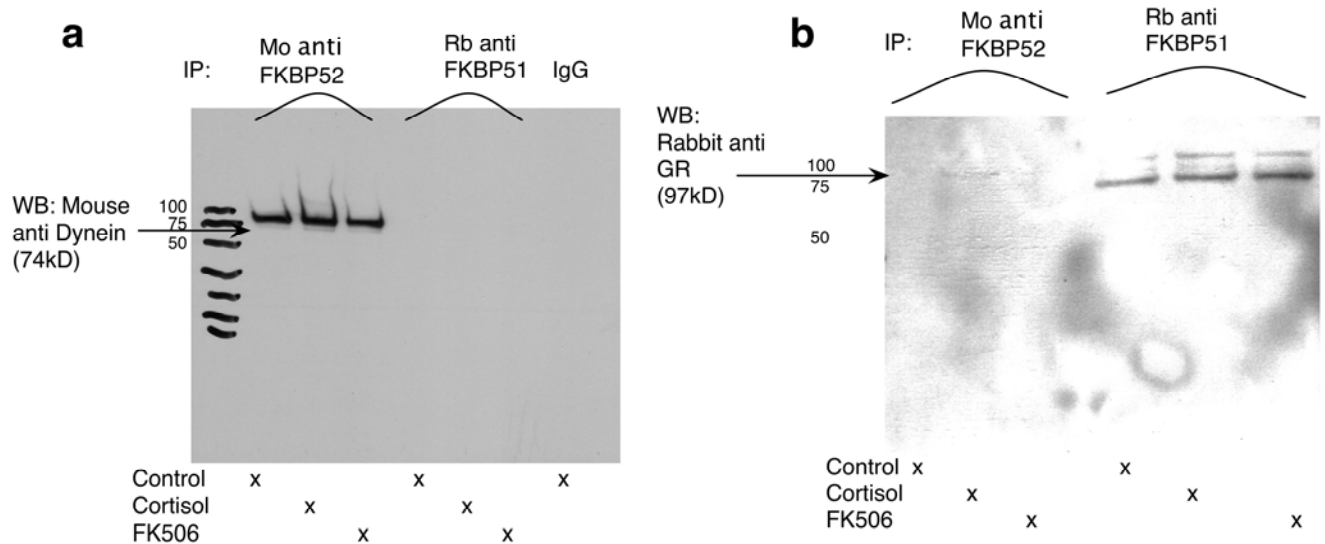


**Figure 4-4. Co-immunoprecipitation of (A) Dynein and (B) GR with FKBP52 and FKBP51.**

**FKBP51 and FKBP52 were immunoprecipitated from whole cell lysates according to Section 3.2.2. Cells were preincubated in and immunoprecipitation buffers supplemented with 100 nM cortisol or 10  $\mu$ M FK506.**

**Immunoprecipitation products were eluted in tris-tricine running buffer and separated by SDS-PAGE and probed for dynein (74 kD) (A) or GR (97 kD) (B). Dynein was detected with FKBP51. GR was detected with FKBP52 only in the presence of cortisol.**

#### **4.3.2 FK506 Inhibits Cortisol-Induced Redistribution of GR and FKBP51 in Neurons**

Since FK506 interrupted the FKBP52 interaction with dynein, we sought to determine whether there was a cellular consequence of FK506 to GR localization. We imaged GR in neurons exposed to cortisol with and without pre-incubation with FK506. To this end, we expanded our study to include a primary human mixed neuron and glia culture system composed mainly of neurons and occasional astrocytes, Figure 4-5 shows Neurofilament/Microtubule Associated Protein-2 (MAP2) and Glial Fibrillary Acidic Protein (GFAP) immunofluorescence of the cultures used. The GR was present in astrocytes (Figure 4-5a) which showed characteristic blebbing of processes (left), and stereotypical cell shape in culture (right). The neurofilament (NF) and MAP2 antigens together were used to identify the neurons (Figure 4-5b) that stained for the GR; as illustrated in Figure 4-5 and Figure 4-6. Immunolabeling of GFAP and NF/MAP2 showed that the neuronal cells and astrocytes were distinct (Figure 4-5c) indicating that neurons and astrocytes at four weeks were mature as detailed in Appendix B.

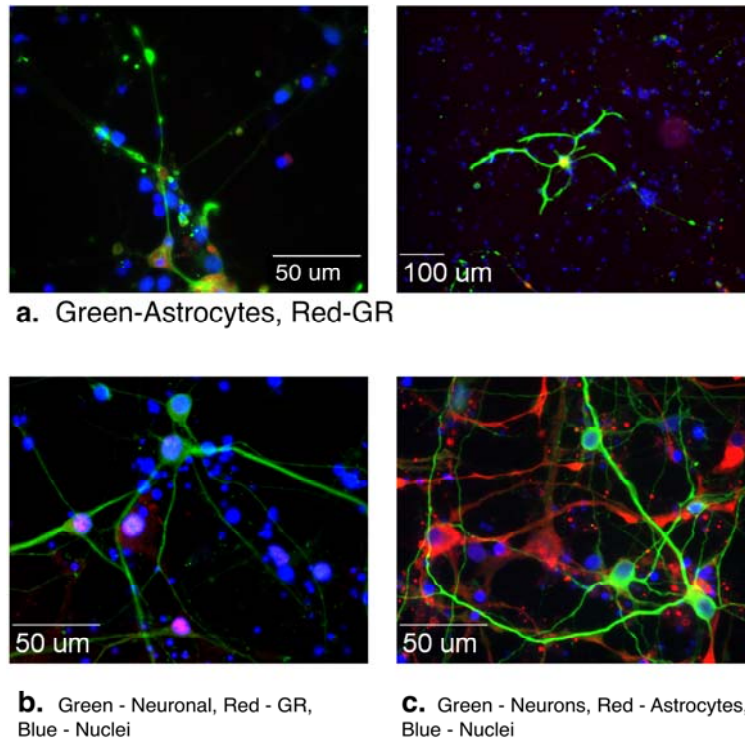


**Figure 4-5. Characterization of primary human neuron-glia cultures.** Primary human neuron-glia cultures were cultivated according to Appendix B and cultured according to Section 4.2.1. Cultures on glass coverslips were permeabilized in 1% TritonX-100, blocked with normal serum, and incubated with primary antibody overnight at 4°C. Coverslips were incubated in Alexafluor 488 and Alexafluor 547 conjugated secondary antibodies at RT for 2 hr. Nuclei were counterlabeled with Hoechst, 10 min RT (blue). (A) Astrocytes labeled with anti-GFAP (green) and GR (red) indicate astrocytic expression of GR at 40X (left) and 100X (right). (B) Neuronal cells were immunofluorescently labeled with neurofilament and MAP2 (green) and GR (red). (C) Together neurons labeled for neurofilament and MAP2 (green) and astrocytes labeled for GFAP (red) in culture indicate maturation of neurons and approximately 1:1 mixture glia:neurons.

Neuronal immunofluorescence for GR was apparent in nuclei without 100 nM cortisol, (Fig. 4-4b and 4-5, top). In a time-dependent fashion, staining of nuclear GR increased with exposure to 100 nM cortisol, indicated at  $\Delta$ s in Figure 4-6. After 30 minutes of 100 nM cortisol

exposure, GR was present in the nucleus of more neurons and glia and was more apparent in the soma, too (Fig. 4-5, bottom-left),  $\Delta$ s point to GR in soma and neuronal nuclei. By 180 minutes, abundant punctate staining for GR in the nucleus, as expected, (Fig. 4-5, bottom-right).

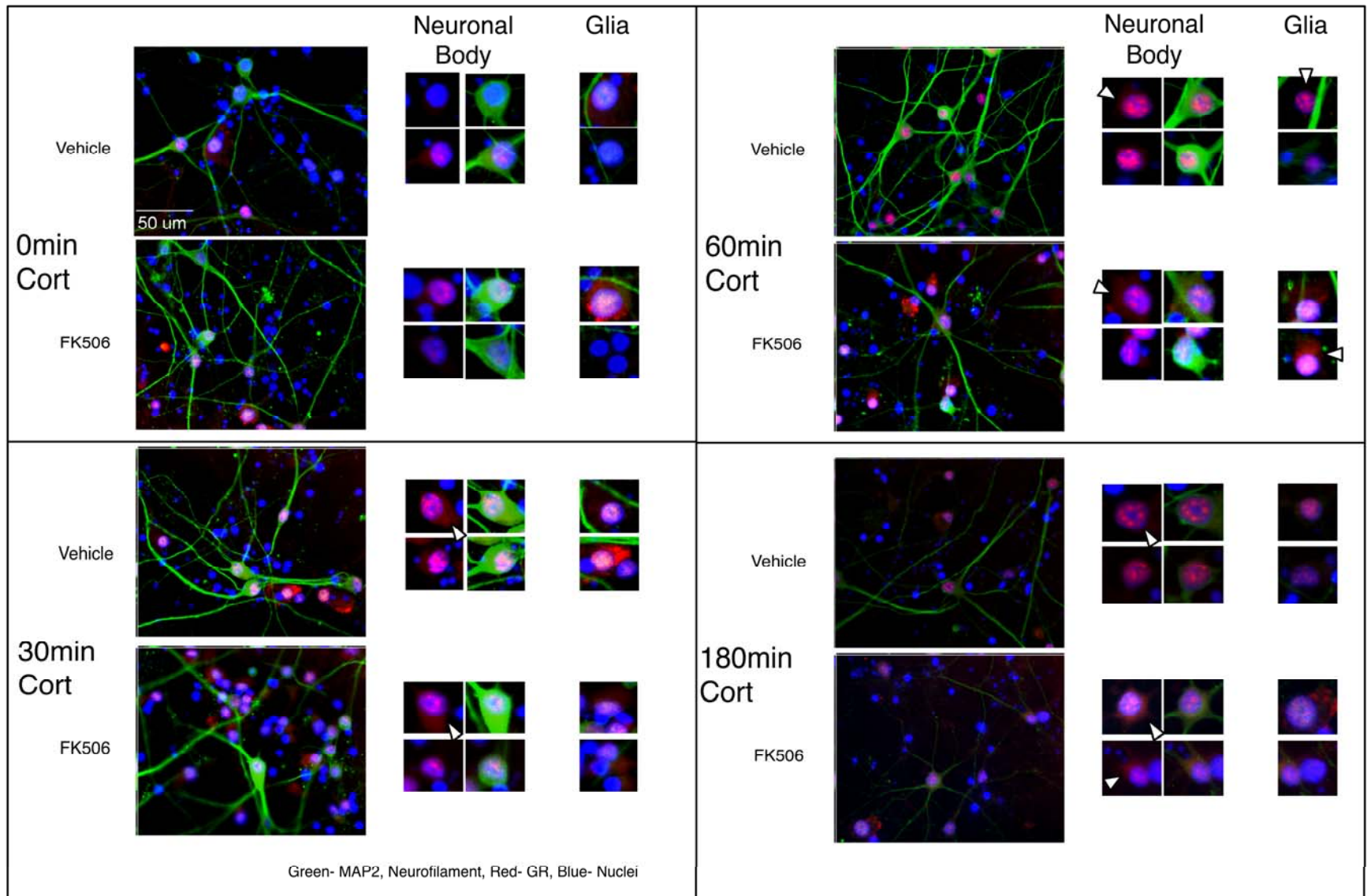


**Figure 4-6. Cortisol-induced nuclear translocation of GR slowed in primary human neuronal cultures with preincubation with 10  $\mu$ M FK506.** Primary human neuron-glia cultures were pre-treated with vehicle (1:500 ethanol) or 10  $\mu$ M FK506 for 2 hr and subsequently treated with 100 nM Cortisol for 30, 60, 180 min. Cells were labeled for neurons with MAP2 and neurofilament (green), immunostained for GR (red), and nuclei counterstained with Hoechst (blue). More focal subnuclear staining of GR was apparent in a time-dependent manner with cortisol. More cytoplasmic GR is delineated with  $\Delta$  at 60 min at 180 min if pretreated with FK506.

With 10  $\mu$ M FK506 present, the nuclear GR labeling remained more diffuse, however some punctate complexes did form. GR stained in the soma of neurons in the presence of 10  $\mu$ M FK506, in contrast non-FK506 controls had little cytoplasmic GR after 180 minutes of cortisol treatment. Figure 4-6, bottom-right,  $\Delta$ 's point to GR in soma in FK506-treated cells and the same area in non-FK506 control at 180 min cortisol exposure.

Cortisol also induced increased nuclear staining of GR in glia cells as well at 60 min and 180 min, as indicated by  $\Delta$  in Figure 4-6. The sublocalization of the GR is more diffuse in the FK506 pretreated cultures.

FKBP51 is a cytoplasmic chaperone-type protein, the putative inhibitor to the FKBP52 adapter-protein that would link it to the motor protein dynein. We found, as shown by others [62], that FKBP51 stained diffusely throughout the nucleus and cytoplasm of cells, shown in Figure 4-7, top;  $\blacktriangle$ s point to FKBP51 staining in z-axis imaging in Figure 4-7. In the presence of cortisol, the distribution of FKBP51 is not changed (Figure 4-7, middle). However, with FK506 treatment, FKBP51 stains perinuclearly and in the soma of neurons (Figure 4-7, middle and bottom).

Because FK506 apparently altered the cortisol-mediated distribution of GR in neuronal cells, we hypothesized that FK506 may alter gene transcription of a GR-responsive gene.

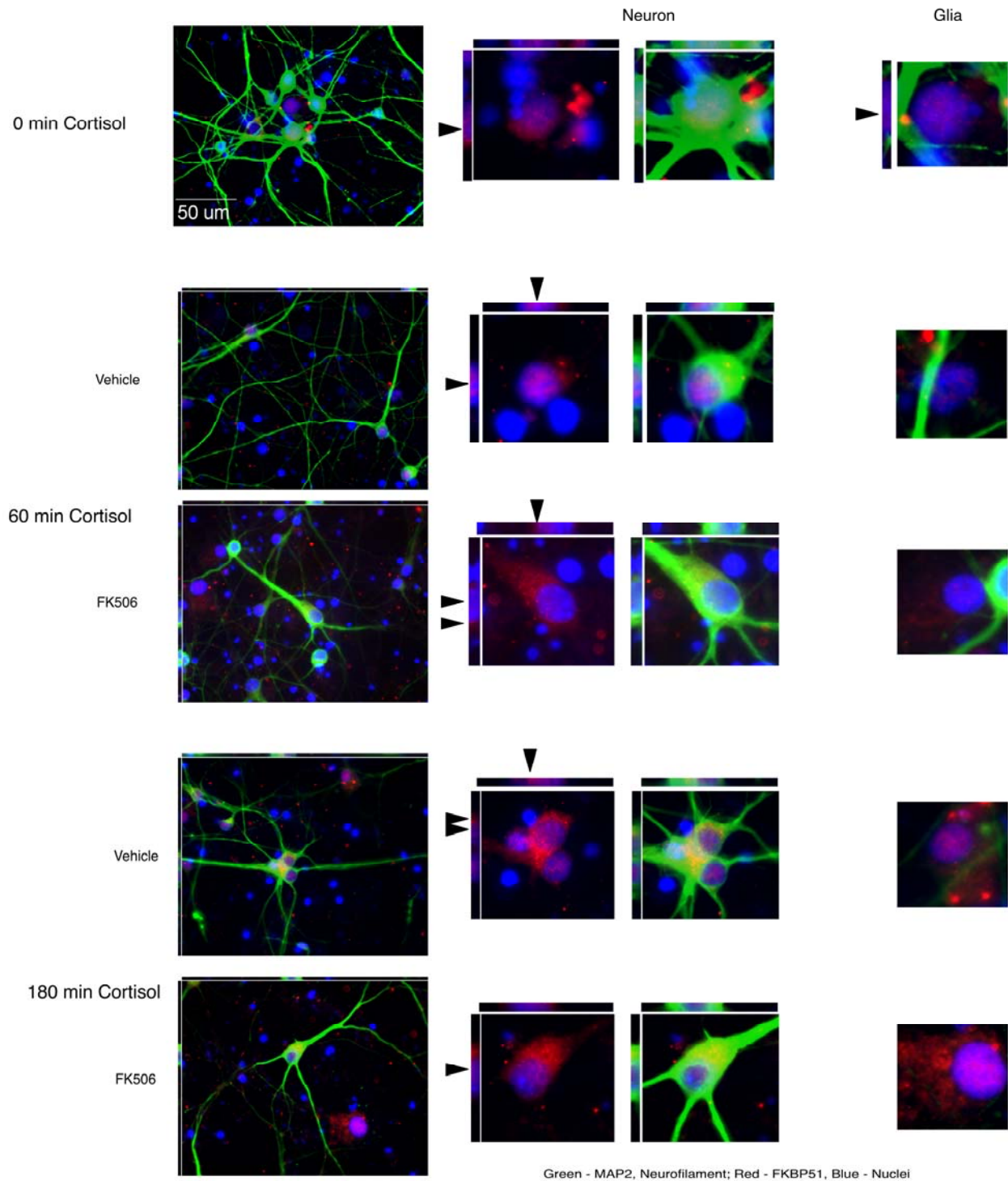


**Figure 4-7. Localization of FKBP51 in primary human neuronal cultures is altered in the presence of 10  $\mu$ M FK506. Primary human neuron-glia cultures were pre-treated with vehicle (1:500 ethanol) or 10  $\mu$ M FK506 for 2 hr and subsequently treated with 100 nM Cortisol for 60 and 180 min. Cells were labeled for neurons with MAP2 and neurofilament (green), immunostained for FKBP51 (red), and nuclei counterstained**

with Hoechst (blue). 3-D reconstruction showed diffused nuclear staining of FKBP51 with and without cortisol present as indicated in top panels with ▲. Pretreatment with FK506 caused exclusion of FKBP51 from the nucleus.

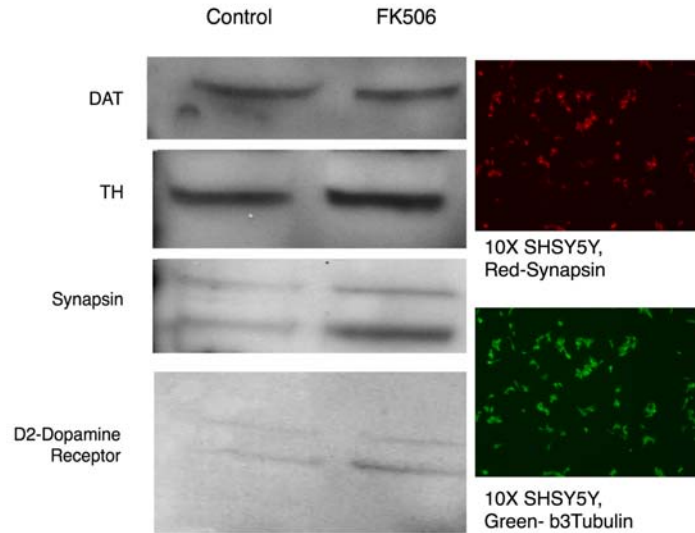


**Figure 4-8. SH-SY5Y Cells Express DAT, TH, Synapsin, D2DR, and  $\beta$ -3-Tubulin.** Total cell lysate from differentiated SH-SY5Y cells treated with or without 10  $\mu$ M FK506 for 24 hr was separated by SDS PAGE and transferred to PVDF membrane. Lysates were probed for dopamine transporter (DAT), tyrosine hydroxylase (TH), synapsin, and D2-dopamine receptor. Differentiated SH-SY5Y cells were grown on glass coverslips, fixed in 4% paraformaldehyde, permeablized in 1% triton-X100, and immunolabeled for Synapsin (red) and  $\beta$ -III-tubulin. Differentiated SH-SY5Y cells, with and without FK506, are of the dopaminergic neuronal phenotype.

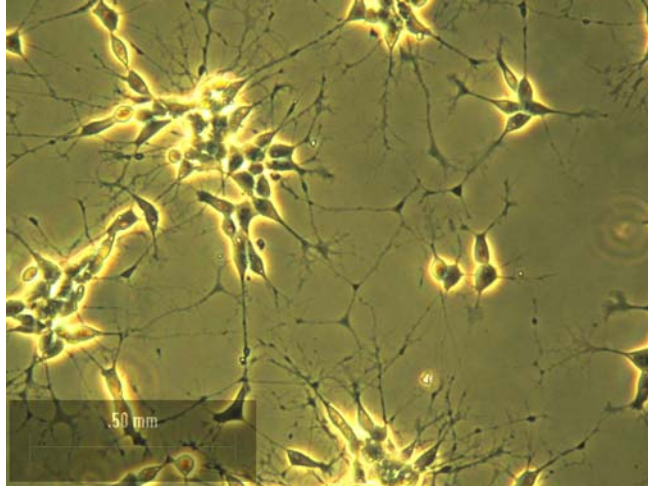


**Figure 4-9. Differentiated SH-SY5Y Cells Show Neuritic Networks and Arborization.** SH-SY5Y cells were grown in glass coverslips coated with poly-ornithine and laminin, after differentiated in retinoic acid for 6 days, cells extend neuritic networks and arborization. Cells were imaged in culture in phase contrast using 20X objective.

For reproducibility and quantitation, the SH-SY5Y cell line is more efficacious than primary neuronal cells, and therefore was used for qPCR of these genes after exposure to cortisol, in the presence or absence of FK506. First, we determined that the SH-SY5Y cells are appropriate in vitro models of neuronal cell system, through western blotting and fluorescence microscopy, we determined that they express the DAT, TH, Synapsin, and  $\beta$ -3-tubulin; which are markers of neuronal differentiation (Figure 4-8). The cells also show neuritic networks and arborization (Figure 4-9). Two genes, *FKBP5* and *Bcl2-L1*, are induced by cortisol and GR-mediated gene transcription [179, 225]. The *FKBP5* gene encodes the FKBP51 protein, contains glucocorticoid-responsive elements, and has polymorphisms that are associated with mood disorders [140-142, 179]. The *Bcl2-L1* gene encodes the protein Bcl-xL, a mitochondrial member of the Bcl2 family, thought to link mitochondria function, metabolism, and synaptic

transmission [226]. We found that *FKBP5* and *Bcl2L1* mRNA were both elevated 30% at 30 min in response to exposure to cortisol, shown in Figure 4-10a and 4-10b. *FKBP5* expression returns to baseline at 24 hours, Figure 4-10a, while *Bcl2L1* remains elevated for up to 48 hours, Figure 4-10b. Treatment with FK506 did not totally ablate the *FKBP5* response, but rather delayed it. The *Bcl2L1* response, however, remained below or close to baseline for 48 hours if FK506 was present. These data are consistent with the model that pretreatment with FK506, in neurons, having altered the nuclear distribution, slows and inhibits GR-responsive gene induction.

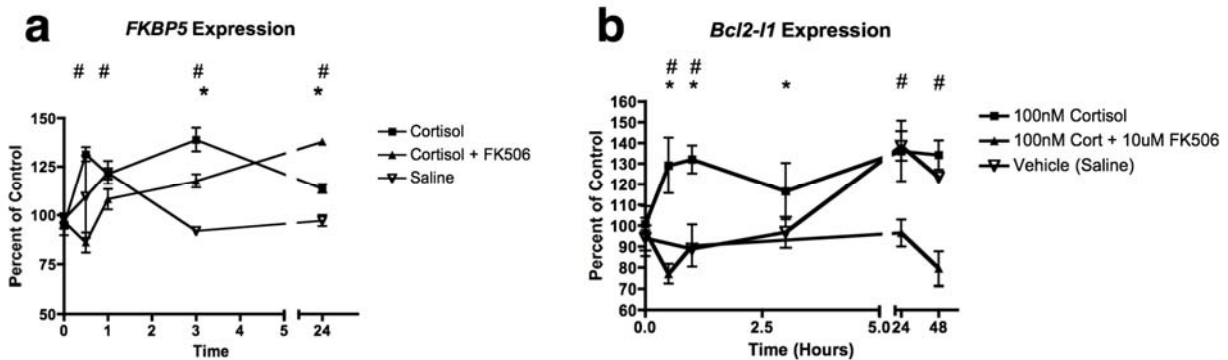


**Figure 4-10. FK506 Inhibits Cortisol - Induced Gene Expression of (A) *FKBP5* and (B) *Bcl2-L1* in Differentiated SH-SY5Y cells.** Differentiated SH-SY5Y cells were exposed 100 nM cortisol for up to 48 hr with (▲) or without (■) pretreatment with 10  $\mu$ M FK506. Saline controls are indicated by ▽, plotted are mean and standard deviation of 3 measurements. RNA was isolated and qRT-PCR was performed as described in Section 4.2.6, percent of control comparing to Time 0 for each treatment and time point for the (a) *FKBP5* and (b) *Bcl2-L1* transcripts are plotted. One way ANOVA and Dunn's multiple comparison tests compared the treatments ( $p < 0.05$  for significance). \* Indicate significant difference at a particular timepoint of 100 nM Cortisol compared to Vehicle Control, and # indicate significant difference between 100 nM Cortisol compared to the FK506 pre-treated group. There is low induction of *FKBP5* (A) with cortisol treatment (■) that is slowed but not abrogated by FK506 (▲). Induction of *Bcl2-L1* is abrogated by FK506 (▲). The vehicle control (▽) elevated *Bcl2-L1* (B) expression after 24 hr compared to Time point 0, which was not observed in the Cortisol +FK506 group (▲).

### 4.3.3 siRNA Knockdown of *FKBP4* Slows GR Translocation

Since FKBP52 protein distribution is predominantly neuronal and acts to promote GR trafficking, we sought to determine whether *FKBP4* siRNA would inhibit the nuclear translocation of GR. For efficacy and consistency of siRNA delivery, the SH-SY5Y cell line was used. Phase contrast image of cells shown in Figure 4-9. Treatment of SH-SY5Y cells with 100 µg/mL cycloheximide to inhibit protein translation and determine the half-life of FKBP52 showed that FKBP52 is quite stable with a half-life of  $13.6 \pm 2.2$  hr (mean  $\pm$  95% confidence interval) and siRNA knockdown would require at least 24 hr (Figure 4-11a). The siRNA experiment followed by cortisol exposure was performed in duplicate in biologically independent samples. Exposure to 250 ng siRNA for 24 hr achieved 70% reduction in FKBP52 protein, and at 24 hours there was a 15% reduction in mRNA of the *FKBP4* gene (Figure 4-11b). Figure 4-11b shows Western Blots for FKBP52 and Actin on the same gel for protein loading control, the independent experiments are illustrated as Repitition (Rep) 1 and Rep 2. Since our final measurement is of GR immunoreactivity, we wanted to ensure that any difference observed in GR localization was not due to changes in GR amount, and Western blot for GR showed no change in GR level in si-Control and si-*FKBP4* (Figure 4-11b).

The si-RNA exposures were performed in 24 well plates, and the protein yield is quite low from SH-SY5Y cells, therefore, we utilized the avidin-biotin-complex (ABC) system for amplification of western blot signal as described in the Materials and Methods. It is for this reason also that Actin and FKBP52 were probed simultaneously. A non-specific band occurs near 50kD and we wanted to confirm that we were measuring the correct band. To do so, whole

cell lysates from SH-SY5Y cells was separated by PAGE and transferred to a PVDF membrane, which was cut into three 2-lane strips, of 10  $\mu$ g and 20 $\mu$ g protein. Western blotting was performed as described in the Materials and Methods except that the strips were incubated separately, the first was treated like normal (Figure 4-11c, left), the second was incubated without primary antibody (Figure 4-11c, center-left), and the third was incubated without primary or secondary antibody (Figure 4-11c, center-right). Immunoprecipitation for FKBP52 was performed and Western for FKBP52 on the Total protein compared to the immunoprecipitate showed also the same non-specific band in the protein lysate (Figure 4-11c, right), which binds to the ABC reagent, (Figure 4-11c, left).

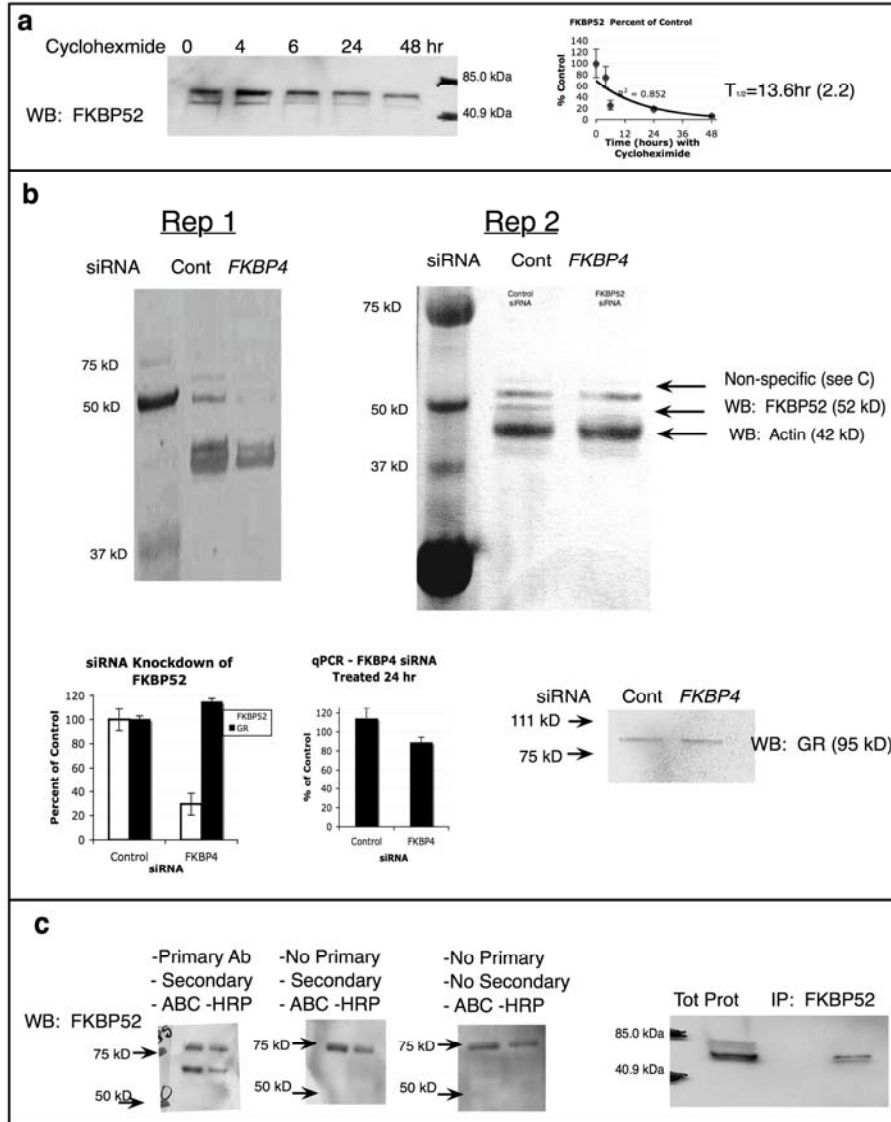


**Figure 4-11. Confirmation of siRNA knockdown of *FKBP4* in SH SY5Y cells.** The half-life of FKBP52 was determined by incubating differentiated SHSY5Y cells with 100  $\mu\text{g}/\text{mL}$  cycloheximide for various time points, and cell lysates were subjected to western and densitometry analysis, triplicate measurements and nonlinear regression to exponential decay ( $R^2 = 0.852$ ) determined that FKBP52 has a half-life of 13.6 (2.2) hr (mean and 95%CI) (A). Differentiated SHSY5Y cells on glass coverslips in 24 well plates were exposed to 250 ng siRNA generated against the *FKBP4* gene or against a control gene, encoding GFP provided by the manufacturer, for 24 hr; protein was isolated for Western and densitometry analysis and RNA isolated for qRT-PCR (B). Two independent siRNA experiments are illustrated (B) and achieved a 70% reduction in protein and 15% reduction in mRNA. To ensure that a difference in GR

immunofluorescence was not due to altered GR protein content, GR was measured by Western analysis, triplicate measurements (mean and SD) of fold-control versus median control value are illustrated (B). To test the appearance of non-specific bands in the western blots, membranes were developed with primary antibody (C-left), without primary antibody (C-middle) and without both secondary and antibody (C-right center), and determined that the non-specific band is from the avidin-biotin amplification system (C). Immunoprecipitation of FKBP52 from cell lysates and probing for FKBP52 by Western blot further confirmed that the non-specific band is a component in total protein, which could be removed through pre-clearing the lysate (C-right) with streptavidin magnetic beads (C).

#### 4.3.3.1 Immunofluorescence Imaging and Quantification of Nuclear and Cytoplasmic GR

After exposure to either si-*FKBP4* or si-control, cells were exposed to 100 nM cortisol for 0, 15, 30, and 60 minutes. Immunofluorescent labeling for GR showed nuclear translocation of the GR for both si-*FKBP4* and si-control. We quantified the intensity of cytoplasmic and nuclear signals as described in the Methods and constructed intensity histograms, illustrated below representative images for each treatment (Figure 4-12). The distribution was fit by nonlinear regression to model the intensity of nuclear and cytoplasmic signals across 10 images per treatment, of approximately 300 cells each and shows 95% confidence intervals. For the nuclear staining, the geometric mean intensity  $\hat{I}$  is reported with 95% CI, for cytoplasmic staining, the intensity of half-maximal frequency,  $I_{1/2}$  is reported with 95% CI, as calculated from the nonlinear regressions as described in the Methods. The values were compared by two-way ANOVA with  $p < 0.05$  set as statistically significant, and the F ratios are determined to compare the contribution of Time (with cortisol) or treatment with siRNA (Control or *FKBP4*) to observed changes in GR staining intensity. Post test with Bonferroni's correction for multiple comparison comparing intensity among the time points (0-60 min Cortisol) and comparing

within the time points (si-Control or si-*FKBP4* for a particular time point) are calculated to determine the contribution of either factor to changes observed in nuclear or cytoplasmic fluorescence intensity.

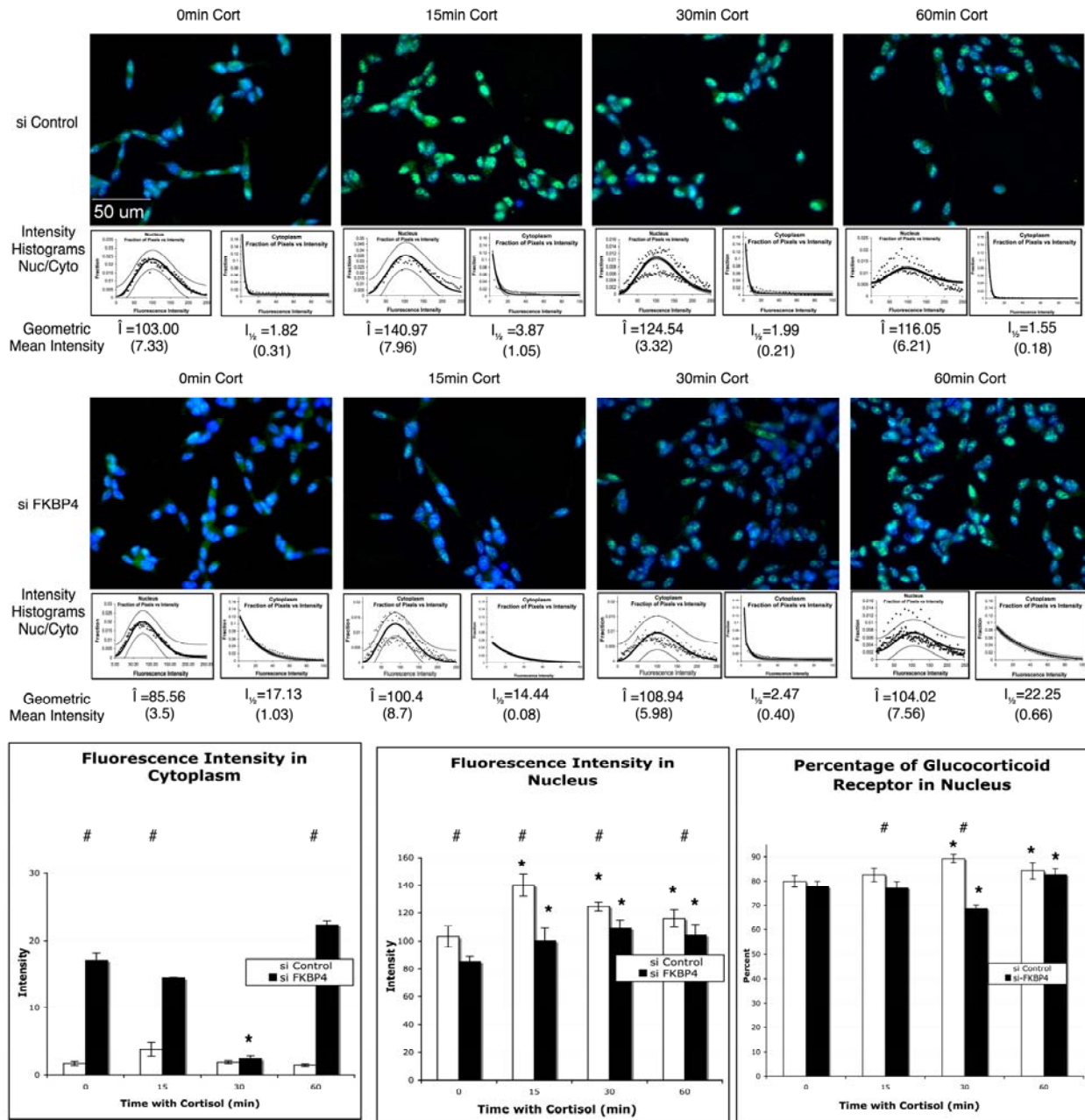


**Figure 4-12.** Quantification of nuclear and cytoplasmic immunofluorescent staining of GR after treatment with 100 nM cortisol and siRNA to *FKBP4*. Differentiated SHSY5Y cells were grown on glass coverslips and exposed to 250 nmol control (top) and *FKBP4* (bottom) siRNA for 24 hr and then 100 nM cortisol for 0, 15,

30, 60 min. Following fixation, cells were fluorescently labeled for GR (green) and nuclei (blue). Using Image J and Slidebook, nuclear and non-nuclear GR staining was partitioned according to the Methods and Supplementary Information and quantified in 10 images for each treatment. Fluorescence histograms were plotted and fitted by non-linear regression to a Boltzman distribution for nuclear staining and exponential decay distribution for cytoplasmic staining and normalized, which are shown below representative images. Geometric mean ( $\hat{I}$ , for nuclear) and half-maximal ( $I_{1/2}$ , for cytoplasmic) intensities with 95% confidence intervals are shown below the images. The total percentage of nuclear fluorescence intensities among the conditions are plotted below the images. Two-way ANOVA compared the effects of siRNA or time-with cortisol on  $\hat{I}$  (bottom center),  $I_{1/2}$ (bottom left), and %Nuclear GR (bottom right). Significance is represented by \* ( $p < 0.01$ ) between the siRNA groups at a particular timepoint and # represent significant difference due to time with cortisol. Si-*FKBP4* contributed to lower nuclear staining intensity, slower nuclear translocation, and higher cytoplasmic staining intensity.

#### 4.3.3.2 Analysis of Nuclear Fluorescence Intensity

In the si-Control group, the geometric mean intensity ( $\hat{I} \pm 95\%$  confidence interval) increased in the nucleus from  $103.00 \pm 7.33$  to  $140.97 \pm 7.96$  and  $124.54 \pm 3.32$  at 30 min and 60 min, respectively, indicating a rapid increase in nuclear GR staining. In the si-*FKBP4* group, the baseline intensity was lower and fluorescence intensity slower than the si-Control group. The increase was significant at each time point, increasing from baseline  $85.56 \pm 3.5$  to  $100.4 \pm 8.7$  at 15 min to  $108.94 \pm 5.98$  at 30 min. The effects of Time (with cortisol) and si-RNA (either Control of *FKBP4*) were analyzed by two-way ANOVA and Bonferroni's post tests. Time with cortisol had a significant effect on  $\hat{I}$ ,  $F_{3,72} = 60.8$ ; while the siRNA had a **larger** effect on  $\hat{I}$ ,  $F_{1,72} = 206.3$  ( $p < 0.0001$ ).

The Bonferroni post test, correcting for multiple comparisons (Significance set to  $p = 0.05/4 = 0.0125$ ), to compare the two siRNA groups at each time point indicated that nuclear  $\hat{I}_{\text{si-Control}}$  is consistently higher at each time point than  $\hat{I}_{\text{siFKBP4}}$ , Table 4-1, this is clear in the bar graphs at the bottom of Figure 4-12. To test whether Time with 100 nM cortisol has an effect on nuclear GR intensity within the siRNA groups, Bonferroni's post test (Significance set to  $p = 0.05/6 = 0.00167$ ) compared  $\hat{I}$  at each time point (15, 30, 60 mins) to time 0. These data indicate that GR staining increased in the nucleus in both si-control and siFKBP4, illustrated in Figure 4-12 and analyzed in Table 4-2. The increase is more rapid and intense in the si-control than the si-FKBP4 group, indicated by the  $t$ -statistic being higher in the Control comparisons in Table 4-2 and illustrated in Figure 4-12, bottom. The  $t$ -statistic is reported because all the  $p$  values are below the threshold for calculation using GraphPad Prism software, larger  $t$  indicates more significant difference between  $\hat{I}$ 's.

**Table 4-1. Bonferroni post test comparing nuclear  $\hat{I}_{\text{siControl}}$  vs  $\hat{I}_{\text{siFKBP4}}$  at each time point after treatment with 100 nM cortisol showing effect of si-RNA.**

<u>Time (min)</u>	<u><math>\hat{I}_{\text{si Control}}</math></u>	<u><math>\hat{I}_{\text{si FKBP4}}</math></u>	<u>Difference</u>	<u><math>t</math></u>	<u><math>p</math></u>
0	103.00	85.56	-17.44	5.92	<0.001
15	140.00	100.40	-39.60	13.43	<0.001
30	124.50	108.90	-15.60	5.29	<0.001
60	116.10	104.00	-12.03	4.08	<0.001

**Table 4-2. Bonferroni post test comparing nuclear  $\hat{I}_0$  vs  $\hat{I}_{\text{Time points}}$  at each siRNA group, showing effect of Time with 100 nM cortisol.**

<b><u>siRNA, time</u></b>	<b><u><math>\hat{I}_0</math></u></b>	<b><u><math>\hat{I}_{\text{time}}</math></u></b>	<b><u>Difference</u></b>	<b><u><math>t</math></u></b>	<b><u>p</u></b>
Control, 15min	103.00	140.00	37.00	12.55	<0.0001
Control, 30 min	103.00	124.50	21.50	7.29	<0.0001
Control, 60 min	103.00	116.10	13.10	4.44	<0.0001
FKBP4, 15min	85.56	100.40	14.84	5.04	<0.0001
FKBP4, 30min	85.56	108.90	23.34	7.92	<0.0001
FKBP4, 60min	85.56	104.00	18.44	6.26	<0.0001

#### **4.3.3.3 Analysis of Cytoplasmic Fluorescence Intensity**

Because the cytoplasmic fluorescence histogram fit a decay distribution, for cytoplasmic fluorescence, the intensity of max-maximal frequency,  $I_{1/2} \pm 95\%CI$ , is reported in Figure 4-12. Time with cortisol had a significant effect on  $I_{1/2}$ ,  $F_{3,72} = 23.39$ ; while the siRNA had a **more** significant effect on  $I_{1/2}$ ,  $F_{1,72} = 187.2$ . We found significant difference between the siRNA groups, with increased cytoplasmic GR fluorescence intensity in the si-*FKBP4* group at all time points except at 30 mins, Table 4-3. We found that changes in  $I_{1/2}$  due to Time with cortisol were less striking than in the nucleus, Table 4-4.

**Table 4-3. Bonferroni post test comparing cytoplasmic  $I_{\text{siControl}}$  vs  $I_{\text{siFKBP4}}$  at each time point, showing effect of siRNA group on cytoplasmic intensity.**

<u>Time (min)</u>	<u>si Control</u>	<u>si FKBP4</u>	<u>Difference</u>	<u>t</u>	<u>p</u>
0	1.82	17.13	15.31	8.90	<0.0001
15	3.87	14.44	10.57	6.15	<0.0001
30	1.99	2.47	0.48	0.28	0.7803
60	1.55	22.25	20.70	12.04	<0.0001

**Table 4-4. Bonferroni post test comparing cytoplasmic  $I_0$  vs  $I_{\text{time point}}$  in each siRNA group, showing effect of Time with 100 nM cortisol on cytoplasmic intensity.**

<u>siRNA, time</u>	<u><math>I_0</math></u>	<u><math>I_{\text{time}}</math></u>	<u>Difference</u>	<u>t</u>	<u>p</u>
Control, 15min	1.82	3.87	-2.05	1.19	0.238
Control, 30min	1.82	1.99	-0.17	0.10	0.9206
Control, 60min	1.82	1.55	0.27	0.16	0.8733
FKBP4, 15min	17.13	14.44	2.69	1.57	0.1208
FKBP4, 30 min	17.13	2.47	14.66	8.53	<0.0001
FKBP4, 60 min	17.13	22.25	-5.22	2.98	0.0039

#### 4.3.3.4 Analysis of Percentage of GR in Nucleus

By summing the nuclear fluorescence, accounting for intensity of pixels and pixel count; and by considering the total overall GR fluorescence; the percentage of GR intensity in the nucleus is calculated, plotted in the bottom Figure 4-12, and analyzed by two-way ANOVA and Bonferroni post test. The percentage of GR intensity in the nucleus was affected by both factors, siRNA ( $F_{1,72} = 125.5$ ) and by Time with cortisol ( $F_{3,72} = 10.52$ ), the **greater** effect by siRNA.

The Bonferroni post test to compare the two siRNA groups at each time point indicated that the percentage of GR in the nucleus is higher in the siControl group than si*FKBP4* group at 15 min and 30 min (Table 4-5) and illustrated in the bar graph at the bottom of Figure 4-12. To test whether Time with 100 nM cortisol has an effect on nuclear GR intensity within the siRNA groups, Bonferroni's post test compared percentage of GR in the nucleus at each time point (15, 30, 60 mins) to time 0. The si-Control groups significantly increased GR in nucleus at 30 and 60 mins, while the si*FKBP4* groups had lower percent GR in the nucleus at 30 mins, and increased to si-Control level at 60 mins, Table 4-6. This analysis is consistent with the  $\hat{I}$  and  $I_{1/2}$  analyses in that the nuclear translocation in the si-Control group is rapid, but slowed in the si*FKBP4* group.

**Table 4-5. Bonferroni post test comparing %GR in Nucleus<sub>siControl</sub> vs %GR in Nucleus<sub>siFKBP4</sub> at each time point, showing effect of siRNA group on percent of GR in nucleus.**

<b><u>Time (min)</u></b>	<b><u>%GR Nuc<sub>siControl</sub></u></b>	<b><u>%GR Nuc<sub>siFKBP4</sub></u></b>	<b><u>Difference</u></b>	<b><u>t</u></b>	<b><u>p</u></b>
0	79.85	77.65	-2.19	1.64	0.1054
15	82.48	77.14	-5.34	3.99	0.0002
30	89.32	68.58	-20.74	15.50	<0.0001
60	84.27	82.55	-1.72	1.28	0.2047

**Table 4-6. Bonferroni post test comparing %GR in Nucleus  $T_{Time0}$  vs %GR in Nucleus  $T_{Time\ point}$  in each siRNA group, showing effect of Time with 100 nM cortisol on %GR in Nucleus for each group.**

<b>siRNA, time</b>	<b>%GR Nuc <math>T_0</math></b>	<b>%GR Nuc <math>T_{time}</math></b>	<b>Difference</b>	<b><math>t</math></b>	<b><math>p</math></b>
Control, 15min	79.85	82.48	2.63	1.97	0.0527
Control, 30 min	79.85	89.32	9.47	7.07	<0.0001
Control, 60 min	79.85	84.27	4.42	3.30	0.0015
FKBP4, 15min	77.65	77.14	-0.51	0.38	0.7051
FKBP4, 30min	77.65	68.58	-9.07	6.78	<0.0001
FKBP4, 60min	77.65	82.55	4.90	3.66	0.0005

## 4.4 DISCUSSION

### 4.4.1 FKBP52 and FKBP51 Co-Immunoprecipitations

Past reports have shown that the GR exists in complex with heat shock proteins such as HSP90, HSP70, and the large molecular weight immunophilins FKBP52 and FKBP51 [79, 227-229]. Davies et al propose that the first step in activation of the GR is a switch from being bound to FKBP51, which does not interact with dynein, to being bound to FKBP52, which does bind dynein [14]. Since these immunophilins are present in the brain, we hypothesized that their function in neurons and glia would be a form of modulation of cortisol-mediated glucocorticoid activation. Using a neural cell line and primary neuronal cultures in vitro, we show that this system is pertinent to neural and glia cells; and that the FKBP52/FKBP51 dynamics may be an intracellular feedback mechanism to GR signaling.

Using immunoprecipitation, we detected the molecular motor protein dynein in complex with FKBP52, but not FKBP51 (Figure 4-4). Further, there appears to be more dynein present with FKBP52 when cells were pre-incubated, and immunoprecipitation and wash buffers were supplemented, with cortisol. GR immunoprecipitated with FKBP52 only in the presence of cortisol, but not the ligand FK506 or control conditions (Figure 4-4). GR was detected in immunoprecipitations with FKBP51, in small amounts, under control conditions or in the presence of cortisol, but not with FK506 present. This observation is in line with previously published reports whereby FK506 disrupts the interaction between both FKBP52 and FKBP51 with GR [210]. Furthermore, since GR was present with FKBP51 in the presence of cortisol, cortisol may **not be sufficient for dissociation** of GR from FKBP51, but is **necessary for association** of GR with FKBP52.

Until recently, the effects of FK506 on GR-FKBP51 was not studied. In 2008, a report showed also that FKBP51 nuclear localization was altered due to HSP90 inhibitor [62]. Using HeLa cells, Normal- (N-TM5 cells) and Glaucoma- (GTM-5 cells) Trabecular Meshwork cells, they showed cell-type dependency on the GR-FKBP51 interaction and FK506-effects, showing FK506 inhibiting GR-induction in the normal cells, but not in the glaucoma cells [62]. The co-immunoprecipitation in Section 4.3.1 and the neuronal cells in Section 4.3.2 respond similarly to the GTM-5 cells. By this model, a cell could modulate its ability to respond to glucocorticoids through GR by altering the concentration of these adapter proteins, FKBP51 and FKBP52.

#### **4.4.1.1 Limitations and Further Questions**

Immunoprecipitation depends upon binding of a specific antibody in solution to an epitope in a protein of interest, the antibody is immobilized on a solid substrate, and other components in the mixture are washed out. Anything complexed with the protein of interest should remain bound

and eluted and further detected. This method can yield false negatives and false positive. Too stringent washing conditions may wash away a component in the mixture. If an interaction is too transient or dependent upon a high concentration of specific ions, like  $\text{Ca}^{2+}$  or  $\text{Mg}^{2+}$ , then components may be lost and not detected. If it known or hypothesized that an interaction depends on a cofactor or ion, buffers can be supplemented with the putative cofactor. For this reason, buffers were supplemented with cortisol or FK506 in the co-immunoprecipitation experiments to determine whether interactions depended upon or were interrupted by those two components.

Non-specific binding of either primary antibody, secondary antibody, or the immobilizing agent to any cell-lysate component can yield false-positives. The lysate should be pre-cleared prior to incubation with primary antibody. Our study used specific antibodies, but other antibody sets from various species could be used to yield cleaner results. We immunoprecipitated for FKBP51 and FKBP52 and detected either GR or dynein by Western blot. Ideally, we could immunoprecipitate GR or dynein and probe for the immunophilins to confirm that the interaction we detected is not a false-positive. Although we were unable to immunoprecipitate GR using antibodies from AbCam (AbCam ab2768 and AbCam ab3578), recently AbCam ab3579 antibody has been made available and is marketed for chromatin-immunoprecipitation and may work in our system, finally, Binder and coworkers were able to immunoprecipitate GR using a rabbit anti GR from Santa Cruz Biotechnology (sc1003).

Another technique commonly called “pulldown” could be utilized. The classic method is to fuse the protein of interest, for example FKBP52 using cloning techniques to glutathione-S transferase (GST), or GST-tagged. The fusion protein would be incubated with lysate, supplemented with the cofactors of interest, and the GST-tagged FKBP52 and its binding-

partners immobilized on a solid glutathione column. The complexes would be eluted using free glutathione to compete away that glutathione column to GST interaction, and putative binding partners probed for. Since glutathione was shown to bind to the ryadonine receptor at the site FKBP12-binding, a different tag should be utilized for immunophilins, for example maltose-binding protein, amylose column (amylose is polymerized maltose), and eluted using free maltose. These pull-down methods would not be dependent upon combinations of antibody and species antibody and would yield clean results in the final Western blot.

#### **4.4.2 Immunofluorescence of GR and FKBP51 in Neuronal Cultures**

The GR is known to be a dynamic protein both in the nucleus and in the cytoplasm, involved in the formation of various DNA and protein complexes and also to undergo proteolysis inside the nucleus [230-233]. Since a portion of the GR may have already been involved in DNA-transcription factor complexes, prior to any cortisol exposure, our images seem to indicate that FK506 interrupts an interaction that would cause GR to be maintained in the nucleus or involved in focal protein complexes; putatively it interrupts the interaction with an immunophilin chaperone protein like FKBP51. At the longer time point, 180 minutes of cortisol exposure, fewer aggregates are formed in the nucleus and the distribution is more diffuse. Furthermore, there is more cytoplasmic **FKBP51** and **GR** staining noted in the presence of FK506. This would support the notion that perhaps FKBP51-binding promotes stability of GR and the formation of foci, perhaps protecting it from proteolysis FKBP51, in this case, would be acting as a chaperone protein associated with GR in the nucleus.

It is unknown what other proteins FKBP51 binds to in the nucleus, aside from GR. It is also unknown whether FKBP51 binds GR when it is DNA-bound. While the staining of GR in

the nucleus showed specific foci, which became more clear and distinct over time with cortisol, the FKBP51 nuclear staining remained diffuse. GR likely is in complex with FKBP51 in the nucleus when it is not DNA bound or in foci, but rather soluble in the nucleus, potentially FKBP51 protects non-DNA-bound-GR from proteolysis in the nucleus or nuclear export; by potentially serving as an adapter protein to other chaperones like HSP90. Others have shown diffuse nuclear staining of FKBP51 in trabecular meshwork cells, (GTM-5 and NTM-5 cells), mouse embryonic fibroblasts (MEF), and rat intestinal epithelia (RIE) cells [62, 234]. After treatment with FK506, FKBP51 was excluded from the nucleus and showed cytoplasmic, potentially perinuclear staining, a similar staining pattern was observed in osteosarcoma cells (U2OS cell line) and in megakaryocytes (MK cells) [234, 235]. The differential localization of FKBP51, nuclear versus perinuclear, seems to be cell-type dependent. This suggests that nuclear localization of FKBP51 is dependent on some component present in MEF cells, neurons, glia, GTM-5, NTM-5, REI cells that is not present in MK cells or U2OS. Our observations in Section 4.3.2 suggest that FK506 interrupts this interaction in neurons and glia.

#### **4.4.2.1 Limitations and Further Questions**

We showed increase GR nuclear localization and altered subnuclear localization due to addition of cortisol whereby GR staining formed distinct foci over time. Pretreatment with FK506 altered this change, GR staining was more diffuse, and more was apparent in the cytoplasm. Quantitative analysis of nuclear localization of GR or GR staining would increase our confidence in the significance of the results. Quantification methods similar to the GR localization described in the Materials and Methods Section 4.2.8 could be adapted. Because the study was performed in mixed-type cell culture from primary human forebrain tissue, the

cultures contained heterogeneous mixture of cell-types, neurons of different sizes, and extracellular debris, which showed up as background in fluorescence imaging.

The quantification described in Section 4.2.8 was quite sensitive; results were confounded when a thin-layer green-pass light filter was misaligned on the fluorescence microscope. In imaging SH-SY5Y cells shown in Section 4.3.3, the experimenter only focused on nuclei through the blue filter in order to not bias the results, and only when the quantification showed skewed result, was the problem made aware. The Nearest Neighbor Algorithm of deconvolution from 3-D steps is a stringent process and when background fluorescence signal from extracellular debris is removed, true signal is also lost. If the cultures from one coverslip differed too much from another coverslip, the differences due to high background or lost signal due to background subtraction could hide differences due to treatment. Therefore a qualitative assessment is presented here.

Nevertheless, other techniques could be quite informative regarding GR, FKBP52, and FKBP51 subnuclear, perinuclear, or cytoplasmic localization or dynamic trafficking. Tracking of proteins in live cells using fluorescent-protein tags during cortisol and FK506 treatment would show how the localization changes over time. Fluorescence-resonance energy transfer (FRET) of tagged proteins would show firstly whether GR and FKBP51 were interacting directly and secondly could quantify how the interaction changes based on treatments.

It is unknown whether FKBP51 interacts with GR when the GR is DNA-bound. Gel-shift and super-shift assays could be performed to test this. DNA of a known length containing GR-responsive elements could be incubated with cell lysate from cells expressing GR and FKBP51, the DNA-protein complexes that formed would be run in an agarose gel and imaged using ethidium bromide. If proteins were bound to the DNA, the DNA band would be shifted to

higher molecular weight. A supershift could be detected if antibodies to FKBP51 were added, further shifting the DNA band to higher molecular weight, indicating FKBP51 is present in the GR-DNA complex. Depleting the lysate of GR, using GR-knocked down cells or GR-knockout animal to obtain the lysate would show whether this putative interaction is GR-dependent. Whether FKBP51 binds GR while GR is DNA-bound would be informative, because FK506 excluded FKBP51 from the nucleus. FK506 is an FDA-approved drug in use as an immunosuppressant in organ transplants, if FK506 has an effect on GR signaling and aberrant GR signaling is implicated in mood disorders described in Chapter 2, then this drug or its analogue may be a target for controlling GR signaling.

#### **4.4.3 Knockdown of FKBP52 by siRNA Slows Cortisol-Induced GR Nuclear Localization**

In the cytoplasm, FKBP52 is hypothesized to be an accessory protein for GR trafficking to the nucleus. To test this hypothesis in neuronal cells, we knocked down FKBP52 by siRNA in differentiated SH-SY5Y cells. We treated the FKBP52-deficient cells with cortisol and stained for GR using immunofluorescence. FKBP52-deficiency did not totally abrogate nuclear translocation of GR. As shown in Figure 4-12, in the si-Control group, the nuclear GR fluorescence intensity rapidly increased. The statistical analysis showed that the cortisol-induced increase in nuclear GR localization in the FKBP52-deficient cells was **slower** and **less robust**. The FKBP52-deficient cells formed GR aggregates, but they were fewer and less intense than those seen in controls and the staining remained diffuse in the nucleus. In the FKBP52-knockdown cells, GR could be seen in neuritic processes even after cortisol exposure, and the fluorescence intensity was measurably higher.

We hypothesized that the nuclear translocation of GR would be abrogated by the absence of FKBP52. We observed a significant reduction in the nuclear immunofluorescence signal for GR in the FKBP52 knockdown (Figure 4-12, bottom). However, calculating percentage of GR signal in the nucleus only showed a 5% difference at 15 min, 20% difference at 30 min, and no difference at 60 min (Table 4-5). The biological significance of 20% difference after 30 min of cortisol exposure is unclear. We wish to extrapolate the data from this body of work toward chronic conditions like HIV-infection and MDD as discussed in Chapter 2, and the we see no difference in GR nuclear localization at 60 min, indicating the effect of FKBP52 must be in the kinetics of relatively early cortisol-induced GR trafficking. However, if a spike in cortisol levels due to a stressful event caused ligand-induced GR signaling in neurons, and the physiologic cortisol levels dissipated quickly, FKBP52 may play a role in these transient stress-induced short cortisol spikes.

A microtubule-associated protein called Double-cortin-like was recently shown to regulate the transport of GR in neuroprogenitor cells [236]. If SH-SY5Y cells express Double-cortin-like, then this would be a factor independent of FKBP52 and FKBP51 regulating GR translocation. A double-knockdown for both Double-cortin-like and FKBP52 would inform us as to the importance of these two factors. The Double-cortin-like (DCL) mRNA is generated by splicing of the Double-cortin-like-kinase (DCLK) mRNA, and these transcripts are expressed in the brain, and splicing is differential throughout CNS development [237]. DCL is involved in cortical development and is expressed in migrating neuroprecursors in the developing mouse brain and disappears from cortical neurons in after embryonic day 13 from cortical projections and is only found in glial afterwards [238]. We showed in Section 3.3.5 that FKBP52 is expressed in cortical neurons of the adult human brain. It would be relevant to determine whether

the differentiated SH-SY5Y cells studied in Section 4.3.3 or the neuron-glia cultures studied in Section 4.3.2 express DCL as this protein may influence GR translocation in the cell culture system but not extrapolate to adult CNS studied in Chapter 3.

#### **4.4.4 Conclusion**

Taken together, these studies suggest that FK506 disrupts the interactions between the GR and both FKBP51 and FKBP52. Cortisol is necessary for the association of FKBP52 with GR, but not sufficient for dissociation of FKBP51 from GR. Treatment with FK506 did not alter the ability of the GR to form nuclear aggregates, but the aggregates were fewer and more diffuse. Also, there was appreciable GR present in the cytoplasm after 180 minutes if FK506 was present compared to cells that were not treated with FK506. This is evidence that association of GR with immunophilins supports GR stability in the nucleus. Based on this, we propose that changing the GR-immunophilin interaction, using FK506, affects the formation and stability of GR in neuronal nuclei.

In conclusion, we propose that immunophilins may be modulators of the cortisol-HPA axis response to stress and related chronic brain disorders. Altering neuronal gene expression through controlling GR-mediated signaling pathways may represent a novel and potent therapeutic intervention.

## 5.0 CONCLUSION AND FUTURE DIRECTIONS

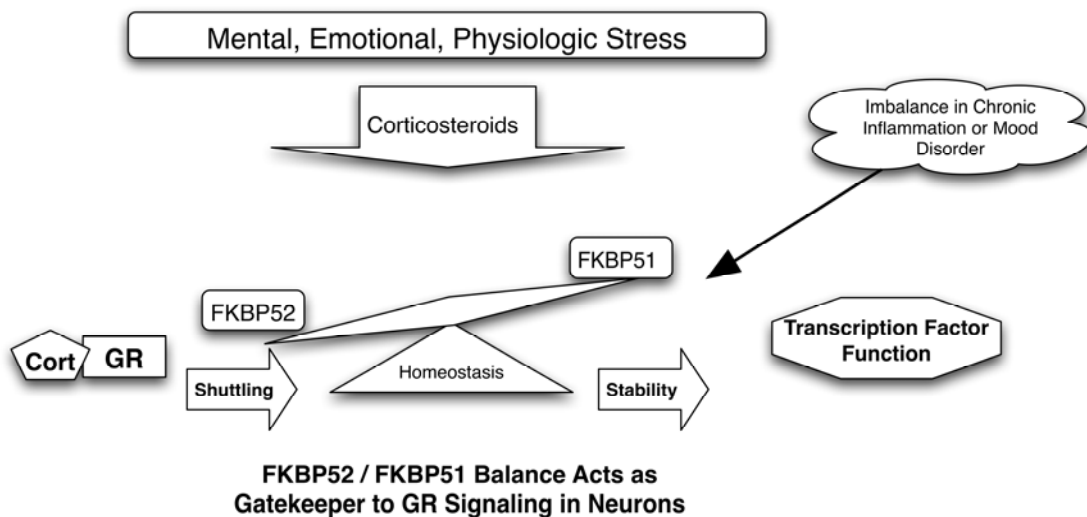


**Figure 5-1. Model of control of GR signaling in neurons by immunophilins; dysregulation in chronic inflammation or mood disorder. The working model is that FKBP52 and FKBP51 balance to act as gatekeepers to GR signaling in mature neurons. FKBP51 may act to promote stability of of GR in the nucleus and cytoplasm, while FKBP52 links GR to the retrograde molecular motor dynein. Factors such as chronic stress, genetic components, or paracrine signaling from nearby activated microglia may cause an imbalance in immunophilin expression, leading to aberrant GR signaling in the brain, and thus contributing to HPA axis dysfunction.**

This body of work presents a potential mechanism whereby neurons could regulate cellular glucocorticoid signaling. Figure 5-1 illustrates this model, chronic inflammation or environmental factors leading to mood disorder could lead to an imbalance in the levels of FKBP52 and FKBP1 which could lead to aberrant GR activation, either acute or chronic. That

may have lasting impact on neurons in the central nervous system. Cellular glucocorticoid signaling in neurons of the frontal cortex could have an impact on surrounding tissue by altering synaptic and dendritic fields. The pathology of disease in psychiatric disorders is subtle and molecular etiology is likely subtle and complex as well. Therefore, these high molecular weight immunophilin proteins, may be part of a feedback system that is a recent addition to the mammalian genetic milieu, which may be part of the biochemical basis for stress-related disease.

## **5.1 IMMUNOPHILINS AND GLUCOCORTICOID RECEPTOR**

We show here the importance of FKBP52 in cortisol-induced trafficking of GR in neurons. However, more questions are raised about FKBP51. The formation of puncta in the nucleus was inhibited by FK506, and FKBP51 was absent in the nucleus when FK506 was present. Does FKBP51 affect the stability or dynamics of GR in the nucleus? Which gene transcripts, specific to GR are altered? Similar cell culture studies as those presented in Chapter 4 knocking down expression of FKBP51 will help answer some of these questions. Furthermore, more sophisticated techniques described in Section 4.4.1.1 and 4.4.2.1 to measure kinetics of protein-protein interactions with the immunophilins and hormone receptors may provide insights into cellular physiology of hormone receptor and adapter protein interplay.

In Chapter 2, a simple phylogenetic analysis illustrated the divergence of the larger molecular weight immunophilin FKBP52 in mammals and primates. FKBP51 is a recent addition to the immunophilin repertoire. Hormone and steroid signaling are important molecular regulators for development and function of tissues. The brain is sometimes said to be a slave to hormones. It is interesting that these two proteins, recently evolved and diverged, play a role in

subtle modulation of glucocorticoid signaling, a cell can regulate its “readiness” to respond to acutely elevated cortisol. In Chapter 3, we showed that in a human model of chronic viral infection (HIV), these proteins are dysregulated in a neuronal population that responds to chronic glucocorticoid exposure with decreased neuritic arborization, which may be pertinent to mood. Future studies that build on this body of work may reveal a molecular basis for mood disorders.

## **5.2 IMMUNOPHILINS IN HIV AND DEPRESSION**

In Chapter 3, we uncovered some interesting information with regard to the expression of immunophilins FKBP52 and FKBP51 in HIV infection and depression. They appear to be increased in the frontal cortex of HIV-infected individuals (Section 3.3.1 and 3.3.2). Since expression of the immunophilins seems to generally neuronal in the region analyzed; for example in large pyramidal neurons for FKBP51 and in pyramidal neurons and interneurons for FKBP52 (Section 3.3.5), the increase is likely not due to direct infection of a cell. Rather, our evidence points to neuronal increase in immunophilin expression due to soluble factors secreted by HIV-infected microglia (Section 3.3.4). Since HIV-infected microglia produce the cytokines  $TNF\alpha$ ,  $IL-1\alpha$ , and  $IL-1\beta$  [184], and these cytokines can cause altered GR signaling [24-26, 177], and these protein play a role in GR signaling [81, 137], it would make sense that neuronal GR signaling is altered by HIV-infected microglia through changes in immunophilin expression due to cytokine production.

HIV patients were shown to be hypercortisolemic [18, 19] and have an increased risk of developing MDD [171, 186]. The results presented here may point to immunophilins as a

molecular basis for susceptibility; however it is important to remember that the genes interact with the environment to produce the disease. In this case, the environment is HIV-infection, not all HIV patients develop MDD, and there are other factors involved. These factors may be psychosocial stress or drug abuse.

We analyzed two SNP's previously identified to be associated with PTSD, depression, and dissociative disorder that may be associated with our MDD population (See Summary in Table 3-8 and Discussion in Section 3.4.3). The SNP's may have different roles in MDD found in HIV and non-HIV patients. The polymorphism located in Intron II, near a hormone responsive element, and the polymorphism located in the 3'UTR, may affect either transcription of the mRNA or translation of the protein, respectively. Studies into the molecular consequences of these polymorphisms would be interesting. For instance, does the SNP located near on intronic hormone responsive element affect the transcription of *FKBP5*? Does the SNP located in the 3'UTR affect interaction with micro-RNA's and affect mRNA stability and protein translation? Is it tissue specific?

In order to determine whether the intronic SNP affects *FKBP5* transcription, an experiment could be designed utilizing primary cells from a genotyped source. Since *FKBP5* is cortisol-responsive and the putative element we are testing is an HRE, treatment with cortisol would show differential effects in cells derived from CC, CT, or TT genotyped cases. Isolation of DNA and amplification of the specific region or even de novo synthesis of the desired region using either the C or T allele at the appropriate place, followed by a gel-shift assay described in Section 4.4.2.1 could test whether the allele affects binding of transcription factors.

In order to determine whether a micro-RNA targets the SNP in the 3'UTR of the *FKBP5*, Northern analysis, and functional analyses could be used. The specific region containing the

SNP in 3'UTR of *FKBP5* would be amplified by PCR from sources homozygous for the A or C allele (potentially using the same probes as the allelic discrimination assay described in Section 3.2.5) and this product hybridized to a membrane. Micro-RNA from cells would then be isolated, radiolabeled, and used to probe PCR product. To determine whether results would be tissue-specific, micro-RNA's from various tissues or brain regions, or from panels of patients could be isolated. Results from these studies may have social impacts on prevention strategies as well for diseases such as PTSD, MDD, peritraumatic dissociation; for example: screening soldiers for risk alleles before deployment and identifying susceptible populations to receive interventional behavioral, cognitive, or pharmacologic therapy. These results would be interesting because it would provide a *functional* consequence of the SNP's which may relate to the etiology of the diseases that they associate with, and provide insights for development of therapeutic strategies.



## APPENDIX A

### DENSITOMETRIC ANALYSIS OF WESTERN BLOTS

#### A.1 PURPOSE

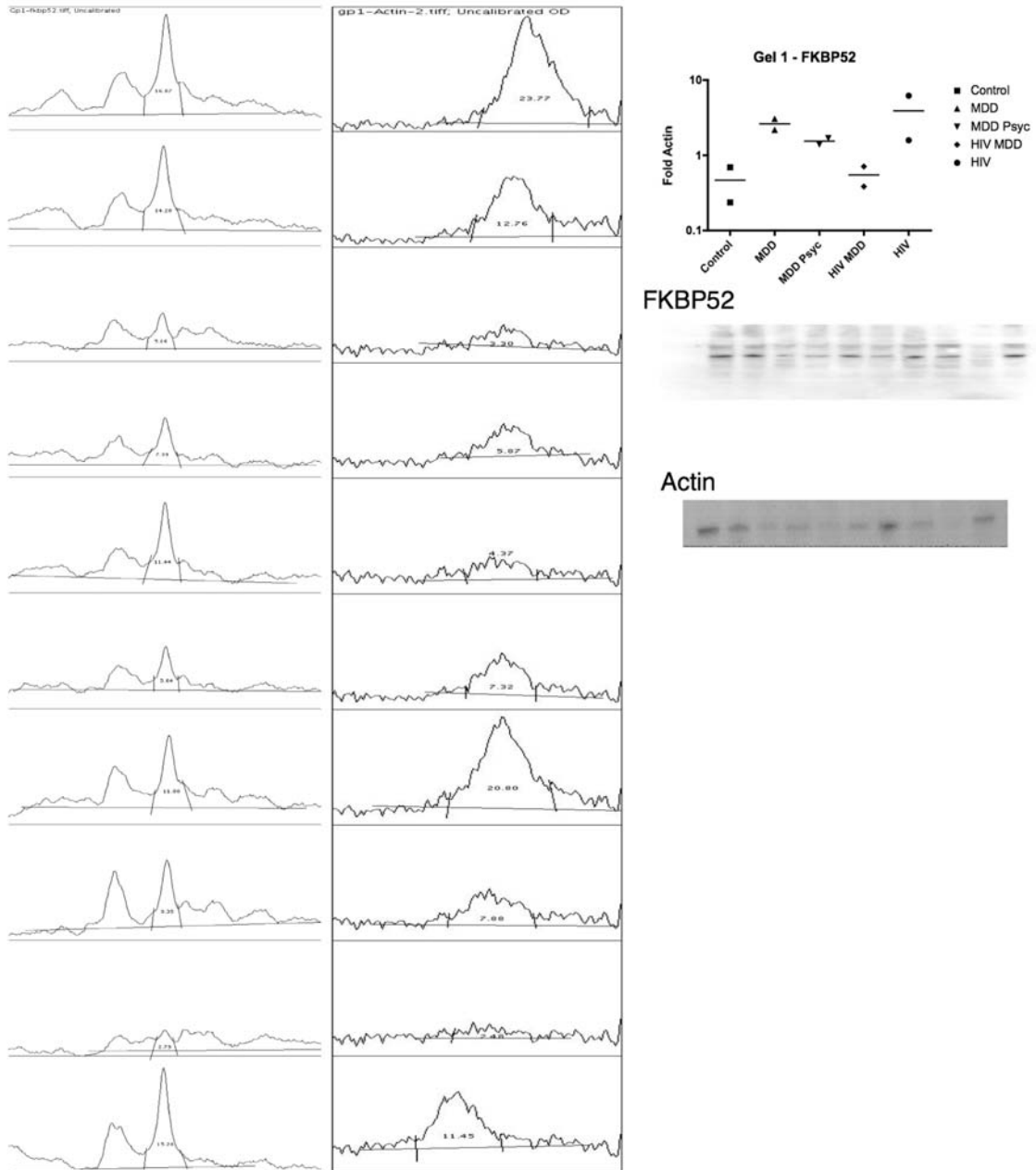
In order to compare protein levels in the autopsy study and obtain the data for Section 3.3.1, densitometric measurements were taken of the Western Blots depicted in Figure 3-5 and Figure 3-7 to obtain the plots. To assess protein transfer, loading, and quality in the western blot polyvinylfluoridine (PVDF) membranes, protein stains were performed prior to further Western blotting.

#### A.2 PROCEDURE

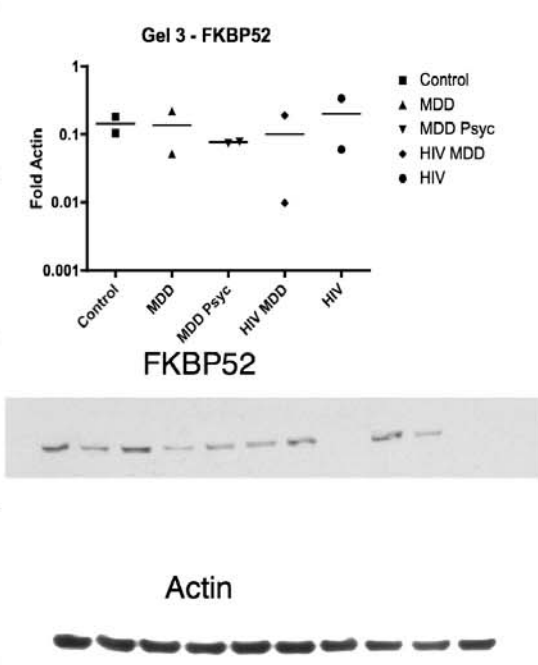
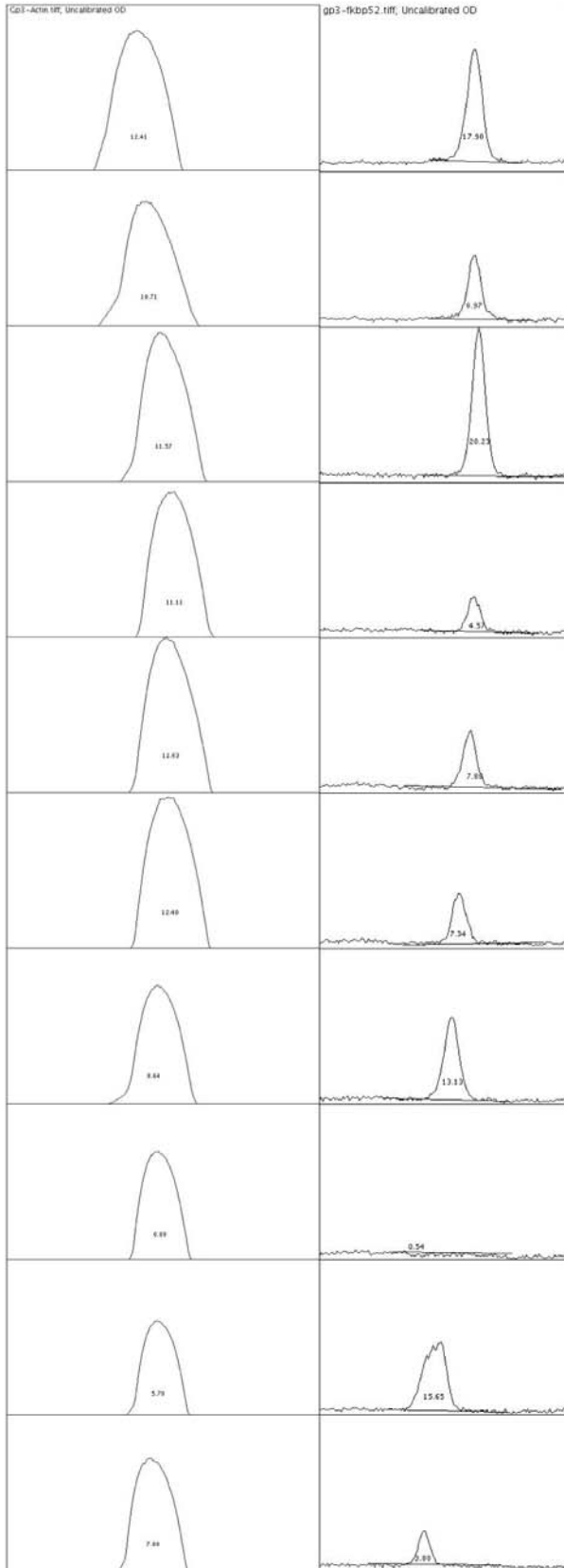
The program Image J was utilized to measure the density of bands in Western blots illustrated in Section 3.3.1 [239]. Lanes were outlined and histograms of optical density were constructed. The area under the curve was measured for each band of the immunophilin proteins and actin.  $\text{Fold-Actin} = \text{Area}_{\text{FKBP}} / \text{Area}_{\text{Actin}}$ . Normalized Fold Actin as plotted in the y axis of Figures 3-6 and 3-8 is calculated by comparing each Fold-Actin to the average Fold-Actin of the Control Group,  $\text{Normalized Fold-Control} = \text{Fold-Actin}_{\text{Control}} / \text{Fold-Actin}_{\text{patient}}$ . Although the densitometric analysis is not strictly quantitative and has a low signal to noise ratio compared to

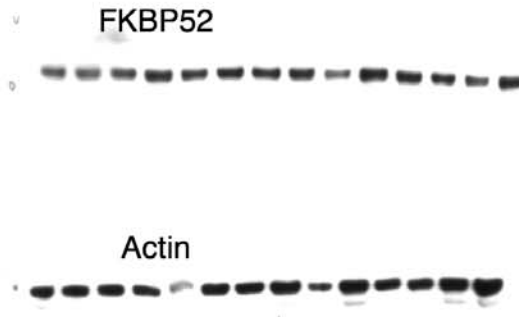
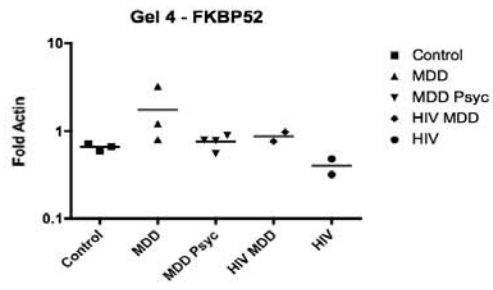
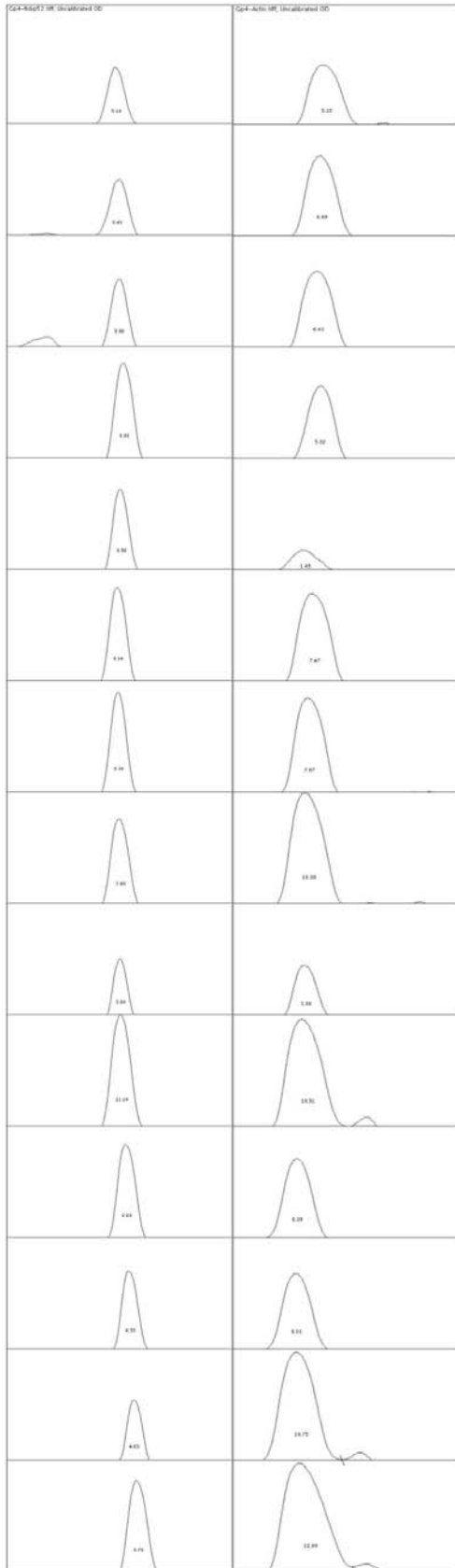
other methods of measurement, calculating Fold-Actin is a way of accounting for protein degradation and loading errors, and is the mathematical basis for the  $\Delta\Delta\text{CT}$  method for determining gene expression in quantitative PCR. Since the tissue is human autopsy tissue with variable handling procedures and postmortem intervals shown in Table 3-1, there was unequal protein degradation from patient to patient, a normalization procedure is necessary for comparison.

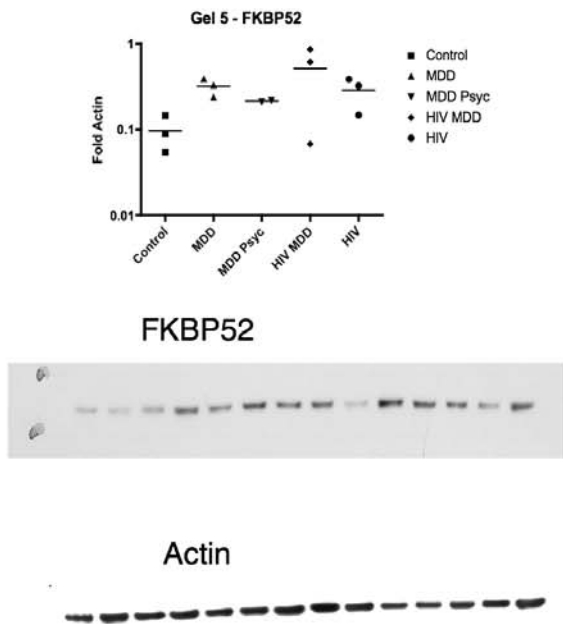
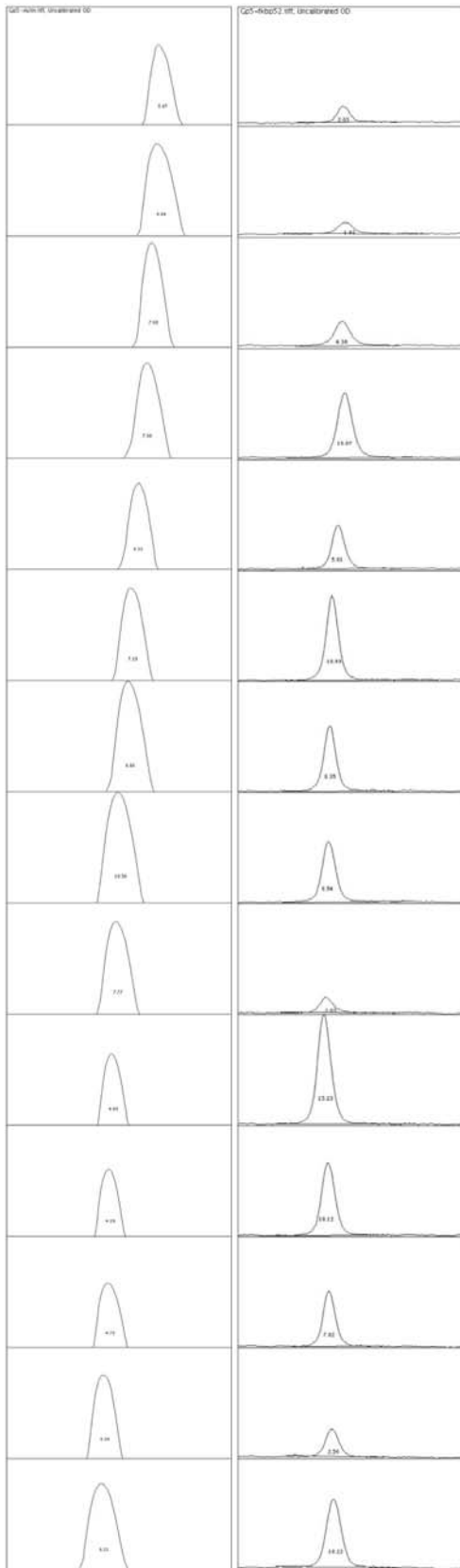
### A.3 RESULTS

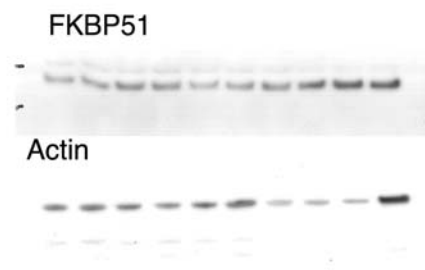
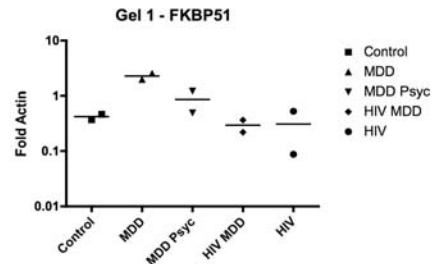
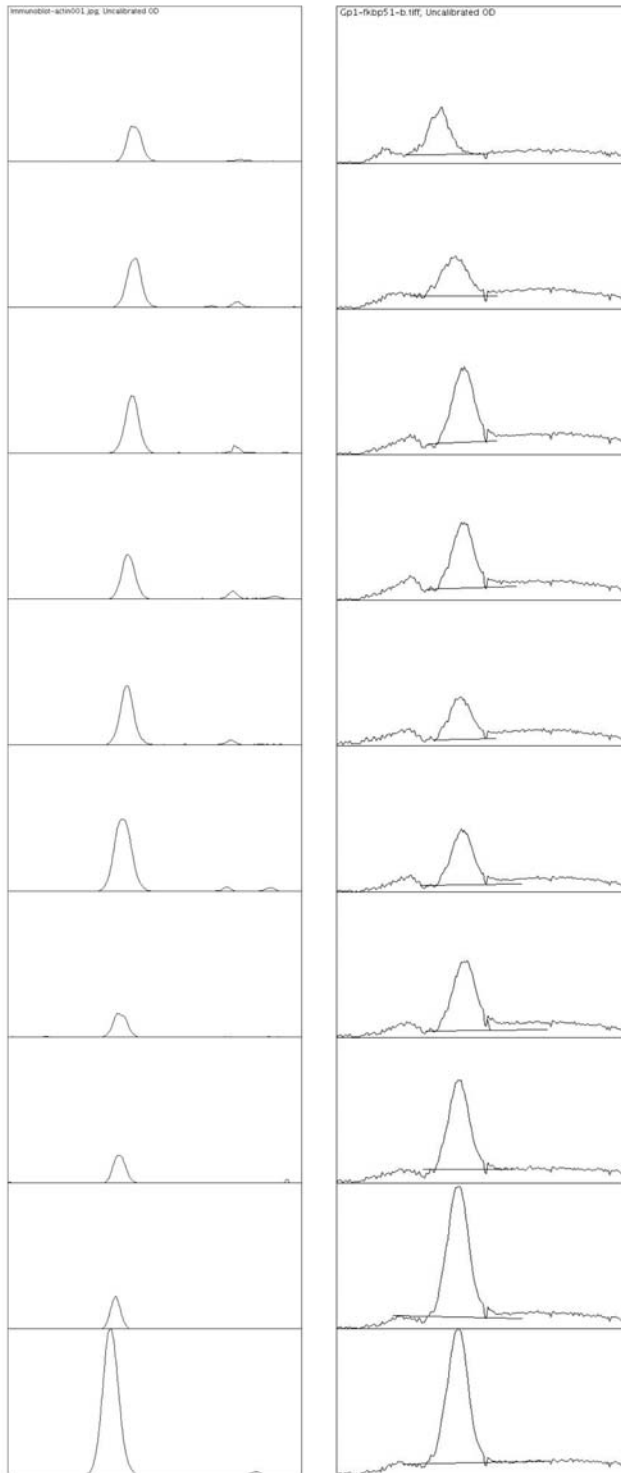


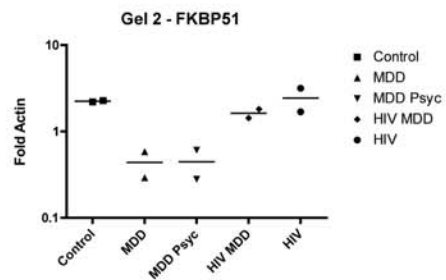
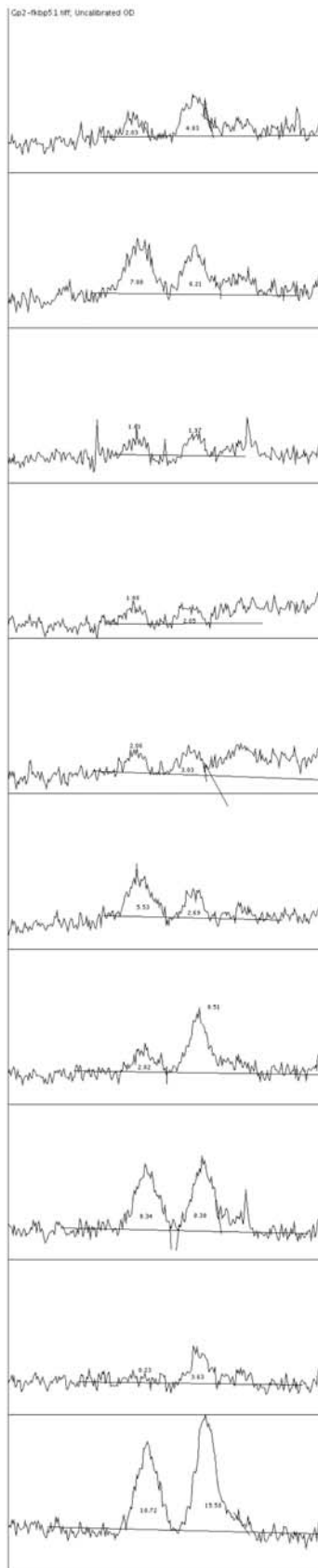
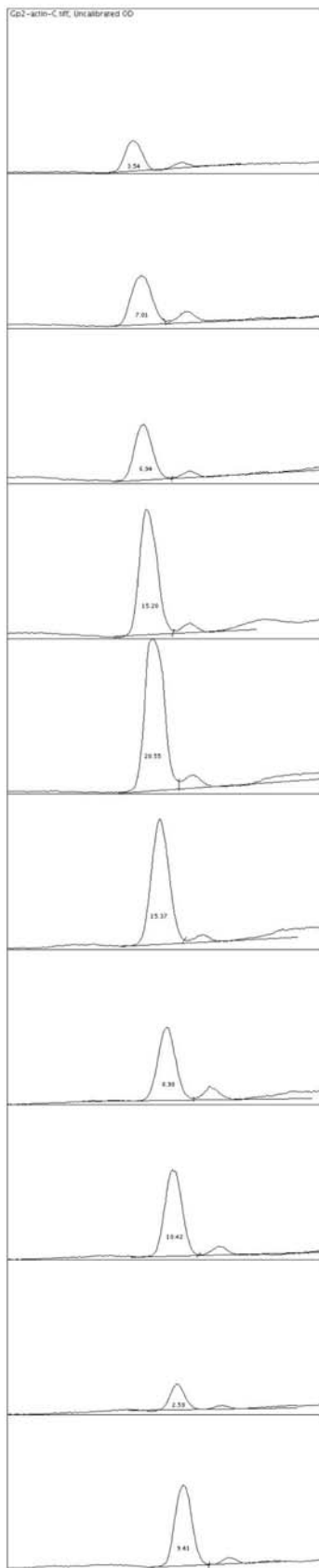








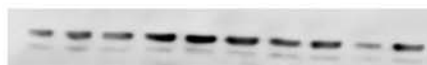


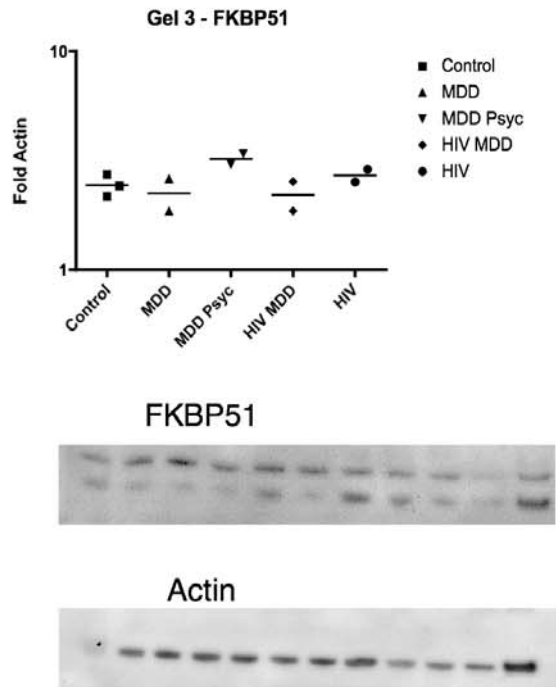
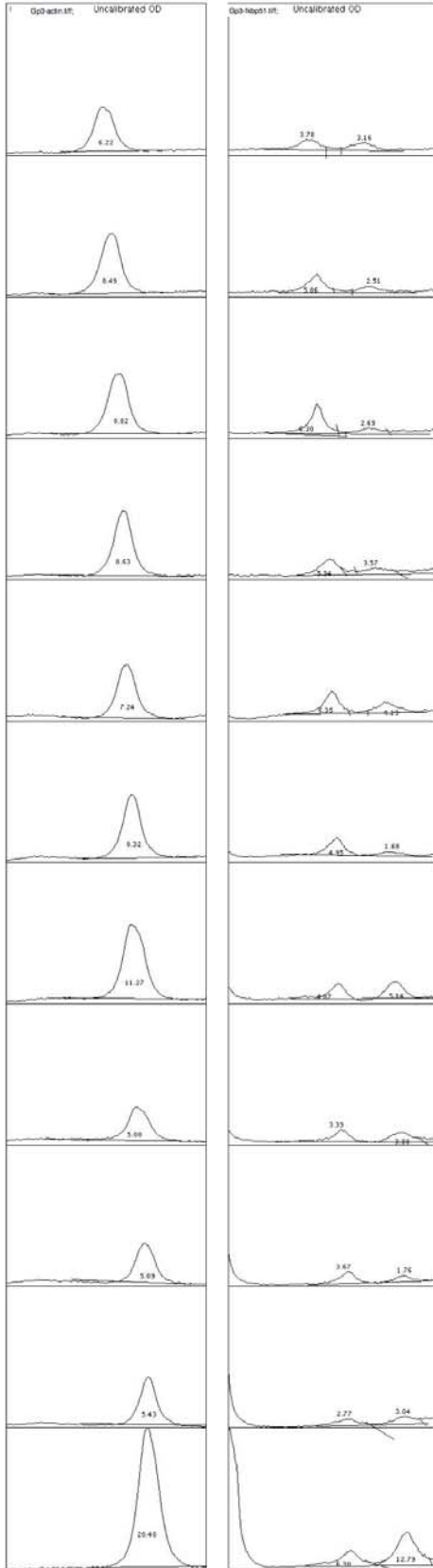


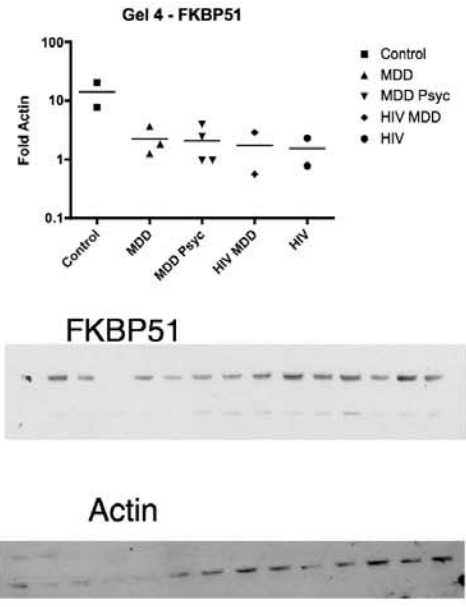
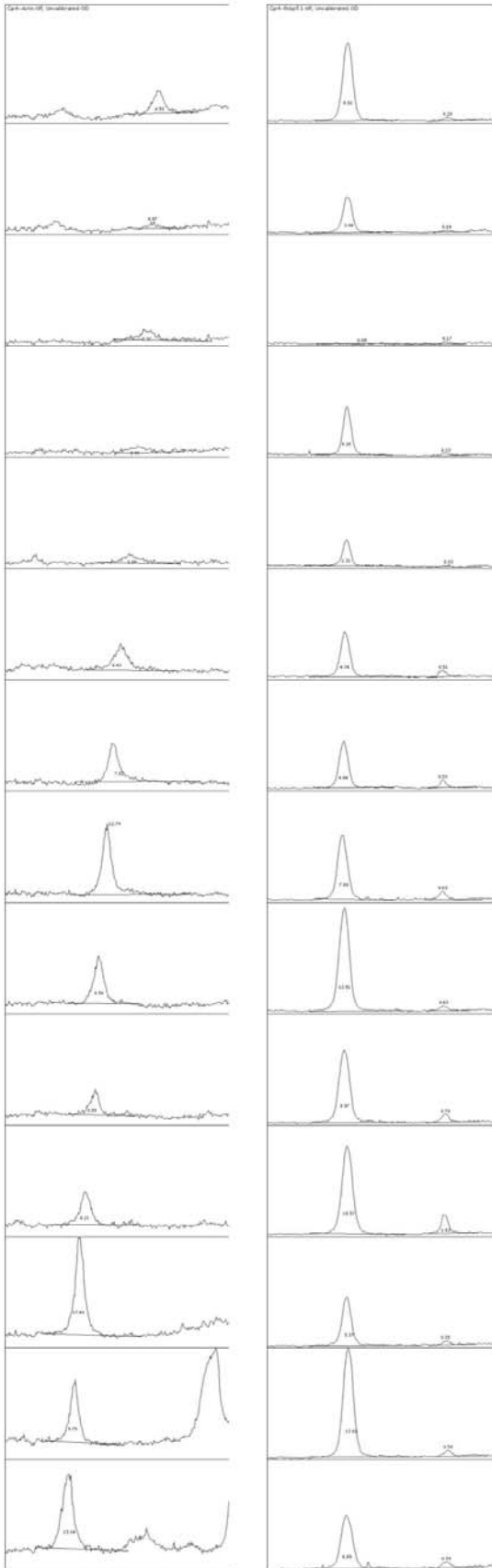
FKBP51

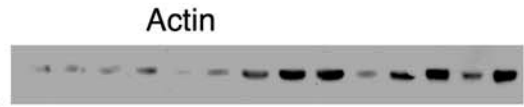
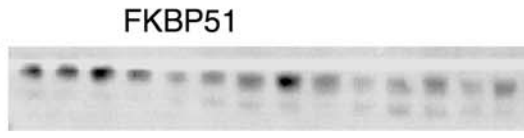
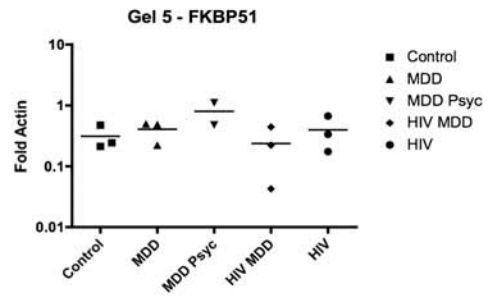
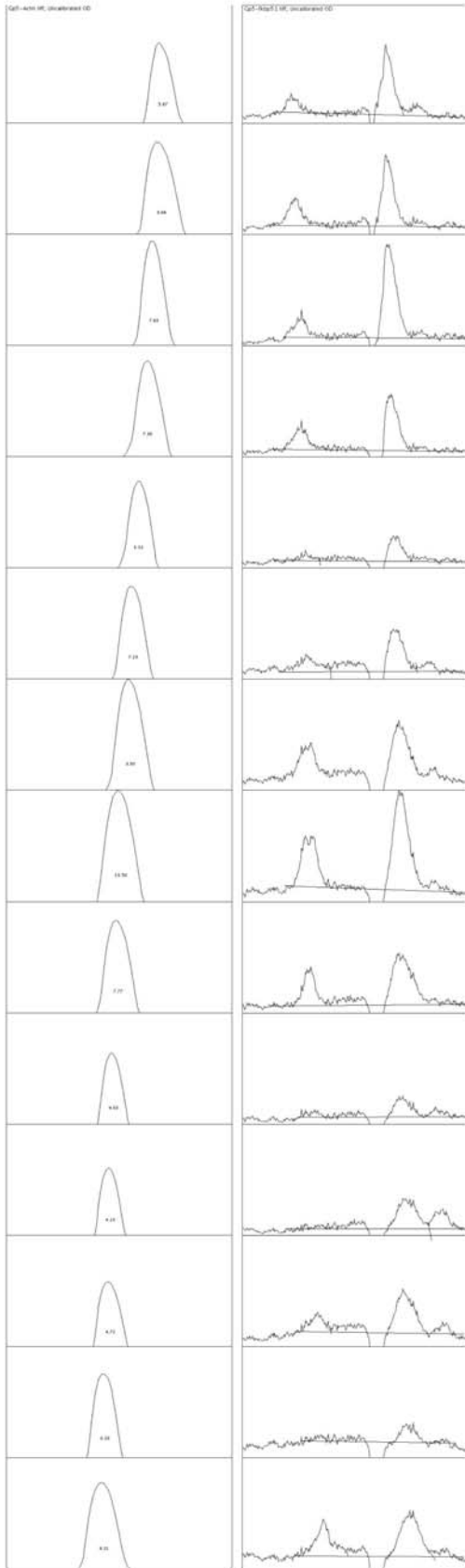


Actin









## **APPENDIX B**

### **PRIMARY HUMAN NEUROGLIA FROM FETAL TISSUE**

#### **B.1 TISSUE PREPARATION**

Human fetal forebrain tissue was acquired according to University of California San Diego Internal Review Board guidelines through Advanced Biosystems (Alameda, CA). Tissue was transferred to a 50mL conical polystyrene tube and kept at 4°C in a Holding Media consisting of Hanks Balanced Salt Solution without Ca<sup>2+</sup> with 1mM glutamine, and 10µg/mL gentamycin sulfate and 25mM HEPES.

1. Tissue was placed in holding media in a sterile Petri dish.
2. Menninges and blood vessels were separated from cellular tissue using forceps separating viable tissue from one petri-dish to the next.
3. Tissue was disaggregated by chopping with a scalpel and transferred to a new conical tube containing 4°C Holding Media.
4. To separate tissue and form a single cell suspension, tissue was drawn back and forth ten times in a 5mL glass pipette.

5. The suspension was shaken gently and stored on ice for 10 minutes to allow extracellular matrix to settle to bottom.

6. Using a 10mL syringe the single cell suspension, supernatant, was removed and passed through a sterile nylon filter into empty 50mL conical tubes.

7. The filtered suspensions were centrifuged at 1000rpm, 4°C for 5 minutes

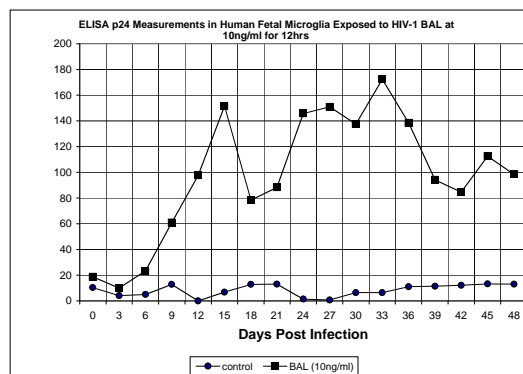
8. Pellets were resuspended in a single tube and cells were counted in Trypan Blue.

9.  $10^6$  cells/mL were plated, and cultures maintained at 37°C, 5%CO<sub>2</sub>.

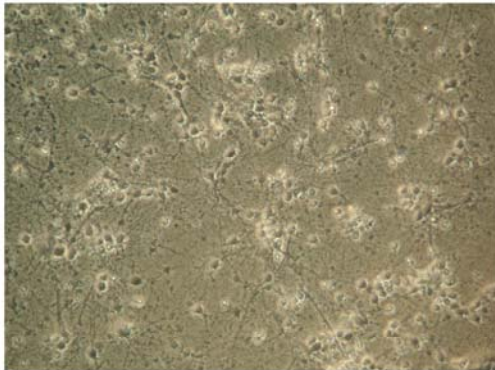
Microglia were cultured in 175cm<sup>2</sup> flasks in 20mL media consisting of high glucose DMEM supplemented with 10% human serum, 25mM HEPES, 10µg/mL gentamycin sulfate, 2mM glutamine.

Neurons are cultured on glass coverslips coated with polyornithine and laminin in 24-well plates using 500µL meda consisting of Neurobasal media with B-27 supplement, 2mM glutamine, and 10µg/mL gentamycin sulfate.

HIV BAL was obtained for the National Institutes of Health AIDS-Reagent Repository Program and microglia were exposed to 104pg of virus as determined by p24 ELISA. Media were changed every three days and supernatant was saved for p24 measurements. Supernatant for exposure to SH-SY5Y cells shown in Section 3.3.4 were used from Day 15 with p24 measurements showing viral propagation in the graph below.



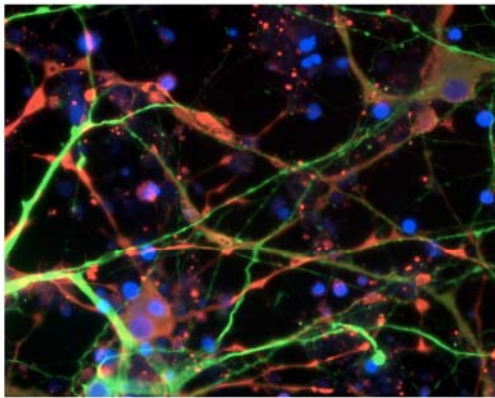
Mixed neuron-glia cultures were maintained in media for four weeks for differentiation according to previously reports. Phase contrast images of a typical live culture is shown below, with MAP2 immunocytochemistry, and MAP2/Neurofilament (green) GFAP (red) immunofluorescence images.



Phase Contrast Live Neuroglia



Immunocytochemistry, Mouse anti MAP2, DAB



Immunofluorescence  
Mouse anti MAP2 (green)  
Mouse anti Neurofilament (green)  
Rabbit anti GFAP (red)  
Hoescht's - Nuclei (blue)

## BIBLIOGRAPHY

1. Steiner, J.P., et al., *High brain densities of the immunophilin FKBP colocalized with calcineurin*. Nature, 1992. **358**(6387): p. 584-7.
2. Dawson, T.M., et al., *The immunophilins, FK506 binding protein and cyclophilin, are discretely localized in the brain: relationship to calcineurin*. Neuroscience, 1994. **62**(2): p. 569-80.
3. Somarelli, J.A., et al., *Structure-based classification of 45 FK506-binding proteins*. Proteins, 2008.
4. Trandinh, C.C., G.M. Pao, and M.H. Saier, Jr., *Structural and evolutionary relationships among the immunophilins: two ubiquitous families of peptidyl-prolyl cis-trans isomerases*. Faseb J, 1992. **6**(15): p. 3410-20.
5. Himukai, R., T. Kuzuhara, and M. Horikoshi, *Relationship between the subcellular localization and structures of catalytic domains of FKBP-type PPIases*. J Biochem, 1999. **126**(5): p. 879-88.
6. Gothel, S.F. and M.A. Marahiel, *Peptidyl-prolyl cis-trans isomerases, a superfamily of ubiquitous folding catalysts*. Cell Mol Life Sci, 1999. **55**(3): p. 423-36.
7. Barik, S., *Immunophilins: for the love of proteins*. Cell Mol Life Sci, 2006. **63**(24): p. 2889-900.
8. Avramut, M. and C.L. Achim, *Immunophilins in nervous system degeneration and regeneration*. Curr Top Med Chem, 2003. **3**(12): p. 1376-82.
9. Vernier, P., et al., *The degeneration of dopamine neurons in Parkinson's disease: insights from embryology and evolution of the mesostriataocortical system*. Annals of the New York Academy of Sciences, 2004. **1035**: p. 231-249.
10. Cara, L.W., *Dendritic reorganization in pyramidal neurons in medial prefrontal cortex after chronic corticosterone administration*. Journal of Neurobiology, 2001. **49**(3): p. 245-253.
11. Cotter, D., et al., *Reduced neuronal size and glial cell density in area 9 of the dorsolateral prefrontal cortex in subjects with major depressive disorder*. Cereb Cortex, 2002. **12**(4): p. 386-94.
12. Webster, M.J., et al., *Regional specificity of brain glucocorticoid receptor mRNA alterations in subjects with schizophrenia and mood disorders*. Mol Psychiatry, 2002. **7**(9): p. 985-94, 924.
13. Sapolsky, R.M. and P.M. Plotsky, *Hypercortisolism and its possible neural bases*. Biol Psychiatry, 1990. **27**(9): p. 937-52.

14. Davies, T.H., Y.M. Ning, and E.R. Sanchez, *A new first step in activation of steroid receptors: hormone-induced switching of FKBP51 and FKBP52 immunophilins*. J Biol Chem, 2002. **277**(7): p. 4597-600.
15. Alexandre Urani, P.G., *Corticosteroid Receptor Transgenic Mice*. Ann N Y Acad Sci, 2003. **1007**(Steroids and the Nervous System): p. 379-393.
16. Florian, H., *High-Quality Antidepressant Discovery by Understanding Stress Hormone Physiology*. Ann N Y Acad Sci, 2003. **1007**(Steroids and the Nervous System): p. 394-404.
17. Sapolsky, R.M., L.C. Krey, and B.S. McEwen, *The neuroendocrinology of stress and aging: the glucocorticoid cascade hypothesis*. Endocr Rev, 1986. **7**(3): p. 284-301.
18. Chittiprol, S., et al., *HPA axis activity and neuropathogenesis in HIV-1 clade C infection*. Front Biosci, 2007. **12**: p. 1271-7.
19. Christeff, N., et al., *Serum cortisol and DHEA concentrations during HIV infection*. Psychoneuroendocrinology, 1997. **22 Suppl 1**: p. S11-8.
20. Valente, S.M., *Depression and HIV disease*. J Assoc Nurses AIDS Care, 2003. **14**(2): p. 41-51.
21. Bagetta, G., et al., *Involvement of interleukin-1beta in the mechanism of human immunodeficiency virus type 1 (HIV-1) recombinant protein gp120-induced apoptosis in the neocortex of rat*. Neuroscience, 1999. **89**(4): p. 1051-66.
22. Yeung, M.C., L. Pulliam, and A.S. Lau, *The HIV envelope protein gp120 is toxic to human brain-cell cultures through the induction of interleukin-6 and tumor necrosis factor-alpha*. AIDS, 1995. **9**(2): p. 137-43.
23. Pariante, C.M., et al., *The Proinflammatory Cytokine, Interleukin-1{alpha}, Reduces Glucocorticoid Receptor Translocation and Function*. Endocrinology, 1999. **140**(9): p. 4359-4366.
24. Joyce, D.A., J.H. Steer, and L.J. Abraham, *Glucocorticoid modulation of human monocyte/macrophage function: control of TNF-alpha secretion*. Inflamm Res, 1997. **46**(11): p. 447-51.
25. Verheggen, M.M., et al., *Modulation of glucocorticoid receptor expression in human bronchial epithelial cell lines by IL-1 beta, TNF-alpha and LPS*. Eur Respir J, 1996. **9**(10): p. 2036-43.
26. Webster, J.C., et al., *Proinflammatory cytokines regulate human glucocorticoid receptor gene expression and lead to the accumulation of the dominant negative beta isoform: a mechanism for the generation of glucocorticoid resistance*. Proc Natl Acad Sci U S A, 2001. **98**(12): p. 6865-70.
27. Tombaugh, G.C., et al., *Glucocorticoids exacerbate hypoxic and hypoglycemic hippocampal injury in vitro: biochemical correlates and a role for astrocytes*. J Neurochem, 1992. **59**(1): p. 137-46.
28. Gillespie, C.F. and C.B. Nemeroff, *Hypercortisolemia and depression*. Psychosom Med, 2005. **67 Suppl 1**: p. S26-8.
29. Wellman, C.L., *Dendritic reorganization in pyramidal neurons in medial prefrontal cortex after chronic corticosterone administration*. J Neurobiol, 2001. **49**(3): p. 245-53.
30. West, M.J., *Regionally specific loss of neurons in the aging human hippocampus*. Neurobiol Aging, 1993. **14**(4): p. 287-93.
31. Smeets, W.J. and A. Reiner, *Phylogeny and development of catecholamine systems in the CNS of vertebrates*. 1994: Cambridge University Press.

32. Achim, C.L., E.T. Tatro, and M. Avramut, *Brain immunophilins as early markers of neurodegeneration*. The FASEB Journal, 2005. **19**: p. Abstract #685.1.
33. Gold, B.G., *Neuroimmunophilin ligands: evaluation of their therapeutic potential for the treatment of neurological disorders*. Expert Opin Investig Drugs, 2000. **9**(10): p. 2331-42.
34. Avramut, M., A. Zeevi, and C.L. Achim, *The immunosuppressant drug FK506 is a potent trophic agent for human fetal neurons*. Brain Res Dev Brain Res, 2001. **132**(2): p. 151-7.
35. Drevets, W.C., et al., *Subgenual prefrontal cortex abnormalities in mood disorders*. Nature, 1997. **386**(6627): p. 824-7.
36. Lupien, S.J., et al., *Increased cortisol levels and impaired cognition in human aging: implication for depression and dementia in later life*. Rev Neurosci, 1999. **10**(2): p. 117-39.
37. Drevets, W.C., et al., *Glucose metabolism in the amygdala in depression: relationship to diagnostic subtype and plasma cortisol levels*. Pharmacol Biochem Behav, 2002. **71**(3): p. 431-47.
38. Roozendaal, B., 1999 Curt P. Richter award. *Glucocorticoids and the regulation of memory consolidation*. Psychoneuroendocrinology, 2000. **25**(3): p. 213-38.
39. Gold, P.W., W.C. Drevets, and D.S. Charney, *New insights into the role of cortisol and the glucocorticoid receptor in severe depression*. Biol Psychiatry, 2002. **52**(5): p. 381-5.
40. Campbell, S., et al., *Lower hippocampal volume in patients suffering from depression: a meta-analysis*. Am J Psychiatry, 2004. **161**(4): p. 598-607.
41. Long, J.M., et al., *What counts in brain aging? Design-based stereological analysis of cell number*. J Gerontol A Biol Sci Med Sci, 1999. **54**(10): p. B407-17.
42. Rowan, M.J., R. Anwyl, and L. Xu, *Stress and long-term synaptic depression*. Mol Psychiatry, 1998. **3**(6): p. 472-4.
43. Miller, D.B. and J.P. O'Callaghan, *Aging, stress and the hippocampus*. Ageing Res Rev, 2005. **4**(2): p. 123-40.
44. Pavlides, C. and B.S. McEwen, *Effects of mineralocorticoid and glucocorticoid receptors on long-term potentiation in the CA3 hippocampal field*. Brain Res, 1999. **851**(1-2): p. 204-14.
45. Li, P., et al., *Structure of the N-terminal domain of human FKBP52*. Acta Crystallogr D Biol Crystallogr, 2003. **59**(Pt 1): p. 16-22.
46. Davies, T.H. and E.R. Sanchez, *Fkbp52*. Int J Biochem Cell Biol, 2005. **37**(1): p. 42-7.
47. Insti, A., 2004-2006.
48. Science, Allen Institute for Brain, *Allen Brain Atlas [Internet]*. 2008, Alen Institute for Brain Science: Seattle, WA.
49. Lein, E.S., et al., *Genome-wide atlas of gene expression in the adult mouse brain*. Nature, 2007. **445**(7124): p. 168-76.
50. Purba, J.S., et al., *Increased number of corticotropin-releasing hormone expressing neurons in the hypothalamic paraventricular nucleus of patients with multiple sclerosis*. Neuroendocrinology, 1995. **62**(1): p. 62-70.
51. Swanson, L.W. and D.M. Simmons, *Differential steroid hormone and neural influences on peptide mRNA levels in CRH cells of the paraventricular nucleus: a hybridization histochemical study in the rat*. J Comp Neurol, 1989. **285**(4): p. 413-35.
52. Tronche, F., et al., *Disruption of the glucocorticoid receptor gene in the nervous system results in reduced anxiety*. Nat Genet, 1999. **23**(1): p. 99-103.

53. Sapolsky, R.M., *Stress, the aging brain, and the mechanisms of neuron death*. 1992, Cambridge, Mass.: MIT Press. xi, 429.
54. Kawamura, A. and M.S. Su, *Interaction of FKBP12-FK506 with calcineurin A at the B subunit-binding domain*. J Biol Chem, 1995. **270**(26): p. 15463-6.
55. Harding, M.W., et al., *A receptor for the immunosuppressant FK506 is a cis-trans peptidyl-prolyl isomerase*. Nature, 1989. **341**(6244): p. 758-60.
56. Siekierka, J.J., et al., *A cytosolic binding protein for the immunosuppressant FK506 has peptidyl-prolyl isomerase activity but is distinct from cyclophilin*. Nature, 1989. **341**(6244): p. 755-7.
57. Gold, B.G. and J.E. Villafranca, *Neuroimmunophilin ligands: the development of novel neuroregenerative/ neuroprotective compounds*. Curr Top Med Chem, 2003. **3**(12): p. 1368-75.
58. Pemberton, T., *Identification and comparative analysis of sixteen fungal peptidyl-prolyl cis/trans isomerase repertoires*. BMC Genomics, 2006. **7**(1): p. 244.
59. Pemberton, T. and J. Kay, *Identification and comparative analysis of the peptidyl-prolyl cis/trans isomerase repertoires of H. sapiens, D. melanogaster, C. elegans, S. cerevisiae, and Sz. pombe*. Comparative and Functional Genomics, 2005. **6**(6): p. 277-300.
60. Somarelli, J.A. and R.J. Herrera, *Evolution of the 12 kDa FK506-binding protein gene*. Biol Cell, 2007. **99**(6): p. 311-21.
61. Denny, W.B., et al., *Squirrel monkey immunophilin FKBP51 is a potent inhibitor of glucocorticoid receptor binding*. Endocrinology, 2000. **141**(11): p. 4107-13.
62. Zhang, X., A.F. Clark, and T. Yorio, *FK506-Binding Protein 51 Regulates Nuclear Transport of the Glucocorticoid Receptor {beta} and Glucocorticoid Responsiveness*. Invest. Ophthalmol. Vis. Sci., 2008. **49**(3): p. 1037-1047.
63. Sinars, C.R., et al., *Structure of the large FK506-binding protein FKBP51, an Hsp90-binding protein and a component of steroid receptor complexes*. PNAS, 2003. **100**(3): p. 868-873.
64. Galat, A., *Sequence diversification of the FK506-binding proteins in several different genomes*. Eur J Biochem, 2000. **267**(16): p. 4945-59.
65. Craescu, C.T., et al., *Three-dimensional structure of the immunophilin-like domain of FKBP59 in solution*. Biochemistry, 1996. **35**(34): p. 11045-52.
66. Wu, B., et al., *Crystallization and preliminary crystallographic studies of the C-terminal domain of human FKBP52*. Acta Crystallogr D Biol Crystallogr, 2003. **59**(Pt 12): p. 2269-71.
67. Aghdasi, B., et al., *FKBP12, the 12-kDa FK506-binding protein, is a physiologic regulator of the cell cycle*. Proc Natl Acad Sci U S A, 2001. **98**(5): p. 2425-30.
68. Avila, G., et al., *FKBP12 binding to RyR1 modulates excitation-contraction coupling in mouse skeletal myotubes*. J Biol Chem, 2003. **278**(25): p. 22600-8.
69. Bultynck, G., et al., *Characterization and mapping of the 12 kDa FK506-binding protein (FKBP12)-binding site on different isoforms of the ryanodine receptor and of the inositol 1,4,5-trisphosphate receptor*. Biochem J, 2001. **354**(Pt 2): p. 413-22.
70. Cameron, A.M., et al., *FKBP12 binds the inositol 1,4,5-trisphosphate receptor at leucine-proline (1400-1401) and anchors calcineurin to this FK506-like domain*. J Biol Chem, 1997. **272**(44): p. 27582-8.

71. Gerard, M., et al., *The aggregation of alpha-synuclein is stimulated by FK506 binding proteins as shown by fluorescence correlation spectroscopy*. FASEB J., 2006: p. 05-5126fje.
72. Zissimopoulos, S. and F.A. Lai, *Interaction of FKBP12.6 with the Cardiac Ryanodine Receptor C-terminal Domain*. J. Biol. Chem., 2005. **280**(7): p. 5475-5485.
73. Zissimopoulos, S., N. Docrat, and F.A. Lai, *Redox Sensitivity of the Ryanodine Receptor Interaction with FK506-binding Protein*. J. Biol. Chem., 2007. **282**(10): p. 6976-6983.
74. Bush, K.T., B.A. Hendrickson, and S.K. Nigam, *Induction of the FK506-binding protein, FKBP13, under conditions which misfold proteins in the endoplasmic reticulum*. Biochem J, 1994. **303 ( Pt 3)**: p. 705-8.
75. Nigam, S.K., et al., *Localization of the FK506-binding protein, FKBP 13, to the lumen of the endoplasmic reticulum*. Biochem J, 1993. **294 ( Pt 2)**: p. 511-5.
76. Hung, D.T. and S.L. Schreiber, *cDNA cloning of a human 25 kDa FK506 and rapamycin binding protein*. Biochem Biophys Res Commun, 1992. **184**(2): p. 733-8.
77. Yang, W.M., Y.L. Yao, and E. Seto, *The FK506-binding protein 25 functionally associates with histone deacetylases and with transcription factor YY1*. Embo J, 2001. **20**(17): p. 4814-25.
78. Jin, Y.J. and S.J. Burakoff, *The 25-kDa FK506-binding protein is localized in the nucleus and associates with casein kinase II and nucleolin*. Proc Natl Acad Sci U S A, 1993. **90**(16): p. 7769-73.
79. Wochnik, G.M., et al., *FK506-binding proteins 51 and 52 differentially regulate dynein interaction and nuclear translocation of the glucocorticoid receptor in mammalian cells*. J Biol Chem, 2005. **280**(6): p. 4609-16.
80. Sanokawa-Akakura, R., et al., *A novel role for the immunophilin FKBP52 in copper transport*. J Biol Chem, 2004. **279**(27): p. 27845-8.
81. Cheung-Flynn, J., et al., *C-terminal sequences outside the tetratricopeptide repeat domain of FKBP51 and FKBP52 cause differential binding to Hsp90*. J Biol Chem, 2003. **278**(19): p. 17388-94.
82. Wu, B., et al., *3D structure of human FK506-binding protein 52: implications for the assembly of the glucocorticoid receptor/Hsp90/immunophilin heterocomplex*. Proc Natl Acad Sci U S A, 2004. **101**(22): p. 8348-53.
83. Crackower, M.A., et al., *Essential role of Fkbp6 in male fertility and homologous chromosome pairing in meiosis*. Science, 2003. **300**(5623): p. 1291-5.
84. Westerveld, G.H., et al., *Mutations in the chromosome pairing gene FKBP6 are not a common cause of non-obstructive azoospermia*. Mol. Hum. Reprod., 2005. **11**(9): p. 673-675.
85. Nakamura, T., et al., *Molecular cloning, characterization, and chromosomal localization of FKBP23, a novel FK506-binding protein with Ca<sup>2+</sup>-binding ability*. Genomics, 1998. **54**(1): p. 89-98.
86. Maestre-Martinez, M., et al., *Solution structure of the FK506-binding domain of human FKBP38*. J Biomol NMR, 2006. **34**(3): p. 197-202.
87. Edlich, F., et al., *Bcl-2 regulator FKBP38 is activated by Ca<sup>2+</sup>/calmodulin*. Embo J, 2005. **24**(14): p. 2688-99.
88. Wang, H.Q., et al., *Interaction of presenilins with FKBP38 promotes apoptosis by reducing mitochondrial Bcl-2*. Hum Mol Genet, 2005. **14**(13): p. 1889-902.

89. Weiwad, M., et al., *A reassessment of the inhibitory capacity of human FKBP38 on calcineurin*. FEBS Lett, 2005. **579**(7): p. 1591-6.
90. Shirane, M. and K.I. Nakayama, *Inherent calcineurin inhibitor FKBP38 targets Bcl-2 to mitochondria and inhibits apoptosis*. Nat Cell Biol, 2003. **5**(1): p. 28-37.
91. Nakagawa, T., et al., *Anchoring of the 26S proteasome to the organellar membrane by FKBP38*. Genes to Cells, 2007. **12**(6): p. 709-719.
92. Patterson, C.E., et al., *Genomic Organization of Mouse and Human 65 kDa FK506-Binding Protein Genes and Evolution of the FKBP Multigene Family*. Genomics, 2002. **79**(6): p. 881-889.
93. Davis, E.C., et al., *Identification of Tropoelastin as a Ligand for the 65-kD FK506-binding Protein, FKBP65, in the Secretory Pathway*. J. Cell Biol., 1998. **140**(2): p. 295-303.
94. Rulten, S., et al., *The human FK506-binding proteins: characterization of human FKBP19*. Mammalian Genome, 2006. **17**(4): p. 322-331.
95. Bennett, P.C., et al., *Cyclosporin A, FK506 and rapamycin produce multiple, temporally distinct, effects on memory following single-trial, passive avoidance training in the chick*. Brain Res, 2002. **927**(2): p. 180-94.
96. Tremmel, D., et al., *FKBP22 is part of chaperone/folding catalyst complexes in the endoplasmic reticulum of Neurospora crassa*. FEBS Letters. **In Press, Corrected Proof**.
97. Zhang, X., et al., *The mouse FKBP23 binds to BiP in ER and the binding of C-terminal domain is interrelated with Ca<sup>2+</sup> concentration*. FEBS Letters, 2004. **559**(1-3): p. 57-60.
98. Rizzo, P.J., *Basic chromosomal proteins in lower eukaryotes: relevance to the evolution and function of histones*. J Mol Evol, 1976. **8**(1): p. 79-94.
99. Clamp, M., et al., *The Jalview Java Alignment Editor*. Bioinformatics, 2004. **20**: p. 426-7.
100. Kissinger, C.R., et al., *Crystal structures of human calcineurin and the human FKBP12-FK506-calcineurin complex*. Nature, 1995. **378**(6557): p. 641-4.
101. Galat, A., *Peptidylprolyl Cis / Trans Isomerases (Immunophilins): Biological Diversity - Targets - Functions*. Current Topics in Medicinal Chemistry, 2003. **3**: p. 1315-1347.
102. Ikura, T. and N. Ito, *Requirements for peptidyl-prolyl isomerization activity: A comprehensive mutational analysis of the substrate-binding cavity of FK506-binding protein 12*. Protein Sci, 2007. **16**(12): p. 2618-25.
103. Park, S.T., et al., *PPIase catalysis by human FK506-binding protein proceeds through a conformational twist mechanism*. J Biol Chem, 1992. **267**(5): p. 3316-24.
104. Griffith, J.P., et al., *X-ray structure of calcineurin inhibited by the immunophilin-immunosuppressant FKBP12-FK506 complex*. Cell, 1995. **82**(3): p. 507-22.
105. Cardenas, M.E., et al., *Immunophilins interact with calcineurin in the absence of exogenous immunosuppressive ligands*. Embo J, 1994. **13**(24): p. 5944-57.
106. Le Bihan, S., et al., *The mammalian heat shock protein binding immunophilin (p59/HBI) is an ATP and GTP binding protein*. Biochem Biophys Res Commun, 1993. **195**(2): p. 600-7.
107. Arevalo-Rodriguez, M., et al., *FKBP12 controls aspartate pathway flux in Saccharomyces cerevisiae to prevent toxic intermediate accumulation*. Eukaryot Cell, 2004. **3**(5): p. 1287-96.
108. Alarcon, C.M. and J. Heitman, *FKBP12 physically and functionally interacts with aspartokinase in Saccharomyces cerevisiae*. Mol. Cell. Biol., 1997. **17**(10): p. 5968-5975.

109. Aracena, P., et al., *Effects of S-glutathionylation and S-nitrosylation on calmodulin binding to triads and FKBP12 binding to type 1 calcium release channels*. *Antioxid Redox Signal*, 2005. **7**(7-8): p. 870-81.
110. Radanyi, C., B. Chambrud, and E. Baulieu, *The Ability of the Immunophilin FKBP59-HBI to Interact with the 90-kDa Heat Shock Protein is Encoded by its Tetratricopeptide Repeat Domain*. *PNAS*, 1994. **91**(23): p. 11197-11201.
111. Patterson, C.E., et al., *Developmental regulation of FKBP65. An ER-localized extracellular matrix binding-protein*. *Mol Biol Cell*, 2000. **11**(11): p. 3925-35.
112. Cameron, A.M., et al., *Calcineurin associated with the inositol 1,4,5-trisphosphate receptor-FKBP12 complex modulates Ca<sup>2+</sup> flux*. *Cell*, 1995. **83**(3): p. 463-72.
113. Zhang, J., et al., *Three-dimensional localization of divergent region 3 of the ryanodine receptor to the clamp-shaped structures adjacent to the FKBP binding sites*. *J Biol Chem*, 2003. **278**(16): p. 14211-8.
114. Van Acker, K., et al., *The 12 kDa FK506-binding protein, FKBP12, modulates the Ca(2+)-flux properties of the type-3 ryanodine receptor*. *J Cell Sci*, 2004. **117**(Pt 7): p. 1129-37.
115. Xin, H.B., et al., *Affinity purification of the ryanodine receptor/calcium release channel from fast twitch skeletal muscle based on its tight association with FKBP12*. *Biochem Biophys Res Commun*, 1995. **214**(1): p. 263-70.
116. Shin, D.W., et al., *Ca(2+)-dependent interaction between FKBP12 and calcineurin regulates activity of the Ca(2+) release channel in skeletal muscle*. *Biophys J*, 2002. **83**(5): p. 2539-49.
117. Bauer, B., et al., *Modulation of p-Glycoprotein Transport Function at the Blood-Brain Barrier*. *Experimental Biology and Medicine*, 2005. **230**(2): p. 118-127.
118. Mizutani, T. and A. Hattori, *New Horizon of MDR1 (P-glycoprotein) Study*. *Drug Metabolism Reviews*, 2005. **37**(3): p. 489 - 510.
119. Hemenway, C.S. and J. Heitman, *Immunosuppressant target protein FKBP12 is required for p-glycoprotein function in yeast*. *J Biol Chem*, 1996. **271**(31): p. 18527-18534.
120. Kamphausen, T., et al., *Characterization of Arabidopsis thaliana AtFKBP42 that is membrane-bound and interacts with Hsp90*. *Plant J*, 2002. **32**(3): p. 263-76.
121. Weiergraber, O.H., A. Eckhoff, and J. Granzin, *Crystal structure of a plant immunophilin domain involved in regulation of MDR-type ABC transporters*. *FEBS Lett*, 2006. **580**(1): p. 251-5.
122. Perez-Perez, J.M., M.R. Ponce, and J.L. Micol, *The ULTRACURVATA2 gene of Arabidopsis encodes an FK506-binding protein involved in auxin and brassinosteroid signaling*. *Plant Physiology*, 2004. **134**(1): p. 101-117.
123. Mealey, K.L., et al., *Immunosuppressant inhibition of P-glycoprotein function is independent of drug-induced suppression of peptide-prolyl isomerase and calcineurin activity*. *Cancer Chemother Pharmacol*, 1999. **44**(2): p. 152-8.
124. Harrell, J.M., et al., *All of the Protein Interactions That Link Steroid Receptor&#183;Hsp90&#183;Immunophilin Heterocomplexes to Cytoplasmic Dynein Are Common to Plant and Animal Cells*. *Biochemistry*, 2002. **41**(17): p. 5581-5587.
125. Liu, F.-L., et al., *The intracellular domain of amyloid precursor protein interacts with FKBP12*. *Biochemical and Biophysical Research Communications*, 2006. **350**(2): p. 472-477.

126. Avramut, M. and C.L. Achim, *Immunophilins and their ligands: insights into survival and growth of human neurons*. *Physiol Behav*, 2002. **77**(4-5): p. 463-8.
127. Sidhu, A., et al., *The role of alpha-synuclein in both neuroprotection and neurodegeneration*. *Ann N Y Acad Sci*, 2004. **1035**: p. 250-70.
128. Sidhu, A., C. Wersinger, and P. Vernier, *Does {alpha}-synuclein modulate dopaminergic synaptic content and tone at the synapse?* *FASEB J.*, 2004. **18**(6): p. 637-647.
129. Maria J. Martí, E.T.J.C., *Clinical overview of the synucleinopathies*. *Movement Disorders*, 2003. **18**(S6): p. 21-27.
130. Polymeropoulos, M.H., et al., *Mutation in the alpha-synuclein gene identified in families with Parkinson's disease*. *Science*, 1997. **276**(5321): p. 2045-7.
131. Galigniana, M.D., et al., *Evidence that the peptidylprolyl isomerase domain of the hsp90-binding immunophilin FKBP52 is involved in both dynein interaction and glucocorticoid receptor movement to the nucleus*. *J Biol Chem*, 2001. **276**(18): p. 14884-9.
132. Pratt, W.B., et al., *Role of hsp90 and the hsp90-binding immunophilins in signalling protein movement*. *Cell Signal*, 2004. **16**(8): p. 857-72.
133. Galigniana, M.D., et al., *Binding of hsp90-Associated Immunophilins to Cytoplasmic Dynein: Direct Binding and in Vivo Evidence that the Peptidylprolyl Isomerase Domain Is a Dynein Interaction Domain*. *Biochemistry*, 2002. **41**(46): p. 13602-13610.
134. Ruff, V.A., et al., *Tissue distribution and cellular localization of hsp56, an FK506-binding protein. Characterization using a highly specific polyclonal antibody*. *J Biol Chem*, 1992. **267**(30): p. 21285-8.
135. Yong, W., et al., *Essential role for Co-chaperone Fkbp52 but not Fkbp51 in androgen receptor-mediated signaling and physiology*. *J Biol Chem*, 2007. **282**(7): p. 5026-36.
136. Tranguch, S., et al., *Cochaperone immunophilin FKBP52 is critical to uterine receptivity for embryo implantation*. *Proc Natl Acad Sci U S A*, 2005. **102**(40): p. 14326-31.
137. Cheung-Flynn, J., et al., *Physiological role for the cochaperone FKBP52 in androgen receptor signaling*. *Mol Endocrinol*, 2005. **19**(6): p. 1654-66.
138. Westberry, J.M., et al., *Glucocorticoid resistance in squirrel monkeys results from a combination of a transcriptionally incompetent glucocorticoid receptor and overexpression of the glucocorticoid receptor co-chaperone FKBP51*. *J Steroid Biochem Mol Biol*, 2006. **100**(1-3): p. 34-41.
139. Scammell, J.G., et al., *Overexpression of the FK506-binding immunophilin FKBP51 is the common cause of glucocorticoid resistance in three New World primates*. *Gen Comp Endocrinol*, 2001. **124**(2): p. 152-65.
140. Binder, E.B., et al., *Polymorphisms in FKBP5 are associated with increased recurrence of depressive episodes and rapid response to antidepressant treatment*. *Nat Genet*, 2004. **36**(12): p. 1319-25.
141. Koenen, K.C., et al., *Polymorphisms in FKBP5 are associated with peritraumatic dissociation in medically injured children*. *Mol Psychiatry*, 2005. **10**(12): p. 1058-9.
142. Gawlik, M., et al., *Is FKBP5 a genetic marker of affective psychosis? A case control study and analysis of disease related traits*. *BMC Psychiatry*, 2006. **6**: p. 52.
143. van Rossum, E.F.C., et al., *Polymorphisms of the Glucocorticoid Receptor Gene and Major Depression*. *Biological Psychiatry*, 2006. **59**(8): p. 681-688.
144. Lee, A.L., W.O. Ogle, and R.M. Sapolsky, *Stress and depression: possible links to neuron death in the hippocampus*. *Bipolar Disord*, 2002. **4**(2): p. 117-28.

145. Stockmeier, C.A., et al., *Cellular changes in the postmortem hippocampus in major depression*. Biol Psychiatry, 2004. **56**(9): p. 640-50.
146. Sapolsky, R.M., et al., *Hippocampal damage associated with prolonged glucocorticoid exposure in primates*. J Neurosci, 1990. **10**(9): p. 2897-902.
147. Heslen, W. and M. Joels, *Modulation of 5HT1A responsiveness in CA1 pyramidal neurons by in vivo activation of corticosteroid receptors*. J Neuroendocrinol, 1996. **8**(6): p. 433-8.
148. Lee, D., et al., *Glucocorticoid modulation of dopamine mediated effects on hypothalamic atrial natriuretic factor neurons*. Mol Psychiatry, 2000. **5**(3): p. 332-6.
149. Garcia, A., et al., *Age-dependent expression of glucocorticoid- and mineralocorticoid receptors on neural precursor cell populations in the adult murine hippocampus*. Aging Cell, 2004. **3**(6): p. 363-71.
150. Pedersen, K.M., et al., *muFKBP38: a novel murine immunophilin homolog differentially expressed in Schwannoma cells and central nervous system neurons in vivo*. Electrophoresis, 1999. **20**(2): p. 249-55.
151. Nielsen, J.V., et al., *Fkbp8: novel isoforms, genomic organization, and characterization of a forebrain promoter in transgenic mice*. Genomics, 2004. **83**(1): p. 181-92.
152. Deng, X., et al., *Reversible Phosphorylation of Bcl2 following Interleukin 3 or Bryostatins Mediated by Direct Interaction with Protein Phosphatase 2A*. J. Biol. Chem., 1998. **273**(51): p. 34157-34163.
153. Erin, N., S.K. Bronson, and M.L. Billingsley, *Calcium-dependent interaction of calcineurin with bcl-2 in neuronal tissue*. Neuroscience, 2003. **117**(3): p. 541-555.
154. Kang, C.B., et al., *Molecular characterization of FK-506 binding protein 38 and its potential regulatory role on the anti-apoptotic protein Bcl-2*. Biochem Biophys Res Commun, 2005. **337**(1): p. 30-8.
155. Edlich, F., et al., *The Bcl-2 Regulator FKBP38-Calmodulin-Ca<sup>2+</sup> Is Inhibited by Hsp90*. J. Biol. Chem., 2007. **282**(21): p. 15341-15348.
156. Bassik, M.C., et al., *Phosphorylation of BCL-2 regulates ER Ca<sup>2+</sup> homeostasis and apoptosis*. Embo J, 2004. **23**(5): p. 1207-16.
157. Kang, C.B., et al., *The flexible loop of Bcl-2 is required for molecular interaction with immunosuppressant FK-506 binding protein 38 (FKBP38)*. FEBS Lett, 2005. **579**(6): p. 1469-76.
158. Breitschopf, K., et al., *Posttranslational modification of Bcl-2 facilitates its proteasome-dependent degradation: molecular characterization of the involved signaling pathway*. Mol Cell Biol, 2000. **20**(5): p. 1886-96.
159. Chang, B.S., et al., *Identification of a novel regulatory domain in Bcl-X(L) and Bcl-2*. Embo J, 1997. **16**(5): p. 968-77.
160. Kohler, A., et al., *The axial channel of the proteasome core particle is gated by the Rpt2 ATPase and controls both substrate entry and product release*. Mol Cell, 2001. **7**(6): p. 1143-52.
161. Ross, C.A. and C.M. Pickart, *The ubiquitin-proteasome pathway in Parkinson's disease and other neurodegenerative diseases*. Trends in Cell Biology, 2004. **14**(12): p. 703-711.
162. Hegde, A.N. and A. DiAntonio, *Ubiquitin and the synapse*. Nat Rev Neurosci, 2002. **3**(11): p. 854-61.
163. Song, S. and Y.K. Jung, *Alzheimer's disease meets the ubiquitin-proteasome system*. Trends Mol Med, 2004. **10**(11): p. 565-70.

164. Ly, C.V. and P. Verstreken, *Mitochondria at the Synapse*. *Neuroscientist*, 2006. **12**(4): p. 291-299.
165. Takamori, S., et al., *Molecular Anatomy of a Trafficking Organelle*. *Cell*, 2006. **127**(4): p. 831-846.
166. Bulgakov, O.V., et al., *FKBP8 is a negative regulator of mouse sonic hedgehog signaling in neural tissues*. *Development*, 2004. **131**(9): p. 2149-59.
167. Nieuwenhuis, E. and C.C. Hui, *Hedgehog signaling and congenital malformations*. *Clin Genet*, 2005. **67**(3): p. 193-208.
168. Sinars, C.R., et al., *Structure of the large FK506-binding protein FKBP51, an Hsp90-binding protein and a component of steroid receptor complexes*. *Proc Natl Acad Sci U S A*, 2003. **100**(3): p. 868-73.
169. Cotter, D., et al., *The density and spatial distribution of GABAergic neurons, labelled using calcium binding proteins, in the anterior cingulate cortex in major depressive disorder, bipolar disorder, and schizophrenia*. *Biol Psychiatry*, 2002. **51**(5): p. 377-86.
170. Porche, D.J. and D.G. Willis, *Depression in HIV-infected men*. *Issues Ment Health Nurs*, 2006. **27**(4): p. 391-401.
171. Bing, E.G., et al., *Psychiatric disorders and drug use among human immunodeficiency virus-infected adults in the United States*. *Arch Gen Psychiatry*, 2001. **58**(8): p. 721-8.
172. Reddy, M.M., et al., *An improved method for monitoring efficacy of anti-retroviral therapy in HIV-infected individuals: a highly sensitive HIV p24 antigen assay*. *J Clin Lab Anal*, 1992. **6**(3): p. 125-9.
173. Haga, H., et al., *Gene-based SNP discovery as part of the Japanese Millennium Genome Project: identification of 190,562 genetic variations in the human genome. Single-nucleotide polymorphism*. *J Hum Genet*, 2002. **47**(11): p. 605-10.
174. Glisovic, T., et al., *RNA-binding proteins and post-transcriptional gene regulation*. *FEBS Letters*, 2008. **582**(14): p. 1977-1986.
175. Konstantinova, I.M., et al., *Role of Proteasomes in Cellular Regulation*, in *International Review of Cell and Molecular Biology*. 2008, Academic Press. p. 59-124.
176. Wilson, V.G. and P.R. Heaton, *Ubiquitin proteolytic system: focus on SUMO*. *Expert Review of Proteomics*, 2008. **5**(1): p. 121-135.
177. Costas, M., et al., *Molecular and functional evidence for in vitro cytokine enhancement of human and murine target cell sensitivity to glucocorticoids. TNF-alpha priming increases glucocorticoid inhibition of TNF-alpha-induced cytotoxicity/apoptosis*. *J Clin Invest*, 1996. **98**(6): p. 1409-16.
178. Zhao, M.L., et al., *Expression of inducible nitric oxide synthase, interleukin-1 and caspase-1 in HIV-1 encephalitis*. *J Neuroimmunol*, 2001. **115**(1-2): p. 182-91.
179. Hubler, T.R. and J.G. Scammell, *Intronic hormone response elements mediate regulation of FKBP5 by progesterins and glucocorticoids*. *Cell Stress Chaperones*, 2004. **9**(3): p. 243-52.
180. Billing, A.M., et al., *Proteomic analysis of the cortisol-mediated stress response in THP-1 monocytes using DIGE technology*. *J Mass Spectrom*, 2007. **42**(11): p. 1433-44.
181. T.G. D'Aversa, E.A.E.J.W.B., *NeuroAIDS: Contributions of the human immunodeficiency virus-1 proteins tat and gp120 as well as CD40 to microglial activation*. *Journal of Neuroscience Research*, 2005. **81**(3): p. 436-446.
182. Scammell, J.G., et al., *Organization of the human FK506-binding immunophilin FKBP52 protein gene (FKBP4)*. *Genomics*, 2003. **81**(6): p. 640-3.

183. Garey, L. and K. Brodmann, *Brodmann's Localisation in the Cerebral Cortex*. 1994, London: Smith Gordon & co Ltd.
184. Achim, C.L., et al., *Macrophage Activation Factors in the Brains of AIDS Patients*. J NeuroAIDS, 1996. **1**(2): p. 1-16.
185. Achim, C.L. and C.A. Wiley, *Inflammation in AIDS and the role of the macrophage in brain pathology*. Curr Opin Neurol, 1996. **9**(3): p. 221-5.
186. Heaton, R.K., et al., *The HNRC 500--neuropsychology of HIV infection at different disease stages. HIV Neurobehavioral Research Center*. J Int Neuropsychol Soc, 1995. **1**(3): p. 231-51.
187. Torrey, E.F., et al., *The stanley foundation brain collection and neuropathology consortium*. Schizophr Res, 2000. **44**(2): p. 151-5.
188. Binder, E.B., et al., *Association of FKBP5 Polymorphisms and Childhood Abuse With Risk of Posttraumatic Stress Disorder Symptoms in Adults*. JAMA, 2008. **299**(11): p. 1291-1305.
189. Rebhan, M., et al., *GeneCards: integrating information about genes, proteins and diseases*. Trends in Genetics, 1997. **13**: p. 163.
190. Lai, E.C., *Micro RNAs are complementary to 3' UTR sequence motifs that mediate negative post-transcriptional regulation*. Nat Genet, 2002. **30**(4): p. 363-4.
191. Shih-Jen Tsai, C.-J.H.T.-J.C.Y.W.Y.Y., *Lack of supporting evidence for a genetic association of the FKBP5 polymorphism and response to antidepressant treatment*. American Journal of Medical Genetics Part B: Neuropsychiatric Genetics, 2007. **144B**(8): p. 1097-1098.
192. Willour, V.L., et al., *Family-based association of FKBP5 in bipolar disorder*. Mol Psychiatry, 2008.
193. Marcus Ising, A.-M.D.A.S.S.L.P.G.U.S.K.S.H.M.U.B.M.I.-M.F.H., *Polymorphisms in the FKBP5 gene region modulate recovery from psychosocial stress in healthy controls*. European Journal of Neuroscience, 2008. **28**(2): p. 389-398.
194. Lekman, M., et al., *The FKBP5-Gene in Depression and Treatment Response--an Association Study in the Sequenced Treatment Alternatives to Relieve Depression (STAR\*D) Cohort*. Biological Psychiatry, 2008. **63**(12): p. 1103-1110.
195. Crayton, J.W., et al., *Effect of corticosterone on serotonin and catecholamine receptors and uptake sites in rat frontal cortex*. Brain Research, 1996. **728**(2): p. 260-262.
196. Glass, J.D., et al., *Clinical-neuropathologic correlation in HIV-associated dementia*. Neurology, 1993. **43**(11): p. 2230-7.
197. Toggas, S.M., et al., *Central nervous system damage produced by expression of the HIV-1 coat protein gp120 in transgenic mice*. Nature, 1994. **367**(6459): p. 188-93.
198. American Psychiatric Association. and American Psychiatric Association. Task Force on DSM-IV., *Diagnostic and statistical manual of mental disorders : DSM-IV*. 4th ed. 2000, Washington, DC: American Psychiatric Association.
199. Bao, A.M., G. Meynen, and D.F. Swaab, *The stress system in depression and neurodegeneration: Focus on the human hypothalamus*. Brain Res Rev, 2007.
200. Carroll, B.J., et al., *Pathophysiology of hypercortisolism in depression*. Acta Psychiatr Scand Suppl, 2007(433): p. 90-103.
201. Miyakawa, T., S. Sumiyoshi, and M. Deshimaru, *Changes induced in the central nervous system of rats by steroid drug*. Acta Neuropathol, 1974. **30**(1): p. 85-9.

202. Chao, H.M., P.H. Choo, and B.S. McEwen, *Glucocorticoid and mineralocorticoid receptor mRNA expression in rat brain*. *Neuroendocrinology*, 1989. **50**(4): p. 365-71.
203. Maccari, S., et al., *Hippocampal type I and type II corticosteroid receptors are modulated by central noradrenergic systems*. *Psychoneuroendocrinology*, 1992. **17**(2-3): p. 103-12.
204. Pavlides, C., et al., *Opposing roles of type I and type II adrenal steroid receptors in hippocampal long-term potentiation*. *Neuroscience*, 1995. **68**(2): p. 387-94.
205. Pariante, C.M. and A.H. Miller, *Glucocorticoid receptors in major depression: relevance to pathophysiology and treatment*. *Biological Psychiatry*, 2001. **49**(5): p. 391-404.
206. Gold, P.W., F.K. Goodwin, and G.P. Chrousos, *Clinical and biochemical manifestations of depression. Relation to the neurobiology of stress (2)*. *N Engl J Med*, 1988. **319**(7): p. 413-20.
207. Sanchez, E.R., *Hsp56: a novel heat shock protein associated with untransformed steroid receptor complexes*. *J Biol Chem*, 1990. **265**(36): p. 22067-70.
208. Callebaut, I., et al., *An immunophilin that binds M(r) 90,000 heat shock protein: main structural features of a mammalian p59 protein*. *Proc Natl Acad Sci U S A*, 1992. **89**(14): p. 6270-4.
209. Harrell, J.M., et al., *Evidence for glucocorticoid receptor transport on microtubules by dynein*. *J Biol Chem*, 2004. **279**(52): p. 54647-54.
210. Davies, T.H., Y.M. Ning, and E.R. Sanchez, *Differential control of glucocorticoid receptor hormone-binding function by tetratricopeptide repeat (TPR) proteins and the immunosuppressive ligand FK506*. *Biochemistry*, 2005. **44**(6): p. 2030-8.
211. Lowy, M.T., *Reserpine-induced decrease in type I and II corticosteroid receptors in neuronal and lymphoid tissues of adrenalectomized rats*. *Neuroendocrinology*, 1990. **51**(2): p. 190-6.
212. Chourbaji, S., M.A. Vogt, and P. Gass, *Mice that under- or overexpress glucocorticoid receptors as models for depression or posttraumatic stress disorder*. *Prog Brain Res*, 2008. **167**: p. 65-77.
213. Gass, P., et al., *Mice with targeted mutations of glucocorticoid and mineralocorticoid receptors: models for depression and anxiety?* *Physiol Behav*, 2001. **73**(5): p. 811-25.
214. Kohda, K., et al., *Glucocorticoid receptor activation is involved in producing abnormal phenotypes of single-prolonged stress rats: a putative post-traumatic stress disorder model*. *Neuroscience*, 2007. **148**(1): p. 22-33.
215. Young, E.A., et al., *Loss of glucocorticoid fast feedback in depression*. *Arch Gen Psychiatry*, 1991. **48**(8): p. 693-9.
216. Brown, G.M., et al., *Pituitary-adrenal function in the squirrel monkey*. *Endocrinology*, 1970. **86**(3): p. 519-29.
217. Reynolds, P.D., et al., *Glucocorticoid resistance in the squirrel monkey is associated with overexpression of the immunophilin FKBP51*. *J Clin Endocrinol Metab*, 1999. **84**(2): p. 663-9.
218. Chrousos, G.P., et al., *Glucocorticoid hormone resistance during primate evolution: receptor-mediated mechanisms*. *Proc Natl Acad Sci U S A*, 1982. **79**(6): p. 2036-40.
219. Ozer, E.J., et al., *Predictors of posttraumatic stress disorder and symptoms in adults: a meta-analysis*. *Psychol Bull*, 2003. **129**(1): p. 52-73.
220. Edinger, R.S., et al., *Effect of immunosuppressive agents on glucocorticoid receptor function in A6 cells*. *Am J Physiol Renal Physiol*, 2002. **283**(2): p. F254-61.

221. White, M.G., et al., *Neuron-enriched second trimester human cultures: growth factor response and in vivo graft survival*. Cell Transplant, 1999. **8**(1): p. 59-73.
222. Leffler, S., *SlideBook*. 1997, Silicon Graphics, Inc.
223. Noursadeghi, M., et al., *Quantitative imaging assay for NF-kappaB nuclear translocation in primary human macrophages*. J Immunol Methods, 2008. **329**(1-2): p. 194-200.
224. Brown, A.M., *A methodology for simulating biological systems using Microsoft Excel*. Comput Methods Programs Biomed, 1999. **58**(2): p. 181-90.
225. Wang, J.-C., et al., *From The Cover: Chromatin immunoprecipitation (ChIP) scanning identifies primary glucocorticoid receptor target genes*. Proceedings of the National Academy of Sciences, 2004. **101**(44): p. 15603-15608.
226. Jonas, E., *BCL-xL Regulates Synaptic Plasticity*. Mol. Interv., 2006. **6**(4): p. 208-222.
227. Riggs, D.L., et al., *The Hsp90-binding peptidylprolyl isomerase FKBP52 potentiates glucocorticoid signaling in vivo*. Embo J, 2003. **22**(5): p. 1158-67.
228. Owens-Grillo, J.K., et al., *A model of protein targeting mediated by immunophilins and other proteins that bind to hsp90 via tetratricopeptide repeat domains*. J Biol Chem, 1996. **271**(23): p. 13468-75.
229. Czar, M.J., et al., *Evidence that the FK506-binding immunophilin heat shock protein 56 is required for trafficking of the glucocorticoid receptor from the cytoplasm to the nucleus*. Mol Endocrinol, 1995. **9**(11): p. 1549-60.
230. Elbi, C., et al., *Molecular chaperones function as steroid receptor nuclear mobility factors*. Proc Natl Acad Sci U S A, 2004. **101**(9): p. 2876-81.
231. Wang, X., J.L. Pongrac, and D.B. DeFranco, *Glucocorticoid receptors in hippocampal neurons that do not engage proteasomes escape from hormone-dependent down-regulation but maintain transactivation activity*. Mol Endocrinol, 2002. **16**(9): p. 1987-98.
232. DeFranco, D.B., *Role of molecular chaperones in subnuclear trafficking of glucocorticoid receptors*. Kidney Int, 2000. **57**(4): p. 1241-9.
233. Deroo, B.J., et al., *Proteasomal inhibition enhances glucocorticoid receptor transactivation and alters its subnuclear trafficking*. Mol Cell Biol, 2002. **22**(12): p. 4113-23.
234. Limited, A.S., *Antibody Review to Mouse Anti FKBP51 ab46002*. 2008, AbCam Incorporated: Cambridge, MA.
235. Giraudier, S., et al., *Overexpression of FKBP51 in idiopathic myelofibrosis regulates the growth factor independence of megakaryocyte progenitors*. Blood, 2002. **100**(8): p. 2932-2940.
236. Fitzsimons, C.P., et al., *The microtubule-associated protein doublecortin-like regulates the transport of the glucocorticoid receptor in neuronal progenitor cells*. Mol Endocrinol, 2008. **22**(2): p. 248-62.
237. Burgess, H.A. and O. Reiner, *Alternative Splice Variants of Doublecortin-like Kinase Are Differentially Expressed and Have Different Kinase Activities*. J. Biol. Chem., 2002. **277**(20): p. 17696-17705.
238. Karin Boekhoorn, A.S.H.K.K.d.P.T.S.P.J.L.E.V., *Doublecortin (DCX) and doublecortin-like (DCL) are differentially expressed in the early but not late stages of murine neocortical development*. J Comp Neurol, 2008. **507**(4): p. 1639-1652.
239. Rasband, W.S., *ImageJ*. 1997-2007, National Institutes of Health, Bethesda, MD, USA.

